CHARACTERIZATION OF THE K1 PROTEIN OF KAPOSI SARCOMA-ASSOCIATED HERPESVIRUS AND DEVELOPMENT OF A NOVEL VACCINE FOR PROTECTION AGAINST RHADINOVIRUS INFECTION

Kwun Wah Wen

A dissertation submitted to the faculty of the University of North Carolina at Chapel Hill in partial fulfillment of the requirements for the degree of Doctor of Philosophy in the Department of Microbiology and Immunology.

Chapel Hill
2010

Approved by:

Blossom Damania, PhD
(Advisor)

Dirk Dittmer, PhD

Nancy Raab-Traub, PhD

Joseph Pagano, MD

Eng-Shang Huang, PhD

ABSTRACT

KWUN WAH WEN: CHARACTERIZATION OF THE K1 PROTEIN OF KAPOSI SARCOMA-ASSOCIATED HERPESVIRUS AND DEVELOPMENT OF A NOVEL VACCINE FOR PROTECTION AGAINST RHADINOVIRUS INFECTION
(Under the direction of Blossom Damania, PhD)

Kaposi sarcoma-associated herpesvirus (KSHV) is the causative agent of Kaposi sarcoma (KS), primary effusion lymphoma (PEL), and multicentric Castleman disease (MCD). KS is the most common malignancy in HIV/AIDS patients worldwide and can lead to significant mortality. There is no cure or vaccine for KSHV infection. KSHV encodes several oncogenic/transforming proteins that are implicated in KSHV-associated malignancies.

Our work is directed towards understanding the functional role of the KSHV K1 protein, which has been shown to activate signaling in B lymphocytes as well as to transform cells. We used tandem affinity purification (TAP) to identify the cellular interacting proteins of K1 and study the mechanisms by which K1 activates signal transduction pathways, inhibits apoptosis, and induces cellular transformation. The functional consequences of the interactions of K1 with its cellular binding partners were investigated with respect to the regulation of K1 expression and its anti-apoptotic function, using pharmacological inhibitors and RNA interference (RNAi). This study thus identified cellular targets essential for K1 function and may also aid in the identification of therapeutic targets that can be used in the treatment of KSHV-associated cancers.

In addition, we examined the role of K1 in the viral lifecycle. We took advantage of a highly related virus, rhesus rhadinovirus (RRV), which is the simian relative of KSHV.

Unlike KSHV, RRV grows to high titers *in vitro* making it a good model to study lytic replication and viral spread. RRV encodes a gene named R1, which is functionally homologous to the KSHV K1 gene. We constructed a RRVΔR1/GFPcc recombinant virus to analyze the contribution of R1 during *de novo* infection, latency, and reactivation of RRV.

Furthermore, we attempted to develop a novel vaccine for protection against rhadinovirus infection in primates using the RRV model system. The latency-associated nuclear antigen (LANA) is critical for the establishment and maintenance of both KSHV and RRV latency. We generated a recombinant virus deleted for RRV LANA, named RRVΔLANA/GFP, and found that this virus was highly lytic and unable to establish latency. A future goal of this aim will be to evaluate the RRVΔLANA/GFP as a vaccine candidate in rhesus macaques.

DEDICATION

To my wife Ting for unlimited love and support throughout my graduate school.
To my parents for constant encouragement of my study and career decisions.
Thank you.

ACKNOWLEDGMENTS

I would like to extend my deepest gratitude to my mentor, Dr. Blossom Damania, for all of her generous guidance and direction. I am especially grateful for her dedication to teaching me how to design appropriate experiments, troubleshoot, and write like a scientist, as well as for her enormous support during difficult times and grant writing.

I would also like to thank both current and former members of the Damania lab for their contributions to this work. Their kindness and friendliness have made my time in the lab very enjoyable. In particular, I am indebted to Dr. Ling Wang, Dr. Prasanna Bhende, Dr. Carlos González, Dr. John West, and Stuart Krall for their friendship and many helpful scientific discussions. I would also like to thank the more recent members of the Damania lab including Aadra Bhatt, Sean Gregory, Dr. Patrick Dillon, and Dr. Sarah Jacobs for helpful scientific discussion, jokes, and laughter. I would like to express my gratitude to Dr. Dirk Dittmer and the members of his laboratory, for technical assistance and engaging discussions.

I would like to thank my thesis committee members Dr. Dirk Dittmer, Dr. Nancy Raab-Traub, Dr. Joseph Pagano, and Dr. Eng-Shang Huang for their useful advice and guidance over the past several years. Their expertise and constructive advice have enabled my projects to progress as smoothly as I could imagine.

I would like to thank my friends in medical school and graduate school for their time and help. I am also indebted to the UNC MD/PhD program, especially Dr. Eugene Orringer and Dr. David Siderovski, for support and advice.

TABLE OF CONTENTS

LIST OF TABLES

LIST OF FIGURES

Chapter One

Chapter Two

Chapter Four

Chapter Five

LIST OF ABBREVIATIONS

ACV	Acyclovir
AIDS	Acquired immune deficiency syndrome
BCBL	Body cavity based lymphoma
BCR	B cell receptor
bFGF	basic fibroblast growth factor
bp	Base pairs of DNA
BJAB	Burkitt lymphoma derived B-cell line
BL	Burkitt lymphoma
BRLF-1	BamH1-R left reading frame number 1
BZLF-1	BamH1-Z left reading frame number 1
CBP	CREB binding protein
CDK	Cyclin dependent kinase
cDNA	Complementary DNA
CHX	Cycloheximide
CIP	Calf intestine phosphatase
CMV	Cytomegalovirus

CPE	Cytopathic effect
Ct	Cycle threshold
CTL	Cytotoxic T-lymphocyte
DAPI	4',6-Diamidino-2-phenylindole
DMEM	Dulbecco's modified eagle media
DMSO	Dimethyl sulfoxide
DNA	Deoxyribonucleic acid
DTT	Dithiothreitol
E	Early class of transcription
EBNA-1	EBV nuclear antigen 1
EBV	Epstein-Barr virus
EC	Endothelial cells
EDTA	Ethyl-diamine tetra-acetic acid
EGFP	Enhanced green fluorescence protein
ER	Endoplasmic reticulum
FLICE	Fas-associated death domain-like interleukin-1beta-converting enzyme
FLIP	Fas-associated death domain-like interleukin-1beta-converting enzyme-inhibitory protein

FOXO	Forkhead box O-class
GAPDH	Glyceraldehyde-3-phosphate dehydrogenase
gB	Glycoprotein B
GCV	Ganciclovir
GFP	Green fluorescence protein
GRP-78	Glucose-regulated protein 78
GSK	Glycogen synthase kinase
HAT	Histone acetyl transferase
HDAC	Histone deacetylase complex
HEK-293	Human endothelial kidney-293 cells
HeLa	Human liver-derived cell line
HEPES	4-(2-hydroxyethyl)-1-piperazineethanesulfonic acid
HHV-8	Human herpesvirus 8 (or KSHV)
HIV	Human immunodeficiency virus
Hsp	Heat shock protein
HSV	Herpes simplex virus
hTERT	Human telomerase reverse transcriptase

HUVEC	Human umbilical vein endothelial cells
HVS	Herpesvirus saimiri
IE	Immediate-early class of lytic transcription
IFA	Immunofluorescence assay
Ig	Immunoglobulin
IHC	Immunohistochemistry
IL	Interleukin
IP	Immunoprecipitation
IRES	Internal ribosome entry sites
IRF	Interferon regulatory factor homologue
ITAM	immunoreceptor tyrosine-based activation motif
JNK	c-Jun N-terminal kinase
kDa	Kilodalton
IE	Immediate early class of transcription
KS	Kaposi sarcoma
KSHV	Kaposi sarcoma-associated herpesvirus
L	Late class of transcription

LANA	Latency-associated nuclear antigen
LUR	Long unique region
MCD	Multicentric Castleman disease
MHV-68	Murine gammaherpesvirus-68
MMP-9	Matrix metalloproteinase 9
mRNA	Messenger RNA
MOI	Multiplicity of infection
MS	Mass spectrometry
MTA	Messenger RNA transport and accumulation protein
mTOR	Mammalian target of Rapamycin
NaB	Sodium butyrate
NERPRC	New England Regional Primate Research Center
NHL	Non-Hodgkin lymphoma
nt	Nucleotide of DNA or RNA
OCT-1	Octamer transcription factor 1
ORF	Open reading frame
ori-Lyt	Lytic origin of DNA replication

ORPRC	Oregon Regional Primate Research Center
PAA	Phosphonoacetic acid
PB	Polybrene
PBMC	Peripheral blood mononuclear cells
PBS	Phosphate-buffered saline
PCR	Polymerase chain reaction
PEL	Primary effusion lymphoma
PFA	Phosphonoformic acid or paraformaldehyde
PFU	Plaque forming unit
PI3K	Phosphotidyl-inositol-3'-OH kinase
PPH	Primary pulmonary hypertension
QPCR	Real-time quantitative PCR
RAP	Replication associated protein (K8/bZIP)
Rb	Retinoblastoma protein
RBP-Jκ	Recombinant signal sequence-binding protein Jκ
RFHV	Retroperitoneal fibromatosis-associated herpesvirus
RFP	Red fluorescence protein

RhF	Rhesus fibroblast cell line
RIPA	Radio-immunoprecipitation assay
R-LANA	RRV latency-associated nuclear antigen
RNA	Ribonucleic acid
RNAi	RNA interference
RRE	Rta-responsive element
RRV	Rhesus monkey rhadinovirus
RT-PCR	Reverse transcriptase PCR
Rta	Replication and transcription activator
RV1	Rhadinovirus 1 lineage
RV2	Rhadinovirus 2 lineage
SAIDS	Simian AIDS
SCID	Severe combined immune deficient
SCIP	Small capsomer interacting protein
SDS-PAGE	Sodium dodecyl sulfate polyacrylamide gel electrophoresis
SH2	Src-homology 2
shRNA	Short hairpin RNA

siRNA	Small interfering RNA
SIV	Simian immunodeficiency virus
TAP	Tandem affinity purification
TBS	Tris buffered saline
TK	Thymidine kinase
TIME	Telomerase immortalized microvascular endothelial cells
TNF	Tumor necrosis factor
TPA	12-*O*-tetradecanoylphorbol-13-acetate
TR	Terminal repeat
TSA	Trichostatin A
UTR	Untranslated region
VEGF	Vascular endothelial growth factor
Vero	African green monkey kidney derived cell line
vGPCR	Viral G protein coupled receptor
vIL-6	Viral interleukin-6
VZV	Varicella-zoster virus
WT	Wild-type

CHAPTER 1

KSHV: MOLECULAR BIOLOGY AND ONCOGENESIS

Kwun Wah Wen and Blossom Damania

A portion of this chapter was published as a review article.

Introduction

The members of the herpesviridae family are well represented in nature and can be found in many different species across the animal kingdom. They are also highly adapted to their hosts and are thought to have coevolved with their hosts for millions of years. Typically, herpesviruses have a double-stranded DNA genome (124-230 kb) enclosed in an icosahedral capsid (~125 nm in diameter) composed of 162 capsomeres. The capsid structure is surrounded by an amorphous tegument layer that separates it from the outer, glycoprotein-decorated, envelope. Common to all human herpesviruses is their ability to adapt very well to the cellular milieu of the infected host and their ability to evade host immune responses to establish life-long latent infection. Based on their biological properties including host range, replication cycle and cell tropism, these viruses are classified into the alpha-, beta-, and gammaherpesvirinae subfamilies (181) (Fig. 1).

There are eight known human herpesviruses (HHV). Most of the human population is infected with one or more of these viruses, and they rarely cause severe disease in the host unless the host immune system is compromised. Human herpesviruses belonging to the alpha subfamily include herpes simplex viruses (HSV) 1 and 2 (HHV-1 and HHV-2), and varicella-zoster virus (VZV; HHV-3). Members of the human betaherpesvirinae include cytomegalovirus (CMV; HHV-5), HHV-6 variants A and B, and HHV-7. Human gammaherpesvirinae include Epstein-Barr virus (EBV; HHV-4) and Kaposi sarcoma-associated herpesvirus (KSHV; HHV-8). Strikingly the members of gammaherpesvirinae are strongly associated with neoplastic disease. For example, EBV is the etiological agent of Burkitt lymphoma, Hodgkin lymphoma, nasopharyngeal carcinoma, T and natural killer cells lymphoma, and post-transplant lymphoma (47, 99, 172, 242). KSHV is the etiological agent

of several human cancers including Kaposi sarcoma (KS) (36, 147), primary effusion lymphoma (PEL) (33), and the plasmablastic variant of multicentric Castleman's disease (MCD) (75, 200). Additionally, there have also been reports of KSHV-associated solid lymphomas of HIV-positive and negative individuals (30) as well as KSHV-associated lymphomas in patients with primary immunodeficiencies such as common variable immunodeficiency (233).

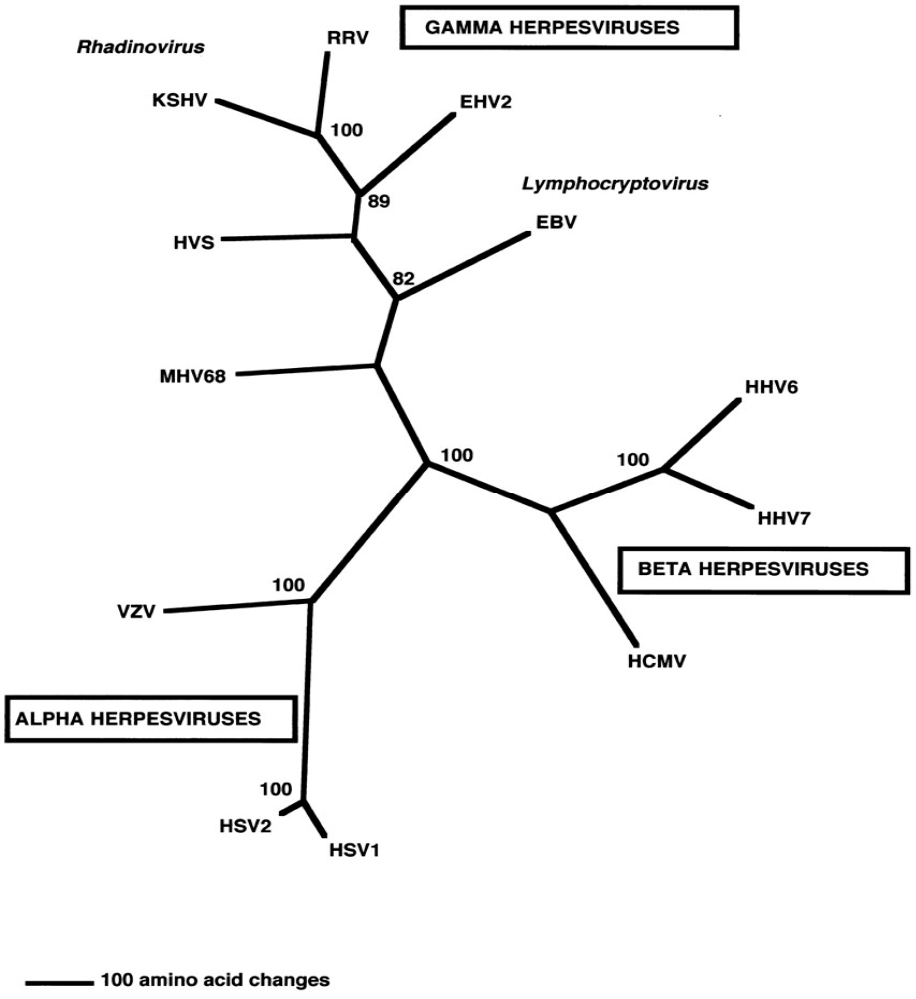

Figure 1. Phylogenetic depiction of the alpha, beta, and gamma subfamilies of herpesviruses. The phylogram is unrooted and was constructed by parsimony analysis using the viral DNA polymerase gene and the neighbor-joining method. (Taken from Damania and Jung (45).)

The gammaherpesviruses have evolved to possess a plethora of viral gene products that intricately subvert normal cellular pathways. The dysregulated signaling pathways include those involved in cell cycle progression, apoptosis, immune surveillance, and antiviral responses. Gammaherpesviruses are masters of altering these pathways in favor of their survival. They are known to establish persistent viral infection, and to evade viral clearance by actively suppressing apoptosis and escaping immune detection. The survival mechanisms used by these viruses are thought to inadvertently contribute to host cell transformation and the development of neoplasia, which is most frequently seen in the setting of immunodeficiency. In this chapter, we will focus on KSHV in terms of its associated clinical diseases and current therapies, as well as viral genes implicated in tumorigenesis and oncogenesis.

Clinical diseases associated with KSHV infection

Kaposi sarcoma. Kaposi sarcoma was named by Dr. Moritz Kaposi, a prominent Hungarian dermatologist, who first described the rare classical form of KS as "idiopathic multiple pigmented sarcoma of the skin" in 1872 (95). Since the 1950s, an infectious agent was suspected to cause KS. The discovery of the causative agent of KS, however, was not intensively pursued until the early 1980s, when the incidence of KS dramatically increased in homosexual and bisexual HIV-positive individuals during the AIDS epidemic. The sudden surge of KS incidence among HIV-infected individuals strongly suggested an infectious agent was involved in the development of KS. In 1994, Chang and Moore used representational difference analysis to characterize DNA fragments obtained from KS biopsies and established an association of a novel human gammaherpesvirus with KS (36). This newly identified virus was named KSHV. KS is a highly vascular tumor of endothelial

lymphatic origin (14, 223). Histologically, the signature KSHV-infected cells are spindle-shaped, poorly differentiated, and highly proliferative (60). KS is also characterized by extravasation of erythrocytes, infiltration of inflammatory cells (macrophages, lymphocytes and plasma cells) and neo-angiogenesis (74). Clinically, KS is characterized by dermatological lesions that are red, brown, or purple in pigmentation. These lesions can be found cutaneously, mucosally, or viscerally. KS can be staged by six overlapping clinicopathologic forms: patch, plaque, nodular, lymphadenopathic, infiltrative, and florid (104, 213). It is important to note that greater than 95% of KS lesions contain KSHV viral DNA. Based on epidemiological and clinical outcomes, KS can be classified into 4 different clinical subtypes. These are classic/sporadic, endemic/African, epidemic/AIDS-associated, and iatrogenic/post-transplant. Classic KS is the form described by Dr. Kaposi. The presentation of classic KS typically occurs with an indolent course in Mediterranean and Eastern European elderly men over 50 years of age. The lesions are generally localized in the upper and/or lower extremities without much involvement with, or spreading to, the lymph nodes and internal organs. Patients diagnosed with classic KS may progress to other secondary malignancies, primarily non-Hodgkin lymphomas (NHL) (71, 89). African endemic KS is commonly seen in Eastern and central African countries such as Uganda, Malawi, and Kenya. Endemic KS may be indolent or aggressive, with more lymph node involvement than classic KS. The aggressive form (also known as lymphadenopathic form) of endemic KS is more commonly found in children at pre-puberty ages, with high fatality rates (62). AIDS-associated KS is the most common and aggressive variant, with the most lymph node/visceral spreading amongst all KS subtypes (17, 20). During the HIV/AIDS epidemic, the incidence of KS concurrently peaked with HIV diagnoses. Due to its strong

association with AIDS, KS was identified as an AIDS-defining illness and served as a marker for HIV disease in the mid-eighties (134). Indeed, KS is the most common malignancy associated with HIV infection and can lead to significant mortality (18). KS is the most common tumor in African men (63, 159, 221). This epidemiologic form of KS is found with increased frequency in homosexual AIDS patients who are relatively young. With the advent of highly active antiretroviral therapy (HAART) in the 1990s, the incidence and mortality of AIDS-associated KS have dramatically dropped (65, 212). However, KS continues to remain the most common AIDS-associated cancer in developed nations and in developing countries (32). Another form of KS, known as iatrogenic/post-transplant KS, is associated with immune suppression after long-term immunosuppressive therapy used to prevent rejection of solid allografts (164). Renal transplant patients are the most likely group to develop this form of KS. Interestingly, the KSHV-infected endothelial cells or lymphocytes found in KS lesions in these patients can originate from donor tissues (12). Reduction or withdrawal of immunosuppressive therapy has been shown to be effective in resolving iatrogenic KS. However, this also increases the likelihood of allograft rejection.

Primary effusion lymphoma. In addition to KS, primary effusion lymphoma (PEL), sometimes referred to as body cavity-based lymphoma (BCBL), has been strongly associated with KSHV (33). PEL is a unique form of NHL found more commonly in immunocompromised AIDS patients. Unlike KS, PEL is derived from clonally expanded malignant B cells and presents as a lymphomatous effusion tumor contained in various body cavities such as the pericardium, pleurum, and peritoneum. There are, however, reports of PEL as a solid mass in lymph nodes and other organs (8). PEL is aggressive and rapidly

progressing, and can cause high fatality. The mean survival time for patients with PEL is approximately two to six months (101). Histologically, PEL cells are larger than normal lymphocytes and erythrocytes, and contain features of both large cell immunoblastic lymphoma and anaplastic large cell lymphoma. PEL cells express CD45, activation-associated antigens, clonal immunoglobulin rearrangements but usually lack B cell-associated antigens (144). PEL cells can be KSHV single-positive or KSHV/EBV double-positive. KSHV genomes are found in PEL cells at a high copy number (50-150 viral genomes per infected cell) (33, 179, 206).

Multicentric Castleman's disease. The plasmablastic variant of multicentric Castleman's disease (MCD) is also highly associated with KSHV; however, the other form of MCD, namely, the hyaline variant of MCD, is not. MCD is a reactive lymphadenopathy that is considered non-neoplastic as polyclonal B-cell populations are usually found in the lesion. However, monoclonal B cell expansion has also been reported for plasmablastic MCD (86, 173). Plasmablastic MCD can have an aggressive and rapid progression leading to high fatality. Histologically, germinal center expansion and vascular endothelial proliferation occur within the involved lymph nodes of MCD. Dysregulated IL-6 levels, likely contributed in part by virally encoded IL-6 (vIL-6) (161), may account for the clinico-pathophysiology of MCD. Like KS and PEL, KSHV genomes are detectable in almost all HIV-positive MCD cases and about fifty percent of HIV-negative MCD cases (60, 200). Additionally, KSHV has been shown to be associated with a plasmablastic variant of MCD.

The KSHV genome

KSHV has a double-stranded DNA genome and its size ranges from 165-170 kb (146, 180). The long unique region (LUR), which is about 138 to 140.5 kb in length and contains all of the KSHV ORFs, is flanked by terminal repeat (TR) sequences at both ends of the linear viral genome. Each TR is 801 bp in length and is highly GC-rich. The number of TRs varies among KSHV isolates, ranging from 16 to 75 (61), which accounts for the variation in the genome sizes of KSHV isolates. The KSHV genome exhibits very high degree of similarity to retroperitoneal fibromatosis-associated herpesvirus (RFHV) and rhesus monkey rhadinovirus (RRV) in the rhadinovirus subfamily of gammaherpesvirinae. RFHV appears to be more closely related to KSHV. Although many of the KSHV ORFs are conserved in alpha- and beta-herpesviruses, the virus does contain a significant number of unique ORFs not found in other herpesviruses (Table 1). These KSHV-specific ORFs are designated K1 to K15, based on their relative locations (from left to right) in the KSHV genome (Fig. 2). Moreover, KSHV also contains several viral genes that have been pirated from the host genome and are homologs of cellular genes (210).

Many viral genes are involved in signal transduction (e.g. K1, K15), cell cycle regulation (e.g. vCyclin, LANA), inhibition of programmed cell death (e.g. K1, vFLIP, vBcl-2) and immune modulation (e.g. viral chemokine receptors, vIRFs, K3, K5). Additionally, a number of KSHV genes are expressed by alternative splicing (reviewed in (191)), by the use of alternative transcriptional start sites, or internal ribosome entry sites (IRES) (121, 126). Very recently, a total of 12 microRNAs have been discovered in the KSHV genome (28, 163, 165, 188). Ten of these microRNAs were found in the non-coding region between K12/Kaposin and K13/Orf71/vFLIP, and two were located within the K12 ORF (Fig. 2). All

of the KSHV microRNAs were expressed during latency (27, 143, 163, 189), with a sub-set of these microRNAs being upregulated during the lytic cycle. Recent evidence has identified cellular and viral targets of these microRNAs, as well as their roles in KSHV pathogenesis (77, 133, 143, 189, 198). Besides microRNAs, KSHV also produces a non-coding RNA transcript that is 1077 bp in size, polyadenylated and exclusively nuclear (PAN) (41, 42, 208, 245). PAN RNA is made during the lytic cycle and has been shown to retain RNA in the nucleus and block the assembly of an export-competent mRNP.

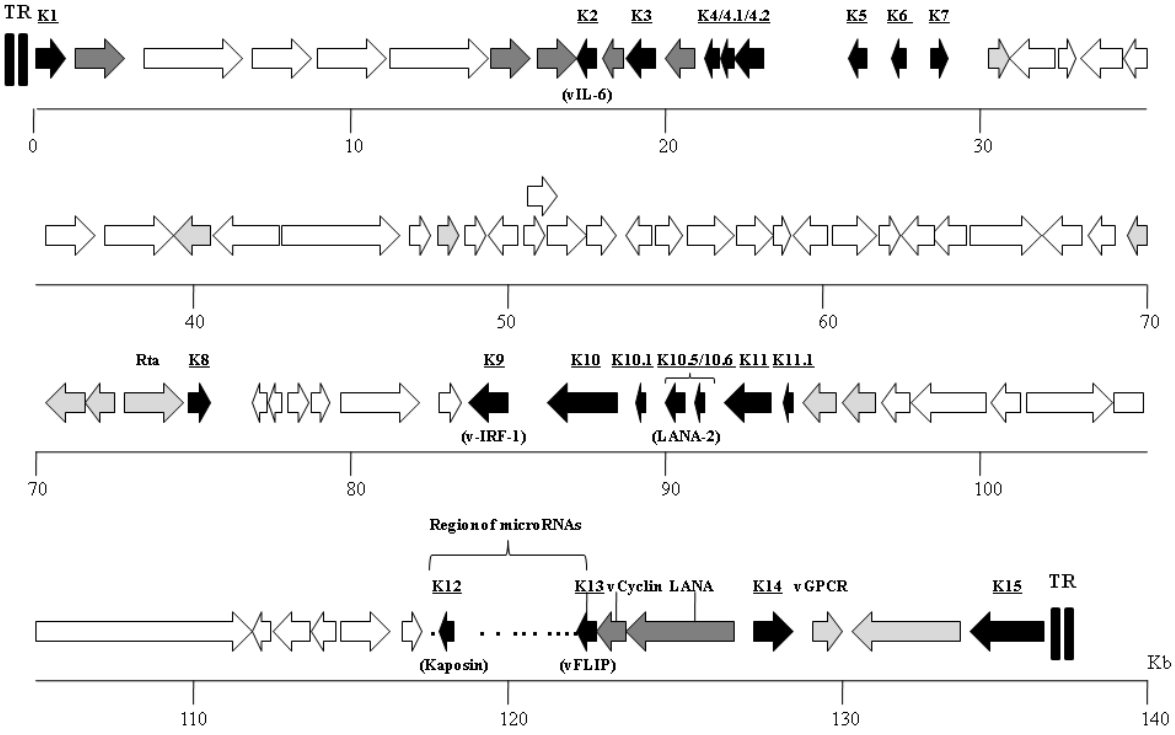

Figure 2. The KSHV genomic open reading frames (ORFs). The arrows represent individuals ORFs and the dots represent the KSHV-encoded microRNAs. ORFs unique to KSHV are labeled K1 through K15 and are indicated by black arrows. Alternative names for some of these unique KSHV genes are in parentheses. Additional ORFs discussed in this chapter are also labeled. The ORFs common to rhadinoviruses are indicated by dark gray arrows, ORFs common to other gammaherpesviruses (e.g. EBV) are indicated by light gray arrows, and ORFs common to most herpesviruses are indicated by white arrows. TR denotes terminal repeats. The numbers on demarcated lines specify the approximate genome positions in Kb.

Table 1. Unique ORFs encoded by KSHV

ORF	Alternative name	Functions
K1 *	VIP	Transformation; B cell activation; inhibition of apoptosis; downregulation of surface B cell receptor (BCR); activation of PI3K/Akt/mTOR kinases
K2 *	vIL-6	IL-6 homolog; B cell proliferation; autocrine/paracrine signaling
K3	MIR1	E3 ubiquitin ligase; immune evasion; inhibition of MHC class I and T cell killing
K4	vMIP-II; vMIP-1b; vCCL-2	MIP-I homolog; angiogenesis; CCR3 and CCR8 binding; chemoattraction of TH2 cells and monocytes (immune modulation)
K4.1	vMIP-III; vBCK; vCCL3	TARC/eotaxin homolog; induction of VEGF-A and angiogenesis; CCR4 binding; chemoattraction of TH2 cells (immune modulation)
K5	MIR2	E3 ubiquitin ligase; immune evasion; inhibition of MHC class I, B7, and ICAM expression
K6	vMIP-I; vMIP-1a; vCCL-1	MIP-I homolog; angiogenesis; CCR5 and CCR8 binding; chemoattraction of TH2 cells and monocytes
K7	Survivin; vIAP	Inhibitor of apoptosis protein (IAP) homolog; inhibition of vGPCR expression and function
K8	K-bZIP	An immediate-early gene that represses RTA transactivation activity and Rta induction of KSHV lytic cycle
K8.1		Viral glycoprotein (structural protein)
K9*	vIRF-1	IRF homolog; Inhibition of type I interferon, p300, p53, and TGF-β; transformation
K10	vIRF-4	IRF homolog
K10.1 K10.5 K10.6	LANA-2 (K10.5); vIRF-3	IRF homolog; inhibition of type I interferon production and apoptosis (PKR-and caspase-3 mediated); inhibition of p53 and NFκB; inhibition of Fas-mediated apoptosis via inhibition of CD95L surface expression
K11 K11.1 K11.5	vIRF-2 (K11.5)	IRF homolog; inhibition of type I interferon and NFκB; inhibition of Fas-mediated apoptosis via inhibition of CD95L surface expression
K12*	Kaposin	Transformation (Kaposin A); cytokine and AU-rich mRNA stabilization by induction of p38 or MK2 signaling (Kaposin B)
K13*	vFLIP	FLIP homolog; transactivator of NF-κB; anti-apoptotic function; transformation
K14	vOx-2	Ox-2 (CD200) homolog; downregulation of myeloid cell activation; regulation of inflammatory cytokine production such as IL-1β, TNF-α, IL-8, IFN-γ and IL-6
K15	LAMP	Activation of the intracellular signaling pathways (Ras/MAPK, NF-κB, and JNK/SAPK), leading to IL-6, IL-8, and Cox-2 induction. A chimeric protein consisting of the CD8 extracellular domain of CD8 and the K15 cytoplasmic domain could inhibit BCR signaling

Note: Only KSHV unique genes marked with an asterisk are discussed in more detail in the text.

The viral lifecycle

Like other herpesviruses, KSHV displays two different phases of its viral lifecycle. Latent KSHV is characterized by a circularized, extra-chromosomal viral genome (episome) and the expression of a very small subset of latent transcripts in the infected cells; no functional or infectious viral particles are produced during latency. In latently infected cells, in all three KSHV-associated malignancies, the expression of OrfK12/Kaposin, K13/Orf71/vFLIP, Orf72/vCyclin, and Orf73/LANA has been detected. In PEL and MCD cells, OrfK10.5/LANA-2/vIRF3 expression was also detected (160). The lytic cycle is characterized by the replication of linear viral genomes, and the expression of more than 80 transcripts in a highly orchestrated temporal order of immediate-early (α), early (β), and late (γ) categories. These categories are defined by sensitivity to cycloheximide and phosphonoacetic acid (PAA) treatment after chemical induction of viral reactivation (57, 66, 92, 162). Unlike early and late genes, immediately-early (IE) genes are not sensitive to the protein synthesis inhibitor cycloheximide, as the expression of IE genes does not rely on viral protein synthesis. IE genes are important for regulating the subsequent transcriptional cascade. KSHV encoded Rta is an IE lytic master switch protein that has been shown to be required and sufficient for initiating the lytic replication cycle to completion. The IE gene K8/K-bZIP appears to antagonize Rta transactivation activity (90, 183). The third IE gene, Orf45, is important for the suppression of interferon induction by lytic viral infection or reactivation (247). In contrast to IE genes, early and late genes are sensitive to cycloheximide, and are distinguished by their dependence on DNA replication. The expression of early genes is independent of viral DNA synthesis and is not inhibited by PAA treatment, whereas the expression of late genes is dependent on the replication of viral genomes and therefore

sensitive to PAA inhibition. To model KSHV lytic replication *in vitro*, chemical induction using *n*-butyrate and 12-O-tetradecanoylphorbol-13-acetate (TPA) to reactivate PEL cells has been reported. TPA treatment can lead to reactivation in about 20-30% of PEL cells (138, 180). The general function of early and late genes is to facilitate the replication of viral genomes, viral assembly and egress.

Rta. Rta (replication and transcription activator) is an immediate-early (IE) gene encoded by KSHV Orf50. As an IE gene, Rta can be expressed in the presence of the protein synthesis inhibitor, cycloheximide. The Rta transcript consists of two exons separated by an intron. Such an arrangement is conserved in all other gamma-2-herpesviruses (205). The Rta transcript is tricistronic, containing Orf50, OrfK8, and OrfK8.1 (246). The major Rta message is spliced out for expression; it is induced in PEL cells within 4 hours of *n*-butyrate treatment (128, 129, 203). Rta is necessary and sufficient to trigger and complete the KSHV lytic cycle. KSHV reactivation has been demonstrated in PEL cells when Rta was ectopically expressed (78, 209). Similar to the HSV-1 IE transactivator protein VP16, Rta protein is virion-associated (13). The Rta protein consists of 691 amino acids and is nuclear (127). Rta is highly phosphorylated and contains an N-terminal DNA binding domain (127) and a C-terminal transactivation domain (228) that are conserved in gammaherpesviruses. When the C-terminal domain was deleted, Rta mutant could no longer function to transactivate other lytic genes. This truncated Rta multimerized with the wild-type Rta and inhibited their activity in a dominant-negative fashion (128). Another line of evidence supporting Rta as the key lytic switch protein was that an Rta deletion virus exhibited defects in reactivation and viral DNA replication upon chemical induction. When Rta was provided *in trans*, such a defect was corrected in cells infected with the Rta deletion virus (235).

The transactivation activity of Rta is mediated by Rta binding to Rta responsive elements (RREs) on the promoters of target genes. An RRE and a TATA box were discovered in the ori-Lyt (223, 225), providing strong evidence for the importance of Rta on the lytic cycle in terms of DNA replication and transcription activation. RREs have been found in various viral promoters including PAN, Orf57/MTA, vIL-6, Kaposin, and Rta itself (205). The RREs of different viral transcripts do not share sequence homology, raising the question of how a viral protein could associate with such a diversity of DNA sequences. As a rare exception, the promoters of Orf57 and K-bZIP share the same 12-bp palindromic RRE sequence (127). Strikingly, Rta associates with several cellular proteins that are known transcriptional regulators. These cellular proteins include: recombination signal sequence-binding protein Jκ (RBP-Jκ), C/EBP-α, Ap-1, Sp1, Sp3, and Oct-1 (40, 118, 186, 229-231, 243). Among these cellular binding candidates of Rta, RBP-Jκ is particularly noteworthy. Rta recruitment of RBP-Jκ could convert this cellular protein from a transcriptional repressor into a transactivator on a number of lytic viral promoters (e.g. PAN, MTA, vIL-6, Kaposin aforementioned) as well as ori-Lyt. This gives rise to a mechanistic understanding of Rta transactivation function on a variety of viral genes. Interestingly, Rta has been shown to upregulate its own expression (Fig. 3). The binding of RBP-Jκ, Oct-1, Sp1, Sp3 and C/EBP-α appears to be responsible for Rta auto-activation (40, 78, 186, 230, 243). Interestingly, Orf57/MTA, the KSHV homolog of HSV-1 ICP27 and EBV SM, binds and synergizes with Rta to promote the lytic transcriptional cascade (130, 157).

The default lifecycle of KSHV is predominantly latent. Thus, transactivation activity of Rta needs to be dampened by the virus in order to switch back to latency after a primary lytic infection. During early infection, LANA expression is induced by Rta-mediated RBP-Jκ

binding to the LANA promoter (110) (Fig. 3). As a negative feedback loop of the lytic cycle, LANA has been shown to downregulate Rta promoter activity as well as physically associate with Rta (109). LANA-1 inhibits Rta expression by recruiting RBP-Jκ to close proximity of Rta promoter. (108) (Fig. 3). In addition to LANA, other viral proteins (e.g. K-bZIP (90, 183), K-RBP (238), and vFLIP (240, 244)) and cellular proteins (e.g. CREB binding protein, histone deacetylases (84), poly(ADP-ribose) polymerase 1 (PARP-1), Ste20-like kinase hKFC (85), HEY1 (236)) may also repress lytic Rta activity. To counteract the inhibitory effects of these proteins, Rta is able to promote the proteasomal degradation of some of these proteins (239). This demonstrates that KSHV proteins finely tune various viral and cellular pathways to achieve an intricate balance between the lytic and latent cycles.

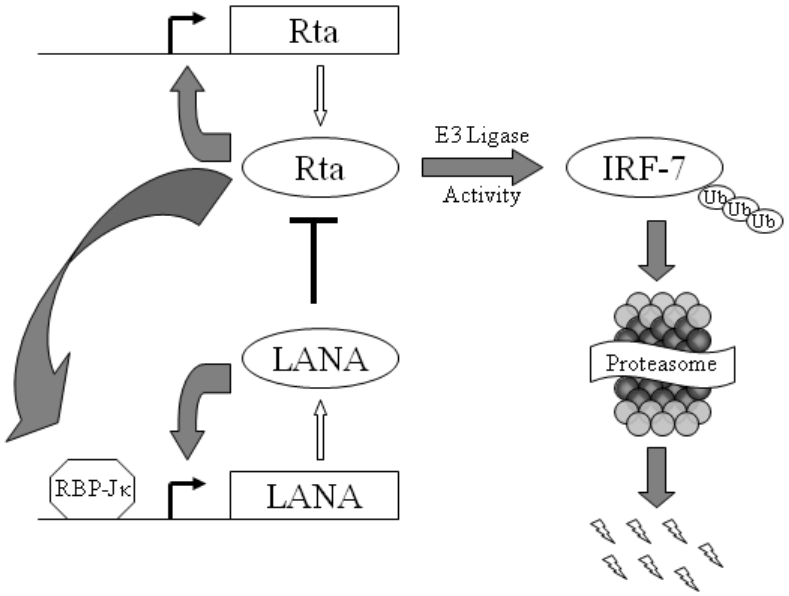

Figure 3. Feedback loops of LANA and Rta to control the switch between latency and lytic replication. Depiction of the regulation of LANA and Rta via positive and negative feedback loops. Both Rta and LANA transactivate their own promoters while Rta also induces LANA expression through interactions with RBP-Jκ. LANA can repress Rta-mediated transactivation through binding of Rta. Rta encodes ubiquitin E3 ligase activity and regulates its own expression through self-ubiquitination and also targets IRF-7 for degradation by the proteasome. (Taken from Dillon and Damania (53))

Putative viral genes involved in KSHV transformation and oncogenesis

Transformation is a key event in the multistep process of oncogenesis. It involves changes in cellular signaling pathways and cell morphology, leading to a state of uncontrolled proliferation. In KSHV, transformation of endothelial cells can lead to chromosome instability (158), alteration of cellular gene expression profiles (167), acquisition of telomerase activity and anchorage-independent growth (69), increase in cell invasiveness (171) as well as long-term proliferation and survival of these cells (69, 224). A number of KSHV-encoded proteins are believed to have transforming and oncogenic properties. They include both latent and lytic proteins: the latent proteins are likely to enhance the survival and proliferation of the infected cells, whereas the lytic viral proteins

are believed to mediate paracrine secretion of growth and angiogenic factors essential for tumor growth and development. This is postulated based partially on the observation that the latent genes (especially those encoded on the latency-associated cassettes) are detectable *in situ* in the majority of KS, PEL, and MCD samples, whereas the lytic genes (e.g. K1, vIL-6, vGPCR) are detectable in only small sub-sets of tumor samples. These oncogenic viral products are described below.

LANA. The latency-associated nuclear antigen (LANA) is required for the maintenance of latency (reviewed in (54, 175, 217)). LANA maintains the episomal KSHV genome in latently infected cells and allows for the co-segregation of viral and host genomes into the daughter cells during mitosis. LANA is able to perform this function by tethering the KSHV episome to the host chromatin (11, 86, 192, 219). When homodimerized, the N-terminus of LANA binds to the nucleosome via interaction with histone H1 and heterochromatin protein 1 (86), while the C-terminus of LANA-1 binds to the terminal repeats of the viral genome (192). LANA is also involved in the replication of the latent viral genome (79) and can autoregulate its expression by binding to its own promoter (93). Furthermore, LANA has been described to interact with multiple cellular proteins including the mSin3A corepressor complex, the DNA methyltransferase Dnmt3a, RBP-Jκ, and cAMP response element-binding protein which results in the transcription repression of several viral and cellular genes (84, 103, 119, 176, 195, 223). Of particular importance is the demonstrated antagonistic effect of LANA on the KSHV Rta promoter (165) (Fig. 3). LANA has been shown to recruit RBP-Jκ to the Rta promoter resulting in chromatin silencing of Rta expression. Furthermore, LANA can also inhibit Rta transactivation through a direct physical interaction (223).

LANA can perturb a plethora of cellular pathways to contribute to tumorigenesis. For example, LANA can physically associate with p53 and inhibit p53-mediated transcription activity and apoptosis (70). LANA can also inactivate the tumor suppressor retinoblastoma (Rb) gene and release E2F transactivator which induces cell to transit through the G1/S cell cycle checkpoint (174). To promote G1/S transition, LANA interacts with the bromodomain-containing protein RING3/Brd2 (48, 83, 166, 220), and can sequester glycogen synthase kinase (GSK)-3β in the nucleus, which prevents GSK-3β from complexing with, and degrading, β-catenin in the cytoplasm. The stabilized β-catenin can translocate into the nucleus, where it complexes with the transcription factors lymphoid enhancing factor (LEF) and T-cell factor (TCF) to transactivate responsive genes including CCND1 and Myc, which have been implicated in cell cycle regulation and oncogenesis (23, 72). LANA can cooperate with the oncogene H-Ras to transform primary rat embryo fibroblasts and render them tumorigenic (174). LANA was also shown to upregulate human telomerase reverse transcriptase (hTERT) gene expression and to immortalize primary HUVEC and increase their proliferation (232). Finally, transgenic mice expressing LANA under the endogenous LANA promoter developed splenic follicular hyperplasia with increased germinal centers as well as lymphomas (67). Based on these findings, LANA appears to at least set the initial stage for sarcomagenesis and lymphomagenesis.

K13/vFLIP. The viral FLICE (Fas-associated death-domain like IL-1 beta-convertase enzyme) inhibitory protein (vFLIP) is also known as K13, and is encoded by Orf71 (55, 66, 92). Latent expression of vFLIP occurs via splicing of the LANA transcript from the tricistronic messenger RNA, and via the use of the IRES in vCyclin coding sequences (19, 80,

126). Similar to cellular FLIPs, vFLIP inhibits death receptor signaling by specifically abrogating the interaction between Fas-associated death domain (FADD) and caspase-8 (15). The inhibition of this pathway blocks Fas-mediated apoptosis, thus providing a survival advantage for KSHV-infected cells (59). In addition to blocking the extrinsic apoptotic pathway, vFLIP also associates with the IKK complex and the heat shock protein 90 (hsp90) to induce NF-κB survival signaling (25, 39, 68, 125). The induced NF-κB signaling is significant in at least two aspects: viral latency and oncogenesis. First, NF-κB activation by vFLIP is critical for vFLIP inhibition of lytic replication via the AP-1 pathway (240, 244). Second, the enhanced NF-κB signaling may be important for the transforming and oncogenic potential of vFLIP as demonstrated in Rat-1 fibroblast assays and tumors in nude mice (207). In primary dermal microvascular endothelial cells, vFLIP expression was shown to induce anoikis (detachment induced apoptosis), but not apoptosis, due to growth factor depletion suggestive of its role in paracrine factor secretion and KS development (64).

vCyclin. This gene is encoded by Orf72, located immediately downstream of the LANA ORF in the latency-associated cassette (55, 211). Expression of vCyclin occurs via splicing of the LANA transcript from the tricistronic messenger RNA. vCyclin is the viral homolog of cellular cyclin D1. Cellular cyclin D1 associates with cyclin-dependent kinases such as CDK6 and CDK4, to form a complex that phosphorylates the retinoblastoma (Rb) protein. Phosphorylated Rb can no longer antagonize E2F's transactivation of S-phase cell cycle genes. vCyclin was shown to complex with CDK6 and inhibit Rb sequestration of E2F from the nucleus; however, vCyclin, unlike its cellular homolog, is insensitive to CDK inhibitors such as p16/INK4a, p21/CIP1 and p27/KIP1 (37, 76, 150, 210). It is believed that vCyclin

has a proliferative effect on latently infected cells and thus promotes their transition into tumor cells. The oncogenic potential of vCyclin was demonstrated in mice lacking functional p53 (218, 219), providing evidence that vCyclin has an auxiliary role in oncogenesis.

Kaposin. The Kaposin transcripts represent the most abundantly expressed viral transcripts during KSHV latency. Kaposin A is encoded by OrfK12, while Kaposins B and C initiate upstream of OrfK12 at two repeat regions (termed DR1 and DR2), and their transcripts extend into OrfK12 (185). Kaposin A has oncogenic potential as demonstrated by focus formation assay in transfected Rat-3 cells. This morphological change is mediated through interaction with cytohesin-1 (100). Cytohesin-1 is a guanine nucleotide exchange factor for the GTPase ARF as well a regulator of cell adhesion. When injected into athymic mice, the transformed Rat-3 cell lines containing Kaposin sequences produced high-grade, highly vascular, undifferentiated sarcomas (142). In contrast to the undetectable protein level of Kaposin A in virus-infected cells, Kaposin B was shown to be the most abundant Kaposin protein in the PEL cell line BCBL-1 (185). Kaposin B functions to stabilize cytokine expression such as IL-6 and GM-CSF by inhibiting degradation of their messages. The inhibition was achieved via Kaposin B binding and activation of MK2 kinase, which inhibits degradation of mRNA containing AU-rich elements (e.g. cytokines) (135). The mRNA stabilization activity is dependent on the direct repeat (DR1 and DR2) elements of Kaposin B (136).

K1. K1 is a 46-kDa type I membrane glycoprotein encoded by the first open-reading frame (106). K1 is also designated VIP (variable ITAM-containing protein) as it contains an immunoreceptor tyrosine-based activation motif (ITAM) (115). The K1 genomic location is equivalent to those of the transforming proteins STP of herpesvirus saimiri (HVS) and LMP-1 of EBV. K1 is expressed at low levels during latency and is upregulated during lytic infection where it demonstrates early kinetics (24, 35). K1 expression has been detected in KS, PEL, and MCD (92, 106, 114, 225). K1 has been shown to transform Rat-1 rodent fibroblasts by inducing morphological changes and foci formation (116), and can functionally substitute for STP in the context of HVS infection of common marmoset to immortalize T lymphocytes to IL-2-independent growth as well as induce lymphomas (116). Transgenic mice expressing the K1 gene showed constitutive activation of NF-κB and Oct-2, increased Lyn tyrosine kinase phosphorylation and activity, as well as increased basic fibroblast growth factor (bFGF) expression (169). Some of these mice developed tumors with features resembling the spindle-cell sarcomatoid tumor and malignant plasmablastic lymphoma (169). Structurally, K1 contains a long N-terminal extracellular domain, a transmembrane domain, and a short C-terminal cytoplasmic tail. The N-terminal domain has a very high sequence variability in different geographical regions and can be glycosylated for multimerization (87, 96, 248). The C-terminus of K1 is well conserved and contains an ITAM that is normally important for lymphocyte activation signaling (115). Upon ligand binding, the ITAM of lymphocyte receptors functions to transduce the extracellular signal to downstream SH2-containing molecules. This subsequently induces calcium mobilization and tyrosine phosphorylation events leading to cellular activation. The ITAM-based signaling of K1, however, appears to be constitutively active, independent of ligand binding (116). In B

cells, K1 has been shown to activate PI3K (p85 subunit), Akt, Vav, and Syk kinases, and to induce NFAT and NF-κB transcriptional activities for cell survival (107, 115, 215) (Fig. 4 & 5). In addition, K1 can prevent death receptor-mediated apoptosis of B lymphocytes by inhibiting the induction of FasL expression and activating the PI3K/Akt pathway (215) (Fig. 4 & 5). Another striking feature of K1 is the induced downregulation of surface B cell receptor by endoplasmic reticular sequestration (113). This may inhibit apoptosis as a consequence of BCR signaling. K1 signaling activity in B-cells has been linked to K1 internalization and since K1 also co-internalizes with BCR, it suggests a possible mechanism of BCR downregulation from the cell surface (214). In epithelial and endothelial cells, K1 expression induced the secretion of angiogenic factors, including vascular endothelial growth factor (VEGF) and matrix metalloproteinase-9 (227). K1 also activated the PI3K/Akt/mTOR pathway in endothelial cells (225) (Fig. 5). In endothelial cells, K1 has been shown to immortalize and extend the life span of primary human umbilical vein endothelial cells (HUVEC) in culture (225). K1 ITAM expression also activates both the VEGF/VEGFR-2 and the PI3K/Akt signaling pathways in HUVEC (225). In C33A epithelial cells, K1 expression also contributes to increased angiogenesis (225). Cumulatively, these data suggest a paracrine model in which K1-mediated secretion of cytokines is involved in the development of KSHV-associated diseases (227). Thus K1 appears to be important in KSHV-associated tumorigenesis and angiogenesis.

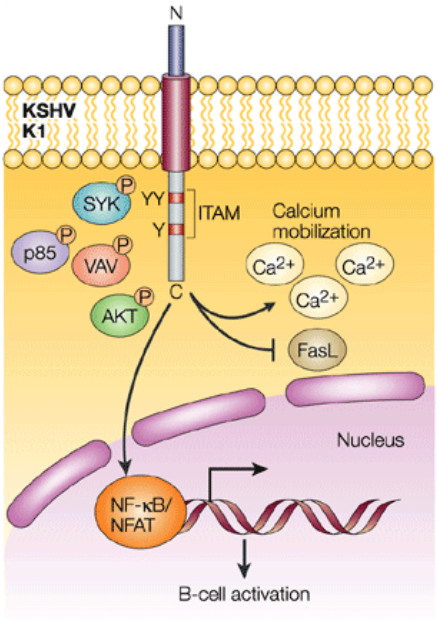

Figure. 4. KSHV K1 modulates cellular signaling events. K1 can mobilize calcium and activate SYK, VAV, p85 and AKT kinase leading to B-cell activation through the induction of the cellular transcription factors NFAT and NF-κB. K1 can also protect cells from Fas-induced apoptosis by preventing the induction of expression of the Fas ligand (Taken from Damania (43))

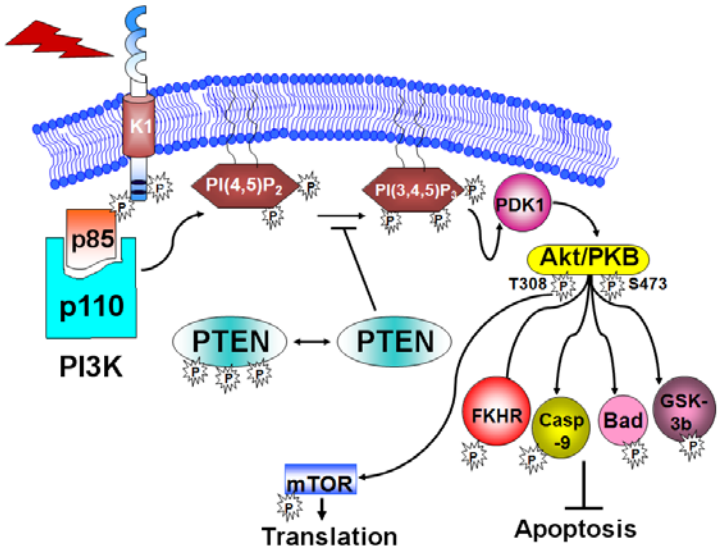

Figure. 5. K1 activates the PI3K/Akt/mTOR signaling pathway in endothelial and B cells.

vGPCR. Viral G-protein-coupled receptor is encoded by Orf74 of KSHV (7, 81). It is expressed early during the lytic cycle and is a viral homolog of the cellular angiogenic IL-8 receptor (34). vGPCR possesses seven transmembrane domains that are universally found in cellular GPCRs (34). The expression of vGPCR can be found in only a small fraction of KS, PEL, and MCD samples (199). This protein has potent oncogenic activities, as evidenced by its ability to transform and form foci in murine NIH3T3 cells as well as to produce tumors when injected into nude mice (9). Like K1, vGPCR can immortalize HUVEC and protect these cells from apoptosis induced by serum starvation (10, 141). A sub-set of vGPCR transgenic mice developed KS-like angioproliferative lesions with surface markers and cytokine profiles resembling those of KS (82, 140, 237). Similar to the situation in KSHV-associated malignancies, the expression of vGPCR was detected in only a small population of cells in the transgenic tumors and in a few other tissues, suggesting that vGPCR-mediated tumor formation is driven by spontaneous lytic reactivation in the background of latently infected cells. To support this argument, endothelial cells with vGPCR expression were demonstrated to cooperate with latent genes to mediate tumorigenesis (140). VEGF secretion, which was linked to angiogenesis (9, 10, 199), was increased in these vGPCR-induced tumors (82). Unlike its cellular homologs, vGPCR signaling is constitutive and independent of ligand binding (182). vGPCR can activate mitogen-activated protein kinases (MAPKs) (199), PLC (10), PI3K (10), and Akt (141) in endothelial cells. These data implicate that like KSHV K1, autocrine/paracrine signaling of vGPCR might contribute to KSHV-associated oncogenesis and angiogenesis. More recently, vGPCR has been shown to increase the expression and secretion of the pro-angiogenic molecule angiopoietin-2 in KSHV infected

lymphatic endothelial cells, the precursor cells of KS spindle cells (216). In PEL cells, vGPCR can activate ERK-2 and p38 pathways, induce the secretion of VEGF and vIL-6, as well as increase the transcription of Rta and Mta (29). Thus, besides its roles in transformation, vGPCR is also involved in promoting the KSHV lytic cycle.

vIL-6. Viral interleukin-6 (vIL-6) encoded by OrfK2 is a homolog of cellular IL-6 (24.6% amino acid sequence identity). Viral IL-6 expression can be detected in KS, PEL, MCD samples to different extents (MCD>PEL>>KS) (160, 203). Interestingly, IL-6 overexpression was suspected to be important in KS and MCD pathogenesis, prior to the identification of this viral homolog (137, 241). Similar to cellular IL-6, vIL-6 signaling triggers the JAK/STAT (Jansus tyrosine kinases signal transducers and activators of transcription) (139), MAPK, and H7-sensitive pathways (156). The JAK/STAT pathway induced by vIL-6 results in increased VEGF expression and signaling in an autocrine/paracrine fashion (124). Unlike its cellular IL-6 homolog, whose signaling depends upon both gp80 (IL-6Rα) and gp130, vIL-6 signaling can be achieved through gp130 alone in BAF cells (139). Therefore, vIL-6 seems to bypass the normal negative feedback loop on gp80. Because of this, vIL-6 signaling is able to evade the interferon response by blocking IFNα signaling induced by viral infection. This could promote cell cycle progression and the proliferation of the infected cells (38), setting the stage for further transformation and tumorigenesis events. Injection of NIH3T3 cells stably expressing vIL-6 into athymic mice resulted in tumor formation, hematopoiesis, and plasmacytosis compared to the control mice. The vIL-6-expressing tumors were also more vascularized, which correlated with an elevated level of VEGF secretion (5). Human PEL cell lines such as BC-1, BCP-1, and BCBL-1 were

also shown to produce elevated levels of VEGF as a result of vIL-6 signaling. When PEL cells were inoculated into nude mice, almost all of them developed PEL-like tumors; however, no tumor formation occurred when PEL-innoculated mice were treated with the neutralizing anti-human VEGF antibody (6), these data suggest that VEGF induction by vIL-6 may contribute to progression of KSHV-associated malignancies. As an alternative mechanism for Kaposi sarcomagenesis, vIL-6 can also induce the expression of angiopoietin-2 in lymphatic endothelial cells infected with KSHV (216).

vIRF-1. The viral interferon regulatory factor-1 is encoded by KSHV OrfK9 (117, 184). In contrast to the other three KSHV-encoded IRFs, the vIRF-1 transcript is unspliced. In PEL cells, the expression of vIRF-1 is low during latency but can be induced to high levels during lytic infection (168). The most apparent function of vIRF-1 is to suppress both type I and type II interferon responses (26, 73, 117). vIRF-1 can compete with cellular IRF3 to interact with the transcriptional coactivator CBP and p300. This interferes with the formation of the IRF3/CBP/p300 complexes (26, 120). In addition to suppressing the host anti-viral response, vIRF-1 can block apoptosis induced by tumor necrosis factor α (TNFα) and p53, respectively (26, 194). Viral IRF-1 can physically associate with p53 and repress its transactivation and apoptotic functions through inhibition of p53 phosphorylation and acetylation (145, 194). Viral IRF-1 is a potential oncogene, as NIH3T3 cells stably expressing vIRF-1 can grow under conditions of serum deprivation. These cells exhibit loss of contact inhibition in soft agar and can form tumors in nude mice (73). Transformation of vIRF-1 expressing NIH3T3 cells was found to be mediated by the induction of Myc proto-oncogene through vIRF-1 activation of the plasmacytoma repressor factor (PRF) element (91).

In addition to their transforming/oncogenic properties in overexpression systems (in isolation), most of the putative oncogenic KSHV gene products (e.g. LANA, vCyclin, vFLIP, vIL-6, Kaposin B, K1, vGPCR, vIRF-1) can be detected in KS, PEL, and MCD specimens, albeit with differential contribution (Table 2). This further corroborates their important roles in the initiation and/or maintenance of KSHV-associated malignancies. Very generally speaking, predominantly latent proteins are expressed in KS and PEL cells, but both latent and lytic proteins are expressed in MCD. Intriguingly, processivity factor-8 (PF-8)/Orf59 and vIRF-1 can be detected in PEL cell line but not in PEL primary tissues (98, 160). Furthermore, PEL cell lines require chemical induction to express vIL-6 while primary PEL tumor cells express vIL-6 without the dependence of lytic reactivation (97, 160, 203). However, a recent report by Chandriani and Ganem found using a very sensitive, limiting dilution-based assay that transcripts of vIL-6 and K1 were present at low levels in latently infected cells in some contexts (35). The discrepancies could also be due to the loss of tumor microenvironment in cell lines or adaptation of PEL cells during passages.

Although we have not described the functions of all the unique genes encoded by KSHV, a brief description of these genes is listed in Table 1.

Table 2. *In situ* detection of KSHV gene products in KS, PEL, and MCD

	KS	PEL	MCD
LANA	RNA & protein	RNA & protein	RNA & protein
vCyclin	RNA	RNA	RNA
vFLIP	RNA	RNA	RNA
Kaposin B	RNA	RNA & protein	?
vIRF-3/LANA-2	-	RNA & protein	RNA & protein*
vIL-6	RNA & protein	RNA & protein	RNA & protein*
K1	RNA & protein	RNA & protein	RNA & protein
vGPCR	RNA	RNA	RNA
Rta/Orf50	RNA	RNA	?
PF-8/Orf59	RNA & protein*	RNA & protein*	RNA & protein*
vIRF-1	RNA	RNA	RNA

Note: * represents a viral gene whose protein levels can be detected in only a small percentage of tumor cells.

Treatment of KS, PEL, and MCD

Treatment options for KS are based on disease severity, the KS subtype, and immune status. For relatively mild and limited KS, local treatment options such as topical alitretrinoin, surgical excision, radiation therapy, and intralesional chemotherapy (e.g. vinblastine) can be used to treat the symptoms. These local therapies do not prevent new KS lesions from developing. For more severe and aggressive KS, systemic chemotherapy with agents such as liposomal anthracyclines (doxorubicin and daunorubicin; first-line) and paclitaxel (second-line) is usually the mainstay of treatment. Other chemotherapeutics include vinorelbine, interferon-α, and interleukin-12. Although the approaches mentioned above have some beneficial effects to the patients, they are not very effective, as they do not target specifically the agent causing the tumor. The mTOR inhibitor, rapamycin (Sirolimus) was tested against

iatrogenic KS and was highly successful (201, 202). In AIDS-KS patients, HAART is recommended to reduce the extent and size of KS lesions. HAART might also reduce the incidence of new KS in HIV-positive individuals. These beneficial effects are likely due to immune reconstitution. In addition to HAART, the tyrosine kinase inhibitor imatinib, and IL-12 also demonstrate some activities against AIDS-KS (102, 123).

PEL patients have very poor prognosis and have a median survival of only two to three months after diagnosis. As in the case of KS, a patient co-infected with HIV is likely to benefit from HAART (152). Complete remission of PEL with HAART is seen occasionally (88, 152, 196). On the other hand, conventional CHOP-like regimens (cyclophosphamide, doxorubicin, vincristine, and prednisone) did not improve survival compared to other HIV-associated NHL (196). For HIV-negative cases of PEL, patients may be given liposomal anthracycline with or without bortezomib (proteasome inhibitor) and prednisone. Bortezomib was reported to be efficacious in treating PEL cell lines when it was used alone or in combination with doxorubicin and Taxol (4). Rapamycin has also shown promise in treating PEL cells in culture and in a xenograft model (197). Although radiation therapy is rarely performed to treat PEL, it may be an option for patients who do not tolerate the above treatment options.

Treatment options for MCD include surgical excision, cytoreduction chemotherapy (CHOP or CVAD), radiation therapy, immune modulators such as steroids and interferon-α, thalidomide, monoclonal antibodies against IL-6 (atlizumab) and CD20 surface marker (rituximab), and inhibitors of KSHV viral replication (reviewed in (31, 32)). The patient responses to these therapeutic options are mixed and therefore, the establishment of treatment regimens requires more epidemiological data. As a general rule of thumb, chemotherapy is

preferred for MCD with severe systemic symptoms; the viral replication inhibitors (especially ganciclovir), interferon-α, and anti-IL-6 and anti-CD20 monoclonal antibodies appear to be the more specific and promising candidates for treating MCD (31).

In conclusion, the current treatment strategies for KS, PEL, and MCD are still sub-optimal. While our understanding of KSHV biology and tumorigenesis has been increasing since the discovery of the virus, we are just beginning to translate knowledge from basic science research into more effective clinical management and therapies. We believe that the use of antiviral agents and small molecules that specifically target the signaling pathways of these tumor cells are potentially more efficacious and have fewer side effects than conventional chemotherapy regimens. More case reports and randomized clinical trials are needed to advance and standardize treatments for KSHV-associated malignancies.

Rhesus rhadinovirus as a model to study KSHV pathogenesis

A detailed understanding of KSHV replication and pathogenesis is important for understanding the biology of the diseases that are associated with this virus. However, *in vivo* studies of KSHV are limited due to the inability of KSHV to persistently infect mice or rhesus macaques (56, 178). Furthermore, difficulties are encountered when trying to study KSHV replication *in vitro* (177). Endothelial cells were previously proposed to study the *de novo* lytic replication and replication of KSHV because they were natural targets of *in vivo* KSHV infection. Nevertheless, cell lines derived from KS lesions rapidly lose the viral genome after serial passage *in vitro* (2, 3, 16, 204, 208). Although several groups have described the use of immortalized human umbilical vein endothelial cells (HUVEC) and microvascular endothelial cells (TIME) to investigate *de novo* KSHV replication (52, 105,

177, 187), the virus replicates lytically only for a limited number of rounds before entering latency in these cells. Hence viral titers of KSHV are quite low in endothelial cells and plaques are rarely observed. Another system to generate lytic virus involves the treatment of KSHV-infected PEL cell lines with chemicals (TPA or *n*-butyrate) (138, 180) or etopic expression of Orf50 (128). Here the problem is that only a small subset (25-30%) of latently infected PEL lymphocytes can be artificially reactivated with TPA (138, 180). Although without chemical induction, KSHV- positive PEL cell lines are mostly latent, about 2-5% of these cells still undergo spontaneous lytic reactivation (180). Thus, the heterogeneous nature of the lytically and latently infected cell populations hampers the dissection of the function of individual viral genes in the context of the whole virus.

We have used rhesus monkey rhadinovirus (RRV) to model KSHV pathogenesis in rhesus fibroblasts (RhF) (149). RRV was first identified by Desrosiers *et al*. in 1997 at the New England Primate Research Center (NEPRC) as a γ_2-herpesvirus of rhesus macaques (*Macaca mulatta*) (49). This isolate was designated H26-95. Additionally, Wong *et al*. at the Oregon Regional Primate Research Center isolated a different strain of RRV (designated 17577) from SIV-infected macaques (234). Sequence analysis revealed that the two RRV isolates are homologous to each other, though not identical (49, 234). Importantly, both genomes exhibit co-linearity with the KSHV genome (1, 193) and all RRV genes have homologs in KSHV (1, 193) (Fig. 6). Wong *et al*. showed that in SIV-infected macaques, RRV induced B-cell hyperplasia resembling KSHV MCD (234) as well as non-Hodgkin lymphoma (154, 155). Mansfield *et al*. reported that RRV also caused an arteriopathy in SIV-infected macaques (131).

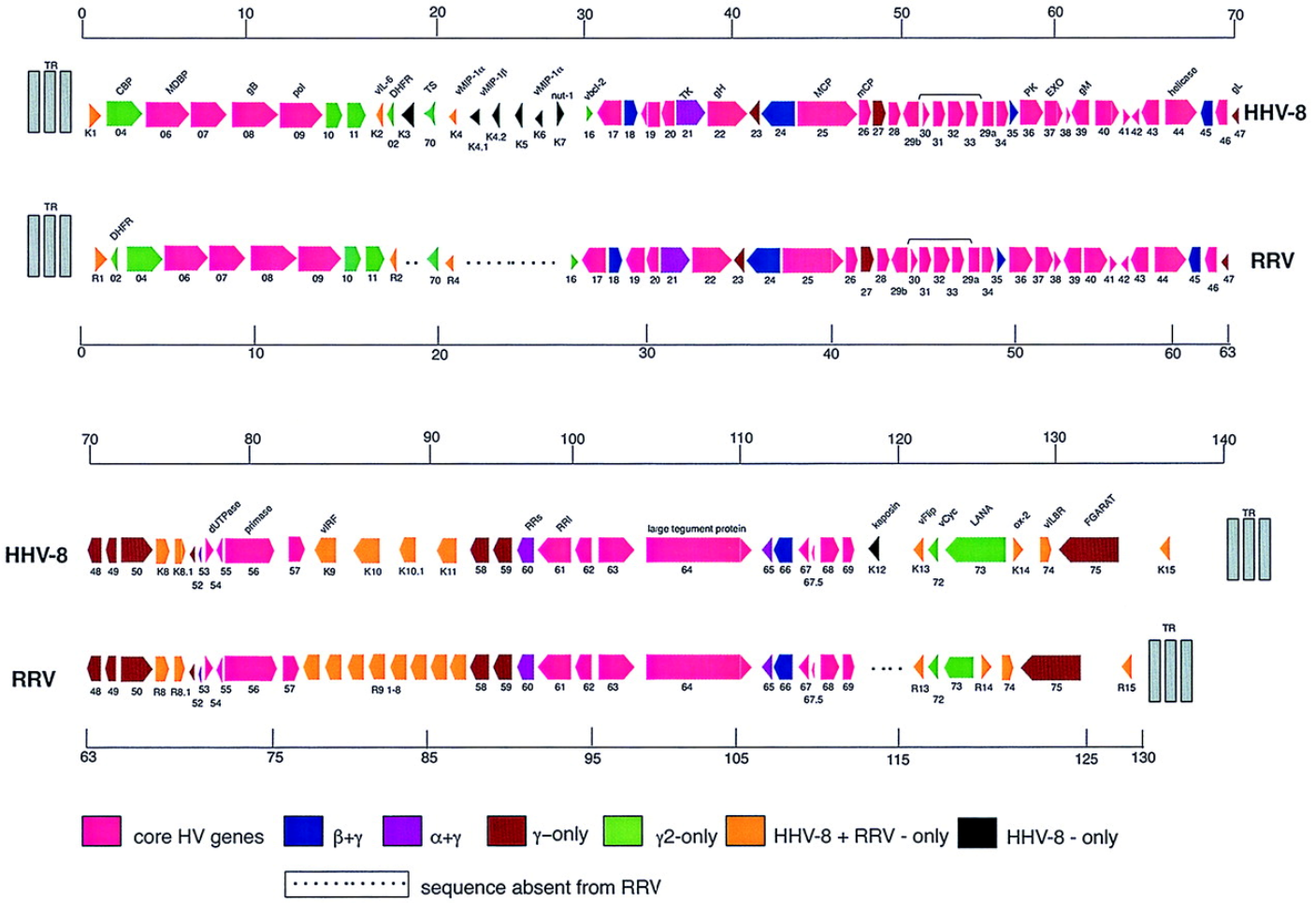

Figure 6. Alignment of KSHV and RRV H26-95 ORFs. ORFs in KSHV and RRV H26-95 that are conserved in the indicated herpesvirus subfamilies or subgroups are signified by the different colors. The square side of the symbol signifies the 5′ end, and the pointed side of the symbol signifies the 3′ end of the depicted ORFs. The ORFs are not drawn to scale (Taken from Alexander *et al.* 2000).

RRV presents several advantages for studying lytic replication. First, the RRV lifecycle can be modeled *in vivo*, in rhesus macaques. Second, rhesus fibroblasts (RhF) support one hundred percent lytic replication of RRV and allows for the production of high titers of virus (approximately 10^6 plaque forming units per ml) without the need to concentrate virus by ultra-centrifugation (148). Our group has demonstrated that the transcription program of RRV is similar to that of KSHV (50, 58). Several laboratories have used the RRV model to study viral gene products, including the viral interleukin-6 (vIL-6) homolog (94, 153), Rta/Orf50, R8/RAP, R8.1 (50, 122), R1 (44, 46), R15 (112, 170), RK15 (226), RRV Orf4 (132), glycoproteins (gB, gH, gL) (22, 111), RCP (151), and the RRV-encoded microRNAs (190, 222). We previously reported the kinetics of gene expression with regard to immediate-early, early, and late genes during RRV lytic infection and have reported they are similar to those seen during KSHV reactivation (50, 58). We also generated a RRV-GFP recombinant virus and devised plaque assays and quantitative real time QPCR assays for the determination of viral titers (51). In this dissertation, we generated and analyzed the replicative properties of recombinant viruses deleted for R1 (Chapter 3) and LANA (Chapter 4) in RRV, to gain insights into their roles in KSHV biology in the context of the whole virus.

Objectives

Expression of the K1 transcript and protein has been detected in KS, PEL, and MCD. The K1 protein has been shown to activate the PI3/Akt/mTOR signaling pathway in B lymphocytes and endothelial cells, inhibit apoptosis in B lymphocytes and epithelial cells, as well as to transform rodent fibrobloasts. This suggests that K1 plays an important role in KSHV infection and transformation. The goal of our study was to identify the cellular proteins that interact with K1 and study the mechanisms by which K1 activates signal

transduction pathways, inhibits apoptosis, and contributes to oncogenesis. Using RRV as a model, we also dissected the role of KSHV K1 in the viral lifecycle. RRV encodes a gene named R1, which is functionally homologous to the KSHV K1 gene. We constructed a RRVΔR1/GFPcc recombinant virus to analyze the contribution of R1 during *de novo* infection, latency, and reactivation of RRV.

The second objective of our study was to develop a novel vaccine for protection against rhadinovirus infection in primates using the RRV model system. The latency-associated nuclear antigen (LANA) is critical for the establishment and maintenance of both KSHV and RRV latency. We generated a recombinant virus deleted for RRV LANA, named RRVΔLANA/GFP, by a homologous recombination approach. We analyzed its biological properties *in vitro* with respect to viral latency and lytic replication.

The objectives of this dissertation are described in further detail below:

1) To identify the cellular binding partners of KSHV K1 and explore the consequences of the interactions of K1 and cellular proteins for K1 signaling and function.

Using tandem affinity purification, we identified the molecular chaperones, Hsp90 and ER-associated Hsp40/Erdj3, as the cellular interacting partners of K1. We showed that Hsp90 and Hsp40/Erdj3 modulated the protein expression and anti-apoptotic function of K1. We also showed that the interaction of K1 with Hsp90 and Hsp40/Erdj3 is relevant in KSHV-associated tumorigenesis by demonstrating co-localization of these proteins in a PEL cell line and their expression in mouse xenograft sections. This study has identified Hsp90 and Hsp40/Erdj3 as being essential for K1 expression and function. These cellular proteins may serve as targets for future therapies for KSHV-associated cancers. *This wok has been published in Oncogene in 2010*.

2) To elucidate the role of KSHV K1 in the viral lifecycle using RRV R1 as a model system.

RRV R1 is the homolog of KSHV K1 (45). Using a cosmid system for RRV (21), the R1 ORF, was disrupted by insertion of a GFP expression cassette. We analyzed the effects of R1 deletion on *de novo* lytic viral replication, reactivation, and the establishment and maintenance of viral latency. This work has led to a detailed understanding of the contribution of K1 to the KSHV lifecycle. *A manuscript has been submitted to the Journal of Virology.*

3) To develop a novel vaccine for protection against rhadinovirus infection.

The LANA proteins of both KSHV and RRV play key roles in the establishment and maintenance of these herpesviruses. We have constructed a RRVΔLANA/GFP in which the RRV LANA open reading frame has been disrupted with a GFP expression cassette generated by homologous recombination. The RRVΔLANA/GFP recombinant virus exhibited significantly elevated lytic replicative properties and failed to establish latency. We also observed significant differences in global viral gene expression between RRVΔLANA/GFP and the wild-type viruses. Several cellular genes that are known to be repressed by KSHV LANA were de-repressed during *de novo* lytic infection with the RRVΔLANA/GFP virus compared to RRV-GFP. *This work has been published in the Journal of Virology in 2009.*

A future goal is to evaluate the RRVΔLANA/GFP as a vaccine candidate in rhesus macaques in collaboration with Dr. Ronald Desrosiers at Harvard Medical School.

REFERENCES

1. **Alexander, L., L. Denekamp, A. Knapp, M. R. Auerbach, B. Damania, and R. C. Desrosiers.** 2000. The primary sequence of rhesus monkey rhadinovirus isolate 26-95: sequence similarities to Kaposi's sarcoma-associated herpesvirus and rhesus monkey rhadinovirus isolate 17577. J Virol **74:**3388-98.

2. **Aluigi, M. G., A. Albini, S. Carlone, L. Repetto, R. De Marchi, A. Icardi, M. Moro, D. Noonan, and R. Benelli.** 1996. KSHV sequences in biopsies and cultured spindle cells of epidemic, iatrogenic and Mediterranean forms of Kaposi's sarcoma. Res Virol **147:**267-75.

3. **Ambroziak, J. A., D. J. Blackbourn, B. G. Herndier, R. G. Glogau, J. H. Gullett, A. R. McDonald, E. T. Lennette, and J. A. Levy.** 1995. Herpes-like sequences in HIV-infected and uninfected Kaposi's sarcoma patients. Science **268:**582-3.

4. **An, J., Y. Sun, M. Fisher, and M. B. Rettig.** 2004. Antitumor effects of bortezomib (PS-341) on primary effusion lymphomas. Leukemia **18:**1699-704.

5. **Aoki, Y., E. S. Jaffe, Y. Chang, K. Jones, J. Teruya-Feldstein, P. S. Moore, and G. Tosato.** 1999. Angiogenesis and hematopoiesis induced by Kaposi's sarcoma-associated herpesvirus-encoded interleukin-6. Blood **93:**4034-43.

6. **Aoki, Y., and G. Tosato.** 1999. Role of vascular endothelial growth factor/vascular permeability factor in the pathogenesis of Kaposi's sarcoma-associated herpesvirus-infected primary effusion lymphomas. Blood **94:**4247-54.

7. **Arvanitakis, L., E. Geras-Raaka, A. Varma, M. C. Gershengorn, and E. Cesarman.** 1997. Human herpesvirus KSHV encodes a constitutively active G-protein-coupled receptor linked to cell proliferation. Nature **385:**347-50.

8. **Arvanitakis, L., E. A. Mesri, R. G. Nador, J. W. Said, A. S. Asch, D. M. Knowles, and E. Cesarman.** 1996. Establishment and characterization of a primary effusion (body cavity-based) lymphoma cell line (BC-3) harboring kaposi's sarcoma-associated herpesvirus (KSHV/HHV-8) in the absence of Epstein-Barr virus. Blood **88:**2648-54.

9. **Bais, C., B. Santomasso, O. Coso, L. Arvanitakis, E. G. Raaka, J. S. Gutkind, A. S. Asch, E. Cesarman, M. C. Gershengorn, and E. A. Mesri.** 1998. G-protein-coupled receptor of Kaposi's sarcoma-associated herpesvirus is a viral oncogene and angiogenesis activator. Nature **391:**86-9.

10. **Bais, C., A. Van Geelen, P. Eroles, A. Mutlu, C. Chiozzini, S. Dias, R. L. Silverstein, S. Rafii, and E. A. Mesri.** 2003. Kaposi's sarcoma associated herpesvirus G protein-coupled receptor immortalizes human endothelial cells by activation of the VEGF receptor-2/ KDR. Cancer Cell **3:**131-43.

11. **Ballestas, M. E., P. A. Chatis, and K. M. Kaye.** 1999. Efficient persistence of extrachromosomal KSHV DNA mediated by latency-associated nuclear antigen. Science **284:**641-4.

12. **Barozzi, P., M. Luppi, F. Facchetti, C. Mecucci, M. Alu, R. Sarid, V. Rasini, L. Ravazzini, E. Rossi, S. Festa, B. Crescenzi, D. G. Wolf, T. F. Schulz, and G. Torelli.** 2003. Post-transplant Kaposi sarcoma originates from the seeding of donor-derived progenitors. Nat Med **9:**554-61.

13. **Bechtel, J. T., R. C. Winant, and D. Ganem.** 2005. Host and viral proteins in the virion of Kaposi's sarcoma-associated herpesvirus. J Virol **79:**4952-64.

14. **Beckstead, J. H., G. S. Wood, and V. Fletcher.** 1985. Evidence for the origin of Kaposi's sarcoma from lymphatic endothelium. Am J Pathol **119:**294-300.

15. **Belanger, C., A. Gravel, A. Tomoiu, M. E. Janelle, J. Gosselin, M. J. Tremblay, and L. Flamand.** 2001. Human herpesvirus 8 viral FLICE-inhibitory protein inhibits Fas-mediated apoptosis through binding and prevention of procaspase-8 maturation. J Hum Virol **4:**62-73.

16. **Benelli, R., A. Albini, C. Parravicini, S. Carlone, L. Repetto, G. Tambussi, and A. Lazzarin.** 1996. Isolation of spindle-shaped cell populations from primary cultures of Kaposi's sarcoma of different stage. Cancer Lett **100:**125-32.

17. **Beral, V., and R. Newton.** 1998. Overview of the epidemiology of immunodeficiency-associated cancers. J Natl Cancer Inst Monogr**:**1-6.

18. **Beral, V., T. A. Peterman, R. L. Berkelman, and H. W. Jaffe.** 1990. Kaposi's sarcoma among persons with AIDS: a sexually transmitted infection? Lancet **335:**123-8.

19. **Bieleski, L., and S. J. Talbot.** 2001. Kaposi's sarcoma-associated herpesvirus vCyclin open reading frame contains an internal ribosome entry site. J Virol **75:**1864-9.

20. **Biggar, R. J., and C. S. Rabkin.** 1996. The epidemiology of AIDS--related neoplasms. Hematol Oncol Clin North Am **10:**997-1010.

21. **Bilello, J. P., J. S. Morgan, B. Damania, S. M. Lang, and R. C. Desrosiers.** 2006. A genetic system for rhesus monkey rhadinovirus: use of recombinant virus to quantitate antibody-mediated neutralization. J Virol **80:**1549-62.

22. **Bilello, J. P., J. S. Morgan, and R. C. Desrosiers.** 2008. Extreme dependence of gH and gL expression on ORF57 and association with highly unusual codon usage in rhesus monkey rhadinovirus. J Virol **82:**7231-7.

23. **Boshoff, C.** 2003. Kaposi virus scores cancer coup. Nat Med **9:**261-2.

24. **Bowser, B. S., S. M. DeWire, and B. Damania.** 2002. Transcriptional regulation of the K1 gene product of Kaposi's sarcoma-associated herpesvirus. J Virol **76:**12574-83.

25. **Bubman, D., I. Guasparri, and E. Cesarman.** 2007. Deregulation of c-Myc in primary effusion lymphoma by Kaposi's sarcoma herpesvirus latency-associated nuclear antigen. Oncogene **26:**4979-86.

26. **Burysek, L., W. S. Yeow, B. Lubyova, M. Kellum, S. L. Schafer, Y. Q. Huang, and P. M. Pitha.** 1999. Functional analysis of human herpesvirus 8-encoded viral interferon regulatory factor 1 and its association with cellular interferon regulatory factors and p300. J Virol **73:**7334-42.

27. **Cai, X., and B. R. Cullen.** 2006. Transcriptional origin of Kaposi's sarcoma-associated herpesvirus microRNAs. J Virol **80:**2234-42.

28. **Cai, X., S. Lu, Z. Zhang, C. M. Gonzalez, B. Damania, and B. R. Cullen.** 2005. Kaposi's sarcoma-associated herpesvirus expresses an array of viral microRNAs in latently infected cells. Proc Natl Acad Sci U S A **102:**5570-5.

29. **Cannon, M., N. J. Philpott, and E. Cesarman.** 2003. The Kaposi's sarcoma-associated herpesvirus G protein-coupled receptor has broad signaling effects in primary effusion lymphoma cells. J Virol **77:**57-67.

30. **Carbone, A., A. Gloghini, E. Vaccher, M. Cerri, G. Gaidano, R. Dalla-Favera, and U. Tirelli.** 2005. Kaposi's sarcoma-associated herpesvirus/human herpesvirus type 8-positive solid lymphomas: a tissue-based variant of primary effusion lymphoma. J Mol Diagn **7:**17-27.

31. **Casper, C.** 2005. The aetiology and management of Castleman disease at 50 years: translating pathophysiology to patient care. Br J Haematol **129:**3-17.

32. **Casper, C., and A. Wald.** 2007. The use of antiviral drugs in the prevention and treatment of Kaposi sarcoma, multicentric Castleman disease and primary effusion lymphoma. Curr Top Microbiol Immunol **312:**289-307.

33. **Cesarman, E., Y. Chang, P. S. Moore, J. W. Said, and D. M. Knowles.** 1995. Kaposi's sarcoma-associated herpesvirus-like DNA sequences in AIDS-related body-cavity-based lymphomas. N Engl J Med **332:**1186-91.

34. **Cesarman, E., R. G. Nador, F. Bai, R. A. Bohenzky, J. J. Russo, P. S. Moore, Y. Chang, and D. M. Knowles.** 1996. Kaposi's sarcoma-associated herpesvirus contains G protein-coupled receptor and cyclin D homologs which are expressed in Kaposi's sarcoma and malignant lymphoma. J Virol **70:**8218-23.

35. **Chandriani, S., and D. Ganem.** Array-based transcript profiling and limiting-dilution RT-PCR analysis identify additional latent genes in KSHV. J Virol.

36. **Chang, Y., E. Cesarman, M. S. Pessin, F. Lee, J. Culpepper, D. M. Knowles, and P. S. Moore.** 1994. Identification of herpesvirus-like DNA sequences in AIDS-associated Kaposi's sarcoma. Science **266:**1865-9.

37. **Chang, Y., P. S. Moore, S. J. Talbot, C. H. Boshoff, T. Zarkowska, K. Godden, H. Paterson, R. A. Weiss, and S. Mittnacht.** 1996. Cyclin encoded by KS herpesvirus. Nature **382:**410.

38. **Chatterjee, M., J. Osborne, G. Bestetti, Y. Chang, and P. S. Moore.** 2002. Viral IL-6-induced cell proliferation and immune evasion of interferon activity. Science **298:**1432-5.

39. **Chaudhary, P. M., A. Jasmin, M. T. Eby, and L. Hood.** 1999. Modulation of the NF-kappa B pathway by virally encoded death effector domains-containing proteins. Oncogene **18:**5738-46.

40. **Chen, J., K. Ueda, S. Sakakibara, T. Okuno, and K. Yamanishi.** 2000. Transcriptional regulation of the Kaposi's sarcoma-associated herpesvirus viral interferon regulatory factor gene. J Virol **74:**8623-34.

41. **Conrad, N. K., V. Fok, D. Cazalla, S. Borah, and J. A. Steitz.** 2006. The challenge of viral snRNPs. Cold Spring Harb Symp Quant Biol **71:**377-84.

42. **Conrad, N. K., and J. A. Steitz.** 2005. A Kaposi's sarcoma virus RNA element that increases the nuclear abundance of intronless transcripts. Embo J **24:**1831-41.

43. **Damania, B.** 2004. Oncogenic gamma-herpesviruses: comparison of viral proteins involved in tumorigenesis. Nat Rev Microbiol **2:**656-68.

44. **Damania, B., M. DeMaria, J. U. Jung, and R. C. Desrosiers.** 2000. Activation of lymphocyte signaling by the R1 protein of rhesus monkey rhadinovirus. J Virol **74:**2721-30.

45. **Damania, B., and J. U. Jung.** 2001. Comparative analysis of the transforming mechanisms of Epstein-Barr virus, Kaposi's sarcoma-associated herpesvirus, and Herpesvirus saimiri. Adv Cancer Res **80:**51-82.

46. **Damania, B., M. Li, J. K. Choi, L. Alexander, J. U. Jung, and R. C. Desrosiers.** 1999. Identification of the R1 oncogene and its protein product from the rhadinovirus of rhesus monkeys. J Virol **73:**5123-31.

47. **Deacon, E. M., G. Pallesen, G. Niedobitek, J. Crocker, L. Brooks, A. B. Rickinson, and L. S. Young.** 1993. Epstein-Barr virus and Hodgkin's disease: transcriptional analysis of virus latency in the malignant cells. J Exp Med **177:**339-49.

48. **Denis, G. V., C. Vaziri, N. Guo, and D. V. Faller.** 2000. RING3 kinase transactivates promoters of cell cycle regulatory genes through E2F. Cell Growth Differ **11:**417-24.

49. **Desrosiers, R. C., V. G. Sasseville, S. C. Czajak, X. Zhang, K. G. Mansfield, A. Kaur, R. P. Johnson, A. A. Lackner, and J. U. Jung.** 1997. A herpesvirus of rhesus monkeys related to the human Kaposi's sarcoma-associated herpesvirus. J Virol **71:**9764-9.

50. **DeWire, S. M., M. A. McVoy, and B. Damania.** 2002. Kinetics of expression of rhesus monkey rhadinovirus (RRV) and identification and characterization of a polycistronic transcript encoding the RRV Orf50/Rta, RRV R8, and R8.1 genes. J Virol **76:**9819-31.

51. **DeWire, S. M., E. S. Money, S. P. Krall, and B. Damania.** 2003. Rhesus monkey rhadinovirus (RRV): construction of a RRV-GFP recombinant virus and development of assays to assess viral replication. Virology **312:**122-34.

52. **Dezube, B. J., M. Zambela, D. R. Sage, J. F. Wang, and J. D. Fingeroth.** 2002. Characterization of Kaposi sarcoma-associated herpesvirus/human herpesvirus-8 infection of human vascular endothelial cells: early events. Blood **100:**888-96.

53. **Dillon, P. J., and B. Damania.** 2009. Human Kaposi's Sarcoma-associated Herpesvirus: Molecular Biology and Oncogenesis. *In* J.-H. J. Ou and T. S. B. Yen (ed.), Human Oncogenic Viruses. World Scientific Publishing Co.

54. **Dittmer, D.** 2008. KSHV viral latent lifecycle. *In* B. Damania and J. Pipas (ed.), DNA Tumor Viruses. Springer.

55. **Dittmer, D., M. Lagunoff, R. Renne, K. Staskus, A. Haase, and D. Ganem.** 1998. A cluster of latently expressed genes in Kaposi's sarcoma-associated herpesvirus. J Virol **72:**8309-15.

56. **Dittmer, D., C. Stoddart, R. Renne, V. Linquist-Stepps, M. E. Moreno, C. Bare, J. M. McCune, and D. Ganem.** 1999. Experimental transmission of Kaposi's sarcoma-associated herpesvirus (KSHV/HHV-8) to SCID-hu Thy/Liv mice. J Exp Med **190:**1857-68.

57. **Dittmer, D. P.** 2003. Transcription profile of Kaposi's sarcoma-associated herpesvirus in primary Kaposi's sarcoma lesions as determined by real-time PCR arrays. Cancer Res **63:**2010-5.

58. **Dittmer, D. P., C. M. Gonzalez, W. Vahrson, S. M. DeWire, R. Hines-Boykin, and B. Damania.** 2005. Whole-genome transcription profiling of rhesus monkey rhadinovirus. J Virol **79:**8637-50.

59. **Djerbi, M., V. Screpanti, A. I. Catrina, B. Bogen, P. Biberfeld, and A. Grandien.** 1999. The inhibitor of death receptor signaling, FLICE-inhibitory protein defines a new class of tumor progression factors. J Exp Med **190:**1025-32.

60. **Dupin, N., C. Fisher, P. Kellam, S. Ariad, M. Tulliez, N. Franck, E. van Marck, D. Salmon, I. Gorin, J. P. Escande, R. A. Weiss, K. Alitalo, and C. Boshoff.** 1999. Distribution of human herpesvirus-8 latently infected cells in Kaposi's sarcoma, multicentric Castleman's disease, and primary effusion lymphoma. Proc Natl Acad Sci U S A **96:**4546-51.

61. **Duprez, R., V. Lacoste, J. Briere, P. Couppie, C. Frances, D. Sainte-Marie, E. Kassa-Kelembho, M. J. Lando, J. L. Essame Oyono, B. Nkegoum, O. Hbid, A. Mahe, C. Lebbe, P. Tortevoye, M. Huerre, and A. Gessain.** 2007. Evidence for a multiclonal origin of multicentric advanced lesions of Kaposi sarcoma. J Natl Cancer Inst **99:**1086-94.

62. **Dutz, W., and A. P. Stout.** 1960. Kaposi's sarcoma in infants and children. Cancer **13:**684-94.

63. **Echimane, A. K., A. A. Ahnoux, I. Adoubi, S. Hien, K. M'Bra, A. D'Horpock, M. Diomande, D. Anongba, I. Mensah-Adoh, and D. M. Parkin.** 2000. Cancer incidence in Abidjan, Ivory Coast: first results from the cancer registry, 1995-1997. Cancer **89:**653-63.

64. **Efklidou, S., R. Bailey, N. Field, M. Noursadeghi, and M. K. Collins.** 2008. vFLIP from KSHV inhibits anoikis of primary endothelial cells. J Cell Sci **121:**450-7.

65. **Eltom, M. A., A. Jemal, S. M. Mbulaiteye, S. S. Devesa, and R. J. Biggar.** 2002. Trends in Kaposi's sarcoma and non-Hodgkin's lymphoma incidence in the United States from 1973 through 1998. J Natl Cancer Inst **94:**1204-10.

66. **Fakhari, F. D., and D. P. Dittmer.** 2002. Charting latency transcripts in Kaposi's sarcoma-associated herpesvirus by whole-genome real-time quantitative PCR. J Virol **76:**6213-23.

67. **Fakhari, F. D., J. H. Jeong, Y. Kanan, and D. P. Dittmer.** 2006. The latency-associated nuclear antigen of Kaposi sarcoma-associated herpesvirus induces B cell hyperplasia and lymphoma. J Clin Invest **116:**735-42.

68. **Field, N., W. Low, M. Daniels, S. Howell, L. Daviet, C. Boshoff, and M. Collins.** 2003. KSHV vFLIP binds to IKK-gamma to activate IKK. J Cell Sci **116:**3721-8.

69. **Flore, O., S. Rafii, S. Ely, J. J. O'Leary, E. M. Hyjek, and E. Cesarman.** 1998. Transformation of primary human endothelial cells by Kaposi's sarcoma-associated herpesvirus. Nature **394:**588-92.

70. **Friborg, J., Jr., W. Kong, M. O. Hottiger, and G. J. Nabel.** 1999. p53 inhibition by the LANA protein of KSHV protects against cell death. Nature **402:**889-94.

71. **Friedman-Birnbaum, R., S. Weltfriend, and I. Katz.** 1990. Kaposi's sarcoma: retrospective study of 67 cases with the classical form. Dermatologica **180:**13-7.

72. **Fujimuro, M., and S. D. Hayward.** 2003. The latency-associated nuclear antigen of Kaposi's sarcoma-associated herpesvirus manipulates the activity of glycogen synthase kinase-3beta. J Virol **77:**8019-30.

73. **Gao, S. J., C. Boshoff, S. Jayachandra, R. A. Weiss, Y. Chang, and P. S. Moore.** 1997. KSHV ORF K9 (vIRF) is an oncogene which inhibits the interferon signaling pathway. Oncogene **15:**1979-85.

74. **Gessain, A., and R. Duprez.** 2005. Spindle cells and their role in Kaposi's sarcoma. Int J Biochem Cell Biol **37:**2457-65.

75. **Gessain, A., A. Sudaka, J. Briere, N. Fouchard, M. A. Nicola, B. Rio, M. Arborio, X. Troussard, J. Audouin, J. Diebold, and G. de The.** 1996. Kaposi sarcoma-associated

herpes-like virus (human herpesvirus type 8) DNA sequences in multicentric Castleman's disease: is there any relevant association in non-human immunodeficiency virus-infected patients? Blood **87:**414-6.

76. **Godden-Kent, D., S. J. Talbot, C. Boshoff, Y. Chang, P. Moore, R. A. Weiss, and S. Mittnacht.** 1997. The cyclin encoded by Kaposi's sarcoma-associated herpesvirus stimulates cdk6 to phosphorylate the retinoblastoma protein and histone H1. J Virol **71:**4193-8.

77. **Gottwein, E., N. Mukherjee, C. Sachse, C. Frenzel, W. H. Majoros, J. T. Chi, R. Braich, M. Manoharan, J. Soutschek, U. Ohler, and B. R. Cullen.** 2007. A viral microRNA functions as an orthologue of cellular miR-155. Nature **450:**1096-9.

78. **Gradoville, L., J. Gerlach, E. Grogan, D. Shedd, S. Nikiforow, C. Metroka, and G. Miller.** 2000. Kaposi's sarcoma-associated herpesvirus open reading frame 50/Rta protein activates the entire viral lytic cycle in the HH-B2 primary effusion lymphoma cell line. J Virol **74:**6207-12.

79. **Grundhoff, A., and D. Ganem.** 2003. The latency-associated nuclear antigen of Kaposi's sarcoma-associated herpesvirus permits replication of terminal repeat-containing plasmids. J Virol **77:**2779-83.

80. **Grundhoff, A., and D. Ganem.** 2001. Mechanisms governing expression of the v-FLIP gene of Kaposi's sarcoma-associated herpesvirus. J Virol **75:**1857-63.

81. **Guo, H. G., P. Browning, J. Nicholas, G. S. Hayward, E. Tschachler, Y. W. Jiang, M. Sadowska, M. Raffeld, S. Colombini, R. C. Gallo, and M. S. Reitz, Jr.** 1997. Characterization of a chemokine receptor-related gene in human herpesvirus 8 and its expression in Kaposi's sarcoma. Virology **228:**371-8.

82. **Guo, H. G., M. Sadowska, W. Reid, E. Tschachler, G. Hayward, and M. Reitz.** 2003. Kaposi's sarcoma-like tumors in a human herpesvirus 8 ORF74 transgenic mouse. J Virol **77:**2631-9.

83. **Guo, N., D. V. Faller, and G. V. Denis.** 2000. Activation-induced nuclear translocation of RING3. J Cell Sci **113 (Pt 17):**3085-91.

84. **Gwack, Y., H. Byun, S. Hwang, C. Lim, and J. Choe.** 2001. CREB-binding protein and histone deacetylase regulate the transcriptional activity of Kaposi's sarcoma-associated herpesvirus open reading frame 50. J Virol **75:**1909-17.

85. **Gwack, Y., H. Nakamura, S. H. Lee, J. Souvlis, J. T. Yustein, S. Gygi, H. J. Kung, and J. U. Jung.** 2003. Poly(ADP-ribose) polymerase 1 and Ste20-like kinase hKFC act as transcriptional repressors for gamma-2 herpesvirus lytic replication. Mol Cell Biol **23:**8282-94.

86. **Hall, P. A., M. Donaghy, F. E. Cotter, A. G. Stansfeld, and D. A. Levison.** 1989. An immunohistological and genotypic study of the plasma cell form of Castleman's disease. Histopathology **14:**333-46; discussion 429-32.

87. **Hayward, G. S.** 1999. KSHV strains: the origins and global spread of the virus. Semin Cancer Biol **9:**187-99.

88. **Hocqueloux, L., F. Agbalika, E. Oksenhendler, and J. M. Molina.** 2001. Long-term remission of an AIDS-related primary effusion lymphoma with antiviral therapy. Aids **15:**280-2.

89. **Iscovich, J., P. Boffetta, and P. Brennan.** 1999. Classic Kaposi's sarcoma as a first primary neoplasm. Int J Cancer **80:**173-7.

90. **Izumiya, Y., T. J. Ellison, E. T. Yeh, J. U. Jung, P. A. Luciw, and H. J. Kung.** 2005. Kaposi's sarcoma-associated herpesvirus K-bZIP represses gene transcription via SUMO modification. J Virol **79:**9912-25.

91. **Jayachandra, S., K. G. Low, A. E. Thlick, J. Yu, P. D. Ling, Y. Chang, and P. S. Moore.** 1999. Three unrelated viral transforming proteins (vIRF, EBNA2, and E1A) induce the MYC oncogene through the interferon-responsive PRF element by using different transcription coadaptors. Proc Natl Acad Sci U S A **96:**11566-71.

92. **Jenner, R. G., M. M. Alba, C. Boshoff, and P. Kellam.** 2001. Kaposi's sarcoma-associated herpesvirus latent and lytic gene expression as revealed by DNA arrays. J Virol **75:**891-902.

93. **Jeong, J., J. Papin, and D. Dittmer.** 2001. Differential regulation of the overlapping Kaposi's sarcoma-associated herpesvirus vGCR (orf74) and LANA (orf73) promoters. J Virol **75:**1798-807.

94. **Kaleeba, J. A., E. P. Bergquam, and S. W. Wong.** 1999. A rhesus macaque rhadinovirus related to Kaposi's sarcoma-associated herpesvirus/human herpesvirus 8 encodes a functional homologue of interleukin-6. J Virol **73:**6177-81.

95. **Kaposi, M.** 1872. Idiopathisches multiples Pigmentsarkom der Haut Arch Dermatol Syph **4:**265-273.

96. **Kasolo, F. C., M. Monze, N. Obel, R. A. Anderson, C. French, and U. A. Gompels.** 1998. Sequence analyses of human herpesvirus-8 strains from both African human immunodeficiency virus-negative and -positive childhood endemic Kaposi's sarcoma show a close relationship with strains identified in febrile children and high variation in the K1 glycoprotein. J Gen Virol **79 (Pt 12):**3055-65.

97. **Katano, H., and T. Sata.** 2000. Human herpesvirus 8 virology, epidemiology and related diseases. Jpn J Infect Dis **53:**137-55.

98. **Katano, H., Y. Sato, T. Kurata, S. Mori, and T. Sata.** 2000. Expression and localization of human herpesvirus 8-encoded proteins in primary effusion lymphoma, Kaposi's sarcoma, and multicentric Castleman's disease. Virology **269:**335-44.

99. **Kieff, E., and A. B. Rickinson.** 2001. Epstein-Barr virus and its replication, p. 2511-2573. *In* D. M. Knipe (ed.), Fields virology, 4th ed, vol. 2. Lippincott Williams & Wilkins, Philadelphia, PA.

100. **Kliche, S., W. Nagel, E. Kremmer, C. Atzler, A. Ege, T. Knorr, U. Koszinowski, W. Kolanus, and J. Haas.** 2001. Signaling by human herpesvirus 8 kaposin A through direct membrane recruitment of cytohesin-1. Mol Cell **7:**833-43.

101. **Komanduri, K. V., J. A. Luce, M. S. McGrath, B. G. Herndier, and V. L. Ng.** 1996. The natural history and molecular heterogeneity of HIV-associated primary malignant lymphomatous effusions. J Acquir Immune Defic Syndr Hum Retrovirol **13:**215-26.

102. **Koon, H. B., G. J. Bubley, L. Pantanowitz, D. Masiello, B. Smith, K. Crosby, J. Proper, W. Weeden, T. E. Miller, P. Chatis, M. J. Egorin, S. R. Tahan, and B. J. Dezube.** 2005. Imatinib-induced regression of AIDS-related Kaposi's sarcoma. J Clin Oncol **23:**982-9.

103. **Krithivas, A., D. B. Young, G. Liao, D. Greene, and S. D. Hayward.** 2000. Human herpesvirus 8 LANA interacts with proteins of the mSin3 corepressor complex and negatively regulates Epstein-Barr virus gene expression in dually infected PEL cells. J Virol **74:**9637-45.

104. **Kyalwazi, S. K.** 1981. Kaposi's sarcoma: clinical features, experience in Uganda. Antibiot Chemother **29:**59-69.

105. **Lagunoff, M., J. Bechtel, E. Venetsanakos, A. M. Roy, N. Abbey, B. Herndier, M. McMahon, and D. Ganem.** 2002. De novo infection and serial transmission of Kaposi's sarcoma-associated herpesvirus in cultured endothelial cells. J Virol **76:**2440-8.

106. **Lagunoff, M., and D. Ganem.** 1997. The structure and coding organization of the genomic termini of Kaposi's sarcoma-associated herpesvirus. Virology **236:**147-54.

107. **Lagunoff, M., R. Majeti, A. Weiss, and D. Ganem.** 1999. Deregulated signal transduction by the K1 gene product of Kaposi's sarcoma-associated herpesvirus. Proc Natl Acad Sci U S A **96:**5704-9.

108. **Lan, K., D. A. Kuppers, and E. S. Robertson.** 2005. Kaposi's sarcoma-associated herpesvirus reactivation is regulated by interaction of latency-associated nuclear antigen with recombination signal sequence-binding protein Jkappa, the major downstream effector of the Notch signaling pathway. J Virol **79:**3468-78.

109. **Lan, K., D. A. Kuppers, S. C. Verma, and E. S. Robertson.** 2004. Kaposi's sarcoma-associated herpesvirus-encoded latency-associated nuclear antigen inhibits lytic replication by targeting Rta: a potential mechanism for virus-mediated control of latency. J Virol **78:**6585-94.

110. **Lan, K., D. A. Kuppers, S. C. Verma, N. Sharma, M. Murakami, and E. S. Robertson.** 2005. Induction of Kaposi's sarcoma-associated herpesvirus latency-associated nuclear antigen by the lytic transactivator RTA: a novel mechanism for establishment of latency. J Virol **79:**7453-65.

111. **Lang, S. M., and R. E. Means.** Characterization of cytoplasmic motifs important in rhesus rhadinovirus gB processing and trafficking. Virology **398:**233-42.

112. **Langlais, C. L., J. M. Jones, R. D. Estep, and S. W. Wong.** 2006. Rhesus rhadinovirus R15 encodes a functional homologue of human CD200. J Virol **80:**3098-103.

113. **Lee, B. S., X. Alvarez, S. Ishido, A. A. Lackner, and J. U. Jung.** 2000. Inhibition of intracellular transport of B cell antigen receptor complexes by Kaposi's sarcoma-associated herpesvirus K1. J Exp Med **192:**11-21.

114. **Lee, B. S., M. Connole, Z. Tang, N. L. Harris, and J. U. Jung.** 2003. Structural analysis of the Kaposi's sarcoma-associated herpesvirus K1 protein. J Virol **77:**8072-86.

115. **Lee, H., J. Guo, M. Li, J. K. Choi, M. DeMaria, M. Rosenzweig, and J. U. Jung.** 1998. Identification of an immunoreceptor tyrosine-based activation motif of K1 transforming protein of Kaposi's sarcoma-associated herpesvirus. Mol Cell Biol **18:**5219-28.

116. **Lee, H., R. Veazey, K. Williams, M. Li, J. Guo, F. Neipel, B. Fleckenstein, A. Lackner, R. C. Desrosiers, and J. U. Jung.** 1998. Deregulation of cell growth by the K1 gene of Kaposi's sarcoma-associated herpesvirus. Nat Med **4:**435-40.

117. **Li, M., H. Lee, J. Guo, F. Neipel, B. Fleckenstein, K. Ozato, and J. U. Jung.** 1998. Kaposi's sarcoma-associated herpesvirus viral interferon regulatory factor. J Virol **72:**5433-40.

118. **Liang, Y., and D. Ganem.** 2004. RBP-J (CSL) is essential for activation of the K14/vGPCR promoter of Kaposi's sarcoma-associated herpesvirus by the lytic switch protein RTA. J Virol **78:**6818-26.

119. **Lim, C., H. Sohn, Y. Gwack, and J. Choe.** 2000. Latency-associated nuclear antigen of Kaposi's sarcoma-associated herpesvirus (human herpesvirus-8) binds ATF4/CREB2 and inhibits its transcriptional activation activity. J Gen Virol **81:**2645-52.

120. **Lin, R., P. Genin, Y. Mamane, M. Sgarbanti, A. Battistini, W. J. Harrington, Jr., G. N. Barber, and J. Hiscott.** 2001. HHV-8 encoded vIRF-1 represses the interferon antiviral response by blocking IRF-3 recruitment of the CBP/p300 coactivators. Oncogene **20:**800-11.

121. **Lin, S. F., D. R. Robinson, G. Miller, and H. J. Kung.** 1999. Kaposi's sarcoma-associated herpesvirus encodes a bZIP protein with homology to BZLF1 of Epstein-Barr virus. J Virol **73:**1909-17.

122. **Lin, S. F., D. R. Robinson, J. Oh, J. U. Jung, P. A. Luciw, and H. J. Kung.** 2002. Identification of the bZIP and Rta homologues in the genome of rhesus monkey rhadinovirus. Virology **298:**181-8.

123. **Little, R. F., K. Aleman, P. Kumar, K. M. Wyvill, J. M. Pluda, E. Read-Connole, V. Wang, S. Pittaluga, A. T. Catanzaro, S. M. Steinberg, and R. Yarchoan.** 2007. Phase 2 study of pegylated liposomal doxorubicin in combination with interleukin-12 for AIDS-related Kaposi sarcoma. Blood **110:**4165-71.

124. **Liu, C., Y. Okruzhnov, H. Li, and J. Nicholas.** 2001. Human herpesvirus 8 (HHV-8)-encoded cytokines induce expression of and autocrine signaling by vascular endothelial growth factor (VEGF) in HHV-8-infected primary-effusion lymphoma cell lines and mediate VEGF-independent antiapoptotic effects. J Virol **75:**10933-40.

125. **Liu, L., M. T. Eby, N. Rathore, S. K. Sinha, A. Kumar, and P. M. Chaudhary.** 2002. The human herpes virus 8-encoded viral FLICE inhibitory protein physically associates with and persistently activates the Ikappa B kinase complex. J Biol Chem **277:**13745-51.

126. **Low, W., M. Harries, H. Ye, M. Q. Du, C. Boshoff, and M. Collins.** 2001. Internal ribosome entry site regulates translation of Kaposi's sarcoma-associated herpesvirus FLICE inhibitory protein. J Virol **75:**2938-45.

127. **Lukac, D. M., L. Garibyan, J. R. Kirshner, D. Palmeri, and D. Ganem.** 2001. DNA binding by Kaposi's sarcoma-associated herpesvirus lytic switch protein is necessary for transcriptional activation of two viral delayed early promoters. J Virol **75:**6786-99.

128. **Lukac, D. M., J. R. Kirshner, and D. Ganem.** 1999. Transcriptional activation by the product of open reading frame 50 of Kaposi's sarcoma-associated herpesvirus is required for lytic viral reactivation in B cells. J Virol **73:**9348-61.

129. **Lukac, D. M., R. Renne, J. R. Kirshner, and D. Ganem.** 1998. Reactivation of Kaposi's sarcoma-associated herpesvirus infection from latency by expression of the ORF 50 transactivator, a homolog of the EBV R protein. Virology **252:**304-12.

130. **Malik, P., D. J. Blackbourn, M. F. Cheng, G. S. Hayward, and J. B. Clements.** 2004. Functional co-operation between the Kaposi's sarcoma-associated herpesvirus ORF57 and ORF50 regulatory proteins. J Gen Virol **85:**2155-66.

131. **Mansfield, K. G., S. V. Westmoreland, C. D. DeBakker, S. Czajak, A. A. Lackner, and R. C. Desrosiers.** 1999. Experimental infection of rhesus and pig-tailed macaques with macaque rhadinoviruses. J Virol **73:**10320-8.

132. **Mark, L., O. B. Spiller, M. Okroj, S. Chanas, J. A. Aitken, S. W. Wong, B. Damania, A. M. Blom, and D. J. Blackbourn.** 2007. Molecular characterization of the rhesus rhadinovirus (RRV) ORF4 gene and the RRV complement control protein it encodes. J Virol **81:**4166-76.

133. **Marshall, V., T. Parks, R. Bagni, C. D. Wang, M. A. Samols, J. Hu, K. M. Wyvil, K. Aleman, R. F. Little, R. Yarchoan, R. Renne, and D. Whitby.** 2007. Conservation of virally encoded microRNAs in Kaposi sarcoma--associated herpesvirus in primary effusion lymphoma cell lines and in patients with Kaposi sarcoma or multicentric Castleman disease. J Infect Dis **195:**645-59.

134. **Mbulaiteye, S. M., R. J. Biggar, J. J. Goedert, and E. A. Engels.** 2003. Immune deficiency and risk for malignancy among persons with AIDS. J Acquir Immune Defic Syndr **32:**527-33.

135. **McCormick, C., and D. Ganem.** 2005. The kaposin B protein of KSHV activates the p38/MK2 pathway and stabilizes cytokine mRNAs. Science **307:**739-41.

136. **McCormick, C., and D. Ganem.** 2006. Phosphorylation and function of the kaposin B direct repeats of Kaposi's sarcoma-associated herpesvirus. J Virol **80:**6165-70.

137. **Miles, S. A., A. R. Rezai, J. F. Salazar-Gonzalez, M. Vander Meyden, R. H. Stevens, D. M. Logan, R. T. Mitsuyasu, T. Taga, T. Hirano, T. Kishimoto, and et al.** 1990. AIDS Kaposi sarcoma-derived cells produce and respond to interleukin 6. Proc Natl Acad Sci U S A **87:**4068-72.

138. **Miller, G., L. Heston, E. Grogan, L. Gradoville, M. Rigsby, R. Sun, D. Shedd, V. M. Kushnaryov, S. Grossberg, and Y. Chang.** 1997. Selective switch between latency and lytic replication of Kaposi's sarcoma herpesvirus and Epstein-Barr virus in dually infected body cavity lymphoma cells. J Virol **71:**314-24.

139. **Molden, J., Y. Chang, Y. You, P. S. Moore, and M. A. Goldsmith.** 1997. A Kaposi's sarcoma-associated herpesvirus-encoded cytokine homolog (vIL-6) activates signaling through the shared gp130 receptor subunit. J Biol Chem **272:**19625-31.

140. **Montaner, S., A. Sodhi, A. Molinolo, T. H. Bugge, E. T. Sawai, Y. He, Y. Li, P. E. Ray, and J. S. Gutkind.** 2003. Endothelial infection with KSHV genes in vivo reveals that vGPCR initiates Kaposi's sarcomagenesis and can promote the tumorigenic potential of viral latent genes. Cancer Cell **3:**23-36.

141. **Montaner, S., A. Sodhi, S. Pece, E. A. Mesri, and J. S. Gutkind.** 2001. The Kaposi's sarcoma-associated herpesvirus G protein-coupled receptor promotes endothelial cell survival through the activation of Akt/protein kinase B. Cancer Res **61:**2641-8.

142. **Muralidhar, S., A. M. Pumfery, M. Hassani, M. R. Sadaie, M. Kishishita, J. N. Brady, J. Doniger, P. Medveczky, and L. J. Rosenthal.** 1998. Identification of kaposin (open reading frame K12) as a human herpesvirus 8 (Kaposi's sarcoma-associated herpesvirus) transforming gene. J Virol **72:**4980-8.

143. **Murphy, E., J. Vanicek, H. Robins, T. Shenk, and A. J. Levine.** 2008. Suppression of immediate-early viral gene expression by herpesvirus-coded microRNAs: implications for latency. Proc Natl Acad Sci U S A **105:**5453-8.

144. **Nador, R. G., E. Cesarman, A. Chadburn, D. B. Dawson, M. Q. Ansari, J. Sald, and D. M. Knowles.** 1996. Primary effusion lymphoma: a distinct clinicopathologic entity associated with the Kaposi's sarcoma-associated herpes virus. Blood **88:**645-56.

145. **Nakamura, H., M. Li, J. Zarycki, and J. U. Jung.** 2001. Inhibition of p53 tumor suppressor by viral interferon regulatory factor. J Virol **75:**7572-82.

146. **Neipel, F., J. C. Albrecht, and B. Fleckenstein.** 1998. Human herpesvirus 8--the first human Rhadinovirus. J Natl Cancer Inst Monogr**:**73-7.

147. **Neipel, F., and B. Fleckenstein.** 1999. The role of HHV-8 in Kaposi's sarcoma. Semin Cancer Biol **9:**151-64.

148. **O'Connor, C. M., B. Damania, and D. H. Kedes.** 2003. De novo infection with rhesus monkey rhadinovirus leads to the accumulation of multiple intranuclear capsid species during lytic replication but favors the release of genome-containing virions. J Virol **77:**13439-47.

149. **O'Connor, C. M., and D. H. Kedes.** 2007. Rhesus monkey rhadinovirus: a model for the study of KSHV. Curr Top Microbiol Immunol **312:**43-69.

150. **Ojala, P. M., M. Tiainen, P. Salven, T. Veikkola, E. Castanos-Velez, R. Sarid, P. Biberfeld, and T. P. Makela.** 1999. Kaposi's sarcoma-associated herpesvirus-encoded v-cyclin triggers apoptosis in cells with high levels of cyclin-dependent kinase 6. Cancer Res **59:**4984-9.

151. **Okroj, M., L. Mark, A. Stokowska, S. W. Wong, N. Rose, D. J. Blackbourn, B. O. Villoutreix, O. B. Spiller, and A. M. Blom.** 2009. Characterization of the complement inhibitory function of rhesus rhadinovirus complement control protein (RCP). J Biol Chem **284:**505-14.

152. **Oksenhendler, E., J. P. Clauvel, S. Jouveshomme, F. Davi, and G. Mansour.** 1998. Complete remission of a primary effusion lymphoma with antiretroviral therapy. Am J Hematol **57:**266.

153. **Orzechowska, B. U., M. Manoharan, J. Sprague, R. D. Estep, M. K. Axthelm, and S. W. Wong.** 2009. Viral interleukin-6 encoded by rhesus macaque rhadinovirus is associated with lymphoproliferative disorder (LPD). J Med Primatol **38 Suppl 1:**2-7.

154. **Orzechowska, B. U., M. F. Powers, J. Sprague, H. Li, B. Yen, R. P. Searles, M. K. Axthelm, and S. W. Wong.** 2008. Rhesus macaque rhadinovirus-associated non-Hodgkin's lymphoma: animal model for KSHV associated malignancies. Blood.

155. **Orzechowska, B. U., M. F. Powers, J. Sprague, H. Li, B. Yen, R. P. Searles, M. K. Axthelm, and S. W. Wong.** 2008. Rhesus macaque rhadinovirus-associated non-Hodgkin lymphoma: animal model for KSHV-associated malignancies. Blood **112:**4227-34.

156. **Osborne, J., P. S. Moore, and Y. Chang.** 1999. KSHV-encoded viral IL-6 activates multiple human IL-6 signaling pathways. Hum Immunol **60:**921-7.

157. **Palmeri, D., S. Spadavecchia, K. D. Carroll, and D. M. Lukac.** 2007. Promoter- and cell-specific transcriptional transactivation by the Kaposi's sarcoma-associated herpesvirus ORF57/Mta protein. J Virol **81:**13299-314.

158. **Pan, H., F. Zhou, and S. J. Gao.** 2004. Kaposi's sarcoma-associated herpesvirus induction of chromosome instability in primary human endothelial cells. Cancer Res **64:**4064-8.

159. **Parkin, D. M., H. Wabinga, S. Nambooze, and F. Wabwire-Mangen.** 1999. AIDS-related cancers in Africa: maturation of the epidemic in Uganda. Aids **13:**2563-70.

160. **Parravicini, C., B. Chandran, M. Corbellino, E. Berti, M. Paulli, P. S. Moore, and Y. Chang.** 2000. Differential viral protein expression in Kaposi's sarcoma-associated herpesvirus-infected diseases: Kaposi's sarcoma, primary effusion lymphoma, and multicentric Castleman's disease. Am J Pathol **156:**743-9.

161. **Parravicini, C., M. Corbellino, M. Paulli, U. Magrini, M. Lazzarino, P. S. Moore, and Y. Chang.** 1997. Expression of a virus-derived cytokine, KSHV vIL-6, in HIV-seronegative Castleman's disease. Am J Pathol **151:**1517-22.

162. **Paulose-Murphy, M., N. K. Ha, C. Xiang, Y. Chen, L. Gillim, R. Yarchoan, P. Meltzer, M. Bittner, J. Trent, and S. Zeichner.** 2001. Transcription program of human herpesvirus 8 (kaposi's sarcoma-associated herpesvirus). J Virol **75:**4843-53.

163. **Pearce, M., S. Matsumura, and A. C. Wilson.** 2005. Transcripts encoding K12, v-FLIP, v-cyclin, and the microRNA cluster of Kaposi's sarcoma-associated herpesvirus originate from a common promoter. J Virol **79:**14457-64.

164. **Penn, I.** 1988. Secondary neoplasms as a consequence of transplantation and cancer therapy. Cancer Detect Prev **12:**39-57.

165. **Pfeffer, S., A. Sewer, M. Lagos-Quintana, R. Sheridan, C. Sander, F. A. Grasser, L. F. van Dyk, C. K. Ho, S. Shuman, M. Chien, J. J. Russo, J. Ju, G. Randall, B. D. Lindenbach, C. M. Rice, V. Simon, D. D. Ho, M. Zavolan, and T. Tuschl.** 2005. Identification of microRNAs of the herpesvirus family. Nat Methods **2:**269-76.

166. **Platt, G. M., G. R. Simpson, S. Mittnacht, and T. F. Schulz.** 1999. Latent nuclear antigen of Kaposi's sarcoma-associated herpesvirus interacts with RING3, a homolog of the Drosophila female sterile homeotic (fsh) gene. J Virol **73:**9789-95.

167. **Poole, L. J., Y. Yu, P. S. Kim, Q. Z. Zheng, J. Pevsner, and G. S. Hayward.** 2002. Altered patterns of cellular gene expression in dermal microvascular endothelial cells infected with Kaposi's sarcoma-associated herpesvirus. J Virol **76:**3395-420.

168. **Pozharskaya, V. P., L. L. Weakland, J. C. Zimring, L. T. Krug, E. R. Unger, A. Neisch, H. Joshi, N. Inoue, and M. K. Offermann.** 2004. Short duration of elevated vIRF-1 expression during lytic replication of human herpesvirus 8 limits its ability to block antiviral responses induced by alpha interferon in BCBL-1 cells. J Virol **78:**6621-35.

169. **Prakash, O., Z. Y. Tang, X. Peng, R. Coleman, J. Gill, G. Farr, and F. Samaniego.** 2002. Tumorigenesis and aberrant signaling in transgenic mice expressing the human herpesvirus-8 K1 gene. J Natl Cancer Inst **94:**926-35.

170. **Pratt, C. L., R. D. Estep, and S. W. Wong.** 2005. Splicing of rhesus rhadinovirus R15 and ORF74 bicistronic transcripts during lytic infection and analysis of effects on production of vCD200 and vGPCR. J Virol **79:**3878-82.

171. **Qian, L. W., J. Xie, F. Ye, and S. J. Gao.** 2007. Kaposi's sarcoma-associated herpesvirus infection promotes invasion of primary human umbilical vein endothelial cells by inducing matrix metalloproteinases. J Virol **81:**7001-10.

172. **Raab-Traub, N.** 2002. Epstein-Barr virus in the pathogenesis of NPC. Semin Cancer Biol **12:**431-41.

173. **Radaszkiewicz, T., M. L. Hansmann, and K. Lennert.** 1989. Monoclonality and polyclonality of plasma cells in Castleman's disease of the plasma cell variant. Histopathology **14:**11-24.

174. **Radkov, S. A., P. Kellam, and C. Boshoff.** 2000. The latent nuclear antigen of Kaposi sarcoma-associated herpesvirus targets the retinoblastoma-E2F pathway and with the oncogene Hras transforms primary rat cells. Nat Med **6:**1121-7.

175. **Rainbow, L., G. M. Platt, G. R. Simpson, R. Sarid, S. J. Gao, H. Stoiber, C. S. Herrington, P. S. Moore, and T. F. Schulz.** 1997. The 222- to 234-kilodalton latent nuclear protein (LNA) of Kaposi's sarcoma-associated herpesvirus (human herpesvirus 8) is encoded by orf73 and is a component of the latency-associated nuclear antigen. J Virol **71:**5915-21.

176. **Renne, R., C. Barry, D. Dittmer, N. Compitello, P. O. Brown, and D. Ganem.** 2001. Modulation of cellular and viral gene expression by the latency-associated nuclear antigen of Kaposi's sarcoma-associated herpesvirus. J Virol **75:**458-68.

177. **Renne, R., D. Blackbourn, D. Whitby, J. Levy, and D. Ganem.** 1998. Limited transmission of Kaposi's sarcoma-associated herpesvirus in cultured cells. J Virol **72:**5182-8.

178. **Renne, R., D. Dittmer, D. Kedes, K. Schmidt, R. C. Desrosiers, P. A. Luciw, and D. Ganem.** 2004. Experimental transmission of Kaposi's sarcoma-associated herpesvirus (KSHV/HHV-8) to SIV-positive and SIV-negative rhesus macaques. J Med Primatol **33:**1-9.

179. **Renne, R., M. Lagunoff, W. Zhong, and D. Ganem.** 1996. The size and conformation of Kaposi's sarcoma-associated herpesvirus (human herpesvirus 8) DNA in infected cells and virions. J Virol **70:**8151-4.

180. **Renne, R., W. Zhong, B. Herndier, M. McGrath, N. Abbey, D. Kedes, and D. Ganem.** 1996. Lytic growth of Kaposi's sarcoma-associated herpesvirus (human herpesvirus 8) in culture. Nat Med **2:**342-6.

181. **Roizman, B., L. E. Carmichael, F. Deinhardt, G. de-The, A. J. Nahmias, W. Plowright, F. Rapp, P. Sheldrick, M. Takahashi, and K. Wolf.** 1981. Herpesviridae. Definition, provisional nomenclature, and taxonomy. The Herpesvirus Study Group, the International Committee on Taxonomy of Viruses. Intervirology **16:**201-17.

182. **Rosenkilde, M. M., T. N. Kledal, H. Brauner-Osborne, and T. W. Schwartz.** 1999. Agonists and inverse agonists for the herpesvirus 8-encoded constitutively active seven-transmembrane oncogene product, ORF-74. J Biol Chem **274:**956-61.

183. **Rossetto, C., Y. Gao, I. Yamboliev, I. Papouskova, and G. Pari.** 2007. Transcriptional repression of K-Rta by Kaposi's sarcoma-associated herpesvirus K-bZIP is not required for oriLyt-dependent DNA replication. Virology **369:**340-50.

184. **Russo, J. J., R. A. Bohenzky, M. C. Chien, J. Chen, M. Yan, D. Maddalena, J. P. Parry, D. Peruzzi, I. S. Edelman, Y. Chang, and P. S. Moore.** 1996. Nucleotide sequence of the Kaposi sarcoma-associated herpesvirus (HHV8). Proc Natl Acad Sci U S A **93:**14862-7.

185. **Sadler, R., L. Wu, B. Forghani, R. Renne, W. Zhong, B. Herndier, and D. Ganem.** 1999. A complex translational program generates multiple novel proteins from the latently expressed kaposin (K12) locus of Kaposi's sarcoma-associated herpesvirus. J Virol **73:**5722-30.

186. **Sakakibara, S., K. Ueda, J. Chen, T. Okuno, and K. Yamanishi.** 2001. Octamer-binding sequence is a key element for the autoregulation of Kaposi's sarcoma-associated herpesvirus ORF50/Lyta gene expression. J Virol **75:**6894-900.

187. **Sakurada, S., H. Katano, T. Sata, H. Ohkuni, T. Watanabe, and S. Mori.** 2001. Effective human herpesvirus 8 infection of human umbilical vein endothelial cells by cell-mediated transmission. J Virol **75:**7717-22.

188. **Samols, M. A., J. Hu, R. L. Skalsky, and R. Renne.** 2005. Cloning and identification of a microRNA cluster within the latency-associated region of Kaposi's sarcoma-associated herpesvirus. J Virol **79:**9301-5.

189. **Samols, M. A., R. L. Skalsky, A. M. Maldonado, A. Riva, M. C. Lopez, H. V. Baker, and R. Renne.** 2007. Identification of cellular genes targeted by KSHV-encoded microRNAs. PLoS Pathog **3:**e65.

190. **Schafer, A., X. Cai, J. P. Bilello, R. C. Desrosiers, and B. R. Cullen.** 2007. Cloning and analysis of microRNAs encoded by the primate gamma-herpesvirus rhesus monkey rhadinovirus. Virology **364:**21-7.

191. **Schulz, T. F., and Y. Chang.** 2007. KSHV gene expression and regulation, p. 490-513. *In* A. M. Arvin, G. Campadelli-Fiume, E. Mocarski, P. S. Moore, B. Roizman, and R. S. Whitley (ed.), Human Herpesviruses : Biology, Therapy, And Immunoprophylaxis. Cambridge, Great Britain/British Isles.

192. **Schwam, D. R., R. L. Luciano, S. S. Mahajan, L. Wong, and A. C. Wilson.** 2000. Carboxy terminus of human herpesvirus 8 latency-associated nuclear antigen mediates dimerization, transcriptional repression, and targeting to nuclear bodies. J Virol **74:**8532-40.

193. **Searles, R. P., E. P. Bergquam, M. K. Axthelm, and S. W. Wong.** 1999. Sequence and genomic analysis of a Rhesus macaque rhadinovirus with similarity to Kaposi's sarcoma-associated herpesvirus/human herpesvirus 8. J Virol **73:**3040-53.

194. **Seo, T., J. Park, D. Lee, S. G. Hwang, and J. Choe.** 2001. Viral interferon regulatory factor 1 of Kaposi's sarcoma-associated herpesvirus binds to p53 and represses p53-dependent transcription and apoptosis. J Virol **75:**6193-8.

195. **Shamay, M., A. Krithivas, J. Zhang, and S. D. Hayward.** 2006. Recruitment of the de novo DNA methyltransferase Dnmt3a by Kaposi's sarcoma-associated herpesvirus LANA. Proc Natl Acad Sci U S A **103:**14554-9.

196. **Simonelli, C., M. Spina, R. Cinelli, R. Talamini, R. Tedeschi, A. Gloghini, E. Vaccher, A. Carbone, and U. Tirelli.** 2003. Clinical features and outcome of primary effusion lymphoma in HIV-infected patients: a single-institution study. J Clin Oncol **21:**3948-54.

197. **Sin, S. H., D. Roy, L. Wang, M. R. Staudt, F. D. Fakhari, D. D. Patel, D. Henry, W. J. Harrington, Jr., B. A. Damania, and D. P. Dittmer.** 2007. Rapamycin is efficacious against primary effusion lymphoma (PEL) cell lines in vivo by inhibiting autocrine signaling. Blood **109:**2165-73.

198. **Skalsky, R. L., M. A. Samols, K. B. Plaisance, I. W. Boss, A. Riva, M. C. Lopez, H. V. Baker, and R. Renne.** 2007. Kaposi's sarcoma-associated herpesvirus encodes an ortholog of miR-155. J Virol **81:**12836-45.

199. **Sodhi, A., S. Montaner, V. Patel, M. Zohar, C. Bais, E. A. Mesri, and J. S. Gutkind.** 2000. The Kaposi's sarcoma-associated herpes virus G protein-coupled receptor up-regulates vascular endothelial growth factor expression and secretion through mitogen-activated protein kinase and p38 pathways acting on hypoxia-inducible factor 1alpha. Cancer Res **60:**4873-80.

200. **Soulier, J., L. Grollet, E. Oksenhendler, P. Cacoub, D. Cazals-Hatem, P. Babinet, M. F. d'Agay, J. P. Clauvel, M. Raphael, L. Degos, and et al.** 1995. Kaposi's sarcoma-associated herpesvirus-like DNA sequences in multicentric Castleman's disease. Blood **86:**1276-80.

201. **Stallone, G., B. Infante, G. Grandaliano, F. P. Schena, and L. Gesualdo.** 2008. Kaposi's sarcoma and mTOR: a crossroad between viral infection neoangiogenesis and immunosuppression. Transpl Int **21:**825-32.

202. **Stallone, G., A. Schena, B. Infante, S. Di Paolo, A. Loverre, G. Maggio, E. Ranieri, L. Gesualdo, F. P. Schena, and G. Grandaliano.** 2005. Sirolimus for Kaposi's sarcoma in renal-transplant recipients. N Engl J Med **352:**1317-23.

203. **Staskus, K. A., R. Sun, G. Miller, P. Racz, A. Jaslowski, C. Metroka, H. Brett-Smith, and A. T. Haase.** 1999. Cellular tropism and viral interleukin-6 expression distinguish human herpesvirus 8 involvement in Kaposi's sarcoma, primary effusion lymphoma, and multicentric Castleman's disease. J Virol **73:**4181-7.

204. **Staskus, K. A., W. Zhong, K. Gebhard, B. Herndier, H. Wang, R. Renne, J. Beneke, J. Pudney, D. J. Anderson, D. Ganem, and A. T. Haase.** 1997. Kaposi's sarcoma-associated herpesvirus gene expression in endothelial (spindle) tumor cells. J Virol **71:**715-9.

205. **Staudt, M. R., and D. P. Dittmer.** 2007. The Rta/Orf50 transactivator proteins of the gamma-herpesviridae. Curr Top Microbiol Immunol **312:**71-100.

206. **Staudt, M. R., Y. Kanan, J. H. Jeong, J. F. Papin, R. Hines-Boykin, and D. P. Dittmer.** 2004. The tumor microenvironment controls primary effusion lymphoma growth in vivo. Cancer Res **64:**4790-9.

207. **Sun, Q., S. Zachariah, and P. M. Chaudhary.** 2003. The human herpes virus 8-encoded viral FLICE-inhibitory protein induces cellular transformation via NF-kappaB activation. J Biol Chem **278:**52437-45.

208. **Sun, R., S. F. Lin, L. Gradoville, and G. Miller.** 1996. Polyadenylylated nuclear RNA encoded by Kaposi sarcoma-associated herpesvirus. Proc Natl Acad Sci U S A **93:**11883-8.

209. **Sun, R., S. F. Lin, L. Gradoville, Y. Yuan, F. Zhu, and G. Miller.** 1998. A viral gene that activates lytic cycle expression of Kaposi's sarcoma-associated herpesvirus. Proc Natl Acad Sci U S A **95:**10866-71.

210. **Swanton, C., D. J. Mann, B. Fleckenstein, F. Neipel, G. Peters, and N. Jones.** 1997. Herpes viral cyclin/Cdk6 complexes evade inhibition by CDK inhibitor proteins. Nature **390:**184-7.

211. **Talbot, S. J., R. A. Weiss, P. Kellam, and C. Boshoff.** 1999. Transcriptional analysis of human herpesvirus-8 open reading frames 71, 72, 73, K14, and 74 in a primary effusion lymphoma cell line. Virology **257:**84-94.

212. **Tam, H. K., Z. F. Zhang, L. P. Jacobson, J. B. Margolick, J. S. Chmiel, C. Rinaldo, and R. Detels.** 2002. Effect of highly active antiretroviral therapy on survival among HIV-infected men with Kaposi sarcoma or non-Hodgkin lymphoma. Int J Cancer **98:**916-22.

213. **Taylor, J. F., A. C. Templeton, C. L. Vogel, J. L. Ziegler, and S. K. Kyalwazi.** 1971. Kaposi's sarcoma in Uganda: a clinico-pathological study. Int J Cancer **8:**122-35.

214. **Tomlinson, C. C., and B. Damania.** 2008. Critical role for endocytosis in the regulation of signaling by the Kaposi's sarcoma-associated herpesvirus K1 protein. J Virol **82:**6514-23.

215. **Tomlinson, C. C., and B. Damania.** 2004. The K1 protein of Kaposi's sarcoma-associated herpesvirus activates the Akt signaling pathway. J Virol **78:**1918-27.

216. **Vart, R. J., L. L. Nikitenko, D. Lagos, M. W. Trotter, M. Cannon, D. Bourboulia, F. Gratrix, Y. Takeuchi, and C. Boshoff.** 2007. Kaposi's sarcoma-associated herpesvirus-encoded interleukin-6 and G-protein-coupled receptor regulate angiopoietin-2 expression in lymphatic endothelial cells. Cancer Res **67:**4042-51.

217. **Verma, S. C., K. Lan, and E. Robertson.** 2007. Structure and function of latency-associated nuclear antigen. Curr Top Microbiol Immunol **312:**101-36.

218. **Verschuren, E. W., J. G. Hodgson, J. W. Gray, S. Kogan, N. Jones, and G. I. Evan.** 2004. The role of p53 in suppression of KSHV cyclin-induced lymphomagenesis. Cancer Res **64:**581-9.

219. **Verschuren, E. W., J. Klefstrom, G. I. Evan, and N. Jones.** 2002. The oncogenic potential of Kaposi's sarcoma-associated herpesvirus cyclin is exposed by p53 loss in vitro and in vivo. Cancer Cell **2:**229-41.

220. **Viejo-Borbolla, A., M. Ottinger, E. Bruning, A. Burger, R. Konig, E. Kati, J. A. Sheldon, and T. F. Schulz.** 2005. Brd2/RING3 interacts with a chromatin-binding domain in the Kaposi's Sarcoma-associated herpesvirus latency-associated nuclear antigen 1 (LANA-1) that is required for multiple functions of LANA-1. J Virol **79:**13618-29.

221. **Wabinga, H. R., D. M. Parkin, F. Wabwire-Mangen, and S. Nambooze.** 2000. Trends in cancer incidence in Kyadondo County, Uganda, 1960-1997. Br J Cancer **82:**1585-92.

222. **Walz, N., T. Christalla, U. Tessmer, and A. Grundhoff.** A global analysis of evolutionary conservation among known and predicted gammaherpesvirus microRNAs. J Virol **84:**716-28.

223. **Wang, H. W., M. W. Trotter, D. Lagos, D. Bourboulia, S. Henderson, T. Makinen, S. Elliman, A. M. Flanagan, K. Alitalo, and C. Boshoff.** 2004. Kaposi sarcoma herpesvirus-induced cellular reprogramming contributes to the lymphatic endothelial gene expression in Kaposi sarcoma. Nat Genet **36:**687-93.

224. **Wang, L., and B. Damania.** 2008. Kaposi's sarcoma-associated herpesvirus confers a survival advantage to endothelial cells. Cancer Res **68:**4640-8.

225. **Wang, L., D. P. Dittmer, C. C. Tomlinson, F. D. Fakhari, and B. Damania.** 2006. Immortalization of primary endothelial cells by the K1 protein of Kaposi's sarcoma-associated herpesvirus. Cancer Res **66:**3658-66.

226. **Wang, L., M. Pietrek, M. M. Brinkmann, A. Havemeier, I. Fischer, B. Hillenbrand, O. Dittrich-Breiholz, M. Kracht, S. Chanas, D. J. Blackbourn, and T. F. Schulz.** 2009. Identification and functional characterization of a spliced rhesus rhadinovirus gene with homology to the K15 gene of Kaposi's sarcoma-associated herpesvirus. J Gen Virol **90:**1190-201.

227. **Wang, L., N. Wakisaka, C. C. Tomlinson, S. M. DeWire, S. Krall, J. S. Pagano, and B. Damania.** 2004. The Kaposi's sarcoma-associated herpesvirus (KSHV/HHV-8) K1 protein induces expression of angiogenic and invasion factors. Cancer Res **64:**2774-81.

228. **Wang, S., S. Liu, M. Wu, Y. Geng, and C. Wood.** 2001. Kaposi's sarcoma-associated herpesvirus/human herpesvirus-8 ORF50 gene product contains a potent C-terminal activation domain which activates gene expression via a specific target sequence. Arch Virol **146:**1415-26.

229. **Wang, S. E., F. Y. Wu, H. Chen, M. Shamay, Q. Zheng, and G. S. Hayward.** 2004. Early activation of the Kaposi's sarcoma-associated herpesvirus RTA, RAP, and MTA promoters by the tetradecanoyl phorbol acetate-induced AP1 pathway. J Virol **78:**4248-67.

230. **Wang, S. E., F. Y. Wu, M. Fujimuro, J. Zong, S. D. Hayward, and G. S. Hayward.** 2003. Role of CCAAT/enhancer-binding protein alpha (C/EBPalpha) in activation of the Kaposi's sarcoma-associated herpesvirus (KSHV) lytic-cycle replication-associated protein (RAP) promoter in cooperation with the KSHV replication and transcription activator (RTA) and RAP. J Virol **77:**600-23.

231. **Wang, S. E., F. Y. Wu, Y. Yu, and G. S. Hayward.** 2003. CCAAT/enhancer-binding protein-alpha is induced during the early stages of Kaposi's sarcoma-associated herpesvirus (KSHV) lytic cycle reactivation and together with the KSHV replication and transcription activator (RTA) cooperatively stimulates the viral RTA, MTA, and PAN promoters. J Virol **77:**9590-612.

232. **Watanabe, T., M. Sugaya, A. M. Atkins, E. A. Aquilino, A. Yang, D. L. Borris, J. Brady, and A. Blauvelt.** 2003. Kaposi's sarcoma-associated herpesvirus latency-associated nuclear antigen prolongs the life span of primary human umbilical vein endothelial cells. J Virol **77:**6188-96.

233. **Wheat, W. H., C. D. Cool, Y. Morimoto, P. R. Rai, C. H. Kirkpatrick, B. A. Lindenbaum, C. A. Bates, M. C. Ellison, A. E. Serls, K. K. Brown, and J. M. Routes.** 2005. Possible role of human herpesvirus 8 in the lymphoproliferative disorders in common variable immunodeficiency. J Exp Med **202:**479-84.

234. **Wong, S. W., E. P. Bergquam, R. M. Swanson, F. W. Lee, S. M. Shiigi, N. A. Avery, J. W. Fanton, and M. K. Axthelm.** 1999. Induction of B cell hyperplasia in simian

immunodeficiency virus-infected rhesus macaques with the simian homologue of Kaposi's sarcoma-associated herpesvirus. J Exp Med **190:**827-40.

235. **Xu, Y., D. P. AuCoin, A. R. Huete, S. A. Cei, L. J. Hanson, and G. S. Pari.** 2005. A Kaposi's sarcoma-associated herpesvirus/human herpesvirus 8 ORF50 deletion mutant is defective for reactivation of latent virus and DNA replication. J Virol **79:**3479-87.

236. **Yada, K., E. Do, S. Sakakibara, E. Ohsaki, E. Ito, S. Watanabe, and K. Ueda.** 2006. KSHV RTA induces a transcriptional repressor, HEY1 that represses rta promoter. Biochem Biophys Res Commun **345:**410-8.

237. **Yang, T. Y., S. C. Chen, M. W. Leach, D. Manfra, B. Homey, M. Wiekowski, L. Sullivan, C. H. Jenh, S. K. Narula, S. W. Chensue, and S. A. Lira.** 2000. Transgenic expression of the chemokine receptor encoded by human herpesvirus 8 induces an angioproliferative disease resembling Kaposi's sarcoma. J Exp Med **191:**445-54.

238. **Yang, Z., and C. Wood.** 2007. The transcriptional repressor K-RBP modulates RTA-mediated transactivation and lytic replication of Kaposi's sarcoma-associated herpesvirus. J Virol **81:**6294-306.

239. **Yang, Z., Z. Yan, and C. Wood.** 2008. Kaposi's sarcoma-associated herpesvirus transactivator RTA promotes degradation of the repressors to regulate viral lytic replication. J Virol **82:**3590-603.

240. **Ye, F. C., F. C. Zhou, J. P. Xie, T. Kang, W. Greene, K. Kuhne, X. F. Lei, Q. H. Li, and S. J. Gao.** 2008. Kaposi's sarcoma-associated herpesvirus latent gene vFLIP inhibits viral lytic replication through NF-kappaB-mediated suppression of the AP-1 pathway: a novel mechanism of virus control of latency. J Virol **82:**4235-49.

241. **Yoshizaki, K., T. Matsuda, N. Nishimoto, T. Kuritani, L. Taeho, K. Aozasa, T. Nakahata, H. Kawai, H. Tagoh, T. Komori, and et al.** 1989. Pathogenic significance of interleukin-6 (IL-6/BSF-2) in Castleman's disease. Blood **74:**1360-7.

242. **Young, L., C. Alfieri, K. Hennessy, H. Evans, C. O'Hara, K. C. Anderson, J. Ritz, R. S. Shapiro, A. Rickinson, E. Kieff, and et al.** 1989. Expression of Epstein-Barr virus transformation-associated genes in tissues of patients with EBV lymphoproliferative disease. N Engl J Med **321:**1080-5.

243. **Zhang, L., J. Chiu, and J. C. Lin.** 1998. Activation of human herpesvirus 8 (HHV-8) thymidine kinase (TK) TATAA-less promoter by HHV-8 ORF50 gene product is SP1 dependent. DNA Cell Biol **17:**735-42.

244. **Zhao, J., V. Punj, H. Matta, L. Mazzacurati, S. Schamus, Y. Yang, T. Yang, Y. Hong, and P. M. Chaudhary.** 2007. K13 blocks KSHV lytic replication and deregulates vIL6 and hIL6 expression: a model of lytic replication induced clonal selection in viral oncogenesis. PLoS ONE **2:**e1067.

245. **Zhong, W., and D. Ganem.** 1997. Characterization of ribonucleoprotein complexes containing an abundant polyadenylated nuclear RNA encoded by Kaposi's sarcoma-associated herpesvirus (human herpesvirus 8). J Virol **71:**1207-12.

246. **Zhu, F. X., T. Cusano, and Y. Yuan.** 1999. Identification of the immediate-early transcripts of Kaposi's sarcoma-associated herpesvirus. J Virol **73:**5556-67.

247. **Zhu, F. X., S. M. King, E. J. Smith, D. E. Levy, and Y. Yuan.** 2002. A Kaposi's sarcoma-associated herpesviral protein inhibits virus-mediated induction of type I interferon by blocking IRF-7 phosphorylation and nuclear accumulation. Proc Natl Acad Sci U S A **99:**5573-8.

248. **Zong, J. C., D. M. Ciufo, D. J. Alcendor, X. Wan, J. Nicholas, P. J. Browning, P. L. Rady, S. K. Tyring, J. M. Orenstein, C. S. Rabkin, I. J. Su, K. F. Powell, M. Croxson, K. E. Foreman, B. J. Nickoloff, S. Alkan, and G. S. Hayward.** 1999. High-level variability in the ORF-K1 membrane protein gene at the left end of the Kaposi's sarcoma-associated herpesvirus genome defines four major virus subtypes and multiple variants or clades in different human populations. J Virol **73:**4156-70.

CHAPTER 2

HSP90 AND ER-ASSOCIATED HSP40/ERDJ3 ARE REQUIRED FOR THE EXPRESSION AND ANTI-APOPTOTIC FUNCTION OF KSHV K1

Kwun Wah Wen and Blossom Damania

ABSTRACT

Kaposi sarcoma-associated herpesvirus (KSHV) is a member of the gammaherpesvirus family. It is the etiological agent of three different human cancers, Kaposi sarcoma (KS), primary effusion lymphoma (PEL), and multicentric Castleman disease (MCD). The far left-end of the KSHV genome encodes a unique transmembrane glycoprotein called K1. K1 possesses the ability to transform rodent fibroblasts and block apoptosis. K1 has also been shown to activate the PI3K/Akt/mTOR pathway in different cells.

Using tandem affinity purification (TAP), we identified heat shock protein 90β (Hsp90β) and endoplasmic reticulum (ER)-associated Hsp40 (Erdj3/DnaJB11), as cellular binding partners of K1. Interactions of K1 with Hsp90β and Hsp40 were confirmed by co-immunoprecipitation in both directions. Furthermore, K1 also interacted with the Hsp90α isoform. We report that siRNAs directed against Hsp90 and Erdj3, as well as pharmacological inhibitors of Hsp90 dramatically reduced K1 expression, suggesting that K1 is a client protein of these chaperones. Additionally, both Hsp90 and Erdj3 were essential for K1's anti-apoptotic function. Finally, we report that the Hsp90 inhibitors, 17-AAG and 17-DMAG, can suppress the proliferation of KSHV-positive PEL cell lines and exhibited IC_{50} values of 50 nM and below.

INTRODUCTION

Kaposi sarcoma-associated herpesvirus (KSHV), or human herpesvirus-8, is a gammaherpesviruses. This virus has been implicated as the etiological agent of Kaposi sarcoma (KS) (7) and lymphoproliferative diseases of B cell origin, namely, primary effusion lymphoma (PEL) (6) and the plasmablastic variant of multicentric Castleman disease (MCD) (13, 48).

The first open-reading frame (ORF) of KSHV encodes a viral glycoprotein named K1 (20). K1 is the positional homolog of the saimiri transformation protein (STP) of herpesvirus saimiri (HVS) (31) and the R1 oncogene of rhesus monkey rhadinovirus (9). K1 expression has been detected in KS, PEL, and MCD (3, 18, 20, 25). We, and others, have shown that K1 is a transforming protein of KSHV capable of transforming rodent fibroblasts. Injection of these cells into nude mice resulted in the development of large, multifocal, disseminated tumors (9, 40). Additionally, K1 could functionally substitute for the HVS STP oncogene in the context of a virus to transform immortalize peripheral blood mononuclear cells to IL-2 independent growth as well as induce lymphomas (27). Expression of the K1 gene in transgenic mice resulted in constitutive NF-κB activation in both T and B lymphocytes, and tyrosine phosphorylation of the Lyn protein kinase (40). These K1-transgenic mice developed tumors with features resembling spindle-cell sarcomas and malignant plasmablastic lymphoma (40).

K1 is a 46 kDa type I transmembrane glycoprotein, which structurally and functionally resembles a B cell receptor (BCR). The extracellular N-terminal domain of K1 exhibits homology to the variable region of the immunoglobulin λ light chain (26), and K1

appears to interact with the BCR μ chain to inhibit the intracellular transport of BCR and downregulate surface BCR expression (24). In its cytoplasmic tail, K1 contains an immunoreceptor tyrosine-based activation motif (ITAM) that is also found in many immunoglobulin receptors e.g. BCR. The K1 ITAM is comprised of two appropriately spaced Src-homology 2 (SH2) binding motifs (22, 26, 27) and is required for BCR activation events (22, 26). We and others have shown that K1 is capable of activating B lymphocyte signal transduction and interacting with Syk (8, 22, 26). Like BCR, K1 can induce tyrosine phosphorylation of cellular proteins, intracellular mobilization of calcium, and activation of transcription factors (21, 22, 26, 40). However, unlike BCR, K1 signaling appears to be constitutively active and independent of ligand binding (27). K1 signaling activity in B cells has been linked to K1 internalization (49), and K1 also co-internalizes with the BCR (49) resulting in the downregulation of BCR surface expression (24).

We previously reported that K1 activates the phosphatidyl-inositol-3'-OH-kinase (PI3K)/Akt/mammalian target of rapamycin (mTOR) signaling pathway in both B cells and endothelial cells (50, 52). In addition, we and other have shown that K1 can prevent Fas-mediated apoptosis (1, 50, 54) through activation of the PI3K/Akt pathway (50). In epithelial and endothelial cells, K1 expression induced the secretion of angiogenic factors, including vascular endothelial growth factor (VEGF) and matrix metalloproteinase-9 (MMP-9) (53). Cumulatively, these data suggest a paracrine model in which K1-mediated secretion of cytokines is involved in the development of KSHV-associated tumorigenesis and angiogenesis (53).

Molecular chaperones are involved in various cellular processes including and maturation, DNA replication and transcription, protein translocation, and cell signaling. For

example, both heat shock protein (Hsp) 90 and the Hsp40/Hsp70 system act to enhance the Akt pathway which is important for cell survival (12, 19). Hsp40, Hsp70, and Hsp90 are important for the assembly of signaling receptor complexes (32, 38, 47). Hsp90 and the Hsp40/Hsp70 system have been shown to suppress tumor necrosis factor (TNF)- and Fas-induced apoptosis (28, 34). Additionally, Hsp90 overexpression has been detected in a variety of cancers (reviewed in (42)). The KSHV K1 protein targets similar signaling pathways as Hsp90 e.g. the PI3K/Akt pathway, and hinders apoptosis by modulating this pro-survival pathway. Hence the functions of Hsp90, Hsp40, and K1 appear to be concordant.

Using tandem affinity purification, we identified Hsp90β and the ER-associated Hsp40 (Erdj3/DnajB11) as cellular binding partners of K1. We confirmed this finding by performing co-immunoprecipitation in both directions. We also found that K1 interacts with Hsp90α by co-immunoprecipitation. Pharmacological inhibition of Hsp90 function reduced expression of the K1 protein. This suggests that K1 protein expression is dependent on Hsp90 activity. Additionally, when Hsp90β or Erdj3 was knocked down by specific siRNAs, the level of K1 protein as well as the total and phosphorylated levels of Akt were reduced, implicating that Hsp90β and Erdj3 are important for K1 protein expressing and downstream Akt signaling. Knockdown of these chaperones also prevented K1 from promoting cell survival and inhibiting apoptosis. Hence, these molecular chaperones are critical for the expression and function of oncogenic K1. Finally, we report that the Hsp90 inhibitors, 17-AAG and 17-DMAG, were very effective in inhibiting the proliferation of KSHV-positive PEL cell lines.

MATERIALS AND METHODS

Cell culture

293-K1 and 293-Vec stable cells were established and maintained in 1 mg/ml G418 selection in DMEM medium supplemented with 10% FBS, 100 U/mL penicillin, and 100 µg/mL streptomycin in 5% CO_2. BCP-1, JSC-1, and BCBL-1 cell lines were cultured in RPMI 1640 medium supplemented with 10% FBS, 100 U/mL penicillin, 100 µg/mL streptomycin, 2 mM L-glutamate, 0.05 mM 2-mercaptoethanol, and 0.075% sodium bicarbonate in 5% CO_2.

Antibodies

Rabbit anti-K1 antibody was a kind gift from Dr. Jae Jung. Anti-Hsp90 (ab1429) and anti-Hsp70 antibodies (ab2787) were purchased from Abcam. Anti-Hsp90α and Hsp90β antibodies were purchased from Stressgen (SPS-771 and SPA-843). Anti-Hsp40 (DNAJB11) antibody was obtained from Sigma (HPA010814). Anti-Akt and anti-phospho-Akt (S473) were purchased from Cell Signaling, while anti-actin antibody was purchased from Santa Cruz (C16). EZview Anti-FLAG M2 resin was obtained from Sigma for immunoprecipitation of K1. Normal mouse IgG (sc-2025), normal rabbit IgG (sc-2027), and protein A/G PLUS-Agarose (sc-2003) were purchased from Santa Cruz. HRP-conjugated anti-ECS antibody used for FLAG immunoblotting was purchased from Bethyl (A190-101P). Immunoblotting detection was performed by using the ECL Plus kit (Amersham).

Inhibitors and small-interfering RNAs (siRNAs)

Geldanamycin, 17-(Allylamino)-17-demethoxygeldanamycin (17-AAG) and 17-Dimethylamino-ethylamino-17-demethoxygeldanamycin (17-DMAG) were purchased from

Invivogen. Stealth siRNAs targeting Hsp90β and Erdj3 were purchased from Invitrogen. Anti-Luc siRNA-1, Accell non-targeting siRNA pool, and GFP siRNA duplex were purchased from Thermo Scientific. The siRNAs directed against K1 (CCACAACAATTGCAGGATT-UU and CCATGCAACCACACATAAA-UU) were designed by Dharmacon siDESIGN® Center Custom siRNA Design Tool and Invitrogen BLOCK-iT™ RNAi Designer and purchased from Dharmacon.

Tandem affinity purification

We generated the FLAG HA tandem tagged K1 construct (TAP-K1) by QuikChange site-directed mutagenesis. A FLAG-tagged K1 construct previously published (50) was used as the PCR template for mutagenesis. The oligonucleotides 5'-ACGACGACAAGGGTACCTACCCATACGACGTCCCAGACTACGCTCTTTATGTGCTATCGTC-3' and 5'-GACGATAGCACATAAAGAGCGTAGTCTGGGACGTCGTATGGGTAGGTACCCTTGTCGTCGT-3' were used to introduce the HA epitope sequence between FLAG and K1 at the N-terminus. pcDNA3-K1 and empty pcDNA3 vector were transfected into 293 cells using FuGENE 6 reagent (Roche) and selected with 1 mg/ml G418 to establish 293-K1 and 293-Vec stable cells, respectively. Forty confluent flasks (T175) of each cell line were harvested and washed twice in cold PBS. Cells were pelleted and stored at -80^{o}C. 293-K1 and 293-Vec stable cell pellets were thawed and lysed in NP40 buffer supplemented with PMSF, EDTA-free protease inhibitor cocktail (Roche) and phosphatase inhibitor cocktails 1 & 2 (Sigma). The lysates were pelleted and the supernatants (20 mg/ml) were subjected to TAP using the FLAG HA Tandem Affinity Purification Kit (Sigma) according to the manufacturer's instructions. After TAP, the samples were eluted in 2X Laemmli sample buffer and resolved

on a 12% NuPAGE Novex Bis-Tris Mini Gel (Invitrogen) with MOPS SDS Running Buffer (Invitrogen). The gel was Coomassie-stained and submitted to the UNC Proteomics Center for mass spectroscopy. Protein bands unique to K1 expressing cells were excised, trypsin-digested, and subjected to Matrix Assisted Laser Desorption/Ionization-Time Of Flight (MALDI-TOF) mass spectroscopy (MS) analysis.

Immunoprecipitation

For each immunoprecipitation reaction, confluent cells in a 10-cm dish were harvested, washed twice in ice cold PBS, and lysed in RIPA buffer supplemented with PMSF, EDTA-free protease inhibitor cocktail (Roche) and phosphatase inhibitor cocktails 1 & 2 (Sigma). Cell lysates were freeze-thawed twice and centrifuged at 13,000 rpm for 10 min at 4^{o}C. The extract was subjected to pre-clearing with Protein A/G PLUS-Agarose and 1 µg of normal mouse Ig or normal rabbit IgG for 30 min at 4^{o}C with gentle rocking. For FLAG immunoprecipitation, pre-cleared extract was incubated with FLAG resin at 4^{o}C overnight, with gentle rocking. The beads were washed three to four times with RIPA buffer and immunoprecipitated protein complexes were subjected to competitive elution with 3X FLAG peptide. For all other immunoprecipitation reactions, pre-cleared extract was incubated with 1 µg of primary antibody at 4^{o}C for 4 h. 20 µl of Protein A/G PLUS-Agarose was added to the lysate and incubated at 4^{o}C overnight, with gentle rocking. After binding, the resins were washed three to four times with RIPA buffer. Immunoprecipitated protein complexes were eluted in 2X Laemmli sample buffer.

MTS assay

The number of metabolically active cells was assessed by the 3-(4,5-dimethylthiazol-2-yl)-5-(3-carboxymethoxyphenyl)-2-(4-sulfophenyl)-2H-tetrazolium (MTS)–based colorimetric assay. Cells were incubated for 4 days with indicated amounts of drug at a seeding density of 1×10^5 cells/ml in triplicate. The amount of MTS, which is converted to a formazan product represents the number of viable cells. The degree of the conversion was determined by measuring the absorbance at a wavelength of 490 nm.

Caspase-3 assay

For Fas-mediated apoptosis, 293-K1 and 293-Vec stable cells were transfected with siRNAs using Superfect (Qiagen). At 36 h posttransfection, the transfected cells were stimulated with anti-Fas cross-linking antibody (clone CH11, Millipore) at 0.2 μg/ml in 1% fetal bovine serum, and cells were harvested 12 h later (50). Apoptosis was analyzed by using an ApoAlert caspase-3 fluorimetric assay kit from Clontech. Absorbance was read on a FLUOstar Optima fluorometric plate reader with a 400-nm excitation and 505-nm emission filter.

Cell-cycle analysis

Cells fixed in 70% ethanol were resuspended in PBS with 20 μg/mL propidium iodide and 200 μg/mL RNaseA. Flow cytometric analysis was performed with a Becton Dickinson FACScan and ModFitLT V3.2.1 program.

Immunohistochemistry

Tumors from SCID mice injected with BC-1 cells as previously described (2, 46) were excised and mixed in 10% neutral buffered formalin. Tumors were paraffin-embedded and 5-

μm sections were prepared on slides. Slides were deparaffinized using Histochoice Clearing Agent (Sigma) and re-hydrated using graded ethanol, followed by extensive washing with water. Endogenous peroxidase activity was quenched with 3% H_2O_2 in 10% methanol solution, and antigens were exposed by heating sections for 10 minutes in 1 mM EDTA (pH 8.0), and cooled to room temperature. Non-specific antigens were blocked using a blocking buffer (10% normal horse serum [Vector Labs], 5% BSA, and 0.3% TritonX-100) for 1 h at room temperature, followed by overnight incubation at 4^{o}C in blocking buffer containing anti-K1 antibody (1:100 dilution), a kind gift from Dr. Jae Jung, or anti-Hsp90 (1: 10 dilution) (Abcam). Sections incubated in blocking buffer lacking primary antibody were used as negative controls. Sections were washed in PBS, incubated with biotinylated goat secondary antibody (anti-rabbit for K1 and anti-mouse for Hsp90), followed by 1 h incubation in pre-formed Avidin DH- biotinylated horseradish peroxidase H complexes (Vectastain ABC kit, Vector Labs), after which sections were stained with Vector NovaRed substrate or NovaDab substrate, and washed. Sections were counterstained with hematoxylin (Invitrogen), dehydrated using graded alcohols, and mounted using Cytoseal XYL (Richard-Allan Scientific). Dried slides were imaged using a LEICA DM LA histology microscope and LEICA Firecam software.

Confocal immunofluorescence microscopy

BCBL-1 cells were air-dried on slides, fixed in 1% paraformaldehyde and permeabilized with 0.1% Triton X-100. The cells were then blocked with 1:10 goat sera and 1% BSA in PBS, and then incubated overnight with primary antibodies in PBS with 1% BSA. Slides incubated in PBS with 1% BSA lacking primary antibody were used as negative controls.

After several washes in PBS with 1% BSA, the cells were incubated with species-specific fluorophore-conjugated secondary antibodies for 30 min, followed by counterstained with 0.1X DAPI. Slides were mounted with Vetashield (Zymed Labs), coverslipped, and imaged using ZEN 2009 program with the Olympus BX61 confocal microscope.

RESULTS

Tandem affinity purification identifies Hsp90β and Hsp40 (Erdj3) as cellular binding partners of K1.

In order to identify cellular binding partners of K1 in the context of mammalian cells, we performed tandem affinity purification (TAP) (41) since it preserves the endogenous milieu of cellular proteins, and the two sequential column purification steps provide high stringency. We cloned the FLAG and HA epitopes in tandem right after the signal peptide sequence in the N-terminus of K1 using PCR. The double-tagged K1 gene was expressed by the pcDNA3 vector. Stable 293 cells expressing FLAG HA tadem tagged K1 (293-K1) or empty vector (293-Vec) were generated by transfection using FuGENE 6 reagent (Roche) and selection with 1 mg/ml G418 for two weeks. The stable cells were maintained under 1 mg/ml G418 selection. Robust expression of K1 and successful detection of the FLAG and HA epitopes were verified by Western blots.

For tandem affinity purification, forty confluent T175 flasks per stable cell line were harvested and lysed in Nonidet P-40 (NP40) buffer (Invitrogen) supplemented with protease inhibitor cocktail (Roche) and phosphatase inhibitor cocktails (Sigma). The protein lysates (20 mg/ml) were centrifuged and the supernatants were subjected to tandem affinity purification at 4^{o}C as follows. The protein lysates were incubated with anti-FLAG resin overnight with gentle rocking and then transferred to a Spin column. Non-specific, unbound proteins were removing by washing the anti-FLAG resin three times with NP40 supplemented with protease and phosphatase inhibitors. After washing, protein complexes were eluted twice with 150 ng/µl 3X FLAG peptide and then pooled. The elutions were then

subjected to binding to anti-HA resin in a Spin column overnight with gentle rocking. Unbound proteins were removing by washing the anti-HA resin three times with NP40 supplemented with protease and phosphatase inhibitors. Proteins bound to the anti-HA resin were eluted in 2X Laemmli Sample Buffer (LSB) (Sigma) and resolved on a 12% NuPAGE Novex Bis-Tris Mini Gel (Invitrogen) with MOPS SDS Running Buffer (Invitrogen). The gel was Coomassie-stained; protein bands unique to K1 expressing cells were excised, trypsin-digested, and subjected to MALDI-TOF Mass spectrometry analysis (Fig. 1A).

Mass spectrometry identified Hsp90β and the ER-associated Hsp40 (Erdj3) as cellular binding partners of K1 (Fig. 1A). Importantly, the specific protein bands for both Hsp90β and Hsp40 were only visible in the K1 lanes, but not in the empty vector (pcDNA3) lanes (Fig. 1A). Furthermore, the digested peptides fully matched the peptide sequences of Hsp90β and Hsp40 (Erdj3) and achieved very high ion scores (Fig. 1B).

A

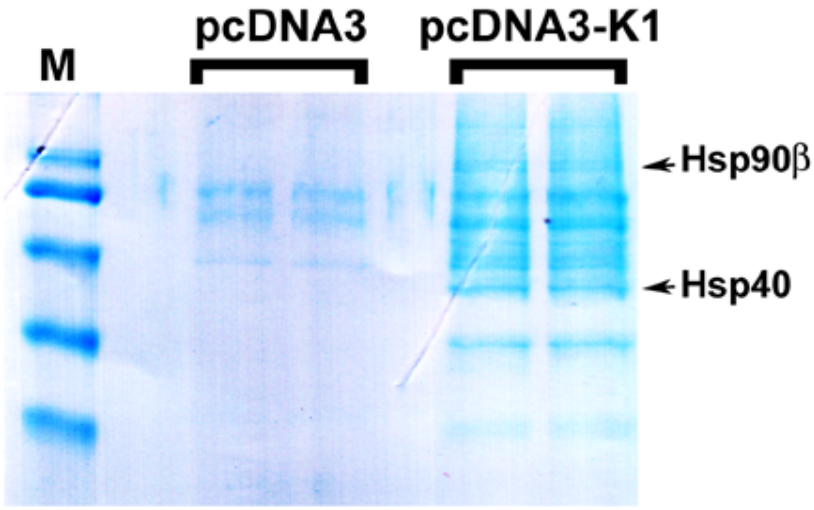

B

Summary of Hsp90β and Hsp40 proteins identified by MALDI-TOF Mass Spectrometry

ACCESSION	PROTEIN IDENTITY	MATCHED/ TOTAL PEPTIDES	PEPTIDE SEQUENCED ION SCORE
CAI20095	heat shock protein 90kDa alpha (cytosolic), class B member 1	15/15	305
T52073	ER-associated Hsp40 co-chaperone - human	19/19	707

Protein spots shown above achieved a Mowse score above the significance threshold ($p < 0.05$).

Figure 1. TAP identified Hsp90β and ER-associated Hsp40 as cellular binding partners of K1. ***A.*** A Coomassie-stained gel of the K1 cellular partners identified by TAP is shown. After TAP, eluted proteins were resolved by SDS-PAGE and visualized by Coomassie staining. Protein bands unique to K1 expressing cells were excised and subjected to MALDI-TOF mass spectrometry (MS). M denotes marker. ***B.*** MS/MS data for the protein identities of Hsp90β and ER-associated Hsp40 are shown.

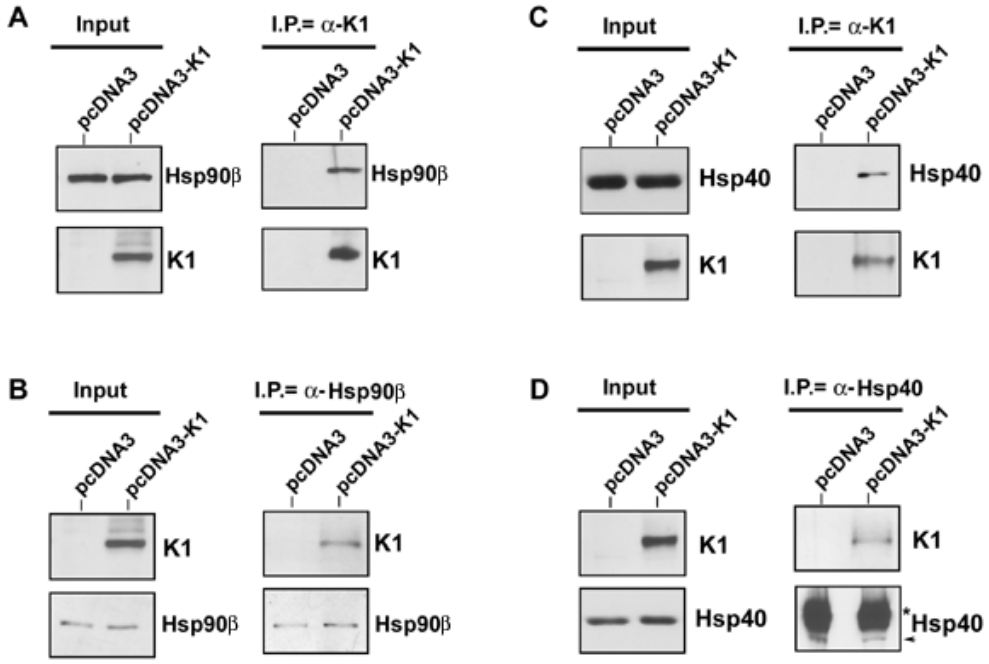

Figure 2. K1 interacts with endogenous Hsp90β and ER-associated Hsp40. ***A.*** Protein lysates from stable 293 cells expressing empty control vector (left lanes) or FLAG-K1 (right lanes) were immunoprecipitated with anti-FLAG antibody. Immunoprecipitation reactions were subjected to SDS-PAGE followed by Western blotting with an anti-Hsp90β antibody. Input lysates showed the presence of Hsp90β in all cell lysates, and K1 protein in the 293-K1 cell lysate. ***B.*** Reverse co-immunoprecipitations were also performed. Lysates from 293-Vec or 293-K1 stable cells were immunoprecipitated with an anti-Hsp90β antibody. Immunoprecipitations were subjected to SDS-PAGE and WB analysis with an anti-FLAG antibody to detect K1 protein expression. Input lysates showed the presence of Hsp90β in all cell lysates, and K1 protein in the 293-K1 cell lysate. These data are representative of at least three independent experiments. ***C. & D.*** Identical co-immunoprecipitations were performed as indicated in panels A and B, respectively, except that anti-Hsp40 antibody was used instead of Hsp90β antibody.

To confirm the TAP results, equivalent micrograms of 293-K1 and 293-Vec lysates were precleared with normal mouse immunoglobulin (Santa Cruz) and protein A/G beads (Santa Cruz) and then used to perform immunoprecipitation with anti-FLAG agarose beads (Sigma) overnight. (Figs. 2A and 2C). The immunoprecipitates were subjected to Western blot analysis with anti-Hsp90β (Fig. 2A) or anti-Erdj3 antibody (Fig. 2C). Interactions of K1

with endogenous Hsp90β and Erdj3 were confirmed by reverse co-immunoprecipitation using anti-Hsp90β (Fig. 2B) or anti-Erdj3/Hsp40 (Fig. 2D), followed by immunoblotting with an anti-FLAG antibody to detect K1 expression. Immunoprecipitation assays performed in both directions strongly corroborated the TAP results, and demonstrated that K1 physically associates with Hsp90β and Erdj3/ER-associated Hsp40. To confirm specificity, we repeated the K1 immunoprecipitation assay with a normal mouse IgG antibody as a negative control. We found that immunoprecipitatons using an anti-FLAG antibody to pull down K1 co-immunoprecipitated Hsp90β and Hsp40, while immunoprecipitation with the control normal mouse IgG antibody did not pull down K1, Hsp90β or Hsp40 (Fig. 3).

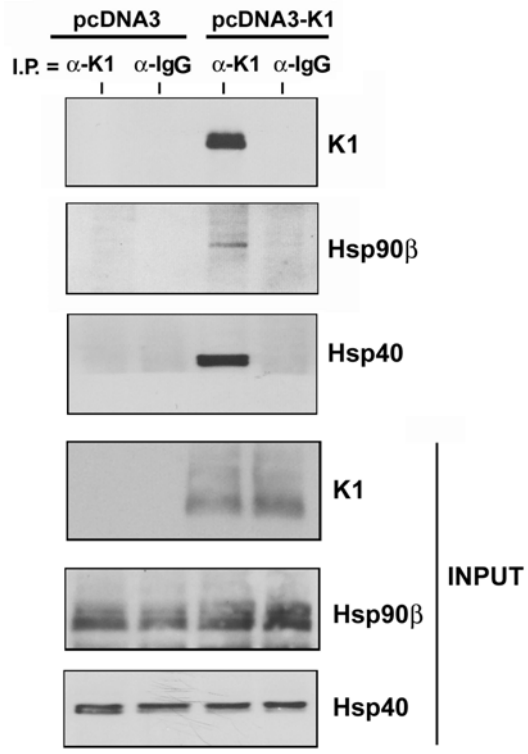

Figure 3. K1 interacts with endogenous Hsp90β and ER-associated Hsp40/Erdj3. Protein lysates from stable 293 cells expressing empty pcDNA3 vector (left 2 lanes) or FLAG-K1 (right 2 lanes) were immunoprecipitated with anti-FLAG antibody or anti-normal mouse IgG. Immunoprecipitates and inputs were subjected to SDS-PAGE followed by Western blots for Hsp90β, Hsp40 or K1. Input lysates show the presence of Hsp90β and Hsp40 in all cell lysates, and K1 protein in the 293-K1 cell lysate only.

Since Hsp90α and Hsp90β show >80% identity and each isoform possesses chaperoning activity (37), we also investigated whether K1 could interact with Hsp90α. Hsp90β is the constitutive form, whereas Hsp90α is more inducible and has been found in the medium and on the cell surface (37). We immunoprecipitated K1 using anti-FLAG resin beads from pre-cleared 293-K1 and 293-Vec lysates, and performed Western blot analysis using anti-Hsp90α antibody. We found that K1 associated with Hsp90α (Fig. 4), indicating that K1 can interact with both α and β isoforms of Hsp90.

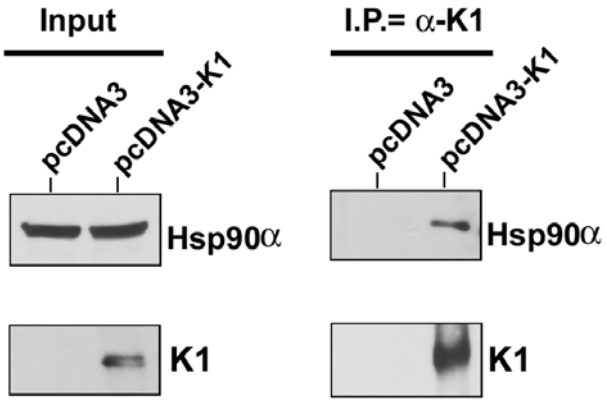

Figure 4. K1 interacts with endogenous Hsp90α. Protein lysates from 293 cells expressing empty control vector (left lane) or FLAG-K1 (right lane) were immunoprecipitated with anti-FLAG antibody. Immunoprecipitation reactions were subjected to SDS-PAGE followed by Western blots for Hsp90α or K1. Input lysates showed the presence of Hsp90α in all cell lysates, and K1 protein in the 293-K1 cell lysate only.

We next investigated whether K1 interacts with heat shock proteins other than Hsp40 and Hsp90. We immunoprecipitated K1 from 293-K1 stable cells with an anti-FLAG antibody. The immunoprecipitates were subjected to Western blot analysis with an anti-Hsp70 antibody (Fig. 5A). We found that K1 failed to interact with Hsp70 suggesting that K1 specifically interacts with Hsp90 and Erdj3/Hsp40.

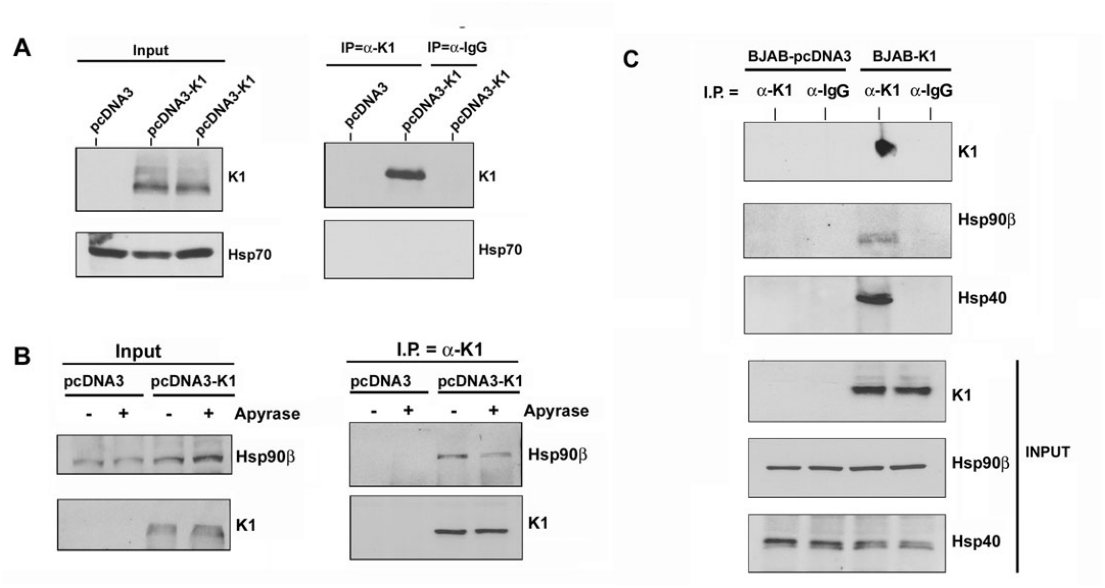

Figure 5. K1 interacts with Hsp90β and Erdj3/Hsp40 in both 293 and BJAB cells. ***A.*** Protein lysates from stable 293 cells expressing empty pcDNA3 control vector or FLAG-K1 were immunoprecipitated with anti-FLAG or control anti-normal mouse Ig antibody. Immunoprecipitation reactions were subjected to SDS-PAGE followed by Western blotting with an anti-Hsp70 antibody. Input lanes show the presence of Hsp70 in all protein lysates and K1 protein in the 293-K1 lysate only. ***B.*** Protein lysates from stable 293-Vec or 293-K1 cells after treatment with vehicle or apyrase were immunoprecipitated with anti-FLAG antibody. Immunoprecipitation reactions were subjected to SDS-PAGE followed by Western blotting with an anti-Hsp90β antibody. ***C.*** Identical co-immunoprecipitations were performed as described in Fig. 2A, except that protein lysates from BJAB B cells transfected with pcDNA3 vector or K1 expression plasmid were immunoprecipitated with anti-FLAG antibody. Immunoprecipitates were subjected to SDS-PAGE followed by Western blotting with an anti-Hsp90β antibody. Input lysates showed the presence of Hsp90β in all cell lysates, and K1 protein in the 293-K1 cell lysate. Immunoprecipitation was also performed with species-matched normal IgG antibody as a negative control.

Hsp90 possesses intrinsic ATPase activity critical for its chaperoning function (35). Apyrase catalyzes the breakdown of ATP and ADP into AMP and inorganic phosphate thereby depleting the ATP content in cells (36, 58). We investigated whether K1's interaction with Hsp90β was dependent on the presence of ATP. We incubated 293-K1 or 293-Vec stable cell lysates with 20 units/ml of apyrase for 30 min, in order to deplete ATP from the samples (36). The ATP-depleted extracts were used to immunoprecipitate K1 and the

immunoprecipitates were subjected to immunoblotting with an anti-Hsp90β (Fig. 5B) or anti-Erdj3/Hsp40 antibody. Notably, ATP depletion by apyrase resulted in less Hsp90β protein being immunoprecipitated with K1 (Fig. 5B), suggesting that ATP levels (and possibly Hsp90 hydrolysis of ATP) modulate K1's interaction with Hsp90β. Interestingly, apyrase treatment did not alter the interaction of K1 with Erdj3/Hsp40, which lacks ATPase activity (data not shown).

Given that K1 expression can be detected in B cells and that K1 perturbs B cell signaling and function, we examined if K1 could interact with Hsp90β and Erdj3/Hsp40 in B cells. Lysates from BJAB cells transfected with FLAG-tagged K1 or pcDNA3 vector plasmids were subjected to immunoprecipitation using an anti-FLAG antibody to pull down K1 or normal mouse IgG as a negative control (Fig. 5C). The K1 immunoprecipitates as well as the input lysates were subjected to Western blot analysis to detect K1, Hsp90β, or Erdj3/Hsp40 (Fig. 5C). Similar to the situation in 293 epithelial cells, we detected specific interactions of Hsp90β with K1 and Erdj3 with K1 in B cells which suggests that these interactions might be relevant in KSHV-associated B lymphoproliferative diseases such as PEL and MCD.

To corroborate the above findings, we also performed co-localization assays for K1 and Hsp90 or Erdj3 in KSHV-positive BCBL-1 cells. Briefly, BCBL-1 were fixed, permeabilized, and then stained with anti-K1 antibody and anti-Hsp90/anti-Erdj3 antibody and examined by confocal microscopy. We found that K1 colocalizes with Hsp90 and Erdj3/Hsp40 (Fig. 6). Additionally, we performed immunohistochemistry on PEL tumor sections (Fig. 7). We found that both K1 and Hsp90 proteins were detected by immunohistochemical staining of tumor sections (Fig. 7).

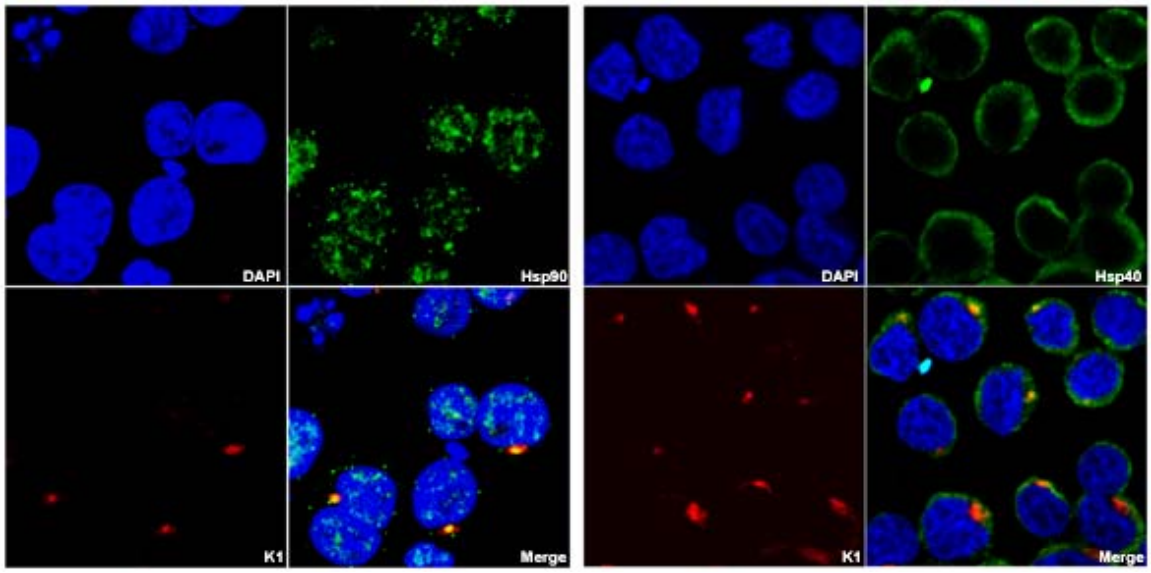

Figure 6. Co-localization of endogenous K1 and Hsp90 or Hsp40/Erdj3 in BCBL-1 cells. BCBL-1 cells were fixed, permeabilized, and subjected to labeling with (i) anti-K1 antibody followed by anti-rabbit IgG-TRITC (ii) anti-Hsp90 antibody followed by anti-mouse IgG-FITC or (iii) anti-Hsp40/Erdj3 followed by anti-goat IgG-FITC. Nuclei were counterstained with DAPI and slides were mounted in Vectashield. Images were taken at 126X and analyzed by confocal microscopy using ZEN 2009 program. For each set, the upper left quadrant shows DAPI (blue); upper right quadrant shows Hsp90 or Hsp40 (green); lower left quadrant shows K1 (red); lower right quadrant shows the merged image. Cells were also stained with no primary antibody and only secondary antibody as a negative control (not shown).

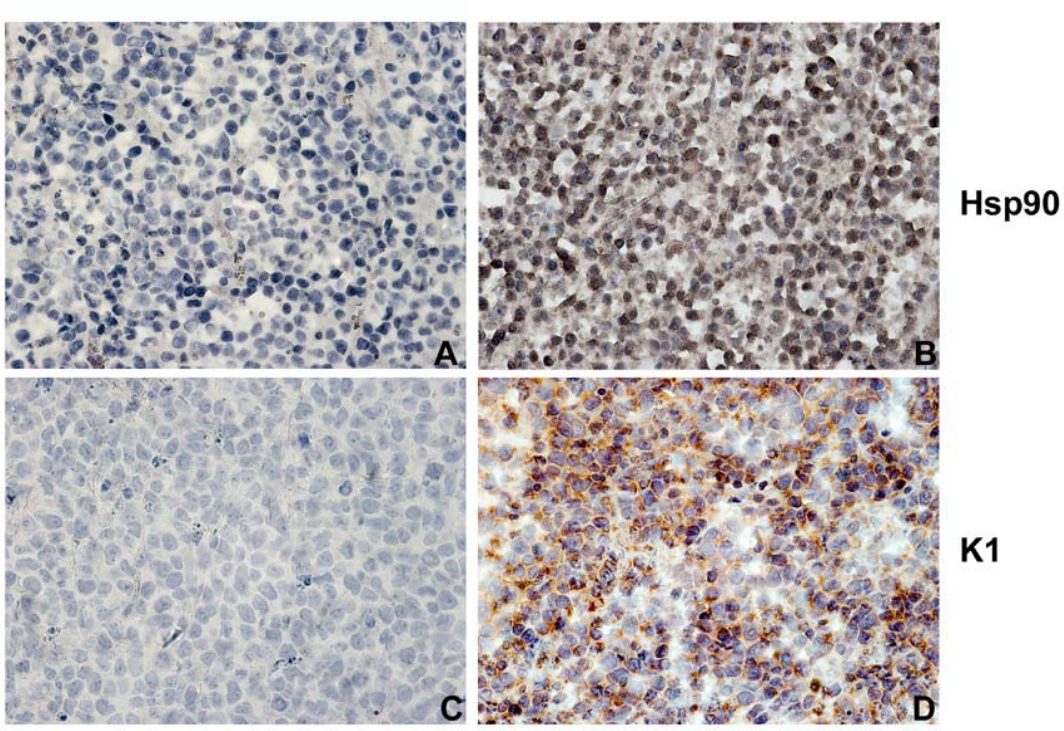

Figure 7. Detection of K1 and Hsp90 in PEL tumors. BC-1 tumors grown in xenografted mice were sectioned and stained with antibodies against K1 or Hsp90. BC-1 tumor sections were stained with Hsp90 antibody followed by NovaDAB secondary antibody (brown stain; panel ***B***) and with K1 antibody followed by NovaRed secondary antibody (red; panel ***D***). Sections that were stained with only secondary antibodies but no primary antibodies for either Hsp90 (Panel ***A***) or K1 (panel ***C***) showed no positive staining. The tissue sections in all four panels were counterstained with hematoxylin (blue).

Hsp90β and Erdj3/Hsp40 associate with the N-terminal domain of K1.

To gain insight into the function and topology of the interaction, we used a panel of FLAG-tagged K1 domain deletion constructs ((ΔC, C-terminal deletion; ΔTM, transmembrane deletion; ΔN, N-terminal deletion)) to determine the K1 domain that interacted with Hsp90β and the ER-associated Hsp40. These constructs were derived from the previously described FLAG-tagged pcDNA3-K1 plasmid (53). In brief, a restriction site was added to both ends of a domain to be deleted by QuikChange site-directed mutagenesis (QIAGEN). The domain deletion mutants were created by restriction digestion and re-

ligation. Expression plasmids for the K1 deletion mutants, the FLAG-tagged wild-type K1, and the control pcDNA3 vector, were transiently transfected into 293 cells. Protein lysates were harvested 48 h post-transfection. Co-immunoprecipitations for K1 with Hsp90β and Hsp40 were performed as described above for Fig. 2. FLAG-tagged K1 was immunoprecipitated with anti-FLAG beads, followed by immunoblotting with anti-Hsp90β (Fig. 8A) or anti-Hsp40/Erdj3 antibody (Fig. 8C). Hsp90β and Hsp40 were detected in all of the samples expressing K1 except for the sample expressing the K1ΔN mutant. Additionally, the reverse immunoprecipitation of Hsp90β (Fig. 8B) or Hsp40 (Fig. 8D) followed by Western blot analysis with anti-FLAG antibody also suggested that the K1ΔN mutant protein does not interact with Hsp90β or Hsp40. Collectively, our data suggest that the N-terminal domain of K1 interacts with the Hsp90β and Hsp40/Erdj3 molecular chaperones.

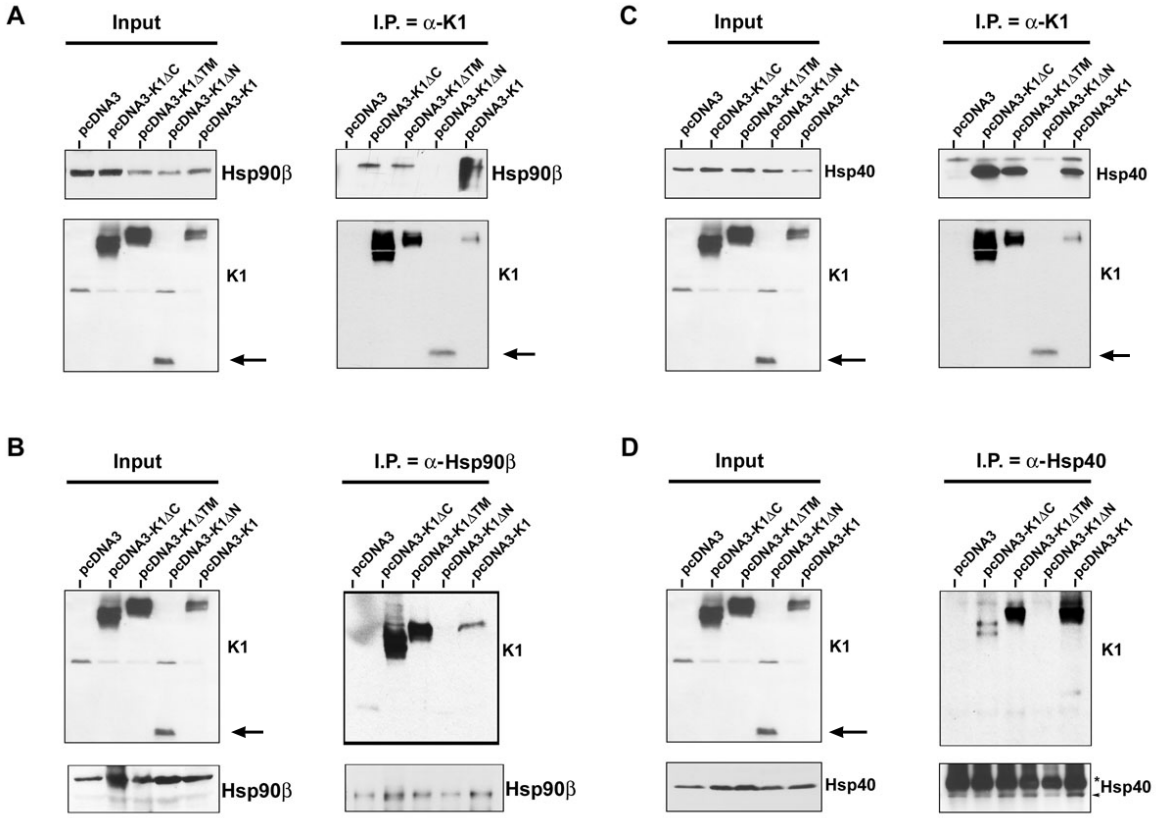

Figure 8. K1 interacts with endogenous Hsp90β and ER-associated Hsp40 through its N-terminus. ***A.*** Co-immunoprecipitation of a panel of K1 constructs with endogenous Hsp90β. 293 cells were transfected with the empty vector or a panel of FLAG-K1 domain deletion mutants (ΔC: C-terminal deletion; ΔTM: transmembrane deletion; ΔN: N-terminal deletion), or the full-length FLAG-K1. Lysates were immunoprecipitated with anti-FLAG resin. Immunoprecipitation reactions were subjected to SDS-PAGE and Western blotting with an anti-Hsp90β antibody. Input lysates showed the presence of Hsp90β in all cell lysates and the presence of K1 mutants in the K1 mutant transfected cells. ***B.*** Reverse co-immunoprecipitations were also performed. Lysates from cells transfected with the vector control or the K1 panel of mutants were immunoprecipitated with an anti-Hsp90β antibody. Immunoprecipitation reactions were subjected to Western blot analysis with an anti-FLAG antibody to detect K1 protein expression. Input lysates showed the presence of Hsp90β in all cell lysates and the presence of K1 mutants in the K1 mutant transfected cells. These data are representative of at least three independent experiments. ***C. & D.*** Identical co-immunoprecipitations were performed as indicated in panels A and B, respectively, except that anti-Hsp40 antibody was used instead of Hsp90β antibody. In panels A-D, arrows indicate the N-terminal deletion mutant of K1.

K1 protein expression is dependent on Hsp90 activity.

As heat shock proteins are molecular chaperones that confer protein stability to their client proteins, we next tested whether the chaperoning activity of Hsp90 affected K1 protein expression. The ansamycin antibiotic, geldanamycin (GA), was used to inhibit the ATPase activity of Hsp90, an activity that is essential for its chaperoning function. Thus, GA prevents the transfer of client proteins to Hsp90. GA inhibits all isoforms of Hsp90, but not Hsp40. After GA treatment, client proteins of Hsp90 are degraded by the proteasomal machinery (55, 57). We treated stable 293-K1 or 293-Vec cells with 1 μM GA, or the vehicle DMSO, for 6 h under serum-starving. Lysates were harvested and subjected to immunoblotting. We found that pharmacological inhibition of Hsp90 with 1μM GA in 293-K1 cells dramatically decreased K1 protein level when compared to DMSO treatment (Fig. 9A). Expectedly, the protein level of phosphorylated Akt (S473), a known client protein of Hsp90 (57), was also diminished in the presence of GA.

We previously reported that K1 can activate and phosphorylate Akt in B and endothelial cells (50, 52). Here we observed the same phenomenon in epithelial cells, where 293-K1 cells showed increased p-Akt (S473) levels compared to 293-Vec samples (Fig. 9A). We next tested whether K1 had any effect on the endogenous levels of Hsp90β and ER-associated Hsp40. Western blot analysis of 293-K1 and 293-Vec cell lysates did not show an appreciable difference in Hsp90β and Hsp40 protein abundance, albeit the total Akt and p-Akt (S473) levels were increased in K1-expressing 293 cells (Fig. 9B).

siRNA-mediated depletion of Hsp90β or ER-associated Hsp40/Erdj3 reduces K1 protein expression.

To confirm the results obtained with pharmacological inhibition of Hsp90, and to rule out any off-target effects of GA that may lead to decreased K1 protein levels, we performed genetic knockdown of Hsp90β or Erdj3/ER-associated Hsp40 using siRNAs. Briefly, 293-K1 cells were transfected) using Superfect reagent (QIAGEN) with 200pmol of pooled Stealth Hsp90β-targeting siRNAs (Invitrogen) or a control luciferase-targeting siRNA (siLUC) (Thermo Scientific). Cells were harvested 48 h post-transfection and the protein lysates were subjected to Western blot analysis. The Hsp90β siRNAs (siHsp90β-1 or siHsp90β-1&2) robustly depleted the endogenous level of Hsp90β without affecting endogenous actin levels (Fig. 9C). Similar to GA treatment, Hsp90β siRNA expression resulted in a reduction of K1 protein expression compared to control luciferase siRNA (Fig. 9C). Hsp90β siRNA knockdown also led to reduced total Akt and p-Akt (S473) levels.

We also tested if K1 protein level is dependent upon ER-associated Hsp40/Erdj3 expression. Using Superfect transfection reagent (QIAGEN), 293-K1 cells were transfected with a pool of three different siRNAs directed against Hsp40/Erdj3 (siHsp40 in Fig. 9D) (Invitrogen) or the irrelevant siLUC (Thermo Scientific) for 48 h. The protein lysates were then subjected to immunoblotting. As shown in Fig. 9D, the pooled siHsp40 siRNAs effectively reduced the endogenous level of Hsp40/Erdj3 compared to the siLUC transfected sample, but did not alter endogenous actin levels. We found that siRNA knockdown of Hsp40/Erdj3 also inhibited K1 protein expression and was accompanied by a slight reduction of the total Akt and p-Akt (S473) levels (Fig. 9D). Taken together, these data suggest that

Hsp90 and Erdj3 are required for the protein stability of K1, and that K1 is a client protein of Hsp90 and the Hsp40/Hsp70 chaperone system.

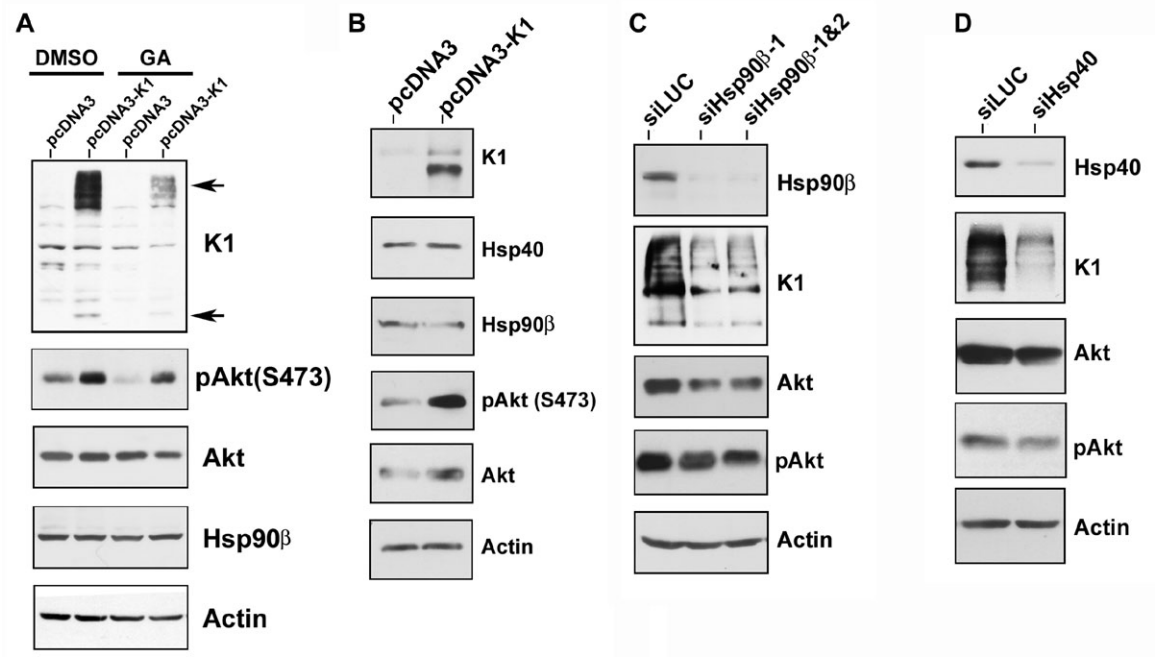

Figure 9. K1 protein expression is dependent on Hsp90 activity and the endogenous levels of Hsp90β and ER-associated Hsp40. ***A.*** Stable 293-Vec cells expressing empty control vector (pcDNA3) or 293-K1 cells expressing FLAG-K1 were treated with 1 μM of the Hsp90 inhibitor, geldanamycin (GA), or DMSO (vehicle), for 6 h in the absence of serum. Cell lysates were harvested and resolved by SDS-PAGE and immunoblotting. Western blots were probed with the indicated antibodies. Arrows indicate monomeric and multimeric forms of the K1 protein. ***B.*** K1 does not affect the endogenous levels of Hsp90β and Hsp40**.** Stable 293-K1 or 293-Vec cell lysates were subjected to SDS-PAGE and Western blot analysis using the indicated antibodies. Each panel is representative of at least three independent experiments. ***C.*** 293-K1 cells were subjected to siRNA targeting luciferase (siLUC; control), or Hsp90β (siHsp90β-1 or siHsp90β-1&2) for 48 h. Cell lysates were harvested and subjected to SDS-PAGE and Western blot analysis. ***D.*** 293-K1 cells were subjected to siRNA targeting luciferase (siLUC; control) or a pool of siRNAs targeting ER-associated Hsp40 (siHsp40) for 48 h. Cell lysates were harvested and subjected to SDS-PAGE and Western blot analysis.

Interaction with Hsp90β and Erdj3 regulates K1 anti-apoptotic function.

We next interrogated whether Hsp90β and Erdj3's association with K1 can modulate its function. In order to examine the impact of Hsp90β or Erdj3 knockdown on K1 function,

we tested the ability of K1 to prevent Fas-mediated apoptosis (1, 50, 54) in the presence of Hsp90β and/or Erdj3 siRNAs (Invitrogen) described above. 293-K1 or 293-Vec cells were transfected with 200 pmol of siRNAs targeting Erdj3 and/or Hsp90β, or K1. To control for any undesirable effect of siRNA transfection on apoptosis, non-targeting siRNA, as well as a GFP-targeting siRNA were used for comparison. Thirty-six hours post-siRNA transfection, the cells were subjected to Fas-receptor antibody stimulation for 12 h to stimulate Fas-receptor dependent apoptosis. Equivalent number of cells (1×10^6) were trypsinized and centrifuged. The pellets were lysed and subjected to a fluorescence-based assay that measures caspase-3 activity as a readout of apoptosis (50). Absorbance was read by the FLUOstar OPTIMA fluorometric plate reader with a 400-nm excitation and 505-nm emission filter. Caspase-3 activity in the antibody stimulated 293-K1 cells was calculated as a percent of the caspase-3 activity in the antibody stimulated 293-Vec control cells. Fig. 10A shows the percent of activated caspase-3 detected in the Fas antibody-stimulated 293-K1 cells compared to the stimulated 293-Vec cells with the same siRNA transfection. Overall, the 293-K1 cells displayed a fifty percent decrease in caspase-3 activation compared to the 293-Vec cells, after Fas-receptor stimulation. This is in concordance with what we and others have previously reported (1, 50, 54). Transfection of either Hsp90β siRNA, Hsp40/Erdj3 siRNA, GFP siRNA, or non-targeting siRNA into the 293-K1 cells, followed by anti-Fas-receptor antibody stimulation, yielded similar levels of caspase-3 activity in these cells (Fig. 10A) indicating that single knockdown of either the Hsp90β or Hsp40 chaperone did not alter K1's ability to prevent Fas-mediated apoptosis. However, when both Hsp90β siRNAs and Hsp40/Erdj3 siRNAs were co-transfected into 293-K1 and 293-Vec cells, the 293-K1 cells now displayed similar levels of caspase-3 activity as the 293-Vec cells (Fig. 10A), suggesting

that both Hsp90β and Erdj3 are required for K1 to exert its anti-apoptotic function, and that knockdown of both chaperones increases the sensitivity of K1-expressing cells to Fas-mediated apoptosis.

In order to look at the role of Hsp90β and Hsp40/Erdj3 on K1's ability to prevent cell death, we repeated the experiment with Fas antibody stimulation but extended the incubation time with the antibody to 18 h (instead of 12 h) to analyze cell death of 293-K1 versus 293-Vec cells transfected with the indicated siRNAs (Fig .10B). Cells were stained with trypan blue and the numbers of viable and dead cells were counted under microscopy in four different fields. Cell death in the Fas antibody stimulated 293-K1 cells was calculated as a percentage of cell death seen in 293-Vec cells stimulated with the same antibody. Overall, the trend in Fig. 10B recapitulates that in Fig. 10A. As a control, a Western blot of K1 expression in 293-K1 cells transfected with siLUC versus K1 siRNA is depicted in Fig. 10C to show effective knockdown of K1 protein levels in the K1 siRNA transfected cells.

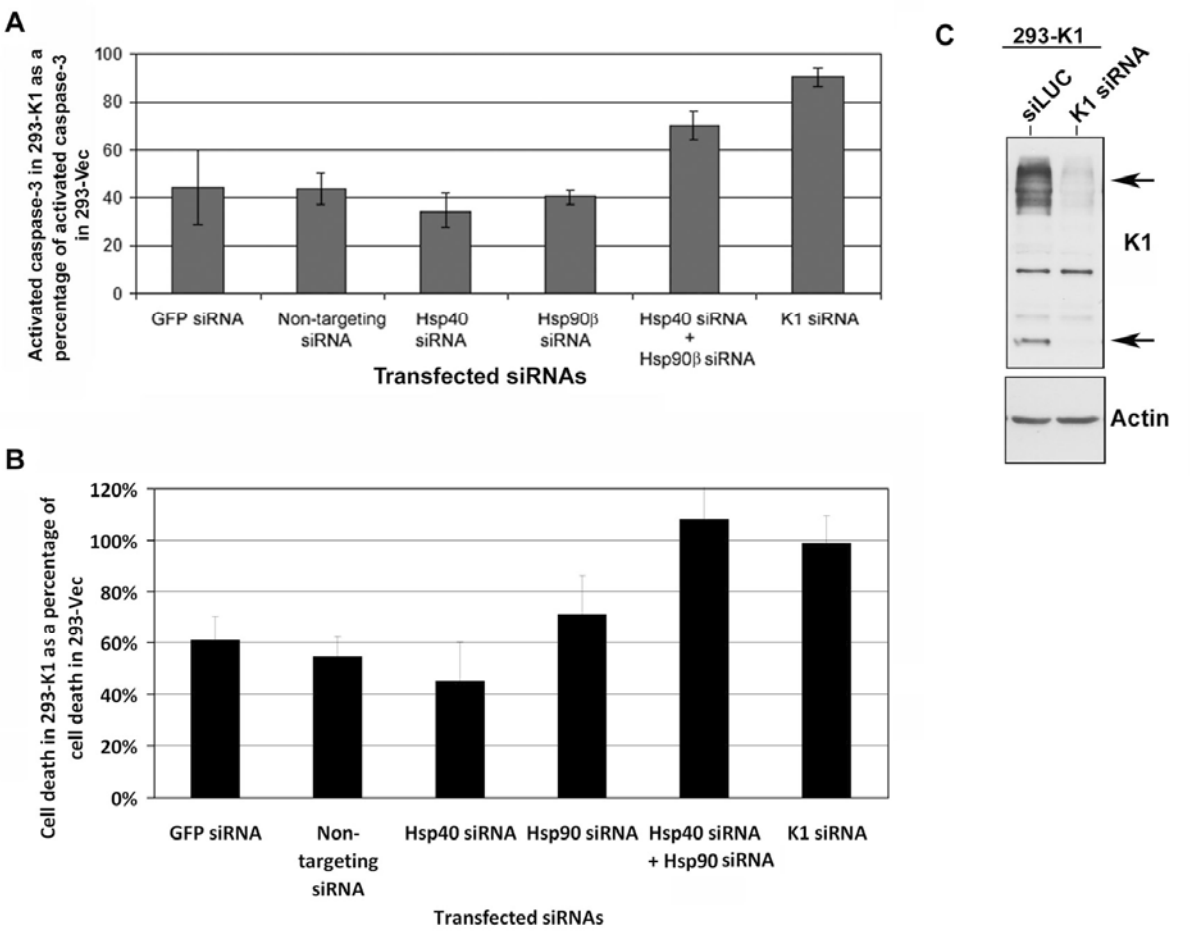

Figure 10. K1 anti-apoptotic function is dependent on the endogenous levels of Hsp90β and ER-associated Hsp40. ***A.*** 293-K1 and 293-Vec stable cells were transfected with the indicated panel of siRNAs. At 36 h post-transfection, anti-Fas antibody was added for 12 h to simulate Fas-receptor-dependent apoptosis. Cells were harvested and subjected to a fluorescence-based caspase-3 assay. Caspase-3 activity was measured using the caspase-3 fluorescent substrate**,** DEVD-AMC. Percent caspase-3 activity in 293-K1 cells compared to 293-Vec cells is plotted on the y-axis, and the siRNA transfected samples are depicted on the x-axis. Error bars represent standard deviations from the mean. The graphs are representative of three independent experiments. ***B.*** The experimental setup was identical to that in panel A, except Fas-antibody induction time was increased to 18 h. Cells were then stained with Trypan blue and counted using a hemocytometer. Each sample was performed in quadruplicate. Cell death in 293-K1 cells was plotted as a percentage of cell death in 293-Vec cells. Error bars represent standard deviations from the mean. ***C.*** 293-K1 cells were transfected with K1 siRNA or control siLUC for 48 h. Protein lysates were subjected to SDS-PAGE and Western blot analysis using an anti-FLAG or actin antibody.

Hsp90 inhibitors decrease the proliferation of KSHV-positive PEL-derived B cell lines *in vitro.*

Because Hsp90 and the ER-associated Hsp40 regulate the protein expression and anti-apoptotic function of K1, we wanted to determine if Hsp90 inhibitors can block proliferation of KSHV-positive PEL cells. PEL cells have previously been shown to express K1 transcripts and protein at low levels (4, 25). We treated PEL cells with DMSO (vehicle control) or 50 nM of the GA-derived Hsp90 inhibitors, 17-AAG and 17-DMAG, that are currently in clinical trials (14, 17) for 0, 24, 48, 72, and 96 hours. We found that both inhibitors suppressed the growth of KSHV-harboring PEL cell lines, BCP-1, BCBL-1, and JSC-1, in a MTS-based cell proliferation assay (Fig. 11A). We also determined the half-maximal inhibitory concentration (IC_{50}) of 17-AAG and 17-DMAG in BCP-1, BCBL-1, and JSC-1 cell lines 72 h post-treatment. The IC_{50} of 17-AAG and 17-DMAG were ~50 nM and ~10 nM, respectively, in all three cell lines (Fig. 11B and 11C). These IC_{50} values are consistent with other tumor cell lines that are dependent on Hsp90 (15). Hence, 17-AAG and 17-DMAG can effectively inhibit KSHV-infected primary effusion lymphoma cell lines *in vitro*. We also investigated the effects of 17-DMAG on 293-K1 cells compared to 293-Vec cells. $1x10^6$ 293-K1 and 293-Vec cells were incubated with 100 nM of 17-DMAG and a Trypan blue exclusion assay was performed at 24, 48 and 72 hours post-treatment. We found that at all three time points tested, there were more live cells present in the 293-K1 cells compared to the 293-Vec cells. This suggests that K1 confers a survival advantage to 293 cells upon Hsp90 inhibition (Fig. 12) and that higher concentrations of drug are required to inhibit K1-expressing 293 cells compared to 293 cells that do not express the K1 protein.

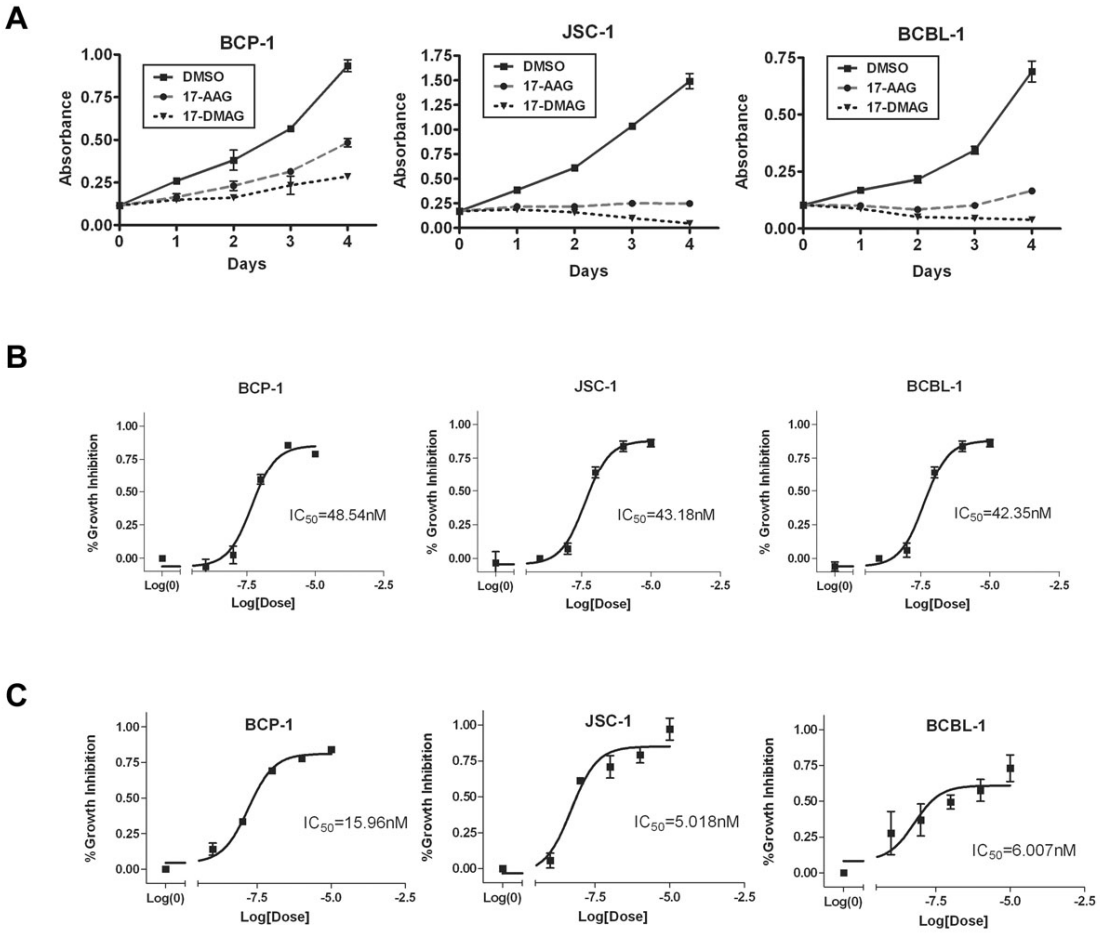

[

Figure 11. The Hsp90 inhibitors, 17-AAG and 17-DMAG, inhibit the proliferation of KSHV-positive PEL cell lines. ***A.*** BCP-1, JSC-1, and BCBL-1 were incubated with 50 nM of 17-AAG or 17-DMAG and subjected to a MTS assay over a period of four days. The absorbance at 490 nm in the presence of 50 nM of 17-AAG or 17-DMAG, or equivalent volume of vehicle control (DMSO) is shown on the vertical axis, and time in days after addition of the drugs is shown on the horizontal axis. Error bars represent standard deviation from the mean. ***B.*** IC_{50} values of 17-AAG on BCP-1, JSC-1, and BCBL-1 were determined after 72 h incubation with 17-AAG. A range of concentrations of 17-AAG was used: 0, 1, 10, 100, 1000, or 10000 nM. A nonlinear fit, sigmoidal curve was generated by plotting percent growth inhibition against the log concentration of 17-AAG. Error bars represent SEM. ***C.*** IC_{50} values of 17-DMAG on BCP-1, JSC-1, and BCBL-1 were determined by MTS assays after 72 h incubation with 17-DMAG.

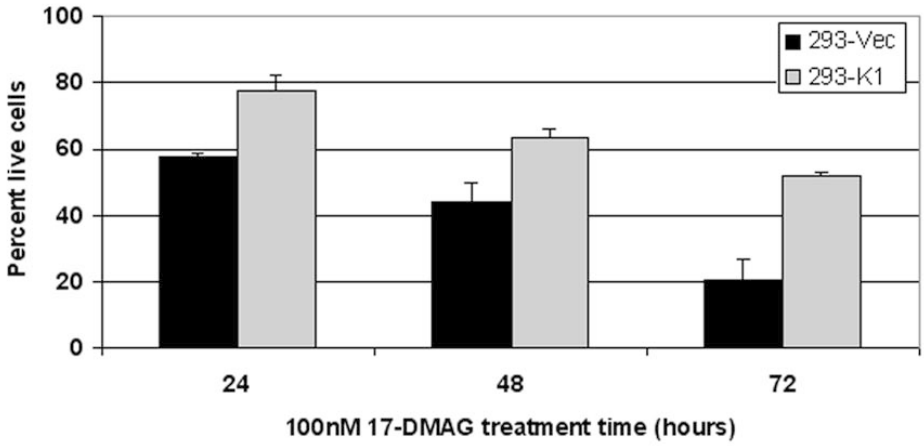

Figure 12. 293-Vec cells are more sensitive to Hsp90 inhibition than 293-K1 cells. 293-K1 or 293-Vec cells were incubated with 17-DMAG for the indicated time-points. Cells were trypsinized, stained with Trypan blue and counted using a hematocytometer. The percentage of lives cells was plotted on the y-axis and the incubation time-points are depicted on the x-axis. Error bars represent standard deviations from the mean.

To address whether the decrease in proliferation of 50 nM 17-AAG and 17-DMAG is due to the induction of cell death, we treated the same three PEL lines above with 50 nM or 500 nM of each inhibitor, or DMSO, for 0, 24, 48, 72, and 96 h and assessed cell viability by a Trypan blue exclusion assay. We found that 500 nM of 17-AAG and 17-DMAG induced an increase in cell death of PEL cells over time (Fig. 13A). In agreement with this observation, we have found that the LC_{50} values of 17-AAG and 17-DMAG in BCP-1 are 464.4 nM and 523.5 nM, respectively (Fig. 13B & 13C) at 72 hours post-treatment. We also confirmed that similar to GA treatment (Fig. 9A), treatment of 293-K1 cells with 500 nM of 17-DMAG inhibited K1 protein expression compared to 293-K1 cells treated with vehicle (DMSO) (Fig. 13D).

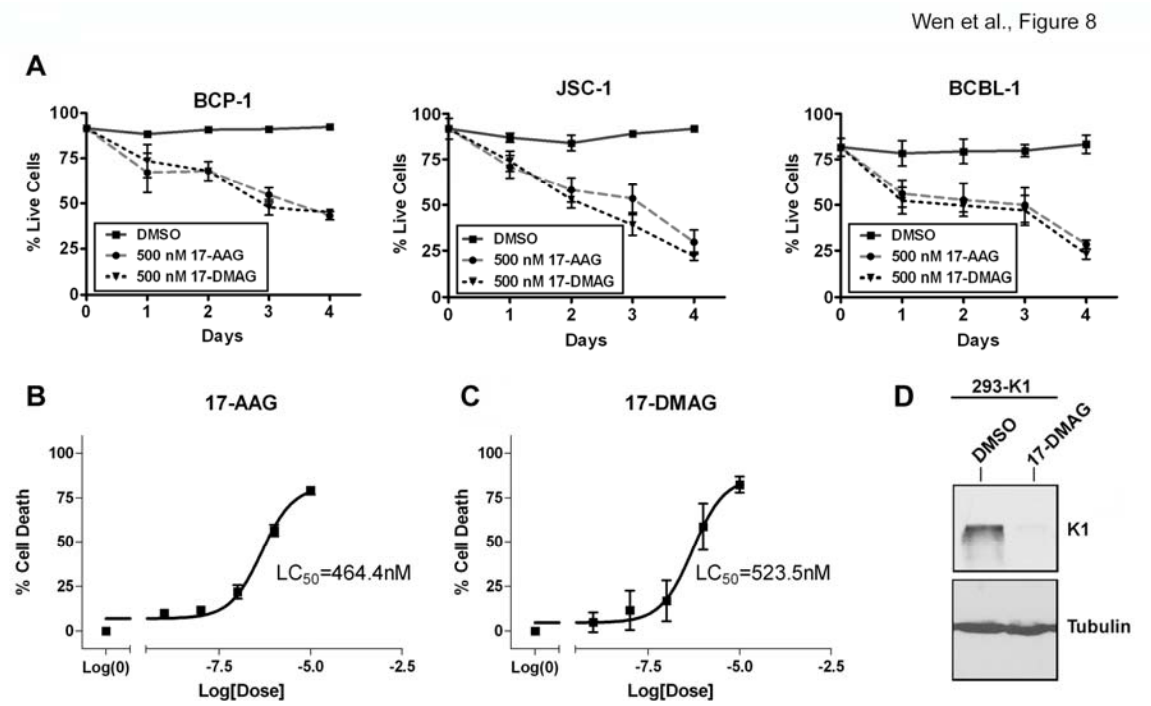

Figure 13. The Hsp90 inhibitors, 17-AAG and 17-DMAG, induce cell death of KSHV-positive PEL cell lines. *A.* BCP-1, JSC-1, and BCBL-1 were incubated with 500 nM of 17-AAG, 17-DMAG, or the equivalent volume of DMSO, and subjected to a Trypan blue exclusion assay over a period of four days. The cells were stained with Trypan blue and counted at the indicated timepoints. Live cells were plotted as a percentage of total cells on the y-axis and the time periods of incubation with 17-AAG or 17-DMAG is depicted on the x-axis. Error bars represent standard deviation from the mean. ***B.*** LC_{50} value of 17-AAG on BCP-1was determined after 72 h incubation with 17-AAG. A range of concentrations of 17-AAG was used: 0, 1, 10, 100, 1000, or 10000 nM. A nonlinear fit, sigmoidal curve was generated by plotting percent growth inhibition against the log concentration of 17-AAG. Error bars represent SEM. ***C.*** LC_{50} value of 17-DMAG on BCP-1 was determined in the same manner as in panel B, except that 17-DMAG was used instead of 17-AAG. ***D.*** 293-K1 cells were treated with 500 nM of 17-DMAG or DMSO vehicle for 72 h. Protein lysates were subjected to SDS-PAGE and Western blot analysis using an anti-FLAG antibody to detect K1 protein levels. An anti-tubulin blot is shown as a control.

On the basis of the inhibitory effect of 17-AAG/17-DMAG on PEL cell proliferation, we speculated that both Hsp90 inhibitors may alter the cell cycle of PEL. We performed cell cycle analysis to address this possibility. JSC-1 and BCBL-1 were treated with 50 nM 17-AAG and 17-DMAG for 48 h, and then subjected to propidium staining and flow cytometry. Both PEL cell lines displayed significant G0/G1 arrest and suppressed DNA synthesis upon Hsp90 inhibition (Fig. 14). 17-DMAG was a stronger inhibitor of the cell cycle than 17-AAG (Fig. 14). Thus, the cell cycle arrest phenotype seen in the presence of 17-AAG and 17-DMAG corroborates the inhibition of cell proliferation we observed in the MTS assay for the different PEL cell lines (Fig. 11).

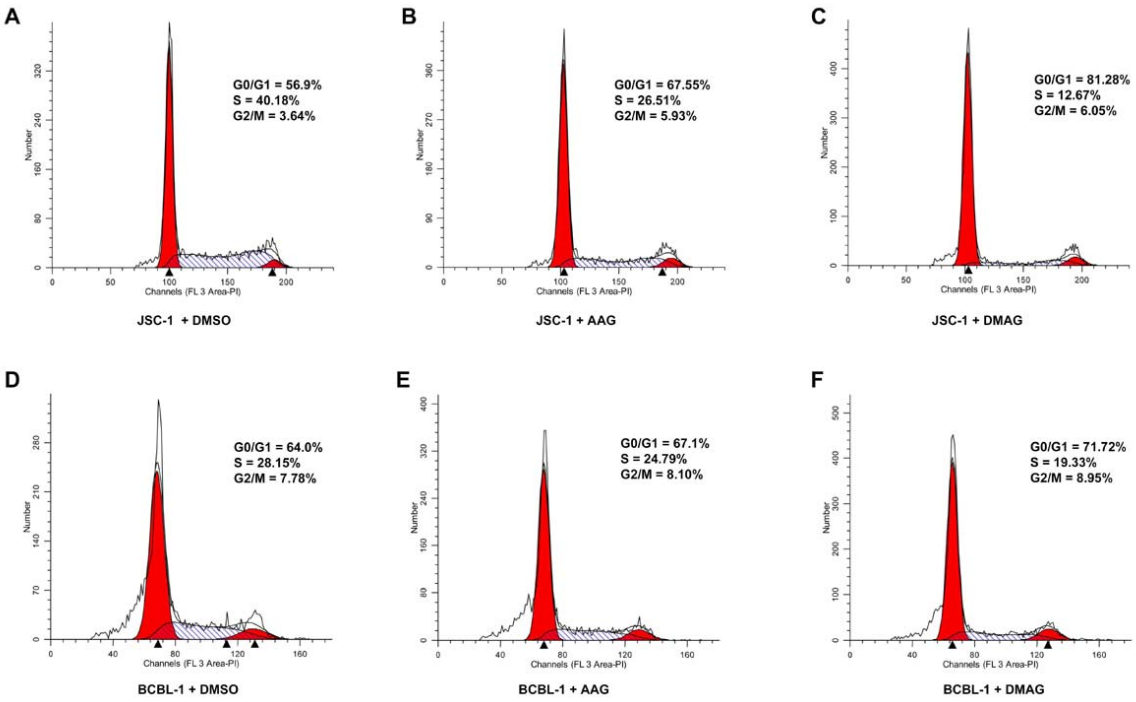

Figure 14. 17-AAG and 17-DMAG induce G0/G1 arrest of KSHV-positive PEL cell lines. 1 x 10^6 live JSC-1 (***A-C***) and BCBL-1 (***D-F***) were incubated with 50 nM of 17-AAG (***B & E***), 17-DMAG, (***C & F***) or equivalent volume of DMSO (***A & D***) for 48 h. The cells were washed with 1X PBS, fixed in 70% ethanol, and stained with propidium iodide and subjected to cell cycle analysis using flow cytometry. The percentages of cells at different stages in the cell cycle (G0/G1, S, G2/M) are shown.

DISCUSSION

KSHV K1 is a viral oncoprotein that has been shown to transform cells, induce tumor formation (9, 40), as well as inhibit apoptosis (1, 50, 54). Furthermore, the K1 protein activates the PI3K/Akt signaling pathway in endothelial cells and B cells (50, 52). Despite the known signal transduction pathway and functions of K1, relatively little is known about how K1 protein expression and function are modulated. Using tandem affinity purification, we identified Hsp90β and the ER-associated Hsp40/Erdj3 protein as cellular partners of K1. This was corroborated by co-immunoprecipitations that confirmed these protein-protein interactions. Importantly, we have shown that K1's interaction with Hsp90β (but not Hsp40/Erdj3) is dependent on the presence of ATP. We also found that K1 can interact with the Hsp90α isoform. The K1-Hsp90 interaction is relevant, as both Hsp90 and K1 have individually been shown to modulate the phosphorylation or function of several important signaling molecules such as VEGF receptor (23, 52, 53), Akt (19, 50, 52), Lyn (39, 40, 51, 56), PDK1 (30, 52), BCR (24, 44, 49), and mTOR (33, 52).

In KSHV, as well as other herpesviruses, Hsp90 also regulates subcellular trafficking and function of viral proteins (5, 11, 16). A novel finding of this report is that K1 appears to be a viral client protein of Hsp90 and the ER-associated Hsp40/Hsp70 system. This is particularly intriguing as it suggests that the protein expression of the K1 viral oncogene can be manipulated with existing Hsp90 inhibitors as well as siRNA/small hairpin RNA targeting against Hsp90 and/or Hsp40/Erdj3 chaperones. In addition, we have shown that K1 interacts and colocalizes with Hsp90 and Hsp40/Erdj3 in B cells. K1 and Hsp90 expression can also be detected in PEL tumors. Thus, our data validate Hsp90 as an important therapeutic target for treating KSHV-associated lymphomas.

Using the Hsp90 inhibitor GA, we showed that Hsp90 ATPase activity and chaperoning function are required for optimal expression of K1. GA inhibits all the known Hsp90 homologs, including cytosolic/extracellular Hsp90α and Hsp90β, as well as Grp94/Gp96 (ER-associated Hsp90), and Trap1 (mitochondria-associated Hsp90). Thus, it is possible that Hsp90 homologs other than Hsp90α and Hsp90β may also associate with K1 and modulate its expression and function. Similar to GA treatment, genetic knockdown of either Hsp90β or Hsp40/Erdj3 using siRNA also dramatically reduced K1 protein expression.

We found that depletion of both endogenous Hsp90β and ER-associated Hsp40 negated the ability of K1 to prevent Fas-mediated apoptosis. However, depletion of only Hsp90β or Hsp40 by itself had no effect. One explanation is that knockdown of both Hsp90β and Hsp40 reduced K1 expression levels more robustly than single knockdowns of these proteins. A second possibility is that there are two different pools of K1 whose expression and/or function are regulated by Hsp90β and Hsp40. K1 has been shown to be expressed on the plasma membrane as well as in the ER (24). Since Hsp90β is predominantly cytosolic and Hsp40/Erdj3 is ER-associated, one may speculate that these different pools of K1 are topologically distinct. Hence, knockdown of the ER-restricted chaperone may reduce K1 levels in the ER, but not affect cytosolic or cell surface levels of K1, and *vice versa*. Thus, single knockdowns of either Hsp90β or Hsp40/Erdj3 may not have reduced K1 protein levels in all cellular compartments to the same extent as double knockdowns of both these chaperones.

Our finding that the N-terminal domain of K1 interacts with Hsp90β and Hsp40 also added an extra layer of complexity to the interaction. Besides being cytosolic, Hsp90α (10, 29) and Hsp90β (45) have been found on the cell surface i.e. extracellularly. Thus, the N-

terminal domain of K1 may co-internalize with extracellular Hsp90. Since K1 internalization has been linked to its signaling function (49), Hsp90 likely plays a role in chaperoning K1 as it is endocytosed. Additionally, since the N-terminal domain of K1 interacts with Hsp90β, it is also possible that Hsp90β interacts with the K1 N-terminus during *de novo* biogenesis of K1 protein when the growing peptide is transiting from the cytoplasm to the ER. Indeed, Hsp90β has been shown to be involved in the protein translation of the BCR (44). Furthermore, since the ER-associated Hsp40/Erdj3 functions as a co-chaperone with Hsp70/BiP for unfolded/nascent proteins, including the unassembled immunoglobulin heavy chain (43), Hsp40/Erdj3 may also participate in the folding of newly synthesized/unfolded or misfolded K1 within the ER.

Our data show that Hsp90 inhibition by 17-AAG and 17-DMAG at low concentrations results in decreased cell proliferation and G0/G1 arrest, albeit at higher concentrations, 17-AAG and 17-DMAG can also induce cell death of KSHV-positive PEL cells. A potential mechanism for these observations is that Hsp90 inhibition leads to a decrease in K1 protein expression, and this has a two pronged effect on the PI3K/Akt/mTOR pathway. This is because Hsp90 inhibition suppresses activation of the PI3K/Akt/mTOR pathway that is normally activated by the K1 viral oncoprotein, and indirectly by Hsp90 through stabilization of and maintenance of Akt kinase activity. Because PI3K, Akt, and mTOR are cell survival kinases, inhibition of Hsp90 destabilizes K1 protein and suppresses its ability to enhance PEL cell proliferation and cell survival through this pathway. This model would predict that Hsp90 inhibition would lead to decreased proliferation of cells that do not express K1 compared to proliferation of cells that do express K1. Indeed, we observed

that more 293-K1 cells survived in the presence of Hsp90 inhibitor compared to 293-Vec cells (Fig. 12).

We also speculate that there are several other KSHV proteins that utilize molecular chaperones to modulate their expression and function. Field *et al*. previously reported that the KSHV latent viral FLICE inhibitory protein (vFLIP) requires Hsp90 to complex with IκB kinase (IKK) and activate the NF-κB pathway (11). Here we report that both Hsp90 and Hsp40 chaperones were needed for K1 protein expression and its anti-apoptotic function. Taken together, our studies provide additional rationale for using Hsp90 inhibitors to treat PEL and other KSHV-related malignancies.

ACKNOWLEDGMENTS

We thank Prasanna Bhende for help with immunohistochemistry and cell cycle analysis and Stuart Krall for technical assistance. We thank Dr. Jae Jung for providing us with the anti-K1 antibody. We thank members of the Damania and Dittmer labs for informative discussions. We also thank the UNC Proteomics Center for processing of the protein samples and subsequent mass spectroscopy analysis. This work was supported by NIH grant CA096500 to BD. KWW was supported in part by NIAID training grant T32-AI007001 and MSTP grant T32-GM008719. BD is a Leukemia & Lymphoma Society Scholar and Burroughs Welcome Fund Investigator in Infectious Disease.

REFERENCES

1. **Berkova, Z., S. Wang, J. F. Wise, H. Maeng, Y. Ji, and F. Samaniego.** 2009. Mechanism of Fas signaling regulation by human herpesvirus 8 K1 oncoprotein. J Natl Cancer Inst **101:**399-411.

2. **Bhatt, A. P., P. M. Bhende, S. H. Sin, D. P. Dittmer, and D. B.** 2010. Dual Inhibition of PI3K & mTOR Inhibits Autocrine and Paracrine Proliferative Loops in PI3K/Akt/mTOR-addicted Lymphomas. Blood (in press).

3. **Bilello, J. P., S. M. Lang, F. Wang, J. C. Aster, and R. C. Desrosiers.** 2006. Infection and persistence of rhesus monkey rhadinovirus in immortalized B-cell lines. J Virol **80:**3644-9.

4. **Bowser, B. S., S. M. DeWire, and B. Damania.** 2002. Transcriptional regulation of the K1 gene product of Kaposi's sarcoma-associated herpesvirus. J Virol **76:**12574-83.

5. **Burch, A. D., and S. K. Weller.** 2005. Herpes simplex virus type 1 DNA polymerase requires the mammalian chaperone hsp90 for proper localization to the nucleus. J Virol **79:**10740-9.

6. **Cesarman, E., Y. Chang, P. S. Moore, J. W. Said, and D. M. Knowles.** 1995. Kaposi's sarcoma-associated herpesvirus-like DNA sequences in AIDS-related body-cavity-based lymphomas. N Engl J Med **332:**1186-91.

7. **Chang, Y., E. Cesarman, M. S. Pessin, F. Lee, J. Culpepper, D. M. Knowles, and P. S. Moore.** 1994. Identification of herpesvirus-like DNA sequences in AIDS-associated Kaposi's sarcoma. Science **266:**1865-9.

8. **Damania, B., M. DeMaria, J. U. Jung, and R. C. Desrosiers.** 2000. Activation of lymphocyte signaling by the R1 protein of rhesus monkey rhadinovirus. J Virol **74:**2721-30.

9. **Damania, B., M. Li, J. K. Choi, L. Alexander, J. U. Jung, and R. C. Desrosiers.** 1999. Identification of the R1 oncogene and its protein product from the rhadinovirus of rhesus monkeys. J Virol **73:**5123-31.

10. **Eustace, B. K., T. Sakurai, J. K. Stewart, D. Yimlamai, C. Unger, C. Zehetmeier, B. Lain, C. Torella, S. W. Henning, G. Beste, B. T. Scroggins, L. Neckers, L. L. Ilag, and D. G. Jay.** 2004. Functional proteomic screens reveal an essential extracellular role for hsp90 alpha in cancer cell invasiveness. Nat Cell Biol **6:**507-14.

11. **Field, N., W. Low, M. Daniels, S. Howell, L. Daviet, C. Boshoff, and M. Collins.** 2003. KSHV vFLIP binds to IKK-gamma to activate IKK. J Cell Sci **116:**3721-8.

12. **Gao, T., and A. C. Newton.** 2002. The turn motif is a phosphorylation switch that regulates the binding of Hsp70 to protein kinase C. J Biol Chem **277:**31585-92.

13. **Gessain, A., A. Sudaka, J. Briere, N. Fouchard, M. A. Nicola, B. Rio, M. Arborio, X. Troussard, J. Audouin, J. Diebold, and G. de The.** 1996. Kaposi sarcoma-associated herpes-like virus (human herpesvirus type 8) DNA sequences in multicentric Castleman's disease: is there any relevant association in non-human immunodeficiency virus-infected patients? Blood **87:**414-6.

14. **Goetz, M. P., D. Toft, J. Reid, M. Ames, B. Stensgard, S. Safgren, A. A. Adjei, J. Sloan, P. Atherton, V. Vasile, S. Salazaar, A. Adjei, G. Croghan, and C. Erlichman.** 2005. Phase I trial of 17-allylamino-17-demethoxygeldanamycin in patients with advanced cancer. J Clin Oncol **23:**1078-87.

15. **Hollingshead, M., M. Alley, A. M. Burger, S. Borgel, C. Pacula-Cox, H. H. Fiebig, and E. A. Sausville.** 2005. In vivo antitumor efficacy of 17-DMAG (17-dimethylaminoethylamino-17-demethoxygeldanamycin hydrochloride), a water-soluble geldanamycin derivative. Cancer Chemother Pharmacol **56:**115-25.

16. **Iscovich, J., A. Fischbein, J. Fisher-Fischbein, L. S. Freedman, S. M. Eng, P. Boffetta, A. Vudovich, C. Glasman, R. Goldschmidt, M. Livingston, B. Heger-Maslansky, P. Brennan, and P. S. Moore.** 2000. Seroprevalence of Kaposi's sarcoma-associated herpesvirus in healthy adults in Israel. Anticancer Res **20:**2119-22.

17. **Ivy, P. S., and M. Schoenfeldt.** 2004. Clinical trials referral resource. Current clinical trials of 17-AG and 17-DMAG. Oncology (Williston Park) **18:**610, 615, 619-20.

18. **Jenner, R. G., M. M. Alba, C. Boshoff, and P. Kellam.** 2001. Kaposi's sarcoma-associated herpesvirus latent and lytic gene expression as revealed by DNA arrays. J Virol **75:**891-902.

19. **Katano, H., Y. Sato, T. Kurata, S. Mori, and T. Sata.** 2000. Expression and localization of human herpesvirus 8-encoded proteins in primary effusion lymphoma, Kaposi's sarcoma, and multicentric Castleman's disease. Virology **269:**335-44.

20. **Lagunoff, M., and D. Ganem.** 1997. The structure and coding organization of the genomic termini of Kaposi's sarcoma-associated herpesvirus. Virology **236:**147-54.

21. **Lagunoff, M., D. M. Lukac, and D. Ganem.** 2001. Immunoreceptor tyrosine-based activation motif-dependent signaling by Kaposi's sarcoma-associated herpesvirus K1 protein: effects on lytic viral replication. J Virol **75:**5891-8.

22. **Lagunoff, M., R. Majeti, A. Weiss, and D. Ganem.** 1999. Deregulated signal transduction by the K1 gene product of Kaposi's sarcoma-associated herpesvirus. Proc Natl Acad Sci U S A **96:**5704-9.

23. **Le Boeuf, F., F. Houle, and J. Huot.** 2004. Regulation of vascular endothelial growth factor receptor 2-mediated phosphorylation of focal adhesion kinase by heat shock protein 90 and Src kinase activities. J Biol Chem **279:**39175-85.

24. **Lee, B. S., X. Alvarez, S. Ishido, A. A. Lackner, and J. U. Jung.** 2000. Inhibition of intracellular transport of B cell antigen receptor complexes by Kaposi's sarcoma-associated herpesvirus K1. J Exp Med **192:**11-21.

25. **Lee, B. S., M. Connole, Z. Tang, N. L. Harris, and J. U. Jung.** 2003. Structural analysis of the Kaposi's sarcoma-associated herpesvirus K1 protein. J Virol **77:**8072-86.

26. **Lee, H., J. Guo, M. Li, J. K. Choi, M. DeMaria, M. Rosenzweig, and J. U. Jung.** 1998. Identification of an immunoreceptor tyrosine-based activation motif of K1 transforming protein of Kaposi's sarcoma-associated herpesvirus. Mol Cell Biol **18:**5219-28.

27. **Lee, H., R. Veazey, K. Williams, M. Li, J. Guo, F. Neipel, B. Fleckenstein, A. Lackner, R. C. Desrosiers, and J. U. Jung.** 1998. Deregulation of cell growth by the K1 gene of Kaposi's sarcoma-associated herpesvirus. Nat Med **4:**435-40.

28. **Lewis, J., A. Devin, A. Miller, Y. Lin, Y. Rodriguez, L. Neckers, and Z. G. Liu.** 2000. Disruption of hsp90 function results in degradation of the death domain kinase, receptor-interacting protein (RIP), and blockage of tumor necrosis factor-induced nuclear factor-kappaB activation. J Biol Chem **275:**10519-26.

29. **Li, W., Y. Li, S. Guan, J. Fan, C. F. Cheng, A. M. Bright, C. Chinn, M. Chen, and D. T. Woodley.** 2007. Extracellular heat shock protein-90alpha: linking hypoxia to skin cell motility and wound healing. Embo J **26:**1221-33.

30. **Matsumura, S., Y. Fujita, E. Gomez, N. Tanese, and A. C. Wilson.** 2005. Activation of the Kaposi's sarcoma-associated herpesvirus major latency locus by the lytic switch protein RTA (ORF50). J Virol **79:**8493-505.

31. **Murthy, S. C., J. J. Trimble, and R. C. Desrosiers.** 1989. Deletion mutants of herpesvirus saimiri define an open reading frame necessary for transformation. J Virol **63:**3307-14.

32. **Nathan, D. F., and S. Lindquist.** 1995. Mutational analysis of Hsp90 function: interactions with a steroid receptor and a protein kinase. Mol Cell Biol **15:**3917-25.

33. **Ohji, G., S. Hidayat, A. Nakashima, C. Tokunaga, N. Oshiro, K. Yoshino, K. Yokono, U. Kikkawa, and K. Yonezawa.** 2006. Suppression of the mTOR-raptor signaling pathway by the inhibitor of heat shock protein 90 geldanamycin. J Biochem **139:**129-35.

34. **Pang, Q., W. Keeble, T. A. Christianson, G. R. Faulkner, and G. C. Bagby.** 2001. FANCC interacts with Hsp70 to protect hematopoietic cells from IFN-gamma/TNF-alpha-mediated cytotoxicity. Embo J **20:**4478-89.

35. **Pearl, L. H., and C. Prodromou.** 2006. Structure and mechanism of the Hsp90 molecular chaperone machinery. Annu Rev Biochem **75:**271-94.

36. **Pedersen, C. B., P. Bross, V. S. Winter, T. J. Corydon, L. Bolund, K. Bartlett, J. Vockley, and N. Gregersen.** 2003. Misfolding, degradation, and aggregation of variant proteins. The molecular pathogenesis of short chain acyl-CoA dehydrogenase (SCAD) deficiency. J Biol Chem **278:**47449-58.

37. **Picard, D.** 2004. Hsp90 invades the outside. Nat Cell Biol **6:**479-80.

38. **Picard, D., B. Khursheed, M. J. Garabedian, M. G. Fortin, S. Lindquist, and K. R. Yamamoto.** 1990. Reduced levels of hsp90 compromise steroid receptor action in vivo. Nature **348:**166-8.

39. **Prakash, O., O. R. Swamy, X. Peng, Z. Y. Tang, L. Li, J. E. Larson, J. C. Cohen, J. Gill, G. Farr, S. Wang, and F. Samaniego.** 2005. Activation of Src kinase Lyn by the Kaposi sarcoma-associated herpesvirus K1 protein: implications for lymphomagenesis. Blood **105:**3987-94.

40. **Prakash, O., Z. Y. Tang, X. Peng, R. Coleman, J. Gill, G. Farr, and F. Samaniego.** 2002. Tumorigenesis and aberrant signaling in transgenic mice expressing the human herpesvirus-8 K1 gene. J Natl Cancer Inst **94:**926-35.

41. **Rigaut, G., A. Shevchenko, B. Rutz, M. Wilm, M. Mann, and B. Seraphin.** 1999. A generic protein purification method for protein complex characterization and proteome exploration. Nat Biotechnol **17:**1030-2.

42. **Schmitt, E., M. Gehrmann, M. Brunet, G. Multhoff, and C. Garrido.** 2007. Intracellular and extracellular functions of heat shock proteins: repercussions in cancer therapy. J Leukoc Biol **81:**15-27.

43. **Shen, Y., and L. M. Hendershot.** 2005. ERdj3, a stress-inducible endoplasmic reticulum DnaJ homologue, serves as a cofactor for BiP's interactions with unfolded substrates. Mol Biol Cell **16:**40-50.

44. **Shinozaki, F., M. Minami, T. Chiba, M. Suzuki, K. Yoshimatsu, Y. Ichikawa, K. Terasawa, Y. Emori, K. Matsumoto, T. Kurosaki, A. Nakai, K. Tanaka, and Y. Minami.** 2006. Depletion of hsp90beta induces multiple defects in B cell receptor signaling. J Biol Chem **281:**16361-9.

45. **Sidera, K., M. Samiotaki, E. Yfanti, G. Panayotou, and E. Patsavoudi.** 2004. Involvement of cell surface HSP90 in cell migration reveals a novel role in the developing nervous system. J Biol Chem **279:**45379-88.

46. **Sin, S. H., D. Roy, L. Wang, M. R. Staudt, F. D. Fakhari, D. D. Patel, D. Henry, W. J. Harrington, Jr., B. A. Damania, and D. P. Dittmer.** 2007. Rapamycin is efficacious against primary effusion lymphoma (PEL) cell lines in vivo by inhibiting autocrine signaling. Blood **109:**2165-73.

47. **Smith, D. F., L. Whitesell, S. C. Nair, S. Chen, V. Prapapanich, and R. A. Rimerman.** 1995. Progesterone receptor structure and function altered by geldanamycin, an hsp90-binding agent. Mol Cell Biol **15:**6804-12.

48. **Soulier, J., L. Grollet, E. Oksenhendler, P. Cacoub, D. Cazals-Hatem, P. Babinet, M. F. d'Agay, J. P. Clauvel, M. Raphael, L. Degos, and et al.** 1995. Kaposi's sarcoma-associated herpesvirus-like DNA sequences in multicentric Castleman's disease. Blood **86:**1276-80.

49. **Tomlinson, C. C., and B. Damania.** 2008. Critical role for endocytosis in the regulation of signaling by the Kaposi's sarcoma-associated herpesvirus K1 protein. J Virol **82:**6514-23.

50. **Tomlinson, C. C., and B. Damania.** 2004. The K1 protein of Kaposi's sarcoma-associated herpesvirus activates the Akt signaling pathway. J Virol **78:**1918-27.

51. **Trentin, L., M. Frasson, A. Donella-Deana, F. Frezzato, M. A. Pagano, E. Tibaldi, C. Gattazzo, R. Zambello, G. Semenzato, and A. M. Brunati.** 2008. Geldanamycin-induced Lyn dissociation from aberrant Hsp90-stabilized cytosolic complex is an early event in apoptotic mechanisms in B-chronic lymphocytic leukemia. Blood **112:**4665-74.

52. **Wang, L., D. P. Dittmer, C. C. Tomlinson, F. D. Fakhari, and B. Damania.** 2006. Immortalization of primary endothelial cells by the K1 protein of Kaposi's sarcoma-associated herpesvirus. Cancer Res **66:**3658-66.

53. **Wang, L., N. Wakisaka, C. C. Tomlinson, S. M. DeWire, S. Krall, J. S. Pagano, and B. Damania.** 2004. The Kaposi's sarcoma-associated herpesvirus (KSHV/HHV-8) K1 protein induces expression of angiogenic and invasion factors. Cancer Res **64:**2774-81.

54. **Wang, S., S. Wang, H. Maeng, D. P. Young, O. Prakash, L. E. Fayad, A. Younes, and F. Samaniego.** 2007. K1 protein of human herpesvirus 8 suppresses lymphoma cell Fas-mediated apoptosis. Blood **109:**2174-82.

55. **Whitesell, L., P. Sutphin, W. G. An, T. Schulte, M. V. Blagosklonny, and L. Neckers.** 1997. Geldanamycin-stimulated destabilization of mutated p53 is mediated by the proteasome in vivo. Oncogene **14:**2809-16.

56. **Woodberry, T., T. J. Suscovich, L. M. Henry, J. N. Martin, S. Dollard, P. G. O'Connor, J. K. Davis, D. Osmond, T. H. Lee, D. H. Kedes, A. Khatri, J. Lee, B. D. Walker, D. T. Scadden, and C. Brander.** 2005. Impact of Kaposi sarcoma-associated herpesvirus (KSHV) burden and HIV coinfection on the detection of T cell responses to KSHV ORF73 and ORF65 proteins. J Infect Dis **192:**622-9.

57. **Xu, W., X. Yuan, Y. J. Jung, Y. Yang, A. Basso, N. Rosen, E. J. Chung, J. Trepel, and L. Neckers.** 2003. The heat shock protein 90 inhibitor geldanamycin and the

ErbB inhibitor ZD1839 promote rapid PP1 phosphatase-dependent inactivation of AKT in ErbB2 overexpressing breast cancer cells. Cancer Res **63:**7777-84.

58. **Zhang, C., and C. L. Guy.** 2005. Co-immunoprecipitation of Hsp101 with cytosolic Hsc70. Plant Physiol Biochem **43:**13-8.

CHAPTER 3

FUNCTIONAL ROLE OF THE R1 PROTEIN IN THE LIFECYCLE OF RHESUS RHADINOVIRUS

Kwun Wah Wen[^], Christine C. Tomlinson[^], Zhigang Zhang, John P. Bilello, Ronald C. Desrosiers, and Blossom Damania

[^]*both authors contributed equally to the work*

(A manuscript has been submitted to the Journal of Virology)

ABSTRACT

Rhesus monkey rhadinovirus (RRV) serves as an *in vitro* and an *in vivo* model for Kaposi sarcoma-associated herpesvirus (KSHV/HHV-8). At the far left end of the RRV genome is a distinct open-reading frame (ORF) designated R1 whose position is equivalent to that of the saimiri transforming protein (STP) of herpesvirus saimiri (HVS) and the K1 protein of KSHV. Similar to K1, the R1 cytoplasmic tail contains motifs capable of binding to the SH2 domains of protein kinases, and R1 has previously been shown to be capable of activating B lymphocyte signaling and interacting with the major B cell kinase, Syk. We disrupted the R1 ORF in the RRV genome by inserting a green fluorescence protein (GFP) expression cassette. We compared the replication kinetics of the wild-type virus, a R1-deleted recombinant virus, and a revertant virus by plaque assays and real-time QPCR-based genome quantification assays. We found that deletion of R1 from the RRV genome did not affect viral replication on rhesus fibroblasts. We also examined the ability of the R1-deleted recombinant virus to establish latency in B cells. We found that the R1-deleted recombinant virus was able to establish latency in B cells more efficiently than the wild-type virus and that the R1-deletion mutant underwent less spontaneous reactivation from infected B cells than wild-type RRV.

INTRODUCTION

Kaposi sarcoma-associated herpesvirus (KSHV) is associated with Kaposi sarcoma (KS), primary effusion lymphoma (PEL), and the plasmablastic variant of multicentric Castleman disease (MCD) (5, 7, 33). Rhesus monkey rhadinovirus (RRV) is a close simian relative of KSHV and was isolated from rhesus macaques at the New England Primate Research Center (NEPRC), from RRV strain H26-95 (12). An additional RRV isolate, termed RRV 17577, was identified by the Oregon Regional Primate Research Center (ORPRC) (32). Analysis of the KSHV and RRV genomic sequences revealed that they are highly homologous and co-linear, with the majority of the open-reading frames (ORFs) in the same genomic locations and orientation. All RRV genes have homologs in KSHV (1, 32).

RRV serves as both an *in vitro* and *in vivo* model for KSHV. Studies of many of the RRV ORFs have shown that they function similarly to their KSHV homologs. The availability of a genetic system to make recombinant viruses and the ability of RRV to replicate lytically on rhesus fibroblasts (RhF) and establish latency in B cells enables one to dissect the contribution of individual ORFs to the viral lifecycle. Additionally, the availability of rhesus macaques as an animal model makes RRV an attractive system to study KSHV pathogenesis. Experimental infection of rhesus macaques with RRV results in a lymphadenopathy similar to MCD (27) as well as non-Hodgkin lymphoma (28). In the context of a dual infection with simian immunodeficiency virus (SIV), the animals developed lymphoproliferative disorders and B-cell hyperplasia (39). Mansfield *et al*. reported that RRV also caused an arteriopathy in SIV-infected macaques (27).

The first open-reading frame (ORF) of KSHV encodes the K1 transforming protein (18). K1 is expressed at low levels during latency and is upregulated during lytic infection where it demonstrates early kinetics (6, 9, 21, 22, 31). K1 contains an immunoreceptor tyrosine-based activation motif (ITAM), which is comprised of two appropriately spaced Src Homology 2 (SH2) binding motifs (24, 26). K1 can interact with multiple SH2 domain-containing cellular proteins, including Lyn, Syk, p85 subunit of PI3K, PLCγ2, RasGAP, Vav and Grb2 (40). In B cells, K1 can activate PI3K (p85 subunit), Akt, Vav, and Syk kinases, and induce NFAT and NF-κB transcriptional activities for cell survival and protection from Fas-mediated apoptosis (3, 24, 26, 30, 34). K1 co-internalizes with the BCR (2) and inhibits intracellular BCR transport via ER sequestration resulting in the downregulation of BCR surface expression. Recently, K1 has been shown to interact with the molecular chaperones Hsp90 and ER-associated Hsp40 in B cells as well as epithelial cells (36).

The first ORF of RRV encodes for R1, a homolog of KSHV K1 (10). Similar to K1, R1 can transform rodent fibroblasts and functionally substitute for the saimiri transforming protein (STP) of herpesvirus saimiri (HVS) to immortalize common marmoset peripheral blood mononuclear cells to IL-2-independent growth *in vitro* (11). When R1-expressing rodent fibroblasts were injected into nude mice, these mice developed multifocal and disseminated tumors (11). The C-terminal cytoplasmic tail of R1 is significantly longer than that of K1 but similar to K1, contains several putative SH2 binding motifs and an ITAM (8). Like K1, R1 is capable of activating B lymphocyte signal transduction as evidenced by tyrosine phosphorylation of cellular proteins, calcium

mobilization from intracellular storage, and activation of the transcription factor NFAT (8).

In Chapter Four, we will demonstrate and discuss the conventional virology technique of homologous recombination in mammalian cells to perform reverse genetics. This approach enabled us to disrupt the LANA ORF in order to study its replicative properties in RRV and explore its vaccine potential against gammaherpesviral infection and persistence. In this chapter, we utilized a relatively less laborious approach to genetically manipulating RRV. When performing homologous recombination, one needs to isolate the recombinant virus away from the "contaminating" wild-type or parental virus. Here we introduce the overlapping cosmid system to functionally disrupt the R1 ORF. This system was generated by Bilello *et al*. (4). In brief, overlapping cosmid clones were engineered to encompass the entire genome of RRV H26-95 (~130 kb), including the terminal repeat (TR) regions that are necessary for viral replication. Importantly, RRV particles resulting from co-transfection of these overlapping cosmids spanning the entire RRV H26-95 genome replicated with similar kinetics and titers to the parental, genetically unaltered RRV H26-95 (4). When developing the cosmid set Bilello *et al*. found that the RRV cosmids were too large (>46 kb including terminal repeat regions) for routine genetic manipulation. To that end, they generated a sub-cosmid clone by truncation of the existing ah28 cosmid, allowing for insertion of a reporter gene upstream of the R1 promoter.

We used the same overlapping cosmid system (4) to disrupt the R1 ORF. Using this system, we genetically inserted a GFP expression cassette in the beginning of the R1 ORF to create a R1 deletion virus named RRVΔR1/GFPcc. We also generated a rescue

virus designated Revertant, and compared the replicative properties of recombinant RRVΔR1/GFPcc and Revertant with the wild-type viruses, RRV-J and RRV-GFPcc, in rhesus fibroblasts (RhF) at twodifferent multiplicities of infection (MOI) (1 and 5) using traditional plaque assays as well as real-time PCR-based genome quantification assays. All four viruses exhibited similar replication kinetics during *de novo* infection of rhesus fibroblasts. However, we found that RRVΔR1/GFPcc established latency more efficiently than the wild-type virus RRV-GFPcc in B cells. RRVΔR1/GFPcc also exhibited less spontaneous reactivation compared to RRV-GFPcc.

MATERIALS AND METHODS

Cell culture

Immortalized RhF have been previously described (14). RhF, 293, and 293T cells were maintained at 37°C and 5% CO_2 in Dulbecco's modified eagle medium (DMEM) H plus Gluta-max supplemented with 10% fetal bovine serum (FBS). BJAB cells were maintained in RPMI 1640 supplemented with 10% FBS.

RRV infection of RhF and BJAB B cells

Approximately 3×10^5 RhF were infected with 1 ml of diluted viral stock in DMEM supplemented with 2% FBS as previously described (37). After two hours of incubation, the virus inoculum was aspirated and the cells were cultured in 1.5 ml of DMEM supplemented with 2% FBS. 2×10^5 BJAB cells were spinoculated in flat-bottom 12-well plates with 1.5 ml of diluted viral stock in complete RPMI medium in the presence of 4 μg/ml of polybrene as previously described (37, 38). The cells were washed once with complete RPMI medium and then allowed to grow and expand in complete RPMI medium.

Plaque assays and quantitative real-time PCR were performed as previously described (37).

Cosmid system and generation of recombinant viruses

Construction of the RRV H26-95 cosmid library has been previously described (4). To generate the recombinant RRVΔR1/GFPcc virus, a portion of the R1 ORF was amplified from the ah28ΔA/H cosmid with primers 5'-

CAGCTGGGATCCACTAGTAGTAACACATAGT ATTTC-3’ and 5'-CAGCTGGAATTCATTTAAATGATTGTACTCATTGTG-3'**.** The amplicon was restriction digested with *Bam*HI and *Eco*RI and then ligated into pSP72 vector at the same sites (R1-RRV pSP72). Site-directed mutagenesis was performed to create a new *Sma*I site in the R1 ORF using primers 5'-CACCACATCCCGGGGATACCTACTTGC-3' and 5'-GCAAGTAGGTATCCCCGGGATGTGGTG-3' by QuikChange site-directed mutagenesis kit (Stratagene) as directed bythe manufacturer. Mutation was verified by DNA sequencing (R1-*Spe*I-*Sma*I pSP72). An EGFP expression cassette was inserted into the newly generated *Sma*I site by amplifying the CMV promoter, EGFP and polyA region from EGFP-N1 vector (Clontech) using primers 5'-GGATATCGTAATCAATTACGGGGTCAT-3' and 5'-TGGATATCACCACAACTAGAATGCAGTG-3' (ΔR1/GFP pSP72). ΔR1/GFP pSP72 was then digested with *Spe*I and *Swa*I and ligated into the same sites in cosmid ah28ΔA/H to generate ah28ΔA/H-ΔR1-GFP.

For construction of the recombinant virus RRVΔR1/GFPcc, cosmids were digested overnight with the I-*Ceu*I homing endonuclease in order to remove the RRV H26-95 sequence from the pSuperCos-1 backbone vector. 293T cells (4.5×10^5 cells/well in six-well plates) were transfected with a combination of digested overlapping cosmids (ah28ΔA/H-ΔR1-GFP, #15A, #1, #37, and ah34) (0.4 μg of each cosmid) using Transfectin reagent (Bio-Rad Laboratories, Hercules, CA) (Fig. 1). Five days post-transfection, medium was harvested and centrifuged at 2, 000 rpm for 10 minutes to remove debris. The supernatants from the three identical cosmid transfection reactions were combined and stored at 4^oC.

To amplify recombinant virus stocks generated in 293T cells, RhF were split and 24 hours later were inoculated with the entire culture supernatant from the transfected 293T cells. Seven days later, the infected cells were split 1:3 and monitored daily for the appearance of GFP-positive viral plaques. Cultures were maintained for 2 weeks before clarified culture medium was harvested. Fresh RhF were inoculated with supernatant from the first passage described above, and maintained without splitting until complete lysis of the RhF monolayer.

To generate a marker rescue virus, cosmid ah28ΔA/H was digested overnight with I-*Ceu*I. Approximately 0.5 μg DNA was nucleofected into RhF using the Amaxa Nucleofection system as described by the manufacturer (program U-23). Following transfection, cells were allowed to recover in complete medium for 24 h. RRVΔR1/GFPcc recombinant virus was used to infect the transfected RhF at an MOI > 1. Upon complete CPE, clarified supernatants were harvested and used to infect fresh RhF monolayers. GFP-negative virus was subjected to at least three rounds of plaque-purification. Seventeen different supernatants were harvested and viral DNA purified using DNeasy kit (QIAGEN, Valencia, CA).

Construction of RRV-GFPcc and RRV-J recombinant viruses has been previously described (4).

Analysis of viral integrity

Virus was harvested from virus-infected RhF by centrifugation at 17, 000 rpm for 3 h. The virus pellet was resuspended in PBS, treated with sarkosyl and subsequently with proteinase K at 60°C for 1 h. Viral DNA was extracted by phenol-chloroform

method. Viral DNA was subjected to diagnostic PCR analysis with the following primers: R1 flanking primers: 5'-CCGTTGTGGTTACAATACACCTG-3' and 5'-TGAACCACCGCACGG AGC-3'; R1 internal primers: 5'-GGGGGTACCCTTCAACCTGTATCGGTGGAGC-3' and 5'-TTGATGATTCAGAGTTCTCGTTGC-3'; GFP internal primers: 5'-CCTGG TCGAGCTGGACGG-3' and 5'-GATCGCGCTTCTCGTTGGG-3'.

For Southern blot analysis, viral DNA was digested with *Not*I. Digestions were electrophoresed through 1% low-melt agarose (NuSieve) in 1X TBE and then transferred to a nylon membrane (Hybond N+) by capillary action. Following UV cross-linking, membranes were pre-hybridized in QuikHyb solution (Stratagene) at 65°C for 15 min. Probes were generated from RRV-DHFR and GFP by random prime method using ^{32}P-dCTP (Roche). Probes were denatured at 95°C for 3 min and added to pre-hybridization solution. Hybridization was carried out for 16 h at 65°C. Probe solution was removed and membranes were washed twice for 15 min with 2X SSC 0.1% SDS at room temperature and once for 30 min at 60°C with 0.1X SSC 0.1% SDS. Membranes were exposed and signals detected on a Phosphor Imager Scanner (Molecular Dynamics).

Plaque assays

$2x10^5$ RhF were plated in 12-well plates. Ten-fold serial dilutions of virus-infected cell supernates were made in DMEM-H supplemented with 2% FBS. Each sample dilution was performed in triplicate. Two hundred microliters of each dilution were overlaid on each well of 12-well dishes and incubated at 37°C for 1 h with redistribution of inoculum every 15 min. Inoculum was removed and cells were overlaid

with 1.5 ml of DMEM with 1.5% methyl cellulose (Sigma M0512), and 2% FBS. Plaque assays were incubated 10 days at 37°C and 5% CO_2. Overlaying medium was aspirated and staining solution (0.8% crystal violet (Sigma C3886), 50% ethanol) was added to each well for 1 h. Plaques were counted under 10X magnification.

Quantitative real-time PCR

For each sample, 10 μg of salmon sperm carrier DNA was added to 200 μl of clarified supernate from infected cells and was processed through the DNeasy Kit (QIAGEN, Valencia, CA) as per the manufacturer's protocol. To quantify viral DNA, SYBR® Green Real-time PCR in 384-well format was performed using the ABI PRISM® 7900 Sequence Detection System (Applied Biosystems Inc., Foster City, CA). To generate a standard curve for cycle thresholds versus genomic copy numbers, the plasmid containing RRV Orf50, rhesus β-tubulin, or human GAPDH was serially diluted to known concentrations in the range of 10^1 to 10^6 plasmid molecules/μl. Each PCR mixture (15 μl) contained 4 μl of viral or standard DNA, 1 μl of Orf50, rhesus β-tubulin, or human GAPDH primer set (final working concentration at 3.33 μM), 7.5 μl of SYBR Green 2X PCR mix (Applied Biosystems), and 2.5 μl of DNase- and RNase- free water (Sigma) in a total volume of 15 μl. Primers for amplification of an 81-bp amplicon internal to the RRV Orf50 sequence were 5′-GTGGAAAGCGGTGTCACAGA-3′ and 5′-TGCGGCGGCCAAAAT-3′. Primers for amplification of an 61-bp amplicon internal to the rhesus β-tubulin sequence were 5'-CCCTTCCCACGCCTCC-3' and 5'-GGCTTCCACGGCTGGTG-3'. Primers for amplifying human GAPDH were 5'-GAA GGT GAA GGT CGG AGT-3' and 5'-GAA GAT GGT GAT GGG ATT TC-3'. PCR

conditions were as follows: 95°C for 15 min, followed by 95°C for 15 sec, 60°C for 1 min repeated for 40 cycles.

RESULTS

Construction of RRVΔR1/GFPcc recombinant virus.

In order to examine the role of R1 in the lifecycle of RRV, we disrupted the R1 ORF from the RRV H26-95 genome using a cosmid-derived genetic system (4). Using cosmid ah28ΔA/H, a GFP expression cassette driven under a CMV promoter was inserted into the R1 ORF at a newly generated *Sma*I site, located approximately 100 bp downstream from the R1 start site, to interrupt the R1 ORF (Fig. 1A). This new cosmid, designated ah28ΔA/H-ΔR1-GFP, was co-transfected with cosmids #15A, #1, #37, and ah34 (Fig. 1B) into 293T cells and amplified in RhF as described in the methods section.

Construction of a revertant virus of RRVΔR1/GFPcc.

A revertant virus was made as a control for the inadvertent introduction of any mutations during the construction or isolation of RRVΔR1/GFPcc. The cosmid ah28ΔA/H was linearized with I-*Ceu*I homing endonuclease overnight and precipitated as described above and transfected into RhF. Twenty-four hours post-transfection, RhF were infected with RRVΔR1/GFPcc. Virus progeny were screened for GFP-negative isolates. In our diagnostic PCR analysis, two revertant viruses, designated rRRV-2.3.1 and rRRV-4.1.1, appeared to be identical to H26-95 (Fig. 2B). The isolate rRRV-2.3.1 (designated "Revertant" from here on) was further analyzed by restriction digest and Southern blot and was included in our subsequent viral replication assays.

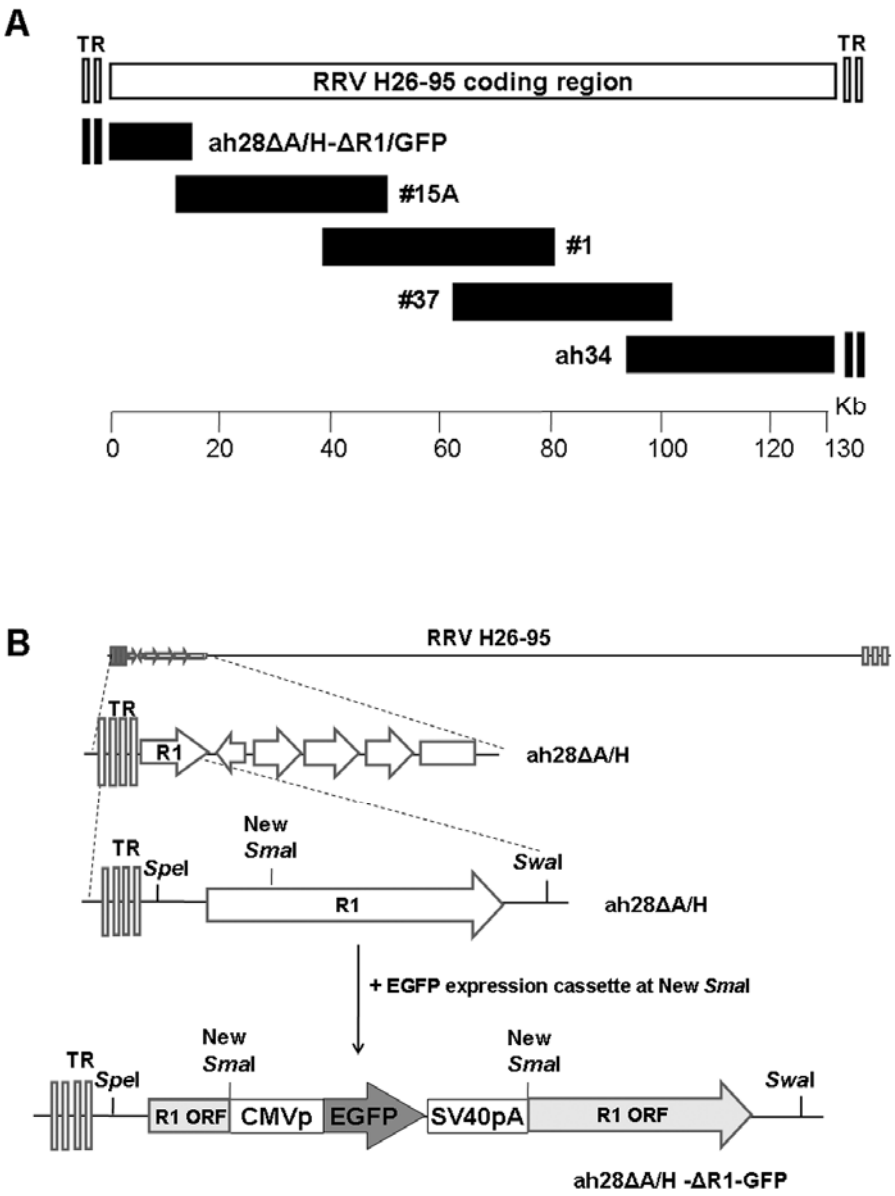

Figure 1. Construction of RRVΔR1/GFPcc. A) A schematic representation of the cosmids (ah28ΔA/H-ΔR1/GFP , #15A, #1, #37, and ah34) used to make RRVΔR1/GFPcc. The black bars indicate the extent and location of each cosmid insert relative to the parental RRV H26-95 genome (top white bar). Each cosmid insert was cloned into the pSuperCos 1 vector following the addition of an I-*Ceu*I homing endonuclease linker. TR denotes terminal repeats. The numbers on demarcated lines specify the approximate genome positions in Kb. **B)** Insertion of GFP expression cassettes into the RRV ah28ΔA/H cosmid. A *Sma*I site was introduced in the N-terminus of the R1 ORF within the ah28ΔA/H cosmid by site-directed mutagenesis. A 1619-bp EGFP expression cassette driven by a CMV promoter was inserted into the new *Sma*I site of R1 within cosmid ah28ΔA/H to disrupt the R1 ORF to generate ah28ΔA/H-ΔR1/GFP. TR denotes terminal repeats.

Analysis of the genomic integrity of the RRVΔR1/GFPcc and revertant viruses.

Viral DNA purified from RRVΔR1/GFPcc and wild-type H26-95 were subject to PCR analysis to ensure proper insertion of the GFP cassette. Primers were designed to amplify regions within the GFP ORF, within the R1 ORF, or flanking the R1 ORF. The ah28ΔA/H-ΔR1-GFP cosmid and the ah28ΔA/H parental cosmid were used as positive and negative controls for GFP insertion, respectively. In Figure 2, lanes 2 and 6 show amplification of the GFP region with a band of 517 bp, when RRVΔR1/GFPcc and ah28ΔA/H-ΔR1-GFP were used as templates, respectively. The R1 internal primers amplified a band of 2322 bp for RRVΔR1/GFPcc or ah28ΔA/H-ΔR1-GFP (lanes 2 and 6), and a band of 712 bp for RRV H26-95, the two revertant viruses, Revertant (rRRV-2.3.1) and rRRV-4.1.1, and the ah28ΔA/H cosmid (lanes 3-7). R1 flanking primers amplified a band of 3415 bp for RRVΔR1/GFPcc or ah28ΔA/H- ΔR1-GFP and a band of 1786 bp for RRV H26-95, Revertant (rRRV-2.3.1), rRRV-4.1.1, and ah28ΔA/H cosmid (lanes 3-7).

Following PCR analysis, viral genomic DNA of RRVΔR1/GFPcc, RRV H26-95, or the revertant virus was subjected to restriction digest. 10 μg of each viral genomic DNA was digested with *Not*I (Fig. 3A and 3B) at 37^{o}C for 3 h. Digested DNA was separated by electrophoresis and stained with ethidium bromide. Restriction digestion of RRVΔR1/GFPcc DNA with *Not*I resulted in two bands of altered mobility (6498 bp and 2003 bp), as compared to the wild-type RRV H26-95, due to the *Not*I site contained in the 3' end of the inserted GFP ORF (Fig. 3A and 3B). RRV H26-95 has no such site. Restriction digest of RRV H26-95 with *Not*I resulted in an expected band of 7757 bp.

To verify that R1 was disrupted by the GFP cassette insertion into the R1 ORF and the rescue virus (Revertant) had the same genetic arrangement as the parental virus RRV H26-95, we performed Southern blot analysis. Viral genomic DNA of RRVΔR1/GFPcc, RRV H26-95, or Revertant was digested with *Not*I restriction enzyme, resolved on 1% agarose by electrophoresis, and then transferred to a nylon membrane (Fig. 3A and 3B). Probe A, a fragment complementary to the RRV DHFR ORF, was generated. As expected the DHFR probe hybridized to the 6498 bp fragment of RRVΔR1/GFPcc and to the 7757 bp fragment of RRV H26-95 or Revertant. Probe B is complimentary to the GFP ORF. Figure 3B depicts the Southern blot performed on the samples using Probe B and shows that the GFP cassette was inserted into the RRVΔR1/GFPcc recombinant virus in the correct site and, as expected, was absent in RRV H26-95 or the revertant virus genome.

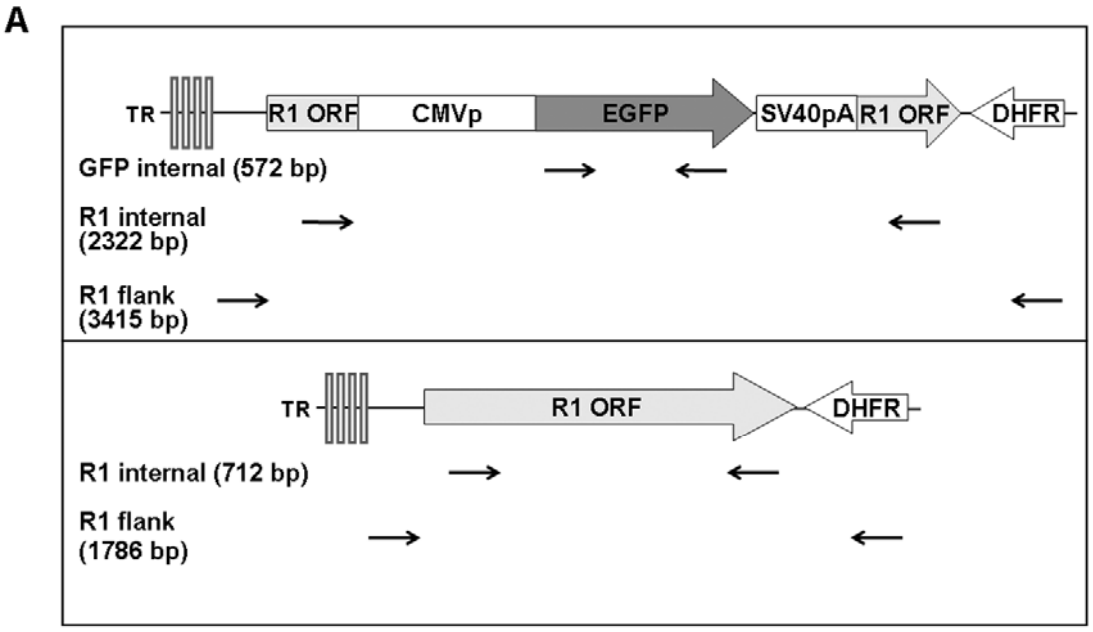

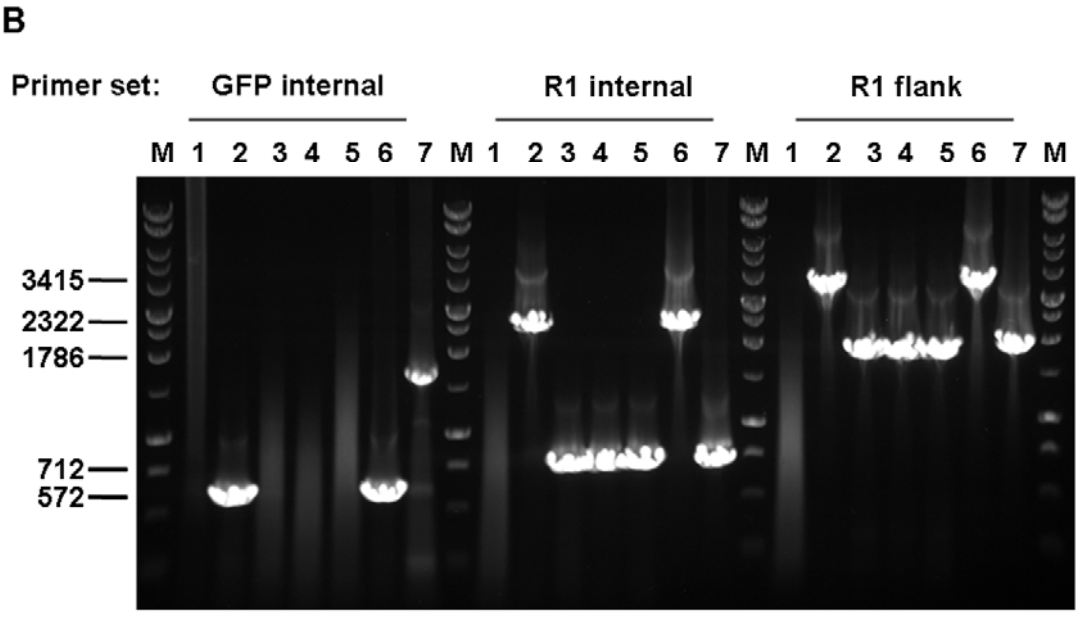

Figure 2. PCR analysis of recombinant viruses. A) A schematic representation of the location of priming sites for templates containing GFP expression cassette (top) and those that do not (bottom). **B)** PCR amplification was performed using oligonucleotides that prime within the GFP cassette (GFP internal), within the R1 ORF (R1 internal) or flanking the R1 ORF (R1 flank). Templates used are as follows: lane 1: non-template control (NTC); lane 2: RRVΔR1/GFPcc DNA; lane 3: RRV H26-95 DNA; lane 4: rRRV-2.3.1 (Revertant) DNA; lane 5: rRRV-4.1.1 DNA; lane 6: ah28ΔA/H-ΔR1/GFP cosmid; lane 7: ah28ΔA/H cosmid. M denotes maker.

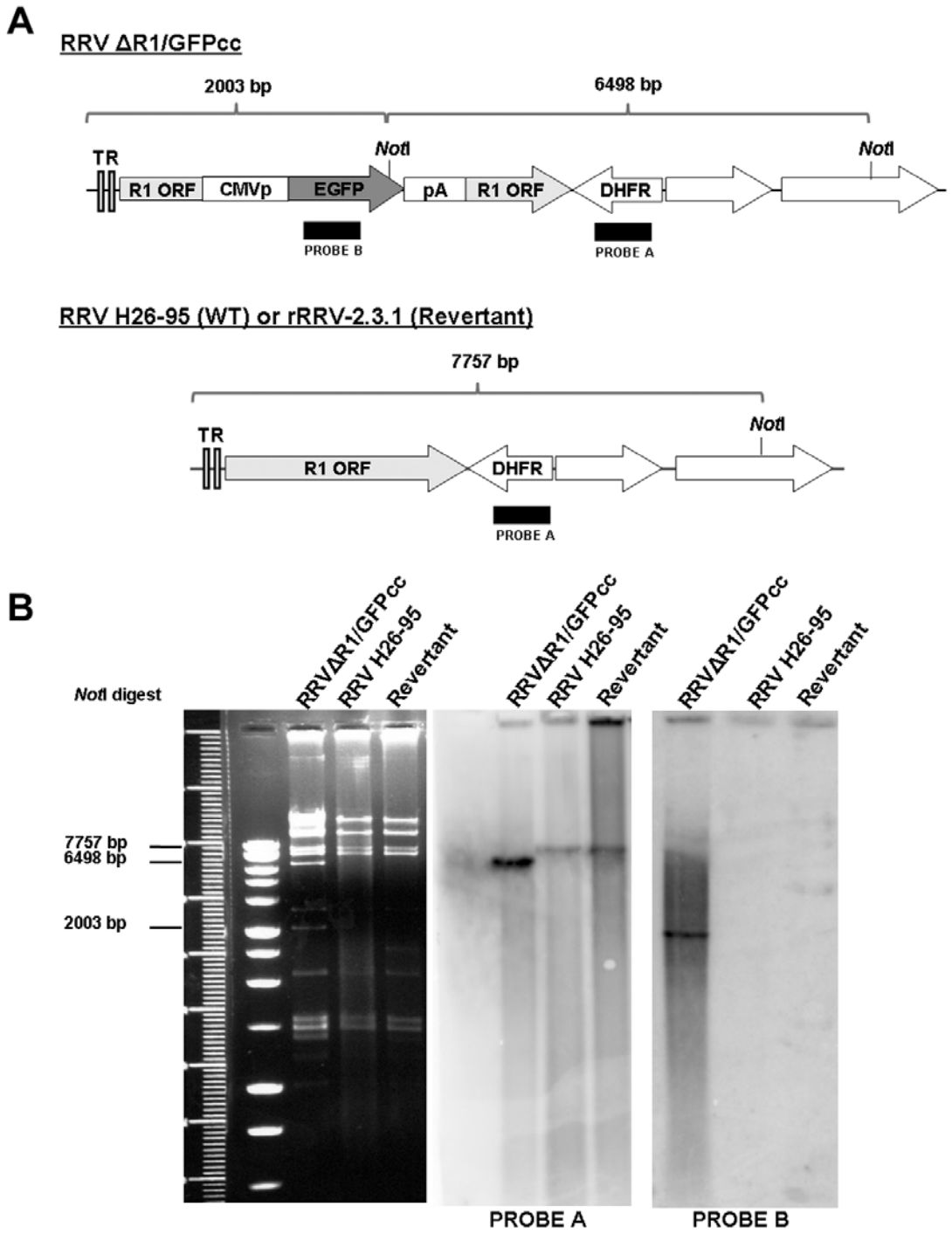

Figure 3. Restriction digest and Southern blot analysis of recombinant viruses. A) Diagram of the 5' region of RRV ΔR1/GFP$_{CC}$ (top) and H26-95 genomes, depicting *Not*I restriction sites and location of probe hybridization sites. **B)** *Not*I digest (left panel) and Southern blots of RRV ΔR1/GFPcc (lane 1), RRV H26-95 (lane 2) and rescue rRRV-2.3.1 (Revertant; lane 3) genomes hybridized with the RRV DHFR probe (Probe A; middle panel) or the GFP probe (probe B; right panel).

Disruption of the R1 gene from RRV does not impact RRV lytic replication in rhesus fibroblasts.

We next determined if the disruption of R1 affected the replication kinetics of RRV. Four viruses, RRVΔR1/GFPcc, Revertant, RRV-GFPcc (a wild-type cosmid-derived RRV H26-95 virus with a GFP expression cassette inserted far upstream of the R1 ORF (4)), and RRV-J (a cosmid-derived wild-type RRV H26-95 (4)) were used in this assay. Two days post-seeding, rhesus fibroblasts were infected with RRVΔR1/GFPcc, RRV-J, RRV-GFPcc, or Revertant at an MOI of 1 or 5 (Figs. 4 and 5, respectively).

After an inoculation period of two hours for optimal adsorption, the supernatants from the infected cells were aspirated and replaced with DMEM containing 2% FBS to allow infections to proceed. At 0, 24, 48, 72, 96, 120, and 144 hours post infection (hpi), cell-free supernatants were harvested by centrifugation at 2,000 rpm for 5 min. For the viral growth curves, the supernatants were serially diluted in triplicate and subjected to traditional plaque assays to measure infectious particles (Fig. 4A and 5A). For the measurement of extracellular viral genome copies by real-time PCR (Fig. 4B and 5B), 200 μl of the clarified supernatant from each infection sample, spiked with salmon sperm DNA, was processed through a DNeasy column (QIAGEN) for DNA isolation. Isolated DNA was then subjected to real-time PCR in triplicate using SYBR® Green mixture containing RRV Rta/Orf50 primers. For the measurement of intracellular viral genome copies by real-time PCR, an identical procedure was performed and the results are shown in Figures 4C and 5C. In order to account for cell death following viral replication in our

data analysis, intracellular viral genomes were also normalized to rhesus genomes using rhesus tubulin as an endogenous control (37) (Fig. 4D and 5D).

We found that RRVΔR1/GFPcc, Revertant, RRV-GFPcc, and RRV-J all replicated to similar levels on rhesus fibroblasts. This was true as measured by plaques assays, as well as a viral genome assay quantitating intracellular and extracellular viral genomes. Since we observed no significant difference in replicative kinetics between RRVΔR1/GFPcc and the other three viruses in RhF that support lytic RRV infection, we conclude that R1 does not impact RRV *de novo* lytic infection and replication.

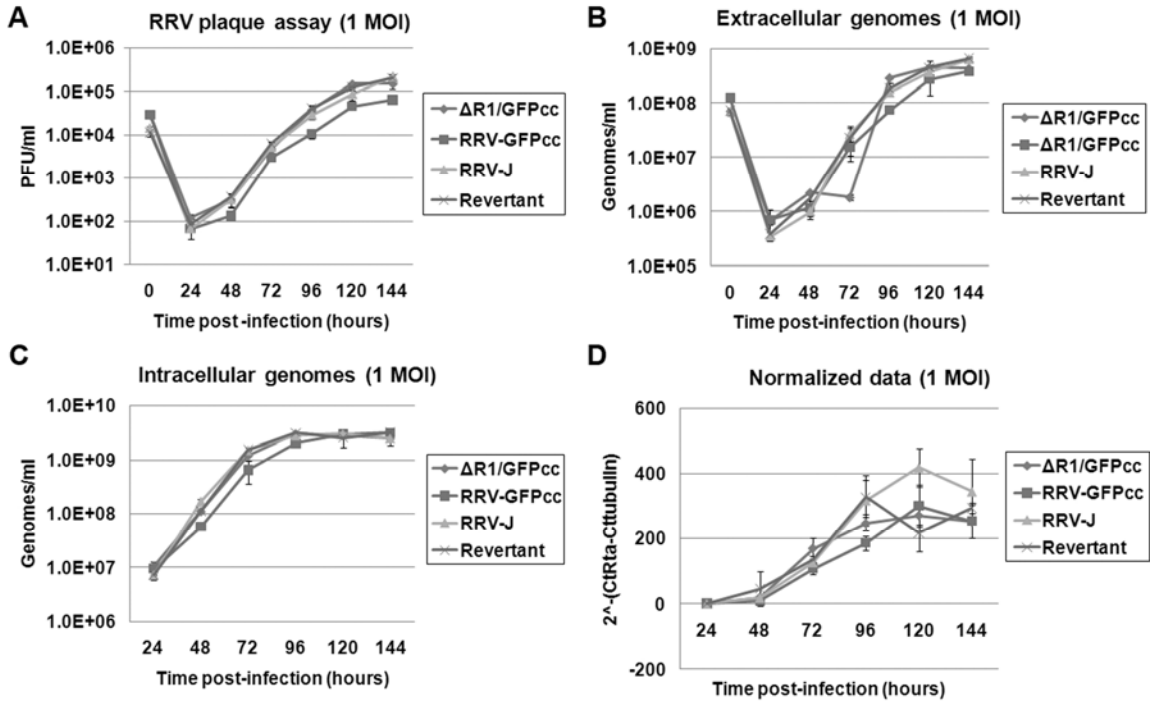

Figure 4. Viral growth curves of RRVΔR1/GFPcc in rhesus fibroblasts at 1 MOI. Equivalent numbers of RhF cells were infected with RRVΔR1/GFPcc, RRV-GFPcc (wild-type with GFP insertion), RRV-J (wild-type without GFP insertion), or Revertant (rRRV-2.3.1) at a MOI of 1. Cell-free supernatants and cell pellets were harvested at indicated points post-infection. **A)** Infectious virus particles from supernatants were quantitated by traditional plaque assay. **B)** Extracellular viral genomes from the same samples as in A) were quantitated by real-time PCR assay. **C)** Intracellular viral genomes extracted from infected cell pellets were quantitated by real-time PCR. **D)** Same as in C) except that the viral genomes were normalized to rhesus β-tubulin. In all panels, results are the averages of duplicate or triplicate samples. Error bars represent standard deviations.

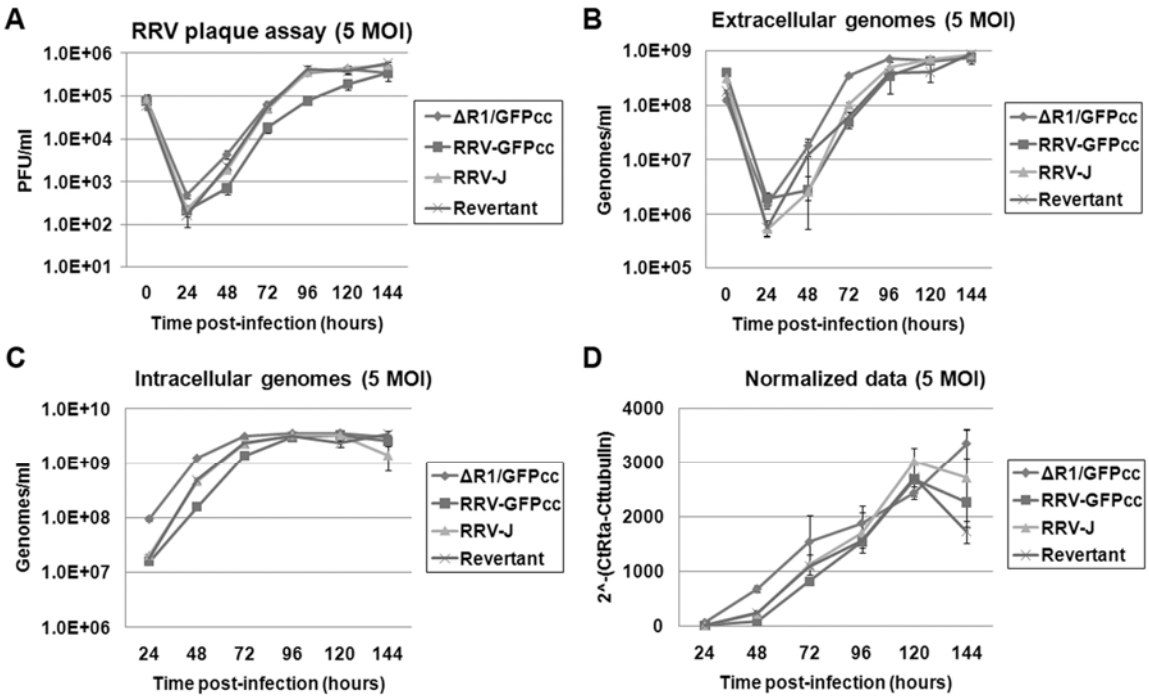

Figure 5. Viral growth curves of RRVΔR1/GFPcc in rhesus fibroblasts at 5 MOI. Equivalent numbers of RhF cells were infected with RRVΔR1/GFPcc, RRV-GFPcc (wild-type with GFP insertion), RRV-J (wild-type without GFP insertion), or Revertant (rRRV-2.3.1) at a MOI of 5. Cell-free supernatants and cell pellets were harvested at indicated points post-infection. **A)** Infectious virus particles from supernatants were quantitated by traditional plaque assay. **B)** Extracellular viral genomes from the same samples as in A) were quantitated by real-time PCR assay. **C)** Intracellular viral genomes extracted from infected cell pellets were quantitated by real-time PCR. **D)** Same as in C) except that the viral genomes were normalized to rhesus β-tubulin. In all panels, results are the averages of duplicate or triplicate samples. Error bars represent standard deviations.

Disruption of the RRV R1 gene leads to an enhanced establishment of latency and lower levels of spontaneous reactivation in B cells.

We next investigated whether R1 played any role in the latent phase of the RRV lifecycle. We have previously reported that RRV establishes latency in the B cell line BJAB (13, 37). We infected BJAB cells with RRVΔR1/GFPcc or RRV-GFPcc (MOI = 0.5) as previously described (15, 37). Seven days post-infection, infected BJAB cells

were sorted by flow cytometry for the presence of green fluorescence. After sorting, equivalent numbers of GFP-positive cells from both RRVΔR1/GFPcc-infected and RRV-GFP-infected BJAB cells were used for further experimentation to assess the maintenance of viral latency. From here onwards, the infected BJAB cells were split equally on the same days and GFP-positive cells were continuously monitored by flow cytometry (Fig. 6) and fluorescence microscopy (Fig. 7) as we previously described (37). The RRVΔR1/GFPcc-infected BJAB sample showed a less rapid loss of GFP-positive cells on days 7, 14, 21, and 28 post-sorting as determined by fluorescence microscopy and flow cytometry (Figure 6). Figure 7 shows the relative GFP-positive cells on days 7, 14, 21, and 28 post-sorting as determined visually by fluorescence microscopy, respectively. To confirm that the higher number of GFP-positive cells in RRVΔR1/GFPcc-infected BJAB cells was a true reflection of a higher percentage of BJAB cells harboring the virus (or intracellular viral genomes), we performed quantitative real-time PCR to calculate RRV genome copy numbers normalized to human GAPDH copy number. RRVΔR1/GFPcc-infected BJAB cells displayed significantly higher intracellular viral genomes compared with RRV-GFPcc infected BJAB cells (Fig. 8A).

We also examined the role of R1 in RRV reactivation. In brief, GFP-positive RRVΔR1/GFPcc or RRV-GFPcc-infected BJAB cells were isolating by flow sorting and equivalent numbers of cells were subjected to reactivation through various means including the phorbol ester 12-O-tetradecanoyl phorbol 13 acetate (TPA) (13, 20), the HDAC inhibitors sodium butyrate (NaB) (13, 20) and trichostatin A (TSA) (13), or by etopic Rta expression (13, 38). A KSHV Rta baculovirus was used because we have

previously reported that KSHV Rta can activate RRV promoters and *vice versa* (9). TPA activates the PKC and ERK signaling pathways leading to Rta activation, whereas NaB and TSA activate Rta and other promoters by inhibiting their silencing via deacetylation. In the absence of artificial induction of viral reactivation, we observed that RRVΔR1/GFPcc-infected BJAB cells released less RRV genomes (i.e. was more latent) than RRV-GFPcc, suggesting that R1 expression enhances spontaneous RRV reactivation (Fig. 8B). Next we investigated the effect of chemical or Rta-mediated induction of reactivation of the RRVΔR1/GFPcc or RRV-GFPcc-infected latent BJAB cells. Interestingly, induction using a cocktail of TPA (25 ng/ml), NaB (0.1 mM), and TSA (100 nM) or by infection with a baculovirus expressing KSHV Rta/Orf50 (38) resulted in approximately equivalent level of reactivation from both RRVΔR1/GFPcc and RRV-GFPcc-infected latent BJAB cells. RRV reactivation was very robust by chemical induction with the TPA/NaB/TSA cocktail and led to almost complete cell death after 24 h. RRV reactivation stimulated by KSHV Rta overexpression was a slower process and yielded similar levels of extracellular genomes at 96 h compared to chemical induction at 24 h but the extracellular RRV genomes accumulated to much higher levels up to 168 h post-induction. Our data suggest that R1 activates signaling pathways that are required for spontaneous viral reactivation from latency and that these pathways are similar to those activated by chemical and Rta induction.

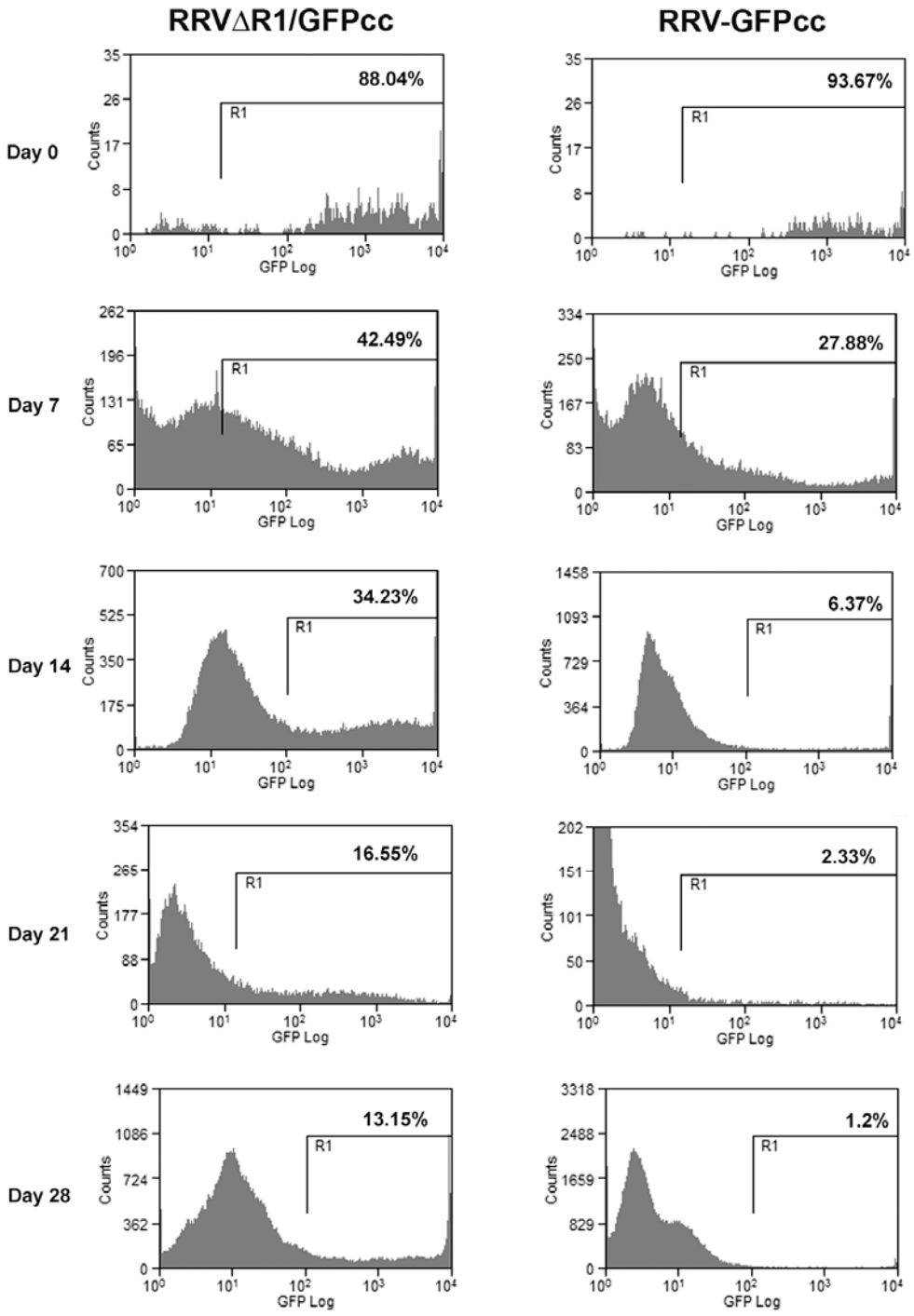

Figure 6. Flow cytometry analysis of RRVΔR1/GFPcc and RRV-GFPcc infected BJAB cells. Flow cytometry analysis was performed to measure the percentage of GFP-positive cells in RRVΔR1/GFPcc or RRV-GFPcc infected BJAB cells immediately after sorting (day 0 post-sorting) and 7, 14, 21, and 28 days post-sorting. The percentages of GFP-positive cells at the indicated time points are shown.

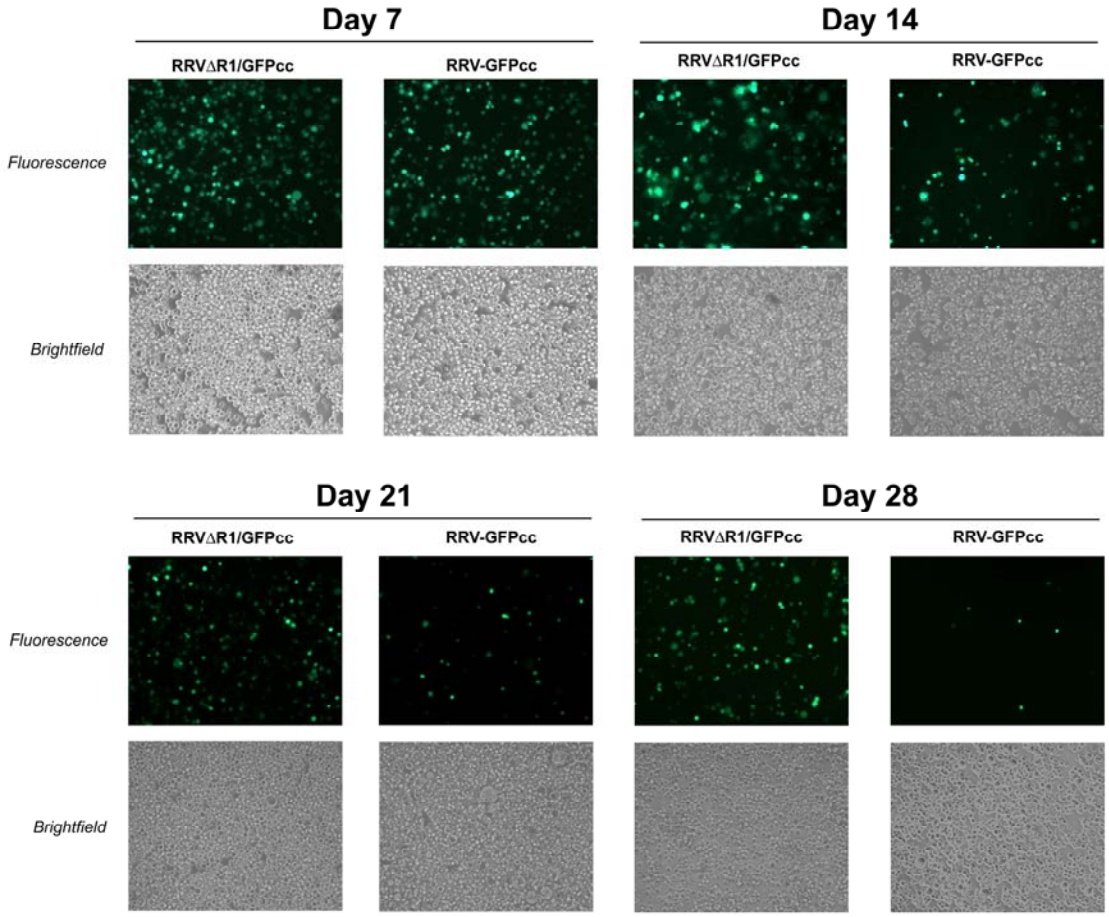

Figure 7. Representative images of RRVΔR1/GFPcc and RRV-GFPcc infected BJAB cells. Brightfield and GFP fluorescence images of RRV-infected GFP-positive BJAB B cells are shown on days 7, 14, 21, and 28 post-sorting.

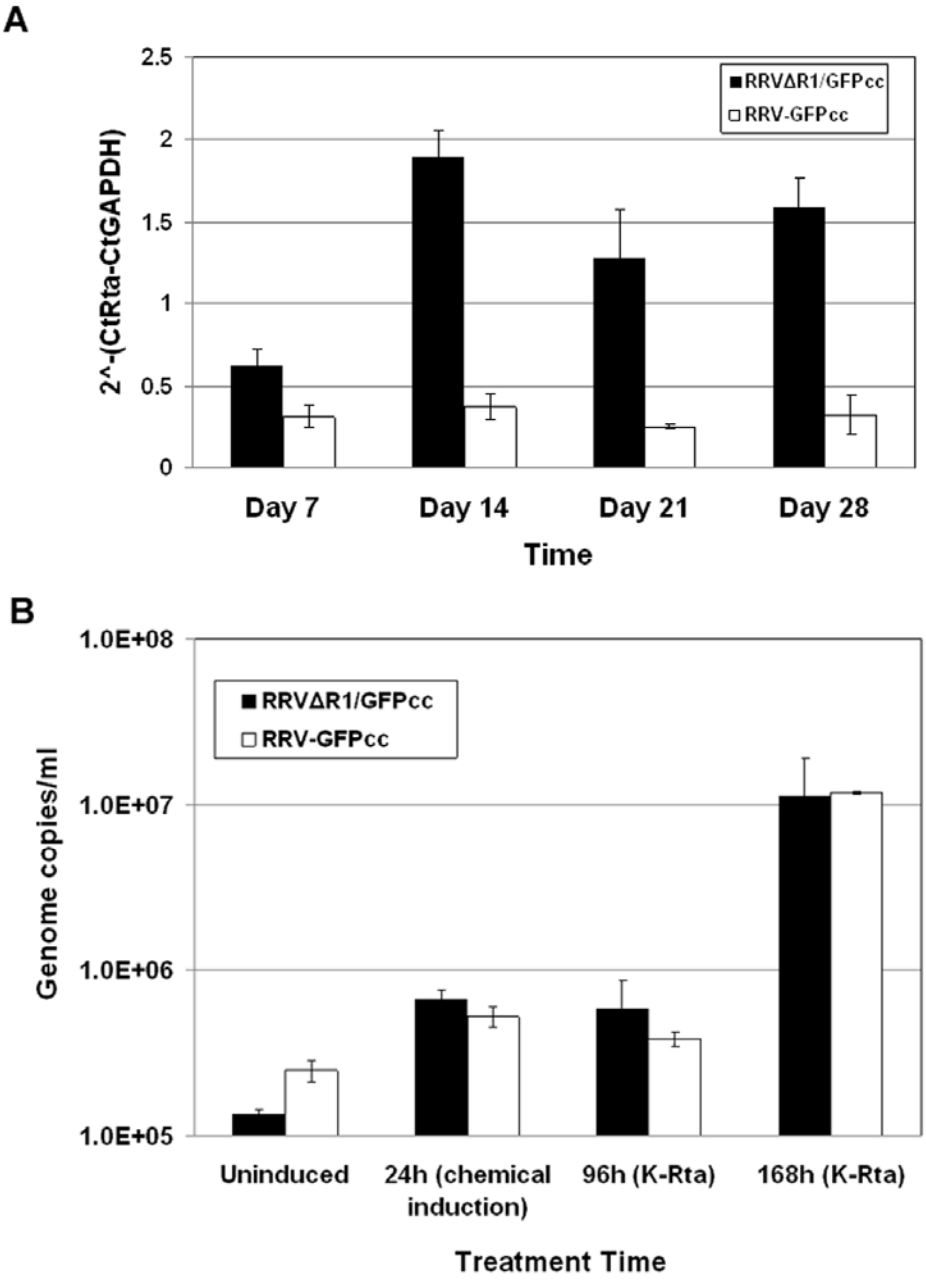

Figure 8. RRVΔR1/GFPcc and RRV-GFPcc latent infection and lytic reactivation in B lymphocytes. A) Intracellular viral genomes of RRVΔR1/GFPcc (■) and RRV-GFPcc (□) infected BJAB cells on days 7, 14, 21, and 28 post-sorting. Intracellular genomes extracted from infected cell pellets were quantitated by real-time PCR to determine viral genome copy number. The viral genomes were normalized to human GAPDH. Results are the averages of triplicate samples. Error bars represent standard deviations. **B)** Extracellular viral genomes were quantitated by real-time PCR assay. RRV-infected B cells were subjected to chemical induction with a mix of TPA (25 ng/ml), NaB (0.1 mM), and TSA (100 nM) for 24 h or KSHV Rta/Orf50-containing baculoviral infection for 96 h or 168 h. DNA from extracellular virus present in the cell supernatant was isolated and subjected to real time quantitative PCR analysis to determine viral genome copy numbers.

DISCUSSION

KSHV cannot establish a robust and persistent infection in mice or rhesus macaques (16, 29) and hence, RRV serves as a unique model to study KSHV pathogenesis *in vivo*. By utilizing an overlapping set of cosmids developed by Bilello *et al*. (4), we generated a R1-deleted virus (RRVΔR1/GFPcc) and an isogenic revertant virus. We confirmed proper placement of the exogenous GFP cassette into the R1 ORF and the integrity of RRVΔR1/GFPcc by diagnostic PCR, restriction digests and Southern blot analysis. The viral genome of recombinant RRVΔR1/GFPcc appeared to be identical to that of the wild-type RRV H26-95, except for the insertion of the GFP expression cassette. We also generated a rescue virus in which the GFP expression cassette was removed by traditional homologous recombination between the RRVΔR1/GFPcc genome and ah28ΔA/H cosmid. The revertant virus showed no genetic difference from the parental RRV H26-95 virus by restriction digest and Southern blot analysis.

Characterization of the recombinant RRVΔR1/GFPcc and revertant viruses in RhF demonstrated that these viruses were replication competent and replicated on RhF with growth kinetics (PFU and viral genome titers) that were similar to those of the wild-type control viruses at single-step growth (5 MOI) or multiple-step growth (1 MOI). Disruption of the R1 gene resulted in a mutant virus more capable of establishing and maintaining latency in BJAB cells. This suggests that R1 fine-tunes the activity of RRV during these phases of the viral lifecycle. Since our data imply that R1 modulates latent infection and spontaneous reactivation, one may speculate that R1 should have a similar effect during *de novo* lytic replication. One possibility for not observing this could be due to cell-type specificity and a difference in the kinases expressed between B cells versus

fibroblasts. R1 has thirteen tyrosine residues in its cytoplasmic tail which may interact with multiple kinases and demonstrate specific interactions with different kinases in different cells.

Whereas RRVΔR1/GFPcc-infected BJAB cells released less virions as measured by extracellular viral genomes than RRV-GFPcc-infected BJAB cells (indicative of a defect in reactivation), both wild-type and RRVΔR1/GFPcc viruses were able to produce similar levels of viral particles upon reactivation induced by a TPA/NaB/TSA chemical cocktail or ectopic Rta overexpression. This suggests that the R1 signaling functions are in the same pathway (and upstream) of the signaling events activated by TPA, NaB, and TSA. In agreement with this model, Lagunoff *et al*. reported blockage of lytic replication by K1 ITAM mutants that could be overcome by TPA treatment, thus suggesting that TPA-mediated signaling pathways could substitute for the loss of K1 signaling (23). Another interesting observation from our study is that KSHV Rta/Orf50 was able to reactivate RRV from latency, which implies that KSHV Rta can functionally complement or substitute for RRV Rta as we previously described using reporter assays (9).

An alternative interpretation of the data is that as a glycoprotein, R1 may function to optimize efficient maturation and/or regress of the virus particle in B cells. This could also account for the observed enrichment of intracellular viral genomes and reduction of extracellular viral genomes. Future directions include electron microscopy to determine the number, subcellular distribution, and morphology of viral particles within RRVΔR1/GFPcc and RRV-GFPcc infected cells. These two scenarios may co-exist and not be mutually exclusive.

An opposing model posits that R1 functions to inhibit viral gene expression and subsequent virus production. In this model, GFP expression would imply spontaneous reactivation (without complete lytic replication) instead of latency. In this scenario, higher intracellular genomes would be the result of increased spontaneous reactivation without complete lytic replication and cell lysis. Although a portion of the viral population may reactivate, the presence of R1 in the viral genome may suppress complete viral replication and lytic replication. In this scenario, R1 contained in the wild-type RRV-GFPcc virus might down-modulate GFP expression driven by the CMV promoter, thus accounting for our observation of fewer GFP-positive cells. In the absence of R1 in RRVΔR1/GFPcc-infected BJAB, the regulation into the latency program may not be as tight. Thus, there would be more GFP-positive cells and more intracellular viral genomes representing a higher percentage of reactivating cells. This model would also predict less intracellular genomes in the wild-type RRV-GFPcc than RRVΔR1/GFPcc as we observed in Figure 8A, although the fact that we do see less extracellular genomes released in Figure 8B in the uninduced condition would be inconsistent with and argue against this alternative model.

To examine whether R1 can suppress viral gene expression, we will isolate total mRNA from RRVΔR1/GFPcc or RRV-GFPcc infected BJAB cells to the RRV QPCR array developed by the Dittmer lab as previously described (17, 37). This would enable us to profile the transcripts that are differentially regulated by RRV in the presence or absence of R1 and determine whether R1 predominantly represses the transcription of the majority of RRV messages. An alternative approach to testing this model is to repeat the latency assay using real time PCR to measure intracellular viral genomes over the course

of the infection, but without flow sorting for GFP-positive cells after infection. This would avoid any bias in enriching cell populations that undergo spontaneous reactivation (GFP-positive) at the expense of excluding cells that are latently infected (GFP-negative).

In addition to its role in viral persistence *in vitro*, R1 may function as an immunoregulatory protein *in vivo*. KSHV K1 has been shown to downregulate BCR surface expression (25). As BCR activation and downstream signaling events may yield to terminal differentiation and apoptosis, K1 modulation of BCR signal transduction may provide a long-term survival advantage *in vivo*. Indeed, K1 expression has been shown to protect cells from Fas-mediated apoptosis (34, 35). Furthermore, the PI3K/Akt pathway activated by K1 is pro-survival and controls Fas-mediated apoptosis (34, 36), R1 also activates B-cell signaling pathways (8) and can also activate the Akt pathway (unpublished). R1 may exhibit a similar phenotype to K1.

In the context of SIV co-infection, experimental infection with wild-type RRV resulted in B cell hyperplasia, persistent lymphadenopathy, and persistent infection in macaques (19, 27, 39). It will be interesting to assess whether rhesus macaques infected with RRVΔR1/GFPcc (compared to RRV-GFPcc) would develop a similar phenotype. In the case of the related gammaherpesvirus HVS, deletion of the left-hand terminal membrane protein, STP, resulted in a mutant virus fully competent in replication but defective in growth transformation of primary T lymphocytes *in vitro* and pathogenesis *in vivo* (18). Because R1 is the positional homolog of STP and deregulates similar signal transduction in B-cells (8), RRVΔR1/GFPcc may have a similar phenotype *in vivo,* perhaps in the context of the development of B-cell hyperplasia.

In conclusion, we have generated a recombinant RRV virus designated RRVΔR1/GFPcc, in which the R1 ORF has been disrupted by the insertion of a GFP expression cassette. This R1 deletion virus exhibited increased persistence in our B cell culture model, but had no effect on replication upon *de novo* infection of rhesus fibroblasts.

ACKNOWLEDGMENTS

We thank Stuart Krall for technical assistance. We also thank members of the Damania and Dittmer labs for helpful discussion. This work was supported by NIH grant CA096500 and HL083469 to BD. KWW was supported in part by NIAID training grant T32-AI007001 and MSTP grant T32-GM008719. CCT was supported in part by NCI training grant T32-CA71341. BD is a Leukemia & Lymphoma Society Scholar and Burroughs Welcome Fund Investigator in Infectious Disease.

REFERENCES

1. **Alexander, L., L. Denekamp, A. Knapp, M. R. Auerbach, B. Damania, and R. C. Desrosiers.** 2000. The primary sequence of rhesus monkey rhadinovirus isolate 26-95: sequence similarities to Kaposi's sarcoma-associated herpesvirus and rhesus monkey rhadinovirus isolate 17577. J Virol **74:**3388-98.

2. **Beral, V., T. A. Peterman, R. L. Berkelman, and H. W. Jaffe.** 1990. Kaposi's sarcoma among persons with AIDS: a sexually transmitted infection? Lancet **335:**123-8.

3. **Bilello, J. P., S. M. Lang, F. Wang, J. C. Aster, and R. C. Desrosiers.** 2006. Infection and persistence of rhesus monkey rhadinovirus in immortalized B-cell lines. J Virol **80:**3644-9.

4. **Bilello, J. P., J. S. Morgan, B. Damania, S. M. Lang, and R. C. Desrosiers.** 2006. A genetic system for rhesus monkey rhadinovirus: use of recombinant virus to quantitate antibody-mediated neutralization. J Virol **80:**1549-62.

5. **Cesarman, E., Y. Chang, P. S. Moore, J. W. Said, and D. M. Knowles.** 1995. Kaposi's sarcoma-associated herpesvirus-like DNA sequences in AIDS-related body-cavity-based lymphomas. N Engl J Med **332:**1186-91.

6. **Chandriani, S., and D. Ganem.** 2010. Array-based transcript profiling and limiting-dilution RT-PCR analysis identify additional latent genes in KSHV. J Virol.

7. **Chang, Y., E. Cesarman, M. S. Pessin, F. Lee, J. Culpepper, D. M. Knowles, and P. S. Moore.** 1994. Identification of herpesvirus-like DNA sequences in AIDS-associated Kaposi's sarcoma. Science **266:**1865-9.

8. **Damania, B., M. DeMaria, J. U. Jung, and R. C. Desrosiers.** 2000. Activation of lymphocyte signaling by the R1 protein of rhesus monkey rhadinovirus. J Virol **74:**2721-30.

9. **Damania, B., J. H. Jeong, B. S. Bowser, S. M. DeWire, M. R. Staudt, and D. P. Dittmer.** 2004. Comparison of the Rta/Orf50 transactivator proteins of gamma-2-herpesviruses. J Virol **78:**5491-9.

10. **Damania, B., M. Li, J. K. Choi, L. Alexander, J. U. Jung, and R. C. Desrosiers.** 1999. Identification of the R1 oncogene and its protein product from the rhadinovirus of rhesus monkeys. J Virol **73:**5123-31.

11. **Damania, B., M. Li, J. K. Choi, L. Alexander, J. U. Jung, and R. C. Desrosiers.** 1999. Identification of the R1 oncogene and its protein product from the Rhadinovirus of Rhesus monkeys. J. Virol. **73:**5123-5131.

12. **Desrosiers, R. C., V. G. Sasseville, S. C. Czajak, X. Zhang, K. G. Mansfield, A. Kaur, R. P. Johnson, A. A. Lackner, and J. U. Jung.** 1997. A herpesvirus of rhesus monkeys related to the human Kaposi's sarcoma-associated herpesvirus. J Virol **71:**9764-9.

13. **DeWire, S. M., and B. Damania.** 2005. The latency-associated nuclear antigen of rhesus monkey rhadinovirus inhibits viral replication through repression of Orf50/Rta transcriptional activation. J Virol **79:**3127-38.

14. **DeWire, S. M., M. A. McVoy, and B. Damania.** 2002. Kinetics of expression of rhesus monkey rhadinovirus (RRV) and identification and characterization of a polycistronic transcript encoding the RRV Orf50/Rta, RRV R8, and R8.1 genes. J Virol **76:**9819-31.

15. **DeWire, S. M., E. S. Money, S. P. Krall, and B. Damania.** 2003. Rhesus monkey rhadinovirus (RRV): construction of a RRV-GFP recombinant virus and development of assays to assess viral replication. Virology **312:**122-34.

16. **Dittmer, D., C. Stoddart, R. Renne, V. Linquist-Stepps, M. E. Moreno, C. Bare, J. M. McCune, and D. Ganem.** 1999. Experimental transmission of Kaposi's sarcoma-associated herpesvirus (KSHV/HHV-8) to SCID-hu Thy/Liv mice. J Exp Med **190:**1857-68.

17. **Dittmer, D. P., C. M. Gonzalez, W. Vahrson, S. M. DeWire, R. Hines-Boykin, and B. Damania.** 2005. Whole-genome transcription profiling of rhesus monkey rhadinovirus. J Virol **79:**8637-50.

18. **Duboise, M., J. Guo, S. Czajak, H. Lee, R. Veazey, R. C. Desrosiers, and J. U. Jung.** 1998. A role for herpesvirus saimiri orf14 in transformation and persistent infection. J Virol **72:**6770-6.

19. **Estep, R. D., M. F. Powers, B. K. Yen, H. Li, and S. W. Wong.** 2007. Construction of an infectious rhesus rhadinovirus bacterial artificial chromosome for the analysis of Kaposi's sarcoma-associated herpesvirus-related disease development. J Virol **81:**2957-69.

20. **Gregory, S. M., J. A. West, P. J. Dillon, C. Hilscher, D. P. Dittmer, and B. Damania.** 2009. Toll-like receptor signaling controls reactivation of KSHV from latency. Proc Natl Acad Sci U S A **106:**11725-30.

21. **Jenner, R. G., M. M. Alba, C. Boshoff, and P. Kellam.** 2001. Kaposi's sarcoma-associated herpesvirus latent and lytic gene expression as revealed by DNA arrays. J Virol **75:**891-902.

22. **Krishnan, H. H., P. P. Naranatt, M. S. Smith, L. Zeng, C. Bloomer, and B. Chandran.** 2004. Concurrent expression of latent and a limited number of lytic genes with immune modulation and antiapoptotic function by Kaposi's sarcoma-associated herpesvirus early during infection of primary endothelial and fibroblast cells and subsequent decline of lytic gene expression. J Virol **78:**3601-20.

23. **Lagunoff, M., D. M. Lukac, and D. Ganem.** 2001. Immunoreceptor tyrosine-based activation motif-dependent signaling by Kaposi's sarcoma-associated herpesvirus K1 protein: effects on lytic viral replication. J Virol **75:**5891-8.

24. **Lagunoff, M., R. Majeti, A. Weiss, and D. Ganem.** 1999. Deregulated signal transduction by the K1 gene product of Kaposi's sarcoma-associated herpesvirus. Proc Natl Acad Sci U S A **96:**5704-9.

25. **Lee, B. S., X. Alvarez, S. Ishido, A. A. Lackner, and J. U. Jung.** 2000. Inhibition of intracellular transport of B cell antigen receptor complexes by Kaposi's sarcoma-associated herpesvirus K1. J Exp Med **192:**11-21.

26. **Lee, H., J. Guo, M. Li, J. K. Choi, M. DeMaria, M. Rosenzweig, and J. U. Jung.** 1998. Identification of an immunoreceptor tyrosine-based activation motif of K1 transforming protein of Kaposi's sarcoma-associated herpesvirus. Mol Cell Biol **18:**5219-28.

27. **Mansfield, K. G., S. V. Westmoreland, C. D. DeBakker, S. Czajak, A. A. Lackner, and R. C. Desrosiers.** 1999. Experimental infection of rhesus and pig-tailed macaques with macaque rhadinoviruses. J Virol **73:**10320-8.

28. **Orzechowska, B. U., M. F. Powers, J. Sprague, H. Li, B. Yen, R. P. Searles, M. K. Axthelm, and S. W. Wong.** 2008. Rhesus macaque rhadinovirus-associated non-Hodgkin's lymphoma: animal model for KSHV associated malignancies. Blood.

29. **Renne, R., D. Dittmer, D. Kedes, K. Schmidt, R. C. Desrosiers, P. A. Luciw, and D. Ganem.** 2004. Experimental transmission of Kaposi's sarcoma-associated herpesvirus (KSHV/HHV-8) to SIV-positive and SIV-negative rhesus macaques. J Med Primatol **33:**1-9.

30. **Samaniego, F., S. Pati, J. E. Karp, O. Prakash, and D. Bose.** 2001. Human herpesvirus 8 K1-associated nuclear factor-kappa B-dependent promoter activity: role in Kaposi's sarcoma inflammation? J Natl Cancer Inst Monogr**:**15-23.

31. **Sarid, R., J. S. Wiezorek, P. S. Moore, and Y. Chang.** 1999. Characterization and cell cycle regulation of the major Kaposi's sarcoma-associated herpesvirus (human herpesvirus 8) latent genes and their promoter. J Virol **73:**1438-46.

32. **Searles, R. P., E. P. Bergquam, M. K. Axthelm, and S. W. Wong.** 1999. Sequence and genomic analysis of a Rhesus macaque rhadinovirus with similarity to Kaposi's sarcoma-associated herpesvirus/human herpesvirus 8. J Virol **73:**3040-53.

33. **Soulier, J., L. Grollet, E. Oksenhendler, P. Cacoub, D. Cazals-Hatem, P. Babinet, M. F. d'Agay, J. P. Clauvel, M. Raphael, L. Degos, and et al.** 1995. Kaposi's sarcoma-associated herpesvirus-like DNA sequences in multicentric Castleman's disease. Blood **86:**1276-80.

34. **Tomlinson, C. C., and B. Damania.** 2004. The K1 protein of Kaposi's sarcoma-associated herpesvirus activates the Akt signaling pathway. J Virol **78:**1918-27.

35. **Wang, S., H. Maeng, D. P. Young, O. Prakash, L. E. Fayad, A. Younes, and F. Samaniego.** 2007. K1 protein of human herpesvirus 8 suppresses lymphoma cell Fas-mediated apoptosis. Blood **109:**2174-82.

36. **Wen, K. W., and B. Damania.** 2010. Hsp90 and ER-associated Hsp40/Erdj3 are required for the expression and anti-apoptotic function of KSHV K1. Oncogene (in press).

37. **Wen, K. W., D. P. Dittmer, and B. Damania.** 2009. Disruption of LANA in rhesus rhadinovirus generates a highly lytic recombinant virus. J Virol **83:**9786-802.

38. **West, J., and B. Damania.** 2008. Upregulation of the TLR3 pathway by Kaposi's sarcoma-associated herpesvirus during primary infection. J Virol **82:**5440-9.

39. **Wong, S. W., E. P. Bergquam, R. M. Swanson, F. W. Lee, S. M. Shiigi, N. A. Avery, J. W. Fanton, and M. K. Axthelm.** 1999. Induction of B cell hyperplasia in simian immunodeficiency virus- infected rhesus macaques with the simian homologue of Kaposi's sarcoma- associated herpesvirus. J Exp Med **190:**827-40.

40. **Woodberry, T., T. J. Suscovich, L. M. Henry, J. N. Martin, S. Dollard, P. G. O'Connor, J. K. Davis, D. Osmond, T. H. Lee, D. H. Kedes, A. Khatri, J. Lee, B. D. Walker, D. T. Scadden, and C. Brander.** 2005. Impact of Kaposi sarcoma-associated herpesvirus (KSHV) burden and HIV coinfection on the detection of T cell responses to KSHV ORF73 and ORF65 proteins. J Infect Dis **192:**622-9.

CHAPTER 4

DISRUPTION OF LANA IN RHESUS RHADINOVIRUS GENERATES A HIGHLY LYTIC RECOMBINANT VIRUS

Kwun Wah Wen, Dirk P. Dittmer and Blossom Damania

ABSTRACT

Rhesus monkey rhadinovirus (RRV) is a γ-herpesvirus that is closely related to human Kaposi sarcoma-associated herpesvirus (KSHV/HHV-8). RRV is the closest relative to KSHV that has a fully sequenced genome and serves as an *in vitro* and an *in vivo* model system for KSHV. The latency-associated nuclear antigen (LANA) protein of both KSHV and RRV plays key roles in the establishment and maintenance of these herpesviruses. We have constructed a RRV recombinant virus (RRVΔLANA/GFP) in which the RRV LANA open-reading frame has been disrupted with a GFP expression cassette generated by homologous recombination. Integrity of the recombinant virus was confirmed by diagnostic PCR, restriction digest, Southern blot analysis, and whole-genome sequencing. We compared single-step and multi-step replication kinetics of RRVΔLANA/GFP, RRV-GFP, wild-type (WT) RRV H26-95, and a revertant virus using traditional plaque assays as well as real-time QPCR based genome quantification assays. The RRVΔLANA/GFP recombinant virus exhibited significantly higher lytic replicative properties compared to RRV-GFP, WT RRV, or the revertant virus. This was observed upon *de novo* infection and in the absence of chemical inducers such as phorbol esters. In addition, by employing a quantitative real-time PCR-based viral array, we are the first to report differences in global viral gene expression between WT and recombinant viruses. The RRVΔLANA/GFP virus displayed increased lytic gene transcription at all timepoints post-infection compared to RRV-GFP. Moreover, we have also examined several cellular genes that are known to be repressed by KSHV LANA and report that these genes are de-repressed during *de novo* lytic infection with the RRVΔLANA/GFP virus compared to RRV-GFP. Finally, we also demonstrate that the RRVΔLANA/GFP virus fails to establish latency in B cells, as measured by the loss of GFP-

positive cells and intracellular viral genomes. Our future goal is to evaluate the RRVΔLANA/GFP as a vaccine candidate in rhesus macaques.

INTRODUCTION

Kaposi sarcoma-associated herpesvirus (KSHV), or human herpesvirus-8, is a member of the γ_2 -herpesviridae subfamily. This virus has been implicated as the etiological agent of Kaposi sarcoma (10) and lymphoproliferative diseases of B cell origin, namely, primary effusion lymphoma (PEL) (9) and the plasmablastic variant of multicentric Castleman disease (MCD) (29, 79).

A detailed understanding of KSHV replication and pathogenesis is important for understanding the biology of the diseases that are associated with this virus. However, *in vivo* studies of KSHV are limited due to the inability of KSHV to persistently infect mice or rhesus macaques (24, 69). Furthermore, difficulties are encountered when trying to study KSHV replication *in vitro* (68). Although several groups have described the use of endothelial cells to investigate *de novo* KSHV replication (20, 45, 68, 73), the virus replicates lytically only for a limited number of rounds before entering latency in these cells. Hence viral titers of KSHV are quite low in endothelial cells and plaques were rarely observed. Another system to generate lytic virus involves the treatment of KSHV-infected PEL cell lines with TPA or *n*-butyrate (57, 71). Here the problem is that only a small subset (25-30%) of latently infected PEL lymphocytes can be artificially reactivated with TPA (57, 71). Thus, the heterogeneous nature of the lytically and latently infected cell populations hampers the dissection of the function of individual viral genes in the context of the whole virus.

We have used rhesus monkey rhadinovirus (RRV) to model KSHV pathogenesis in rhesus fibroblasts (RhF) (60). RRV was first identified by Desrosiers *et al*. in 1997 at the New England Primate Research Center (NEPRC) as a γ_2-herpesvirus of rhesus macaques (*Macaca mulatta*) (16). This isolate was designated H26-95. Additionally, Wong *et al*. at the

Oregon Regional Primate Research Center isolated a different strain of RRV (designated 17577) from SIV-infected macaques (89). Sequence analysis revealed that the two RRV isolates are homologous to each other, though not identical. Importantly, both genomes exhibit co-linearity with the KSHV genome (2, 77) and all RRV genes have homologs in KSHV (2, 77). Wong *et al*. showed that in SIV-infected macaques, RRV induced B-cell hyperplasia resembling KSHV MCD (89) as well as non-Hodgkin lymphoma (61). Mansfield *et al*. reported that RRV also caused an arteriopathy in SIV-infected macaques (55).

RRV presents several advantages for studying lytic replication. First, the RRV lifecycle can be modeled *in vivo*, in rhesus macaques. Second, rhesus fibroblasts (RhF) support one hundred percent lytic replication of RRV and allows for the production of high titers of virus (approximately 10^6 plaque forming units per ml) (59). Our group has demonstrated that the transcription program of RRV is similar to that of KSHV (18, 26). Several laboratories have used the RRV model to study viral gene products, including the viral interleukin-6 (vIL-6) homologue (38), Rta/Orf50, R8/RAP, R8.1 (18, 51), R1 (14, 15), R15 (47, 64), RRV Orf4 (56), and the RRV-encoded microRNAs (75). We previously reported the kinetics of gene expression with regard to immediate-early, early, and late genes during RRV lytic infection and have reported they are similar to those seen during KSHV reactivation (18, 26). We also generated a RRV-GFP recombinant virus and devised plaque assays and quantitative real time QPCR assays for the determination of viral titers (19). This validates the experimental methods used here.

In KSHV, the latency-associated nuclear antigen (K-LANA) maintains latency by tethering the circularized viral episome to the mitotic host chromosomes, which allows the viral genome to co-segregate with the host genome to daughter cells during cellular

replication (6-8, 12, 13, 34, 39, 40, 42, 43, 66, 70, 81, 88, 90, 91). We have previously reported the identification and characterization of RRV LANA (R-LANA) (17). R-LANA shows homology to K-LANA except for the central variable-length internal acidic repeat domain, which is absent in R-LANA. The N- and C-terminal ends of R-LANA show high degree of sequence similarity to K-LANA, containing the same arrangement of chromosome-binding domain, nuclear localization signal, proline/serine-rich and glutamine-rich regions. Similar to K-LANA, R-LANA exhibited a speckled nuclear localization (17). We have previously reported that R-LANA can bind the RRV viral genome and may tether the RRV genome to the host chromosome in a similar fashion as K-LANA (17).

Genetically, both K-LANA and R-LANA are encoded by open reading frame (Orf) 73 of their respective viruses. K-LANA is found in the tricistronic latency-associated cassette, which also includes Orf71/vFLIP and Orf72/vCyclin (23, 74, 83). Differential splicing of the tricistronic cassette results in a 1.7 kb bicistronic transcript containing Orf72 and Orf71. Thus the expression of KSHV Orf71, Orf72, and Orf73 is coordinately driven by the common LANA promoter. Within the bicistronic transcript, there exists an internal ribosome entry site (IRES) in Orf72 for protein translation of Orf71. Although expressed at low levels, monocistronic Orf71 transcript was also detected during KSHV latency, and this transcript was upregulated during lytic reactivation, suggesting that there might be a cryptic promoter for Orf71 expression during the lytic cycle (32). In RRV, similarly arranged tricistronic (LANA, vCyclin, and vFLIP) and bicistronic (vCyclin and vFLIP) transcripts have been previously described by our group (18). In KSHV, LANA has also been shown to transactivate its own promoter (36, 37, 63, 80). Additionally, as a possible mechanism to ensure K-LANA expression during the lytic cycle, Rta (replication transcription activator)

was described to positively regulate K-LANA gene expression by recruiting RBP-Jκ to the LANA promoter (46). K-LANA, on the other hand, has been shown to inhibit Rta transactivation of downstream viral promoters by various mechanisms (reviewed in (85)).

Our lab has previously demonstrated that R-LANA inhibits RRV Rta transactivation of lytic promoters (17). In order to examine the role of R-LANA protein in the RRV lifecycle we have disrupted the expression of R-LANA in the viral genome using homologous recombination. In this report we describe the construction of a RRVΔLANA/GFP knockout virus and compare the replication kinetics of RRVΔLANA/GFP, RRV-GFP, and wild-type (WT) RRV H26-95 at three different multiplicities of infection (0.1, 0.5, and 5) using traditional plaque assays as well as real-time PCR based genome quantification assays. We have also constructed a revertant virus (RRV_{REV}) and find that it behaves similar to WT RRV.

Previously, LANA knockout viruses have been published for KSHV and murine gammaherpesvirus 68 (MHV68) (27, 28, 48, 58). The KSHV LANA deletion virus showed a higher viral replication than wild-type in contrast to the MHV68 LANA-null virus which showed absolutely no difference in replication *in vitro* at high MOI, and a lower amount of replication than wild-type at very low MOIs (28, 48, 58). These experiments yielded important insights, but also raised new questions since these viruses behaved very differently from each other with respect to replication. RRV is the closest relative to KSHV that has a *de novo* infection system. We constructed a RRVΔLANA/GFP knockout virus and have examined RRV LANA's contribution to the lytic and latent cycle. We found that RRVΔLANA/GFP exhibits enhanced lytic replication similar to the KSHV LANA deletion virus. Additionally, this higher lytic replication is seen upon *de novo* infection and in the

absence of chemical inducers like TPA. Furthermore, we are the first to employ a quantitative real-time PCR-based RRV viral array to transcriptionally profile genome-wide viral gene expression during *de novo* infection with RRVΔLANA/GFP and RRV-GFP viruses. We also analyzed several cellular genes that were previously reported to be repressed by KSHV LANA alone and found that they were derepressed in RRVΔLANA/GFP infected cells compared to RRV-GFP infected cells. This suggests that R-LANA modulates transcription of these genes during lytic infection and in the context of the whole virus.

MATERIALS AND METHODS

Cell culture

Immortalized rhesus macaque skin fibroblasts (RhF) with puromycin resistance were described previously (18). Cells were maintained at 37°C and 5% CO_2 in Dulbecco's modified Eagle's medium-H (DMEM-H) with Gluta-max supplemented with 10% fetal bovine serum (FBS), penicillin, and streptomycin. BJAB cells, a human B-cell line that is KSHV negative and Epstein-Barr virus negative were maintained in RPMI 1640 medium supplemented with 10% fetal bovine serum, penicillin, and streptomycin.

Construction of the recombinant RRVΔLANA/GFP virus and the revertant RRV_{REV} virus

RRV isolate H26-95 (16) and RRV-GFP (19) were previously described. To construct RRVΔLANA/GFP, a 3051-bp RRV LANA sequence of RRV H26-95 spanning nucleotides 117207 to 121414 was PCR amplified with primers 5′-CGCCGCGAATTCCGGTCAATGGAGAGCATCAGGTG-3′ and 5′-CGCCGCAAGCTTCGCGCGCTCACATAGACCTATAC-3′. This amplicon was subsequently cloned into pSp72 (Promega) at *Eco*RI and *Hind*III restriction sites to create pSp72-R-LANA-flank (also called R-LANA-flank plasmid). Site-directed mutagenesis was performed to create a *Sac*I site at nucleotide position 40 of the R-LANA ORF with primers 5'-CAGGAACTTCGCAACCCGAGCTCCGATACTATGCCGGAAC-3' and 5'-GTTCCGGCATAGTATCGGAGCTCGGGTTGCGAAGTTCCTG-3'. The resulting plasmid was designated pSp72-R-LANA-flank-new *Sac*I. The EGFP expression cassette driven by the CMV IE promoter with the SV40 polyadenylation signal was PCR amplified from a

pEGFP-N1 (Clontech) plasmid in which the multiple cloning site was removed by digesting with *Bam*HI and *Bgl*II and religating the ends together. The EGFP-N1 cassette primers used were 5′- CAAAAAGAGCTCGTAATCAATTACGGGGTCAT -3′ and 5′- CAAAAAGAGCTCACCACAACTAGAATGCAGTG -3′. The resulting *Sac*I tagged CMV-GFP-pA amplicon was ligated into pSP72-R-LANA-flank-new *Sac*I to form pSp72ΔLANA/GFP (also called R-LANA-flank+GFP plasmid). This plasmid was linearized by *EcoR*I digestion and then transfected into RhF by Amaxa Nucleofection system as described by the manufacturer. Forty-eight hours post-nucleofection, RhF were infected with RRV H26-95 virus at a low MOI. A single GFP-positive virus was isolated and purified by limiting dilution and plaque assay five times. To generate a revertant virus, RhF were nucleofected with *EcoR*I-linearized pSp72-R-LANA-flank plasmid and subsequently infected with RRVΔLANA/GFP at a low MOI. Clear, GFP-negative plaques were isolated and the revertant virus was further separated from RRVΔLANA/GFP by three rounds of plaque purification. This revertant virus was designated RRV_{REV}.

Viral DNA of RRV-H26-95, RRVΔLANA/GFP, or RRV_{REV} was used as a template for PCR analysis with the following primers: R-LANA flanking primers: 5'-CGCCGCGAATTCCGGTCAATGGAGAGCATCAGGTG-3' and 5'-CGCCGCAAGCTTCGCGCGCTCACATAGACCTATAC-3', R-LANA primers: 5'-GAGTTGGAATTC TTAGTGCTGAATTGGCAG-3' and 5'-CGGCAATCTAGATTAGTGCTGAATTGGCAGTCCTCTGTCCATGCGCACTATGC-3'.

Southern hybridization

Virus was harvested from virus-infected RhF by centrifugation at 17,000 rpm for 3 h. The virus pellet was resuspended in PBS, treated with sarkosyl and subsequently with proteinase K at 60°C for 1 h. Viral DNA was extracted by phenol-chloroform method. For Southern blot analysis, 1μg of the viral DNA was digested with *Nhe*I for hybridization with the RRV LANA probe or digested with *Sac*I for hybridization with the GFP probe. Digestion fragments of viral genomic DNA were subjected to electrophoresis through 1% low-melt agarose (NuSieve) and transferred overnight to a nylon membrane (Hybond N+) by capillary action. Following UV cross-linking, membranes were prehybridized in QuikHyb solution at 65°C for 15 min. Probes were generated from a 330-bp RRV LANA fragment restriction digested by *Kpn*I and *Fsp*I (R-LANA ORF nucleotide position 985 through 1315) and a 154-bp GFP fragment (nucleotide position 362 through 515 from the ATG start codon of EGFP-N1 plasmid) derived from PCR by random prime method using ^{32}P labeled dCTP (Roche). Probes were denatured at 95°C for 3 min and added to QuikHyb prehybe solution (Stratagene). Hybridization was carried out for 1 h at 65°C. Probe solution was removed and membranes were washed twice for 15 min with 2× SSC 0.1% SDS at room temperature and once for 30 min at 60°C with 0.1× SSC 0.1% SDS. Membranes were exposed overnight on an X-ray film.

Illumina/Solexa sequencing

Supernatant of RRV-infected RhF was filtered, concentrated by ultracentrifugation, and loaded on a Sepharose CL-4B column (Sigma) to isolate RRV virions. RRV genomic DNA was released by sarkosyl and proteinase K (Qiagen) treatment, and purified by phenol-

chloroform extraction. The viral DNA was further purified using Wizard® SV Genomic DNA Purification System (Promega) as per manufacturer's instructions. Four micrograms of RRVΔLANA DNA were submitted to UNC-CH Genome Analysis Facility and sequenced by the Illumina/Solexa 1G Genome Analyzer using the Illumina DNA sample Prep Kit (FC-102-1001), Standard Cluster Generation Kit (FC-103-1001), and 18-cyle Illumina Sequencing Kit (FC-104-1001). This sample was sheared to 200-300bp length using a Bioruptor. Library preparation then followed standard Illumina protocols for a GA2 sequencer (Illumina, San Diego CA). The Illumina GA2 sequencer was run with 36 cycles using the standard flow cell. Raw Illumina GA2 sequence image data was phased and filtered for quality using default GERALD parameters for unaligned reads (analysis: NONE, Use Bases: 35). Sequence reads were aligned to the RRV genome using the emboss function fuzznuc (72) and CLC Genomics Workbench V2.0.4 (CLC bio Inc.) under Mac OS X 10.5.5. Further analysis was conducted using R (GNU general public license (1)). For junction search, raw sequence data were first converted into a blast database using formatdb and then the predicted junction fragments 5'-ATGTCCCCTGCAGGAACTTCGCAACCCGAGCT_CGTAATCAATTACGGGGTCATTAGTTCAT and 5'-TTTTTTCACTGCATTCTAGTTGTGGTGAGCT_CCGATACTATGCCGGAACGATGTTGCCG (underscore marks the junction) were searched against the Illumina read database.

Quantitative real-time PCR for viral load and cellular gene expression analysis

For each sample, 10 μg of salmon sperm carrier DNA was added to 200 μl of clarified supernatant from infected cells and was processed through the DNeasy Kit (QIAGEN, Valencia, CA) as per the manufacturer's protocol. To quantify viral DNA, SYBR® Green

Real-time PCR in 384-well format was performed using the ABI PRISM® 7900 Sequence Detection System (Applied Biosystems Inc: Foster City, CA). To generate a standard curve for cycle thresholds versus genomic copy numbers, the pcDNA3-RRVOrf50 plasmid was serially diluted to known concentrations in the range of 10^1 to 10^6 plasmid molecules/µl. Each PCR mixture (15 µl) contained 4 µl of viral or standard DNA, 1 µl of Orf50 primer set (final working concentration at 3.33 µM), 7.5 µl of SYBR Green 2X PCR mix (Applied Biosystems), and 2.5 µl of DNase- and RNase- free water (Sigma) in a total volume of 15 µl. Primers for amplification of an 81-bp amplicon internal to the Orf50 sequence were 5′-GTGGAAAGCGGTGTCACAGA-3′ and 5′-TGCGGCGGCCAAAAT-3′. PCR conditions were as follows: 95°C for 15 min, followed by 95°C for 15 s, 60°C for 1 min repeated for 40 cycles. Similar reactions were assembled to assess cellular gene expression. The sequences for real-time PCR primers for the specific cellular genes shown in Table 1 including β-actin (housekeeping control) are provided in Table 2.

Plaque assays

RhF monolayers in 12-well plates were achieved by plating 2×10^5 cells per well 2 days before starting the assay. Ten-fold dilutions of virus-infected cell supernatants were made in DMEM-H supplemented with 2% fetal bovine serum (FBS). Each sample dilution was performed in triplicate. Two hundred microliters of each dilution was placed in each well of 12-well dishes and incubated at 37°C with redistribution of inoculum every 15 min. Importantly, for all infections, we incubated the virus with the cells for exactly two hours, after which the inoculum was aspirated and an overlay of methylcellulose was added to each well. The overlay media consisted of (per well): 1 ml 2×DMEM, 1 ml 1.5% methyl-cellulose

(Sigma M0512), and 40 µl FBS (2%). Cells were then incubated 7 days at 37°C and 5% CO_2. Overlay media was then aspirated and cells were stained with 0.8% crystal violet (Sigma C3886) in a 50% ethanol staining solution for 1 h. Plaques were counted under 10X magnification.

RRV real-time PCR genome array

The RRV quantitative real-time reverse transcription-PCR genome array was previously described (26). Samples were prepared for the viral array as follows: Virus was used to infect RhF at 0.5 MOI. The infected RhF were centrifuged and snap-frozen at −80^{o}C at 12, 24, 48, 72, 96, 120, and 144 hours post-infection. RNA from RRV-infected RhF was isolated using RNAzol (Tel-Test Inc.) as previously described (25, 26). Poly A mRNA was prepared using dT-beads (QIAGEN) and reverse-transcribed using Superscript II reverse transcriptase (Life Technologies) according to the manufacturer's recommendations. Five hundred nanograms of RNA were reverse-transcribed using ABI cDNA archive kit and random hexanucleotide primers (Applied Biosystems, Inc). The reaction mixture was sequentially incubated at 42°C for 45 min, 52°C for 30 min, and 70°C for 10 min. The RT reaction was quenched by heating to 95°C for 5 min and then subject to 0.5 U *RNase*H (Invitrogen) treatment at 37°C for an additional 30 min. Afterwards, the cDNA pool was diluted 25-fold with diethyl pyrocarbonate-treated, distilled H_2O and stored at -80°C. For quantitative real-time PCR, 2.5 µl of primer mix was combined with 7.5 µl SYBR Green 2X PCR mix (Applied Biosystems) and 5 µl cDNA and subjected to real-time QPCR on an MJR Opticon2 cycler using standard cycling conditions.

RRV infection of BJAB cells

2×10^5 BJAB cells were spinoculated in flat-bottom 12-well plates with 1.5 ml of diluted viral stock in complete RPMI medium in the presence of 4 μg/ml of polybrene as previously described (86). The cells were washed once with complete RPMI medium and then allowed to grow and expand in complete RPMI medium.

RESULTS

Generation of a RRVΔLANA/GFP recombinant virus.

Our lab has previously published the generation of a RRV recombinant virus expressing GFP (RRV-GFP) using homologous recombination (19). We used a similar homologous recombination approach to construct a RRVΔLANA/GFP recombinant virus by inserting a GFP expression cassette into the R-LANA ORF to disrupt R-LANA transcription and translation. A 3051 bp RRV LANA sequence of RRV H26-95 spanning nucleotides 117207 to 121414 was PCR amplified and subcloned into the plasmid pSp72 to create pSp72-R-LANA-flank. We then mutagenized a unique *Sac*I restriction site in the R-LANA ORF in the pSp72-R-LANA-flank plasmid at nucleotide position 40 of the R-LANA ORF to generate pSp72-R-LANA-flank-new *Sac*I. The GFP expression cassette was subcloned into this *Sac*I site in an opposite direction to the R-LANA ORF to yield the plasmid pSp72ΔLANA/GFP. Next, the pSp72ΔLANA/GFP plasmid was linearized with *Eco*RI, and RhF were nucleofected with the linearized pSp72ΔLANA/GFP plasmid, followed by RRV infection at a low multiplicity of infection (Fig. 1A). Single GFP-positive viruses were plaque purified for five rounds and one such isolate, named RRVΔLANA/GFP, was chosen for further study. Using a similar procedure, we subsequently generated a rescue virus by nucleofection of RhF with *Eco*RI-linearized pSp72-R-LANA-flank plasmid, followed by infection with RRVΔLANA/GFP at a low multiplicity of infection (Fig. 1B). Clear, GFP-negative plaques were isolated and separated from GFP-positive RRVΔLANA/GFP by plaque purification. One such revertant virus, designated RRV_{REV}, was chosen for further study.

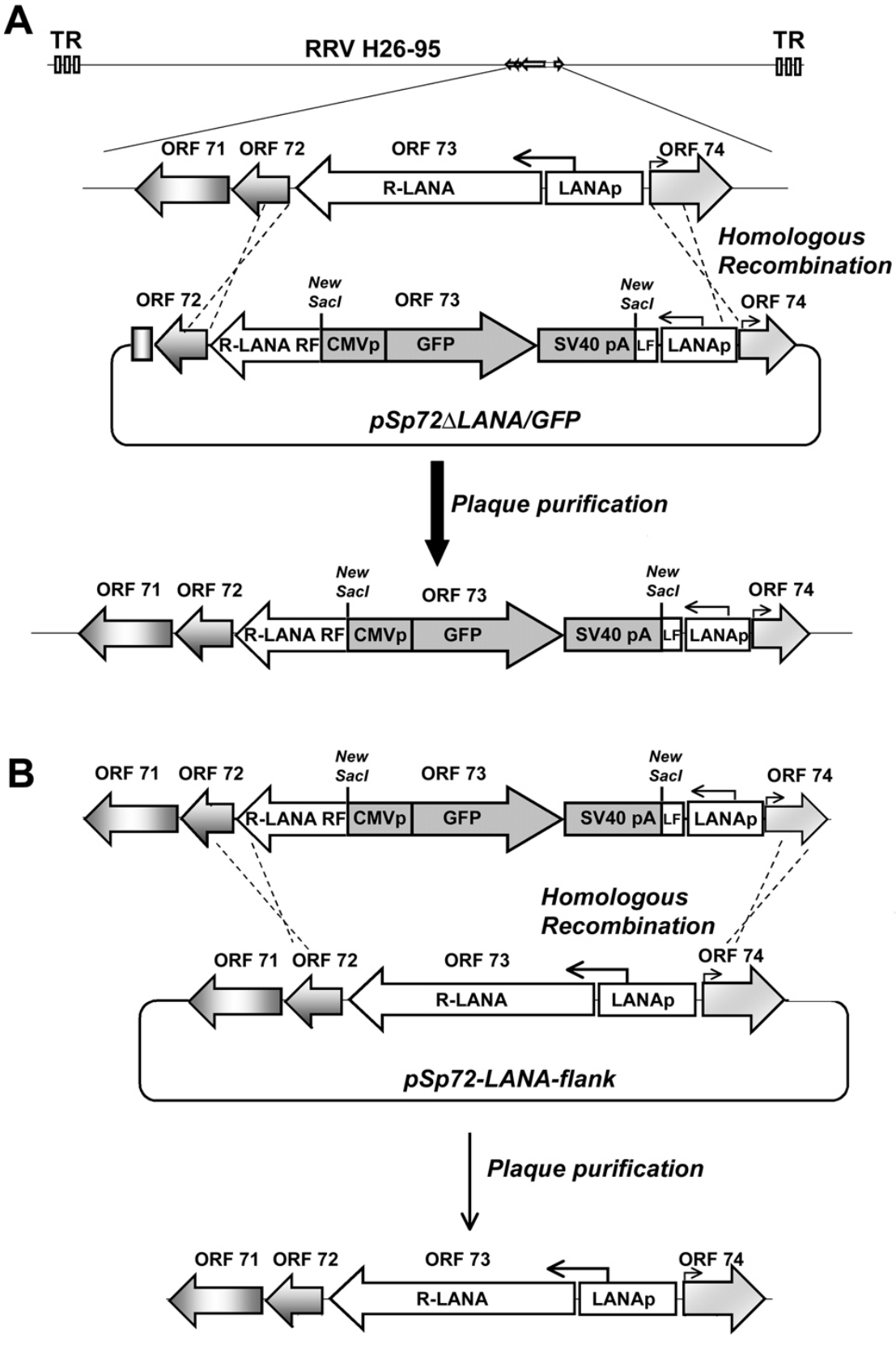
A
TR
RRV H26-95
TR
ORF 71
ORF 72
ORF 73
ORF 74
R-LANA
LANAp
Homologous Recombination
ORF 72
New SacI
ORF 73
New SacI
ORF 74
R-LANA RF
CMVp
GFP
SV40 pA
LF
LANAp
pSp72ΔLANA/GFP
Plaque purification
ORF 71
ORF 72
New SacI
ORF 73
New SacI
ORF 74
R-LANA RF
CMVp
GFP
SV40 pA
LF
LANAp
B
ORF 71
ORF 72
New SacI
ORF 73
New SacI
ORF 74
R-LANA RF
CMVp
GFP
SV40 pA
LF
LANAp
Homologous Recombination
ORF 71
ORF 72
ORF 73
ORF 74
R-LANA
LANAp
pSp72-LANA-flank
Plaque purification
ORF 71
ORF 72
ORF 73
ORF 74
R-LANA
LANAp

Figure 1 (previous page). A schematic representation of the construction of the RRVΔLANA/GFP and RRV_{REV} recombinant viruses. A) Construction of the RRVΔLANA/GFP virus. An EGFP expression cassette driven by a CMV promoter was inserted into the N-terminus of R-LANA (Orf73) to disrupt the R-LANA ORF. This EGFP cassette was cloned into a plasmid containing the coding sequence of R-LANA and flanking ORFs (Orf71 to Orf74). The plasmid (pSp72ΔLANA/GFP) was linearized and transfected into RhF, and then subjected to RRV infection at a low multiplicity of infection (MOI). Single GFP-expressing viral plaques were purified for five rounds and one such isolate, designated RRVΔLANA/GFP, was chosen for further study. **B)** Construction of a revertant RRV_{REV} virus. A plasmid containing the coding sequence of R-LANA flanked by Orf71 and Orf74 (pSp72-R-LANA-flank) was linearized and transfected into RhF. Transfected cells were infected with RRVΔLANA/GFP at a low MOI. GFP-negative viral plaques were purified. One such isolate was designated RRV_{REV} and chosen for further study. LF denotes left flank; RF, right flank.

We have confirmed the correct insertion of the GFP cassette into RRVΔLANA/GFP by diagnostic PCR with two different sets of primers targeting full length R-LANA ORF and its flanking regions, respectively (Fig. 2A, B, C). Cell pellets of RhF infected with RRVΔLANA/GFP were subjected to total DNA isolation on DNeasy columns (Qiagen). Approximately 500 nanograms of total DNA per infected sample were subjected to standard PCR. The R-LANA-flank plasmid (also called pSp72-R-LANA-flank plasmid in Fig. 1B), or parental H26-95 viral DNA, was used as the PCR template as a negative control for GFP insertion. The R-LANA-flank+GFP plasmid (also called pSp72ΔLANA/GFP in Fig. 1A) served as the PCR template for the positive control. The R-LANA primers and R-LANA flanking primers amplified from the R-LANA-flank+GFP plasmid template showed the expected fragment sizes of 2950 bp and 5800 bp, respectively (Fig. 2B & 2C).

The removal of the GFP sequence in rescue virus RRV_{REV} was likewise confirmed by diagnostic PCR (Fig. 2D, 2E, 2F). Total DNA was isolated from RRV_{REV}-infected RhF pellets and subjected to standard PCR. The R-LANA-flank plasmid DNA or H26-95 viral

DNA was used as a control to show the expected amplicon sizes of intact R-LANA (Fig. 2). The PCR products of RRV_{REV} viral DNA show the correct size of 1350 bp for wild-type R-LANA ORF with the full length R-LANA primer set (Fig. 2E), and 4200 bp for wild-type R-LANA flank sequence with the R-LANA flank primer (Fig. 2F).

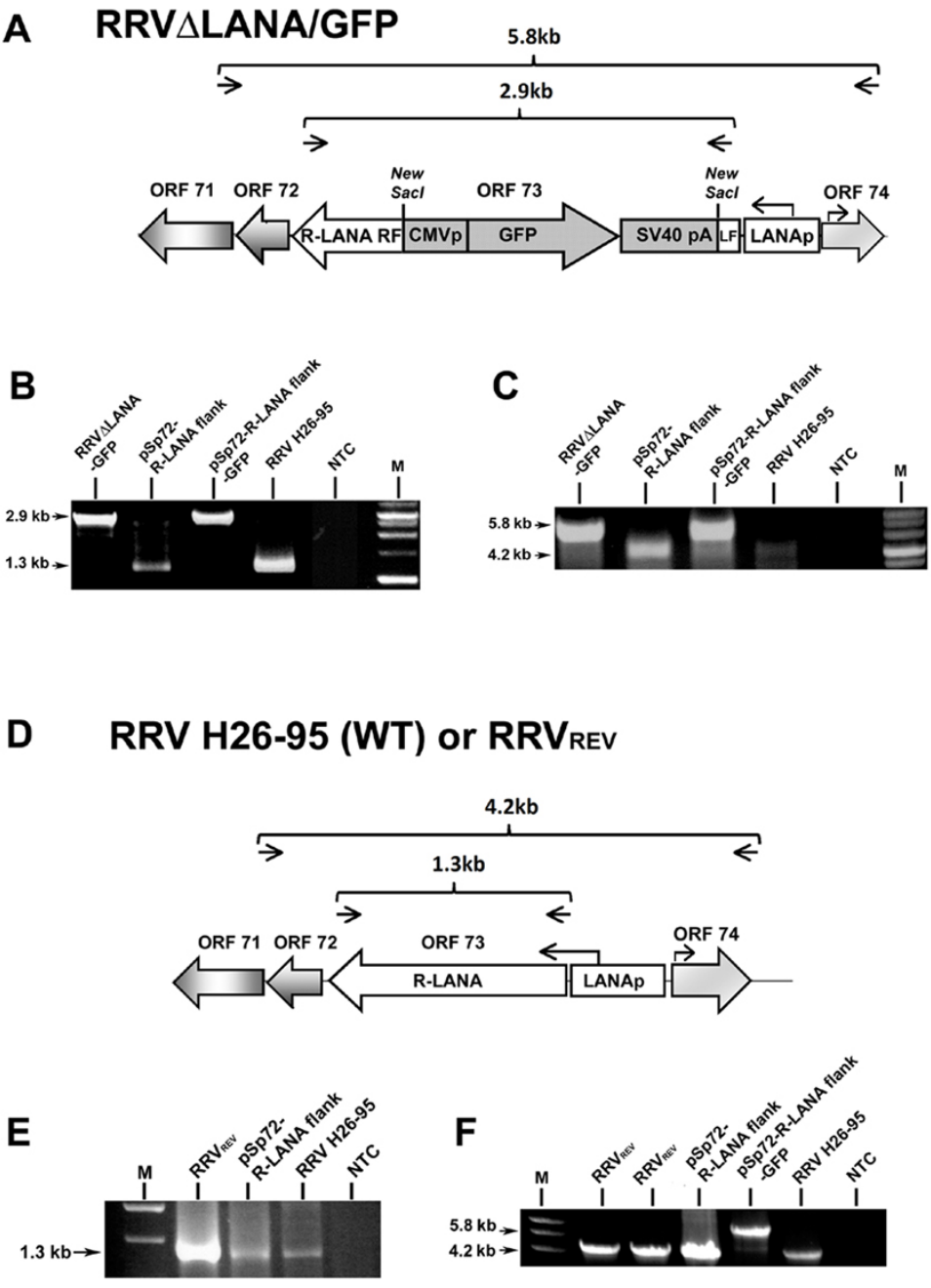

Figure 2 (previous page). PCR analysis of recombinant viruses. A) A schematic representation of PCR diagnosis of RRVΔLANA/GFP virus. Primers (arrows) for either the full length R-LANA ORF (lower bracket) or the R-LANA flanking ORF (upper bracket). **B)** Templates used in the PCR reactions are labeled on top of each lane. NTC denotes non-template control and M denotes marker. With the R-LANA primer set, the expected size for R-LANA (~1350 bp) was seen in R-LANA-flank plasmid (i.e. pSp72-R-LANA-flank plasmid in Fig. 1B) and RRV H26-95 viral DNA. The RRVΔLANA/GFP lane and R-LANA-flank+GFP (i.e. pSp72ΔLANA/GFP in Fig. 1A) plasmid lane show the expected size (~2950 bp) for EGFP cassette (~1600 bp) insertion. **C)** With the R-LANA flanking primer set, an expected size of ~4200 bp was seen with the R-LANA-flank plasmid and RRV H26-95 viral DNA. The RRVΔLANA/GFP lane and R-LANA-flank+GFP plasmid lane show the expected size (~5800 bp) for EGFP cassette insertion. **D)** A schematic representation of PCR diagnosis of RRV_{REV}. Primers (arrows) for either the full length R-LANA ORF (lower bracket) or the R-LANA flanking ORF (upper bracket). **E)** With the full length R-LANA primer set, the PCR product of RRV_{REV} shows the correct size for R-LANA ORF, similar to the amplicon size (~1350 bp) of positive template controls (R-LANA-flank plasmid and RRV H26-95 viral DNA). **F)** PCR using the R-LANA flank primer set displays an expected amplicon size (~4200 bp) for the RRV_{REV} template as indicated by the same amplified fragment size when wild-type R-LANA-flank plasmid or viral DNA H26-95 was used as the template.

To rule out aberrant insertion of the exogenous GFP cassette into the rest of the viral genome, diagnostic Southern blot analysis following restriction digest was performed. We have provided a graphical scheme of the restriction digestion and Southern blotting in Fig. 3A. Virion DNA from wild-type RRV H26-95, RRVΔLANA/GFP, and RRV_{REV} recombinant viruses grown on RhF was isolated and digested with *Nhe*I. The digested DNA fragments were resolved on two separate agarose gels by electrophoresis and the gels were transferred and crosslinked to nitrocellulose membrane. Southern blots were performed using a radiolabeled probe complementary to either the R-LANA or the GFP sequence (Fig. 3A). The R-LANA specific probe hybridized to a predicted 2.4 kb fragment in RRVΔLANA/GFP and a predicted 6.5 kb fragment in RRV H26-95 and RRVΔLANA $_{REV}$ digested with *Nhe*I (Fig. 3B). The GFP-specific probe used in the Southern blot revealed the expected hybridization fragment size of 5.6 kb for *Nhe*I digested RRVΔLANA/GFP virion DNA (Fig.

3C). As expected, the probe did not hybridize to the wild-type H26-95 or the rescue virus DNA. A third Southern blot was performed using the GFP probe (Fig. 3D). Since the GFP cassette in RRVΔLANA/GFP was inserted into the virus at a newly created *Sac*I site, restriction digestion with *Sac*I should release a 1.6 kb fragment corresponding to the size of the exogenous GFP sequence from this recombinant virus. In the Southern blot shown in Fig. 3D, this fragment was detected by the GFP probe in *Sac*I-digested virion DNA of RRVΔLANA/GFP but was absent in the *Sac*I-digested H26-95 and RRV_{REV} genomic DNA, as expected. Ethidium bromide stained gels of *Sac*I single-digested and *Sac*I/*Eco*RI double-digested RRV H26-95 and RRVΔLANA/GFP viral DNA are shown in Fig. 4.

Figure 3 (next page). Restriction digest and Southern blot analysis of recombinant viruses. A) A schematic illustration showing the strategy for *Nhe*I or *Sac*I restriction enzyme digestion and Southern blot analysis of RRVΔLANA/GFP, wild-type H26-95, and RRV_{REV} genomic DNA. R-LANA probe was generated from digestion of a plasmid encoding R-LANA, and the GFP probe was generated from a PCR product of the pEGFP-N1 plasmid. **B)** The R-LANA probe hybridized to a 2.4 kb fragment in RRVΔLANA/GFP digested with *Nhe*I, and a 6.5 kb fragment in RRV H26-95 and RRV_{REV} digested with *Nhe*I. **C)** The GFP probe hybridized to a 5.6 kb fragment of *Nhe*I digested RRVΔLANA/GFP genomic DNA. The GFP probe did not hybridize to the wild-type H26-95 or RRV_{REV} DNA, as expected. **D)** Restriction digestion with *Sac*I released a 1.6 kb fragment corresponding to the size of the exogenous GFP sequence from RRVΔLANA/GFP genomic DNA, but no fragment was detected in the wild-type or revertant viral DNA.

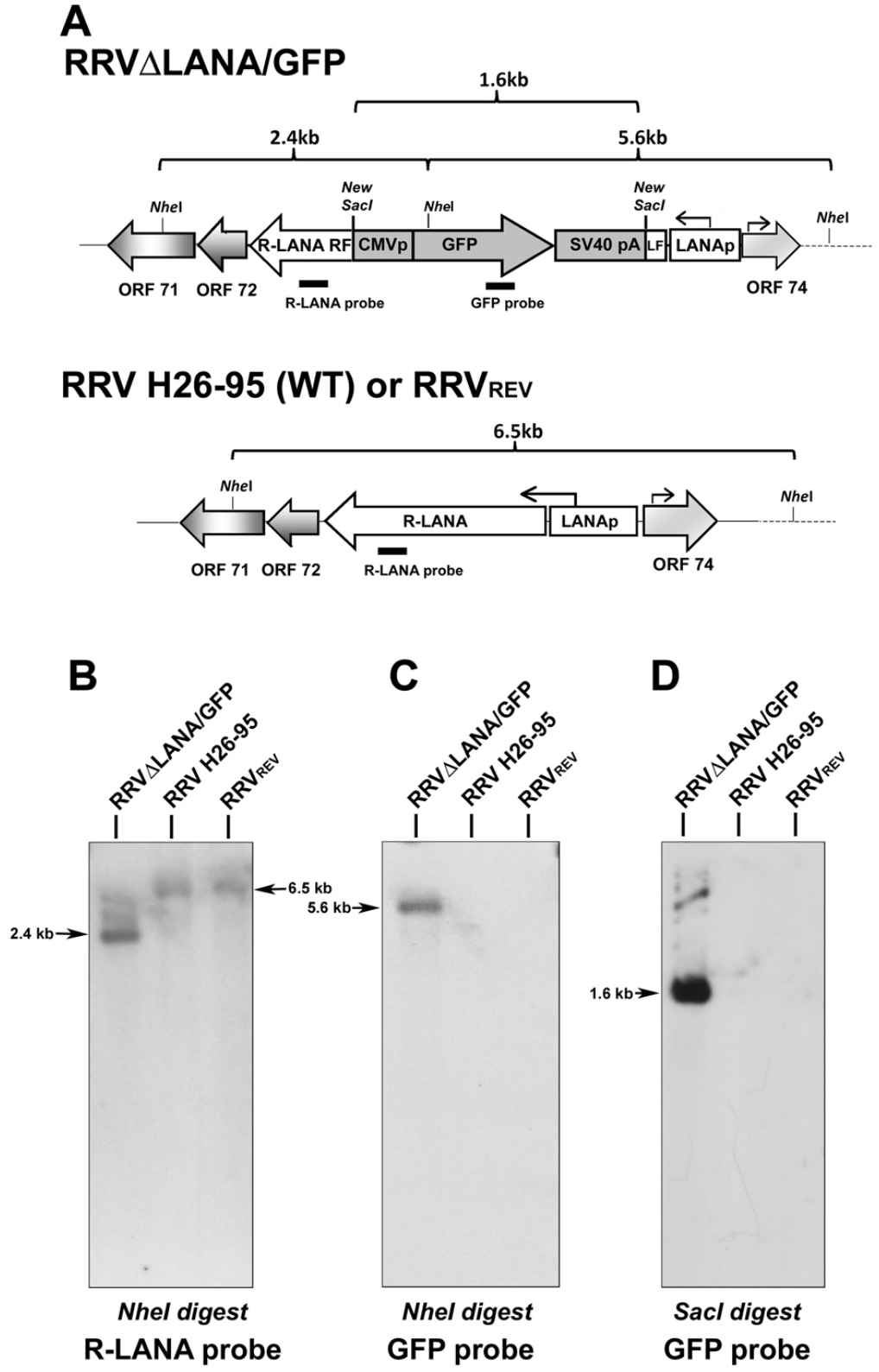
A
RRVΔLANA/GFP
1.6kb
2.4kb
5.6kb
NheI
New SacI
NheI
New SacI
NheI
R-LANA RF
CMVp
GFP
SV40 pA
LF
LANAp
ORF 71
ORF 72
R-LANA probe
GFP probe
ORF 74
RRV H26-95 (WT) or RRVREV
6.5kb
NheI
R-LANA
LANAp
NheI
ORF 71
ORF 72
R-LANA probe
ORF 74
B
C
D
RRVΔLANA/GFP
RRV H26-95
RRVREV
2.4 kb
6.5 kb
5.6 kb
1.6 kb
NheI digest
R-LANA probe
NheI digest
GFP probe
SacI digest
GFP probe

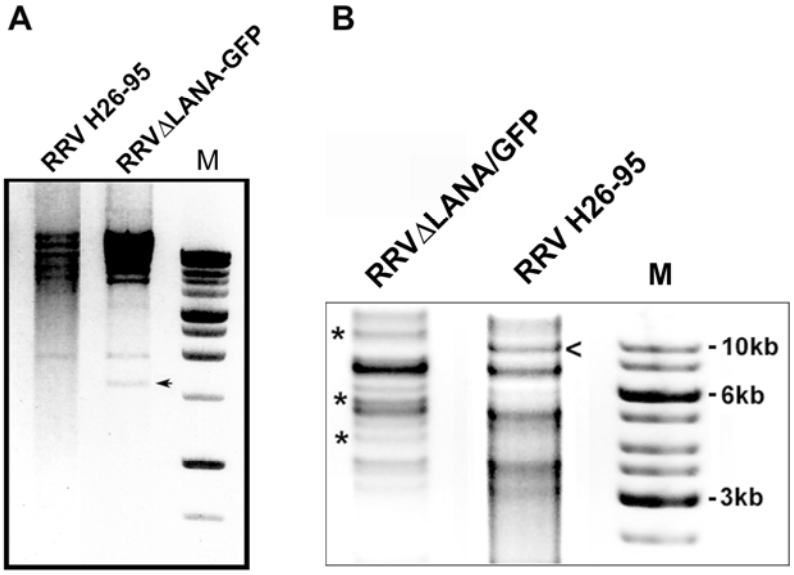

Figure 4. Restriction digestion analysis of recombinant RRVΔLANA/GFP and parental H26-95 genomes. The ethidium bromide-stained agarose gel images were taken with Kodak Gel Logic 200 Imaging system. The image was shown in this figure with reverse contrast. **A)** Viral genomes were restriction digested with *Sac*I, which released a unique 1.6 kb fragment in RRVΔLANA/GFP (marked with an arrow head). **B)** Viral genomes were double-digested with *Eco*RI and *Sac*I. The expected DNA fragments unique for RRVΔLANA/GFP viral DNA were marked with asterisks (*). H26-95 contains only one unique restriction fragment and it was marked with <. M denotes marker.

Whole genome sequencing of the RRVΔLANA/GFP recombinant virus.

The results from these traditional molecular analyses suggest that the RRVΔLANA/GFP recombinant virus is genetically identical to the wild-type RRV H26-95 genome, except for the insertion of the GFP expression cassette in the R-LANA ORF. To further ensure complete genetic integrity at the nucleotide level, we performed genome-wide sequencing of RRVΔLANA/GFP virus using the recently developed Illumina/Solexa sequencing technology. It was crucial to obtain highly pure and abundant viral DNA for such a purpose. Approximately 5×10^8 RhF were subjected to RRVΔLANA/GFP infection and virus was amplified until complete cytopathic effect was observed. Cell-free supernatant of RRV-infected RhF was filtered, ultracentrifuged, and subjected to virion purification on a

sepharose column. RRV genomic DNA was released by sarkosyl and proteinase K treatment, and purified by phenol-chloroform extraction. Further purification of genomic DNA was performed using Wizard® SV Genomic DNA Purification System (Promega). Four micrograms of RRVΔLANA DNA were submitted to the UNC-CH Genome Analysis Facility. We obtained full coverage of the RRVΔLANA/GFP viral genome when the parental RRV H25-95 (AF210726) excluding the 3' terminal repeat was used as the reference sequence. We used stringent alignment parameters. Only reads of 35 nucleotides were used. We obtained 8,179,932 raw reads. 1,451,388 reads matched the AF210726 RRV strain H25-95 sequence excluding any gaps and allowing for at most one mismatch. Maximum coverage was 876 fold excluding the terminal repeats. The detailed coverage distribution is shown in Fig. 5A. Importantly, RRVΔLANA/GFP contained no deletions or rearrangements (average coverage per base pair >100). The RRVΔLANA/GFP genome is identical to the reference H26-95 sequence except at the disrupted R-LANA ORF. A few single nucleotide polymorphisms (SNPs) were present that were also polymorphic in the other RRV 17577 strain and may in fact represent sequencing errors in the initial reference sequence. Correct insertion of the GFP cassette into the R-LANA ORF was verified by comparing the sequenced fragments with the predicted LANA-GFP junctional sequences (Fig. 5B and 5C). Importantly, 476 illumina reads matched the 5' junction without gaps or mismatch and 500 reads matched the 3' junction sequences without gaps or mismatch. This demonstrates that the recombinant virus had the desired structure and no inadvertent secondary mutations.

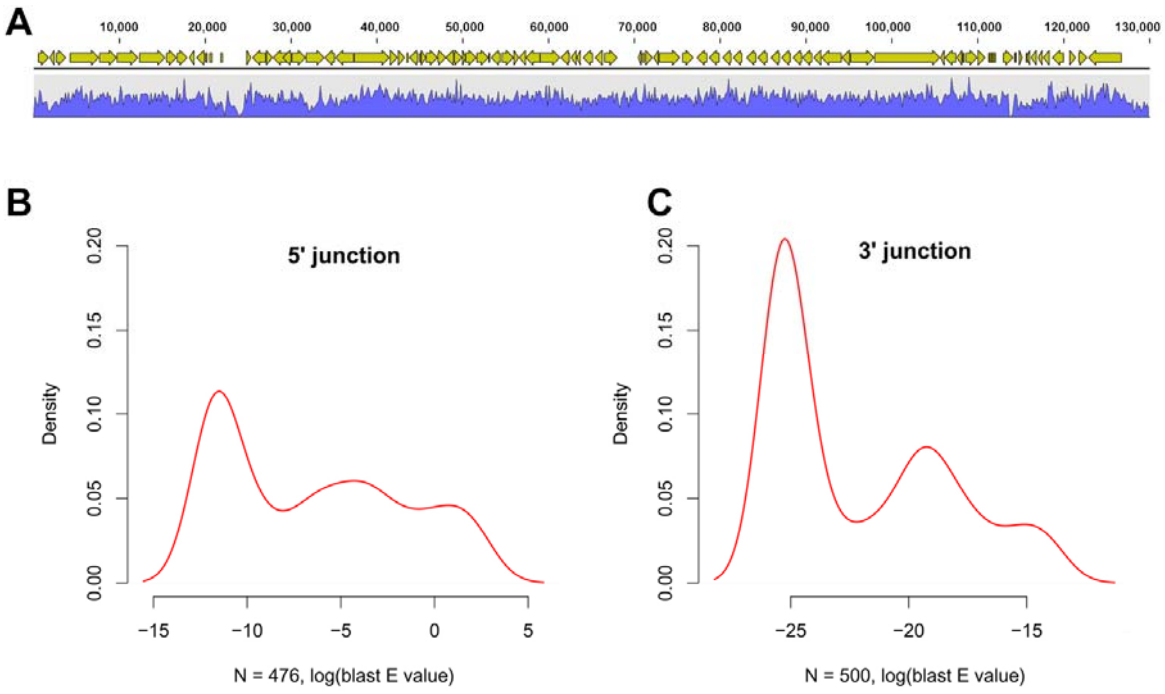

Figure 5. Illumina/Solexa whole viral genome sequencing. A) Coverage of RRVΔLANA/GFP genome by Solexa sequencing reads. Solexa generates 35bp DNA reads. These were aligned to the RRV H26-95 genome using the reference sequence. The arrows on top represent individual RRV ORFs and the numbers represent nucleotide coordinates. The graph below shows the number of reads at each nucleotide position on a linear scale from 0 to 876. Peaks indicate regions of high coverage; valleys indicate regions of low coverage. Complete coverage of the whole RRV H26-95 genome was achieved. Maximum coverage was 876 fold. **B)** Correct insertion of the GFP cassette into the R-LANA ORF was verified by comparing all Solexa fragments with the predicted RRV LANA-GFP junctional sequence. We found 476 Solexa reads that matched the 5' LANA-GFP junctional sequence. Shown is the distribution (density) of BLAST scores log(blast E value) for this comparison. Lower values (< -10) indicate sequence reads that matched the junction sequence perfectly, without any gap or even a single mismatch. **C)** We found 500 Solexa reads that matched the 5' LANA-GFP junctional sequence. Shown is the distribution (density) of BLAST scores log(blast E value) for this comparison. Again, the majority of reads matched perfectly (lowest log(blast E value)). If there was an inadvertent single nucleotide insertion at this site, we would expect the majority (i.e. the peak of the density distribution) not to be associated with the lowest log(blast E value), but with a higher one, indicative of a mismatch.

Absence of R-LANA leads to more lytic replication during *de novo* infection.

As we have previously reported (19), RRV infection of RhF provides a lytic system to study *de novo* viral replication. We wanted to examine the role of R-LANA in lytic replication in the context of the whole virus. Infection with RRVΔLANA/GFP, the parental H26-95 virus, revertant virus RRV_{REV}, and RRV-GFP viruses was performed at 0.5 MOI (Fig. 6), 0.1 MOI (Fig. 7), or 5 MOI (Fig. 8) in duplicate on confluent monolayers of RhF. These three different MOIs were chosen in order to assess whether R-LANA may have variegating effects on lytic viral replication based on multiple-step (0.1 and 0.5 MOI) versus single-step (5 MOI) infection conditions. RRV-GFP virus (19) contains a CMV immediately-early promoter-driven GFP cassette in a non-coding intergenic region of RRV between ORFs 18 and 19. RRV-GFP virus was used to control for any undesirable GFP-related effects on RRVΔLANA/GFP viral replication. After an inoculation period of two hours for optimal adsorption, the supernatants from the infected cells were aspirated and replaced with DMEM containing 2% FBS to allow infections to proceed. At 0, 24, 48, 72, 96, 120, and 144 hours post infection (hpi), cell-free supernatants were harvested by centrifugation at 2,000 rpm for 5 min. For the viral growth curves, the supernatants were serially diluted in triplicate and subjected to traditional plaque assays to measure infectious particles (Fig. 6A, 7A, and 8A). For real-time PCR to measure extracellular viral genome copies (Fig. 6B, 7B, and 8B), 200 μl of the clarified supernatant for each infection sample, spiked with salmon sperm DNA was processed through a DNeasy column (QIAGEN) for DNA isolation. Two hundred microliters of the eluate were collected, 4 μl of which was then subjected to real-time PCR in triplicate using SYBR® Green mixture containing RRV Orf50 primers. To obtain absolute quantification, a standard curve for Orf50 was generated for each real-time PCR run. For

QPCR intracellular viral assays, the infected cells were harvested by trypsinization. Each infected cell pellet was resuspended in 200 µl of PBS and the total DNA content was column-purified by the DNeasy kit (QIAGEN) and eluted in 200 µl of elution buffer. Four microliters of the eluate was then subjected to real-time QPCR in triplicate. The results are shown in Figures 6C, 7C, and 8C. In order to account for cell death following viral replication in our data analysis, intracellular viral genomes were also normalized to rhesus genomes using rhesus tubulin as an endogenous control (Figs. 6D, 7D, and 8D).

The results at all three MOIs show that RRVΔLANA/GFP exhibited significantly faster growth kinetics by replicating to higher titers compared to the other three viruses. This enhanced growth property was more pronounced during earlier timepoints. At later timepoints the levels of RRVΔLANA/GFP viral genomic DNA and RRVΔLANA/GFP infectious particles reached a plateau, while DNA synthesis of the parental H26-95 virus and revertant virus RRV_{REV}, and RRV-GFP continued. This was likely due to the depletion of viable cells available for replication for RRVΔLANA/GFP virus during later timepoints after the virus had replicated through the monolayer of RhF at earlier timepoints. Expectedly, the rescue virus RRV_{REV}, displayed nearly identical growth kinetics as wild-type RRV by plaque assay and genome quantitation assay. As revealed by comparing the growth curves of RRV-GFP virus with the wild-type and revertant viruses, the presence of GFP slightly decreased virus replication at both 0.1 and 0.5 MOI. This is likely due to the cytotoxic effects of GFP expression on the infected RhF. Thus, true assessment of the role of R-LANA on lytic viral replication should be made by comparing the viral growth curves of RRVΔLANA/GFP with that of the RRV-GFP recombinant virus. The RRVΔLANA/GFP virus showed a greater than 10 fold higher level of replication than the RRV-GFP virus at early timepoints. Additionally,

the RRVΔLANA/GFP virus produced more viral genomes and functional virions than the RRV-GFP virus at all timepoints at both 0.1 and 0.5 MOI. At the single-step MOI of 5, the more rampant viral replication by RRVΔLANA/GFP was maintained during early infection up to 72 hpi and then plateaued due to the depletion of viable cells required for replication.

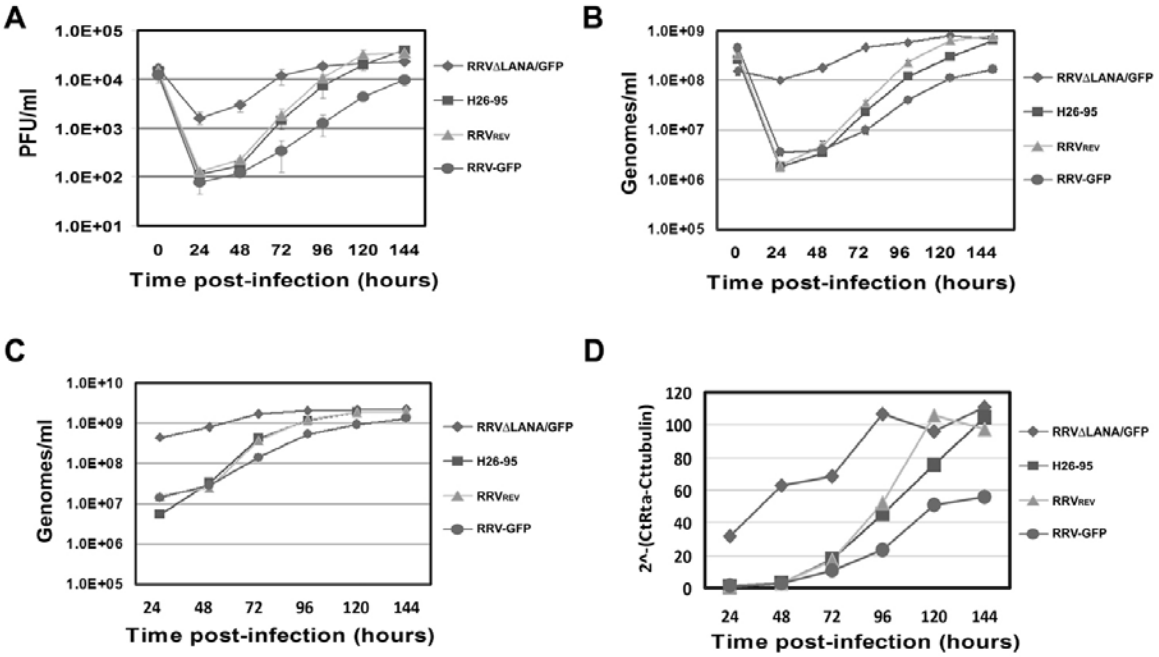

Figure 6. Viral growth curves of RRVΔLANA/GFP in rhesus fibroblasts at 0.5 MOI. Equivalent numbers of RhF cells were infected with RRVΔLANA/GFP (◊), wild-type H26-95 (□), RRV_{REV} (Δ), or RRV-GFP (O) at a MOI of 0.5. Cell-free supernatants and cell pellets were harvested at indicated points post-infection. **A)** Infectious virus particles from supernatants were quantitated by traditional plaque assay. **B)** Extracellular viral genomes from the same samples as in A) were quantitated by real-time PCR assay. In this real-time PCR-based assay, a RRV Orf50/Rta copy number standard curve was used to generate the viral genome copy number. **C)** Intracellular viral genomes extracted from infected cell pellets were quantitated by real-time PCR using a RRV Orf50 standard curve to generate the viral genome copy number. **D)** The viral genomes were normalized to rhesus β-tubulin copy numbers. The same samples as in C) were subjected to real-time PCR with RRV Orf50 primers as described in panel C, and rhesus β-tubulin primers to absolutely quantitate rhesus β-tubulin copy numbers using a rhesus β-tubulin standard curve. During real-time QPCR, the amount of product at each cycle is quantified and the cycle threshold (Ct) at which the product signal crossed a user-defined threshold is recorded. In this figure, dCt is mathematically defined as Ct_{Rta}-$Ct_{tubulin}$, the signal difference between the viral gene Orf50 and the cellular gene rhesus β-tubulin in a sample. The y-axis ($2^{-(Ct_{Rta}-Ct_{tubulin})}$) thus reflects the fold difference, or relative abundance, of RRV viral genomes compared with the cellular genomes. In all panels, results are the averages of duplicate or triplicate samples. Error bars represent standard deviations.

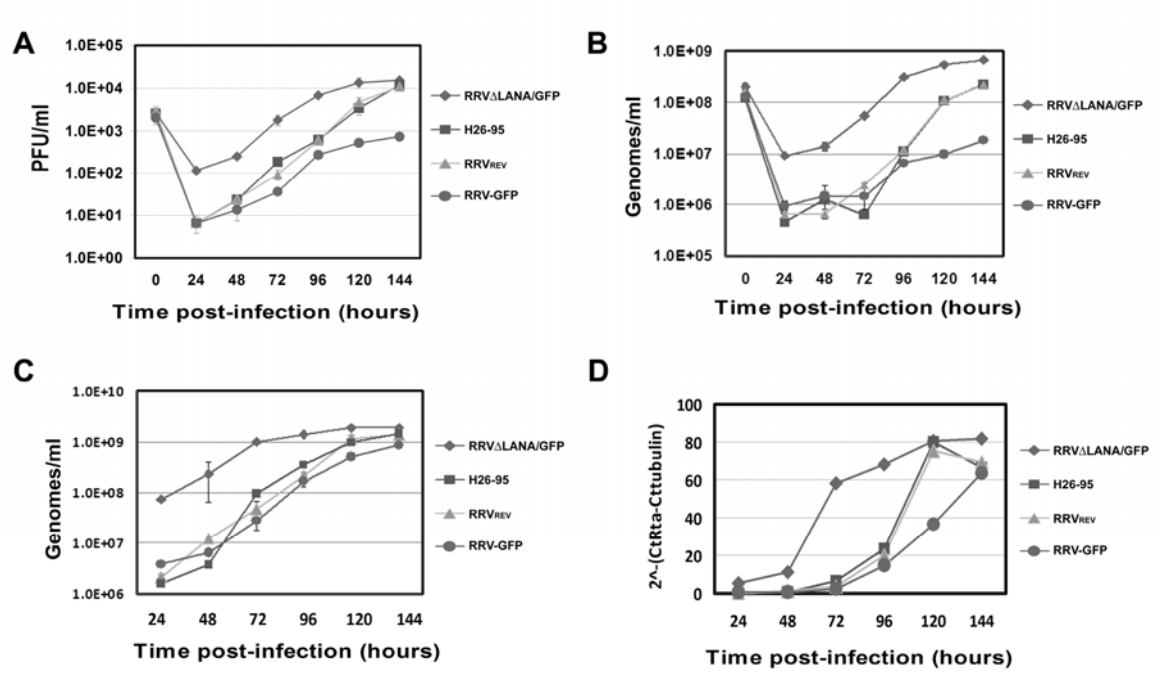

Figure 7. Viral growth curves of RRVΔLANA/GFP in rhesus fibroblasts at 0.1 MOI. Equivalent numbers of RhF cells were infected with RRVΔLANA/GFP (◊), wild-type H26-95 (□), RRV_{REV} (Δ), or RRV-GFP (O) at a MOI of 0.1. Cell-free supernatants and cell pellet were harvested at indicated points postinfection. **A)** Infectious virus particles from supernatants were quantitated by traditional plaque assay. **B)** Extracellular viral genomes from the same samples as in A) were quantitated by real-time PCR assay. In this real-time PCR-based assay, a RRV Orf50 copy number standard curve was used to generate the viral genome copy number. **C)** Intracellular viral genomes extracted from infected cell pellets were quantitated by real-time PCR using a RRV Orf50 standard curve to generate the viral genome copy number. **D)** The viral genomes were normalized to rhesus β-tubulin copy numbers. The same samples as in C) were subjected to real-time PCR with RRV Orf50 primers as described in panel C, and rhesus β-tubulin primers to absolutely quantitate rhesus β-tubulin copy numbers using a rhesus β-tubulin standard curve. In all panels, results are the averages of duplicate or triplicate samples. Error bars represent standard deviations.

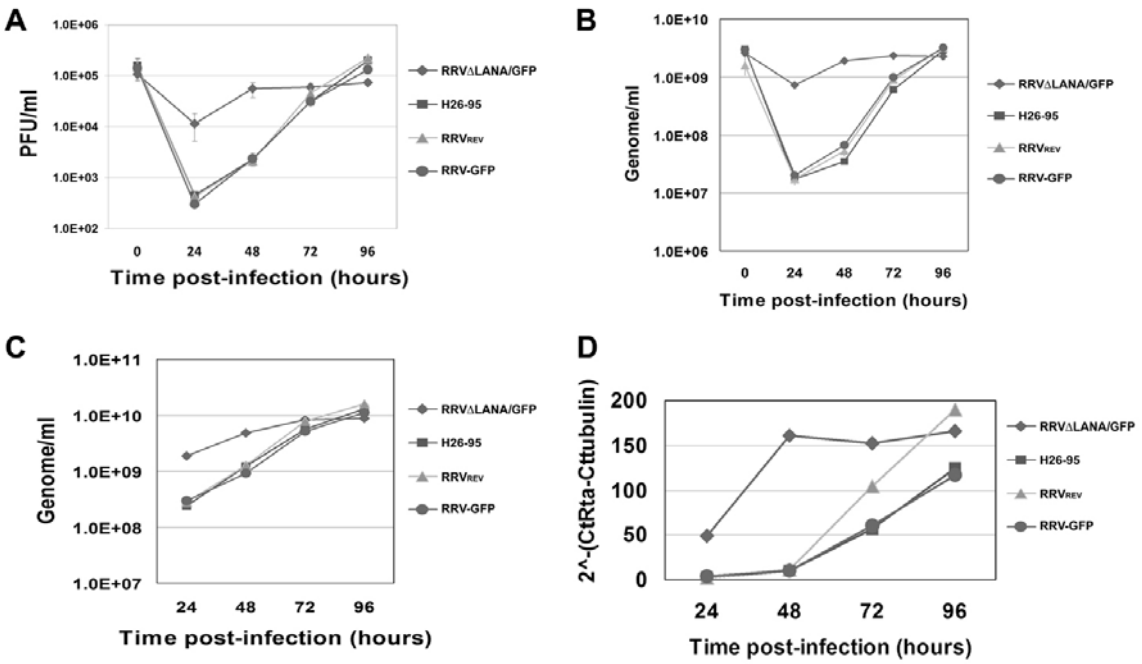

Figure 8. Viral growth curves of RRVΔLANA/GFP in rhesus fibroblasts at 5 MOI. Equivalent numbers of RhF cells were infected with RRVΔLANA/GFP (◊), wild-type H26-95 (□), RRV_{REV} (Δ), or RRV-GFP (O) at a MOI of 5. Cell-free supernatants and cell pellet were harvested at indicated points postinfection. **A)** Infectious virus particles from supernatants were quantitated by traditional plaque assay. **B)** Extracellular viral genomes from the same samples as in A) were quantitated by real-time PCR assay. In this real-time PCR-based assay, a RRV Orf50 copy number standard curve was used to generate the viral genome copy number. **C)** Intracellular viral genomes extracted from infected cell pellets were quantitated by real-time PCR using a RRV Orf50 standard curve to generate the viral genome copy number. **D)** The viral genomes were normalized to rhesus β-tubulin copy numbers. The same samples as in C) were subjected to real-time PCR with RRV Orf50 primers as described in panel C, and rhesus β-tubulin primers to absolutely quantitate rhesus β-tubulin copy numbers using a rhesus β-tubulin standard curve. In all panels, results are the averages of duplicate or triplicate samples. Error bars represent standard deviations.

Absence of R-LANA results in the enhanced transcriptional expression of many RRV genes.

Based on our growth curve experiments (Figs. 6, 7, and 8), RRVΔLANA/GFP virus displayed more lytic viral replication than H26-95, RRV-GFP, and RRV_{REV} viruses. We were therefore interested to determine whether the overall pattern of RRV viral gene expression was altered during *de novo* infection. We used the RRV real-time quantitative PCR viral array our lab previously reported (26) to profile the gene expression of all 84 RRV ORFs following *de novo* infection of RhF at 0.5 MOI. A heat map representation of real-time QPCR data normalized to rhesus tubulin (dCT) from viral infection timepoints at 0, 12, 24, 48, 72, 96, 120, and 144 hpi was generated. The dCT values were subjected to hierarchical clustering using the standard Euclidian correlation method. Beginning at 24 hpi, the RRVΔLANA/GFP infected cells displayed upregulation of the majority of viral genes of immediate-early (IE), early (E), and late (L) classes compared to RRV-GFP infected cells (Fig. 9A). The upregulated RRV IE genes included Orf50/Rta. Furthermore, almost all of the RRV early genes (ORFs R1, 43, 6, 29a, 17, R9-1, 27, 24, 45, 55, R8, 74, 8, and 49) were robustly upregulated in the RRVΔLANA/GFP infected cells compared to RRV-GFP infected cells. Examples of upregulated late transcripts in the RRVΔLANA/GFP infected cells are ORFs 25/MCP, 28/gp150, 29b (packaging protein), 32 (transport protein), 53/gN, R9-3/vIRF, 65/SCIP, 67, 67.5, 69, 75/vFGARAT, 23 (egress protein), and 9/polymerase. Unlike the immediate-early and early genes, the extent of late gene upregulation in the RRVΔLANA/GFP infected cells was not as robust. Indeed, amongst the late genes listed above, only Orf65/SCIP and Orf69 exhibited highly differential expression in the RRVΔLANA/GFP infected cells compared to the RRV-GFP infected cells. The remainder of

the late transcript levels were only modestly increased in the RRVΔLANA/GFP infected cells. Notably, infection with RRVΔLANA/GFP resulted in increased expression of all RRV Rta-responsive genes. These include R8, Orf8/gB, Orf57/MTA, whose expression we previously reported to be induced by RRV Orf50 transient expression using luciferase reporter constructs (18). Transcription of the RRV homologues of KSHV Rta-responsive viral genes (Orf6/ssDBP, R1, Orf9/DNApol, Orf74/vGPCR, and Orf45) were also found to be preferentially elevated in the RRVΔLANA/GFP infected cells compared to RRV-GFP infected cells. Taken together, these data suggest that RRV Rta function may be unchecked in the absence of R-LANA expression, and that R-LANA has an enormous impact on the expression of many RRV viral genes. Only a few RRV genes did not show much R-LANA dependency in their expression profiles, these included Orf38 and OrfR9-3/vIRF. Importantly, genetic disruption of R-LANA did not inhibit the transcription of the adjacent Orf71 and Orf72 genes. Orf72 gene expression was upregulated in the RRVΔLANA/GFP virus, suggesting that unimpeded Rta expression further enhances the R-LANA promoter for this transcript. Orf71 was also increased in the RRVΔLANA/GFP infected cells but less dramatically than Orf72. This result might be due to the predominant effect of the cryptic promoter for monocistronic Orf71 transcript driving Orf71 expression in an Rta-independent fashion during lytic replication as previously described (32). Our array also contained negative controls including primers for KSHV genes (Orf73/LANA, Orf50/Rta, Orf57/MTA, K1, Orf74/vGPCR), human GAPDH, human actin, and murine apoB genes. As expected, the expression of any KSHV, human or mouse transcripts was undetectable in RRV infected rhesus fibroblasts.

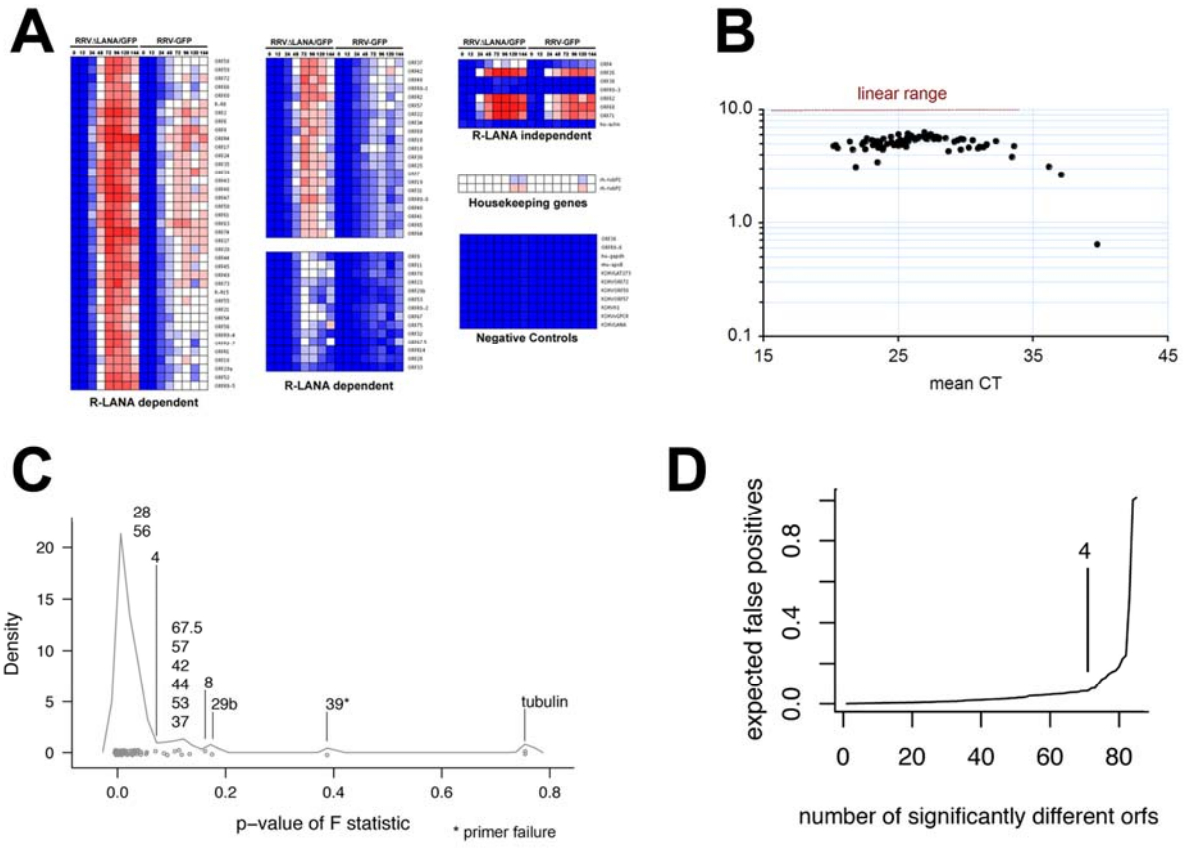

Figure 9. Viral gene profiling of RRVΔLANA/GFP and RRV-GFP infected rhesus fibroblasts. A) A heat map representation of real-time QPCR data normalized to rhesus tubulin (dCT) of infected cells taken at the following timepoints: 0, 12, 24, 48, 72, 96, 120, and 144 hpi. The dCT values were hierarchically clustered using standard Euclidian correlation method. Blue indicates low, white represents intermediate/median, and red represents the highest level of viral mRNA detected relative to rhesus tubulin. **B)** Quality control of RRV QPCR primers for all of the ORFs. There was no significant correlation between the magnitude of the log(SD) and the mean CT, demonstrating that except for three outliers, changes in RRV gene expression did not depend on the overall levels of any particular viral mRNA. **C)** Distribution of RRV ORFs showing differential transcript abundance between samples. We determined for each individual gene in the array whether its relative abundance at each time point differed between wild-type and mutant. The significance of the difference is expressed by the p-value of the F statistic. mRNAs that differed significantly in their transcription pattern yield a low p-value. We then plotted the density, i.e. the distribution of p values for all mRNAs in the array. Individual dots just above the x-axis indicate individual mRNAs. The peak at a low p-value indicates that the majority of mRNAs have differential expression between the wild-type RRV-GFP and mutant RRVΔLANA/GFP viruses. Orf4 has a p-value of 0.076 and is a watershed to differentiate ORFs that exhibit statistically significant differences (peak group left to Orf4) from those that do not (right to Orf4). Orfs 28 and 56 are the only genes within the peak group with $p>0.05$. **D)** A great concern in array analysis is the problem of multiple comparisons. Given

enough comparisons; one would expect some ORFs to show a statistically significant difference by chance alone. These are called false positives. The expected number of false positives (rate) can be calculated based on the total number of genes in the array and the p-values of the individual comparisons. Shown in this panel is a plot of the expected rate of false positive against the number of RRV ORFs considered showing individually statistically significant differences in mRNA levels between wild-type and mutant viruses. Based on the p-value distribution in panel C one would expect less than 1 (<0.02) false positive within the top 71 differentially regulated genes, i.e. those that differed more significantly between wild-type and mutant than Orf 4 (indicated in panel D).

The QPCR primers amplified their respective targets efficiently and independent of the overall levels of any particular viral messages. This is visualized by plotting the log(SD) against the mean raw CT values (Fig. 9B). No correlation was evident. Except for three outliers with mean CT > 35 all data were within the linear range of the assay.

To quantitatively assess whether there was a difference in the transcription profile between the mutant and wild-type viruses, we calculated the difference ddCT in mRNA levels for every mRNA at every time point, which is equivalent to taking the ratio of absolute mRNA levels between RRVΔLANA/GFP and RRV-GFP viruses. Next, we fitted a linear regression curve to the ddCT over time and calculated the p-value using the F statistic (30) to determine whether there was a linear trend over time. For any mRNA with no differences between the mutant and wild-type virus, ddCT would be the same at each timepoint and there would be no significant correlation. This is evidenced by tubulin, which has a p-value of 0.76 (Fig. 9C). Note that this statistic is based on n = 16 data points. A few viral genes showed intermediate dependencies, but the majority of viral mRNAs (n = 72) exhibited a significant linear trend with a mean $p \leq 0.02$. We used q-value calculations (82) to adjust for multiple comparisons (Fig. 9D). This demonstrated that within our total set of 84 genes, we would

expect at most 4 genes to show this trend by chance alone. As we observed 72 genes, this analysis establishes that there is a significant difference between wild-type and recombinant virus mRNA levels and that almost all mRNA transcripts of the RRVΔLANA/GFP were transcribed at higher levels at earlier times than the wild-type virus.

R-LANA modulates the transcription of cellular genes.

We also examined several cellular genes that are known to be repressed by KSHV LANA in the context of lytic infection with the RRVΔLANA/GFP and RRV-GFP viruses. In brief, RhF were infected with either virus (1 MOI) for 48 hours. Total RNA was isolated from infected RhF and one microgram of the RNA was reverse-transcribed using the Promega reverse transcription system and Oligo(dT) primers. The cDNA was then subjected to real time PCR using standard cycling conditions with primers specific to genes that were previously cited to be repressed by LANA (Table 1). The real time PCR primers are shown in Table 2. In real time PCR, higher Ct values correlate with lower abundance of the examined RNA and vice versa. A dCt value is defined as the Ct value of each listed gene minus the Ct value of the endogenous control, rhesus β-tubulin. A negative dCt value indicates a higher expression level of the specific gene compared to the control rhesus β-tubulin gene. The Ct value for each gene (including β-actin) was normalized to the Ct value of rhesus β-tubulin from the same sample to generate dCt ($dCt=Ct_{\text{gene of interest}}-Ct_{\beta\text{-tubulin}}$) values for mock, RRVΔLANA/GFP and RRV-GFP infected cells (Table 1). A ddCt value is defined as the dCt value of each listed gene from an infected sample minus the dCt value of the same gene from a mock infected sample. Negative values of ddCt indicate higher expression of genes in infected compared to mock infected samples. The ddCt values were calculated for

RRVΔLANA/GFP compared to mock-infection, and for RRV-GFP compared to mock infection, respectively. The fold activation of the specific gene in RRVΔLANA/GFP infected cells compared to RRV-GFP infected cells was subsequently deduced and is shown in Table 1. Previous reports have shown that KSHV LANA can repress nuclear receptor coactivator 3 (NCOA3), cAMP responsive element binding protein-like 1 (CREBL1), CCAAT-box binding transcription factor, G1/S-specific cyclin-D2 (CCND2), and forkhead box protein G1B (FKHL1/FOXG1B) when expressed in isolation in B cells or endothelial cells (3, 4, 52). We found that these genes are derepressed i.e. activated during *de novo* lytic infection of RhF with the RRVΔLANA/GFP virus compared to RRV-GFP (Table 1). The β-actin gene serves as a control since its expression did not change in cells infected with either RRVΔLANA/GFP or RRV-GFP. Specifically, An *et al*. showed that the transcriptional factors NCOA3, CREBL1, and CCAAT-box binding transcription factor were down-regulated between 2 and 4.9 fold when LANA expression was induced by doxycycline in BJAB/Tet-On/LANA cells (3). Our data using the RRVΔLANA/GFP virus suggests that R-LANA might also repress the transactivation of cellular and/or viral genes that are dependent on these transcription factors. Since NCOA3 has an intrinsic histone acetyltransferase (HAT) activity (11), one might also speculate that LANA suppression of NCOA3 gene expression could lead to histone remodeling in order to silence genes that are normally activated by NCOA3. Moreover, Shamay *et al*. previously demonstrated that expression of KSHV LANA in TIME endothelial cells resulted in a strong repression of FKHL1/FOXG1B (17 fold) and CCND2 (4.6 fold) gene expression (78). Such repression was due to LANA recruitment of the methyltransferase Dnmt3a and could be reversed using a methyltransferase inhibitor (78). Our finding that the RRVΔLANA/GFP virus infected cells display higher activation of

FKHL1/FOXG1B and CCND2 gene expression than the RRV-GFP infected cells suggests that R-LANA does indeed repress FKHL1/FOXG1B and CCND2 gene expression even in the context of the whole virus. This finding also suggests an epigenetic mechanism for R-LANA mediated silencing of cellular genes, and further corroborates LANA's role in suppressing gene transcription (78).

Table 1. Cellular genes that are activated (derepressed) in RRVΔLANA/GFP infected RhF compared to RRV-GFP infected RhF.

GENE NAME	ACCESSION (*Macaca mulatta*)	Mock (dCt)	RRV-GFP (dCt)	RRVΔLANA (dCt)	RRV-GFP- Mock (ddCt)	RRVΔLANA-Mock (ddCt)	FOLD ACTIVATION $\frac{2^{ddCt}\ RRV\Delta LANA}{2^{ddCt}\ RRV\text{-}GFP}$
NCOA3	XM_001101475	5.473	1.128	2.619	-4.345	-2.854	2.810
CREBL1	XR_014255	6.574	4.835	6.065	-1.739	-0.509	2.344
CCAAT-box binding TF	XM_001084362	8.765	5.425	7.406	-3.34	-1.359	3.946
CCND2	XR_012297	6.253	3.497	5.034	-2.755	-1.219	2.902
FKHL1 / FOXG1B	XM_001106922	13.406	9.521	12.981	-3.885	-0.425	11.005
Actin (control)	NM_001033084	-2.304	-2.796	-2.573	-0.492	-0.269	1.167

Table 2. Real-time QPCR primers for rhesus cellular genes.

GENE NAME	FORWARD PRIMER	REVERSE PRIMER
NCOA3	GGGGATGGTGAGCTGTGACT	TGACATCCAAAATGGTCAGCA
CREBL1	TGAGGTGGGGGTGTTC	GAGCTCTATATTCCGAAAAGG
CCAAT-box binding TF	TTTCAAGTCCTTTCACCCCAG	GCAAGGCTGTTTTTTACCCC
CCND2	ATTGGCTATGATGGTGACAT	CTCTTAAAAGGCAGCTGACTA
FKHL1/FOXG1B	AAGAAAGTTGTTTCAGTTGGC	TTCAATTGAATGGGCAGT
β-actin	CCTTCCATCGTCCACCGCAAA TGCTTCTAGGC	GTCAAGAAAGGGTGTAACGCA ACTAAGTCACA

R-LANA is important for establishment of latency in BJAB cells.

We determined whether R-LANA also modulates the establishment and maintenance of RRV in B cells. To address this question, we infected BJAB B cells with RRVΔLANA/GFP or RRV-GFP (MOI = 0.5) as previously described (19). Seven days post-

infection, infected BJAB cells were sorted by flow cytometry for the presence of green fluorescence. RRVΔLANA/GFP showed higher infectivity of BJAB cells than RRV-GFP on day 0 pre-sorting (data not shown). After sorting, we used equivalent numbers of GFP-positive cells from both RRVΔLANA/GFP-infected and RRV-GFP-infected BJAB cells for further experimentation (Fig. 10A, upper panels). From here onwards, BJAB cells were split every two days and GFP-positive cells were continuously monitored by fluorescence microscopy and flow cytometry. The RRVΔLANA/GFP-infected BJAB sample showed a rapid loss of GFP-positive cells on days 7 and 14 post-sorting as determined by fluorescence microscopy and flow cytometry. Fig. 10A (lower panels) and Fig. 10B show the relative GFP-positive cells on day 14 post-sorting as determined quantitatively by flow sorting and visually by fluorescent microscopy, respectively. To confirm that the dramatic decrease in GFP-positive cells in RRVΔLANA/GFP-infected BJAB cells was due to the loss of RRV particles (or intracellular viral genomes), we performed quantitative real-time PCR to calculate RRV genome copy number. RRVΔLANA/GFP-infected BJAB cells displayed significantly lower intracellular viral genomes compared with RRV-GFP infected BJAB cells (Fig. 10C).

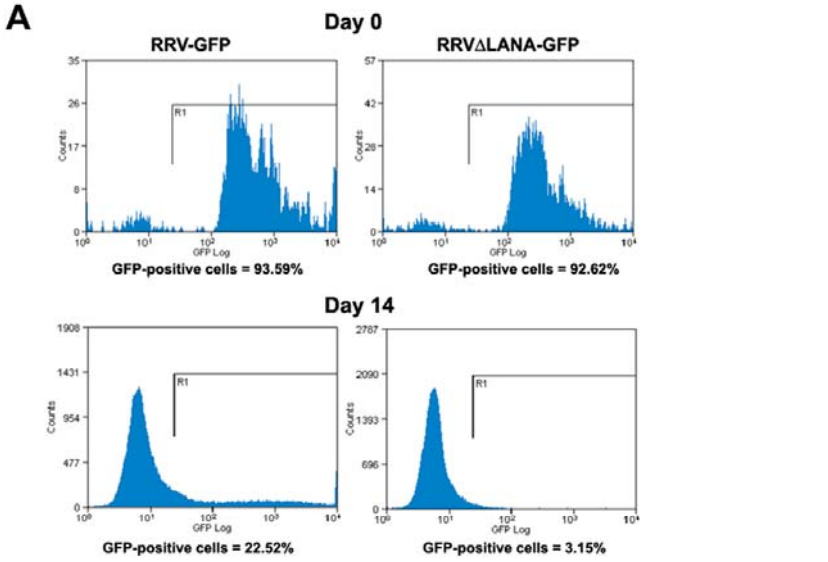
A
Day 0
RRV-GFP
RRVΔLANA-GFP
R1
Counts
GFP Log
GFP-positive cells = 93.59%
GFP-positive cells = 92.62%
Day 14
GFP-positive cells = 22.52%
GFP-positive cells = 3.15%

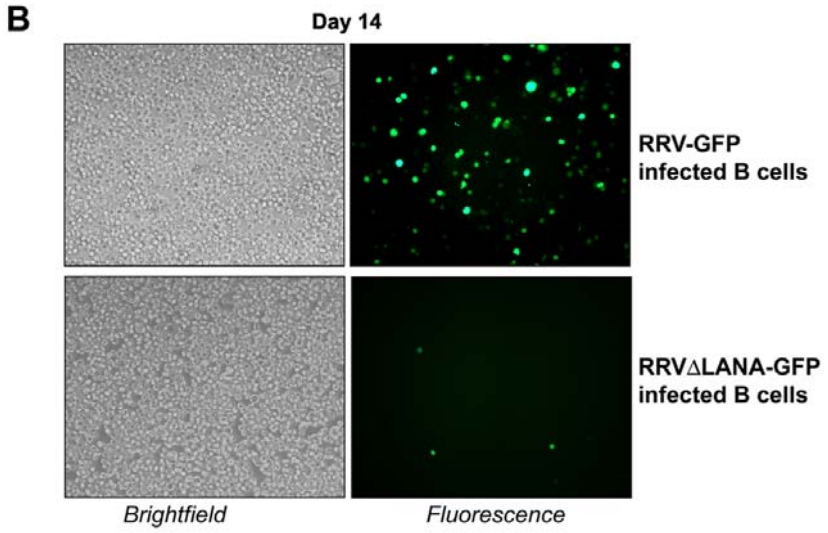
B
Day 14
RRV-GFP
infected B cells
RRVΔLANA-GFP
infected B cells
Brightfield
Fluorescence

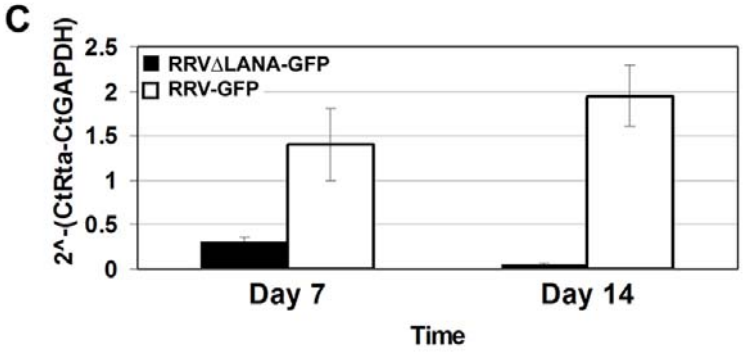
C
2^-(CtRta-CtGAPDH)
RRVΔLANA-GFP
RRV-GFP
2.5
2
1.5
1
0.5
0
Day 7
Day 14
Time

Figure 10 (previous page). RRVΔLANA/GFP and RRV-GFP infection of B lymphocytes. The KSHV-negative PEL cell line, BJAB, was infected with RRVΔLANA/GFP or RRV-GFP virus at 0.5 MOI by spinoculation. Seven days post-infection, infected BJAB cells were sorted by flow cytometry for the presence of green fluorescence. **A)** Flow cytometry analysis of GFP- positive BJAB cells infected with RRVΔLANA/GFP or RRV-GFP virus immediately after sorting (day 0 post-sorting) and 14 days post-sorting. The percentages of GFP-positive cells at the indicated time points are shown below the graphs. **B)** Representative images of RRVΔLANA/GFP and RRV-GFP infected BJAB cells on day 14 post-sorting. Brightfield and GFP fluorescence images of RRV-infected GFP-positive B cells are shown. **C)** Intracellular viral genomes of RRVΔLANA/GFP (■) and RRV-GFP (□) infected BJAB cells on day 7 and day 14 post-sorting. Intracellular genomes extracted from infected cell pellets were quantitated by real-time PCR using a RRV Orf50 standard curve to generate the viral genome copy number. The viral genomes were normalized to human GAPDH copy numbers, which were generated using a human GAPDH standard curve. Results are the averages of triplicate samples. Error bars represent standard deviations.

DISCUSSION

KSHV LANA (K-LANA) has been extensively studied in regard to its molecular functions in regulating cell cycle, apoptosis, immune evasion, as well as viral latency (reviewed in (22, 85)). By comparison, relatively little is known about R-LANA. Given our previous finding that R-LANA can inhibit RRV Rta-mediated transactivation of a sub-set of lytic viral genes (17), we hypothesized that a R-LANA deletion mutant virus would display dysregulated transcription compared to wild-type RRV. Here we report the use of homologous recombination to generate RRVΔLANA/GFP and a revertant RRV_{REV} recombinant virus to gain insight into the replication kinetics of the R-LANA knockout virus. We found that RRVΔLANA/GFP displayed increased lytic activity when the R-LANA ORF was functionally disrupted by insertion of a GFP expression cassette. By generating viral growth curves using traditional plaque assays as well as QPCR viral load assays, we demonstrated increased production of both viral genomes by real-time QPCR, and infectious virion particles by plaque assay, in RRVΔLANA/GFP infected RhF compared to wild-type and RRV-GFP infected RhF. Furthermore, whole-genome profiling of RRV transcripts provided an unbiased scrutiny of all RRV lytic gene expression that was altered by the functionally disrupted R-LANA, suggesting that the observed increase in RRV lytic activity was caused by global upregulation of RRV mRNA transcripts. Because Orf50/Rta is necessary and sufficient for initiation and orchestration of the lytic viral transcriptional cascade, we speculate that the lytic behavior of RRVΔLANA/GFP in our permissive RhF tissue culture system was largely due to unhampered Rta transactivation activity when R-LANA expression was lost. Thus, R-LANA plays a pivotal role in suppressing lytic replication during *de novo* infection.

Several possible mechanisms could explain how R-LANA might inhibit Rta transactivation of Rta-responsive genes. The most obvious explanation is chromatin remodeling, as R-LANA has been implicated in recruiting histone deacetylases (HDACs) (17) , the result of which may lead to histone modification of Rta-responsive viral promoters. Such a mechanism has also been proposed for K-LANA by physical interaction with RBP-Jκ and other cellular proteins (21, 46, 53, 54). Additionally, Lu *et al*. have reported that Orf50 transcription is specifically repressed by KSHV LANA during viral latency (53). In dually infected PELs, K-LANA has been shown to suppress EBV viral genes by regulating the mSin3 corepressor complex (44), although K-LANA was also reported to activate EBV or HIV viral genes (31, 35) as well as cellular genes (5, 41, 84). The transcriptional activation and repression activities have been mapped to the amino and carboxyl termini of K-LANA, respectively (62, 76, 87). In addition to recruiting HDACs for transcription repression, as we previously published (17), R-LANA might sequester histone acetyltransferases (HATs) from Rta or Rta-dependent viral promoters. Our finding that R-LANA decreased the gene expression of the histone acetyltransferase, NCOA3, suggests that R-LANA might also repress HAT-mediated transcription.

In KSHV, both LANA and Rta have been shown to bind CREB-binding protein (CBP), which has HAT activity and can activate transcription (33, 49, 50). Other possibilities by which R-LANA could inhibit Rta function include affecting Rta protein levels and modification of Rta post-translationally in order to downregulate Rta transactivation function. Our preliminary data have excluded these two possibilities (unpublished data). Interestingly, a significant number of RRV genes that were upregulated in the RRVΔLANA/GFP infected cells compared to the RRV-GFP infected cells have not been

previously identified as being Rta-responsive in either the KSHV or RRV viral systems. KSHV LANA has been shown to act as a transcriptional repressor on some cellular promoters such as those that are dependent on CBP or E2F transactivation (49, 50, 65, 67). It is therefore plausible that R-LANA acts as a direct transcriptional repressor of a sub-set of viral genes, independent of its inhibition of Rta transactivation.

The characterization of a KSHVΔLANA virus in the context of lytic replication was recently published (48). The investigators reported that deletion of KSHV LANA resulted in the increased production of KSHV infectious virions after TPA and sodium butyrate treatment of KSHVΔLANA infected cells, as well as enhanced transcription of four Rta-responsive lytic genes including MTA, Orf59, vIL-6, Orf-K8.1 (48). The expression of these homologous genes in RRV was also increased by RRVΔLANA/GFP *de novo* infection of RhF, and increased production of infectious RRV virions was also observed with RRVΔLANA/GFP infection compared to RRV-GFP infection. Importantly, this differential pattern of gene expression was seen in the absence of exogenous artificial inducers such as TPA and butyrate (48).

Furthermore, our study showed for the first time that LANA modulates transcription of cellular genes during lytic infection and in the context of the whole virus. Cellular genes such as NCOA3, cAMP responsive element binding protein-like 1, CCAAT-box binding transcription factor, CCND2, and FKHL1/FOXG1B, which were previously reported to be repressed by KSHV LANA in either B cells or endothelial cells (3, 4, 52), were found to be derepressed in cells infected with RRVΔLANA/GFP compared to RRV-GFP.

Unlike KSHV and RRV, deletion of LANA from MHV68 showed absolutely no difference in replication *in vitro* at high MOI, and the MHV68ΔLANA virus displayed reduced viral titers compared to wild-type virus at very low MOIs upon *de novo* infection of primary murine embryonic fibroblasts or NIH3T3 fibroblasts (27, 28, 48, 58). This paradoxical observation could be attributed to the different cell lines being investigated, mouse versus primate cells. On the other hand, the discrepancies here may reflect that the KSHV LANA protein may be functionally more similar to its primate homologue, RRV LANA, than the murine MHV68 LANA homolog.

Finally, RRVΔLANA/GFP was inefficient in establishing latency in infected BJAB cells. This was similar to what was observed with the KSHV LANA deletion mutant BAC36-ΔLNA, which failed to establish a latent infection in transfected human 293 cells (90). A future goal of our study is to investigate RRVΔLANA/GFP infection in rhesus macaques to determine its behavior *in vivo*. In the case of the MHV68 LANA deletion virus, previous reports suggest that the loss of LANA resulted in a compromised ability of the virus to replicate in the lungs and establish latency in the spleen of infected mice (28, 58). Given the biological properties of the RRVΔLANA/GFP recombinant virus, we hypothesize that such a virus would make a good candidate vaccine, which will protect against challenge with wild-type RRV-GFP virus. This is because the highly lytic nature of this virus results in the dysregulated expression of multiple lytic viral genes, which should expose the virus to the host innate and adaptive arms of the immune system to a greater extent than WT RRV-GFP. Hence, the host should be able to mount a robust immune response against the RRVΔLANA/GFP virus, which may help protect the host from subsequent challenge with wild-type RRV. Furthermore, the inability of this virus to establish latency in dividing cells

means that unlike wild-type RRV-GFP and other herpesviruses, this virus should be lost from proliferating cells since R-LANA is not expressed.

We are currently evaluating the RRVΔLANA/GFP as a vaccine candidate in rhesus macaques in collaboration with Dr. Ronald Desrosiers at Harvard Medical School. We will determine the biological characteristics of the RRVΔLANA/GFP recombinant virus in terms of its persistence, viral load levels in the blood, anti-viral antibodies present in the RRVΔLANA/GFP infected rhesus macaques and to use it as a vaccine to protect against challenge with WT RRV.

In conclusion, we have created a RRVΔLANA/GFP that is more lytic than RRV-GFP, wild-type RRV H26-95, or a revertant RRV_{REV} virus. This recombinant virus displays higher viral loads in rhesus fibroblasts as well as increased expression of a multitude of RRV viral genes during lytic replication in rhesus fibroblasts. Additionally, cellular genes that are normally repressed by LANA are derepressed in RRVΔLANA/GFP infected cells compared to RRV-GFP infected cells. Furthermore, the RRVΔLANA/GFP recombinant virus also fails to successfully establish latent infection in B lymphocytes.

ACKNOWLEDGMENTS

We thank Stuart Krall for assistance with the virus amplification. We are grateful to Chelsey Hilscher for technical contributions to the RRV quantitative PCR array data and Melissa Wills for providing the rhesus tubulin plasmid. We thank members of the Damania and Dittmer labs for informative discussions. We also thank the UNC Genomics Facility for performing Solexa sequencing of the recombinant virus. This work was supported by NIH grant CA096500 and DE018281 to BD and CA109232 to DPD. KWW was supported in part by NIAID training grant T32-AI007001 and MSTP grant T32-GM008719. BD is a Leukemia & Lymphoma Society Scholar and Burroughs Welcome Fund Investigator in Infectious Disease.

REFERENCES

1. http://www.gnu.org/licenses/licenses.html#GPL.

2. **Alexander, L., L. Denekamp, A. Knapp, M. R. Auerbach, B. Damania, and R. C. Desrosiers.** 2000. The primary sequence of rhesus monkey rhadinovirus isolate 26-95: sequence similarities to Kaposi's sarcoma-associated herpesvirus and rhesus monkey rhadinovirus isolate 17577. J Virol **74:**3388-98.

3. **An, F. Q., N. Compitello, E. Horwitz, M. Sramkoski, E. S. Knudsen, and R. Renne.** 2005. The latency-associated nuclear antigen of Kaposi's sarcoma-associated herpesvirus modulates cellular gene expression and protects lymphoid cells from p16 INK4A-induced cell cycle arrest. J Biol Chem **280:**3862-74.

4. **An, J., Y. Sun, and M. B. Rettig.** 2004. Transcriptional coactivation of c-Jun by the KSHV-encoded LANA. Blood **103:**222-8.

5. **Bajaj, B. G., S. C. Verma, K. Lan, M. A. Cotter, Z. L. Woodman, and E. S. Robertson.** 2006. KSHV encoded LANA upregulates Pim-1 and is a substrate for its kinase activity. Virology **351:**18-28.

6. **Ballestas, M. E., P. A. Chatis, and K. M. Kaye.** 1999. Efficient persistence of extrachromosomal KSHV DNA mediated by latency-associated nuclear antigen. Science **284:**641-4.

7. **Barbera, A. J., J. V. Chodaparambil, B. Kelley-Clarke, V. Joukov, J. C. Walter, K. Luger, and K. M. Kaye.** 2006. The nucleosomal surface as a docking station for Kaposi's sarcoma herpesvirus LANA. Science **311:**856-61.

8. **Barbera, A. J., J. V. Chodaparambil, B. Kelley-Clarke, K. Luger, and K. M. Kaye.** 2006. Kaposi's sarcoma-associated herpesvirus LANA hitches a ride on the chromosome. Cell Cycle **5:**1048-52.

9. **Cesarman, E., Y. Chang, P. S. Moore, J. W. Said, and D. M. Knowles.** 1995. Kaposi's sarcoma-associated herpesvirus-like DNA sequences in AIDS-related body-cavity-based lymphomas. N Engl J Med **332:**1186-91.

10. **Chang, Y., E. Cesarman, M. S. Pessin, F. Lee, J. Culpepper, D. M. Knowles, and P. S. Moore.** 1994. Identification of herpesvirus-like DNA sequences in AIDS-associated Kaposi's sarcoma. Science **266:**1865-9.

11. **Chen, H., R. J. Lin, R. L. Schiltz, D. Chakravarti, A. Nash, L. Nagy, M. L. Privalsky, Y. Nakatani, and R. M. Evans.** 1997. Nuclear receptor coactivator ACTR is a novel histone acetyltransferase and forms a multimeric activation complex with P/CAF and CBP/p300. Cell **90:**569-80.

12. **Cotter, M. A., 2nd, and E. S. Robertson.** 1999. The latency-associated nuclear antigen tethers the Kaposi's sarcoma-associated herpesvirus genome to host chromosomes in body cavity-based lymphoma cells. Virology **264:**254-64.

13. **Cotter, M. A., 2nd, C. Subramanian, and E. S. Robertson.** 2001. The Kaposi's sarcoma-associated herpesvirus latency-associated nuclear antigen binds to specific sequences at the left end of the viral genome through its carboxy-terminus. Virology **291:**241-59.

14. **Damania, B., M. DeMaria, J. U. Jung, and R. C. Desrosiers.** 2000. Activation of lymphocyte signaling by the R1 protein of rhesus monkey rhadinovirus. J Virol **74:**2721-30.

15. **Damania, B., M. Li, J. K. Choi, L. Alexander, J. U. Jung, and R. C. Desrosiers.** 1999. Identification of the R1 oncogene and its protein product from the rhadinovirus of rhesus monkeys. J Virol **73:**5123-31.

16. **Desrosiers, R. C., V. G. Sasseville, S. C. Czajak, X. Zhang, K. G. Mansfield, A. Kaur, R. P. Johnson, A. A. Lackner, and J. U. Jung.** 1997. A herpesvirus of rhesus monkeys related to the human Kaposi's sarcoma-associated herpesvirus. J Virol **71:**9764-9.

17. **DeWire, S. M., and B. Damania.** 2005. The latency-associated nuclear antigen of rhesus monkey rhadinovirus inhibits viral replication through repression of Orf50/Rta transcriptional activation. J Virol **79:**3127-38.

18. **DeWire, S. M., M. A. McVoy, and B. Damania.** 2002. Kinetics of expression of rhesus monkey rhadinovirus (RRV) and identification and characterization of a polycistronic transcript encoding the RRV Orf50/Rta, RRV R8, and R8.1 genes. J Virol **76:**9819-31.

19. **DeWire, S. M., E. S. Money, S. P. Krall, and B. Damania.** 2003. Rhesus monkey rhadinovirus (RRV): construction of a RRV-GFP recombinant virus and development of assays to assess viral replication. Virology **312:**122-34.

20. **Dezube, B. J., M. Zambela, D. R. Sage, J. F. Wang, and J. D. Fingeroth.** 2002. Characterization of Kaposi sarcoma-associated herpesvirus/human herpesvirus-8 infection of human vascular endothelial cells: early events. Blood **100:**888-96.

21. **Di Bartolo, D. L., M. Cannon, Y. F. Liu, R. Renne, A. Chadburn, C. Boshoff, and E. Cesarman.** 2008. KSHV LANA inhibits TGF-beta signaling through epigenetic silencing of the TGF-beta type II receptor. Blood **111:**4731-40.

22. **Dittmer, D.** 2008. KSHV viral latent lifecycle. *In* B. Damania and J. Pipas (ed.), DNA Tumor Viruses. Springer.

23. **Dittmer, D., M. Lagunoff, R. Renne, K. Staskus, A. Haase, and D. Ganem.** 1998. A cluster of latently expressed genes in Kaposi's sarcoma-associated herpesvirus. J Virol **72:**8309-15.

24. **Dittmer, D., C. Stoddart, R. Renne, V. Linquist-Stepps, M. E. Moreno, C. Bare, J. M. McCune, and D. Ganem.** 1999. Experimental transmission of Kaposi's sarcoma-associated herpesvirus (KSHV/HHV-8) to SCID-hu Thy/Liv mice. J Exp Med **190:**1857-68.

25. **Dittmer, D. P.** 2003. Transcription profile of Kaposi's sarcoma-associated herpesvirus in primary Kaposi's sarcoma lesions as determined by real-time PCR arrays. Cancer Res **63:**2010-5.

26. **Dittmer, D. P., C. M. Gonzalez, W. Vahrson, S. M. DeWire, R. Hines-Boykin, and B. Damania.** 2005. Whole-genome transcription profiling of rhesus monkey rhadinovirus. J Virol **79:**8637-50.

27. **Forrest, J. C., C. R. Paden, R. D. Allen, 3rd, J. Collins, and S. H. Speck.** 2007. ORF73-null murine gammaherpesvirus 68 reveals roles for mLANA and p53 in virus replication. J Virol **81:**11957-71.

28. **Fowler, P., S. Marques, J. P. Simas, and S. Efstathiou.** 2003. ORF73 of murine herpesvirus-68 is critical for the establishment and maintenance of latency. J Gen Virol **84:**3405-16.

29. **Gessain, A., A. Sudaka, J. Briere, N. Fouchard, M. A. Nicola, B. Rio, M. Arborio, X. Troussard, J. Audouin, J. Diebold, and G. de The.** 1996. Kaposi sarcoma-associated herpes-like virus (human herpesvirus type 8) DNA sequences in multicentric Castleman's disease: is there any relevant association in non-human immunodeficiency virus-infected patients? Blood **87:**414-6.

30. **Glanz, S. A.** 1992. Primer of Biostatistics, 3rd ed. McCgaw-Hill, New York.

31. **Groves, A. K., M. A. Cotter, C. Subramanian, and E. S. Robertson.** 2001. The latency-associated nuclear antigen encoded by Kaposi's sarcoma-associated herpesvirus activates two major essential Epstein-Barr virus latent promoters. J Virol **75:**9446-57.

32. **Grundhoff, A., and D. Ganem.** 2001. Mechanisms governing expression of the v-FLIP gene of Kaposi's sarcoma-associated herpesvirus. J Virol **75:**1857-63.

33. **Gwack, Y., H. Byun, S. Hwang, C. Lim, and J. Choe.** 2001. CREB-binding protein and histone deacetylase regulate the transcriptional activity of Kaposi's sarcoma-associated herpesvirus open reading frame 50. J Virol **75:**1909-17.

34. **Hu, J., A. C. Garber, and R. Renne.** 2002. The latency-associated nuclear antigen of Kaposi's sarcoma-associated herpesvirus supports latent DNA replication in dividing cells. J Virol **76:**11677-87.

35. **Hyun, T. S., C. Subramanian, M. A. Cotter, 2nd, R. A. Thomas, and E. S. Robertson.** 2001. Latency-associated nuclear antigen encoded by Kaposi's sarcoma-associated herpesvirus interacts with Tat and activates the long terminal repeat of human immunodeficiency virus type 1 in human cells. J Virol **75:**8761-71.

36. **Jeong, J., J. Papin, and D. Dittmer.** 2001. Differential regulation of the overlapping Kaposi's sarcoma-associated herpesvirus vGCR (orf74) and LANA (orf73) promoters. J Virol **75:**1798-807.

37. **Jeong, J. H., J. Orvis, J. W. Kim, C. P. McMurtrey, R. Renne, and D. P. Dittmer.** 2004. Regulation and autoregulation of the promoter for the latency-associated nuclear antigen of Kaposi's sarcoma-associated herpesvirus. J Biol Chem **279:**16822-31.

38. **Kaleeba, J. A., E. P. Bergquam, and S. W. Wong.** 1999. A rhesus macaque rhadinovirus related to Kaposi's sarcoma-associated herpesvirus/human herpesvirus 8 encodes a functional homologue of interleukin-6. J Virol **73:**6177-81.

39. **Kelley-Clarke, B., M. E. Ballestas, T. Komatsu, and K. M. Kaye.** 2007. Kaposi's sarcoma herpesvirus C-terminal LANA concentrates at pericentromeric and peri-telomeric regions of a subset of mitotic chromosomes. Virology **357:**149-57.

40. **Kelley-Clarke, B., M. E. Ballestas, V. Srinivasan, A. J. Barbera, T. Komatsu, T. A. Harris, M. Kazanjian, and K. M. Kaye.** 2007. Determination of Kaposi's sarcoma-associated herpesvirus C-terminal latency-associated nuclear antigen residues mediating chromosome association and DNA binding. J Virol **81:**4348-56.

41. **Knight, J. S., M. A. Cotter, 2nd, and E. S. Robertson.** 2001. The latency-associated nuclear antigen of Kaposi's sarcoma-associated herpesvirus transactivates the telomerase reverse transcriptase promoter. J Biol Chem **276:**22971-8.

42. **Komatsu, T., M. E. Ballestas, A. J. Barbera, and K. M. Kaye.** 2002. The KSHV latency-associated nuclear antigen: a multifunctional protein. Front Biosci **7:**d726-30.

43. **Komatsu, T., A. J. Barbera, M. E. Ballestas, and K. M. Kaye.** 2001. The Kaposi' s sarcoma-associated herpesvirus latency-associated nuclear antigen. Viral Immunol **14:**311-7.

44. **Krithivas, A., D. B. Young, G. Liao, D. Greene, and S. D. Hayward.** 2000. Human herpesvirus 8 LANA interacts with proteins of the mSin3 corepressor complex and negatively regulates Epstein-Barr virus gene expression in dually infected PEL cells. J Virol **74:**9637-45.

45. **Lagunoff, M., J. Bechtel, E. Venetsanakos, A. M. Roy, N. Abbey, B. Herndier, M. McMahon, and D. Ganem.** 2002. De novo infection and serial transmission of Kaposi's sarcoma-associated herpesvirus in cultured endothelial cells. J Virol **76:**2440-8.

46. **Lan, K., D. A. Kuppers, S. C. Verma, N. Sharma, M. Murakami, and E. S. Robertson.** 2005. Induction of Kaposi's sarcoma-associated herpesvirus latency-associated nuclear antigen by the lytic transactivator RTA: a novel mechanism for establishment of latency. J Virol **79:**7453-65.

47. **Langlais, C. L., J. M. Jones, R. D. Estep, and S. W. Wong.** 2006. Rhesus rhadinovirus R15 encodes a functional homologue of human CD200. J Virol **80:**3098-103.

48. **Li, Q., F. Zhou, F. Ye, and S. J. Gao.** 2008. Genetic disruption of KSHV major latent nuclear antigen LANA enhances viral lytic transcriptional program. Virology **379:**234-44.

49. **Lim, C., Y. Gwack, S. Hwang, S. Kim, and J. Choe.** 2001. The transcriptional activity of cAMP response element-binding protein-binding protein is modulated by the latency associated nuclear antigen of Kaposi's sarcoma-associated herpesvirus. J Biol Chem **276:**31016-22.

50. **Lim, C., H. Sohn, Y. Gwack, and J. Choe.** 2000. Latency-associated nuclear antigen of Kaposi's sarcoma-associated herpesvirus (human herpesvirus-8) binds ATF4/CREB2 and inhibits its transcriptional activation activity. J Gen Virol **81:**2645-52.

51. **Lin, S. F., D. R. Robinson, J. Oh, J. U. Jung, P. A. Luciw, and H. J. Kung.** 2002. Identification of the bZIP and Rta homologues in the genome of rhesus monkey rhadinovirus. Virology **298:**181-8.

52. **Liu, J., H. J. Martin, G. Liao, and S. D. Hayward.** 2007. The Kaposi's sarcoma-associated herpesvirus LANA protein stabilizes and activates c-Myc. J Virol **81:**10451-9.

53. **Lu, F., L. Day, S. J. Gao, and P. M. Lieberman.** 2006. Acetylation of the latency-associated nuclear antigen regulates repression of Kaposi's sarcoma-associated herpesvirus lytic transcription. J Virol **80:**5273-82.

54. **Lu, F., L. Day, and P. M. Lieberman.** 2005. Kaposi's sarcoma-associated herpesvirus virion-induced transcription activation of the ORF50 immediate-early promoter. J Virol **79:**13180-5.

55. **Mansfield, K. G., S. V. Westmoreland, C. D. DeBakker, S. Czajak, A. A. Lackner, and R. C. Desrosiers.** 1999. Experimental infection of rhesus and pig-tailed macaques with macaque rhadinoviruses. J Virol **73:**10320-8.

56. **Mark, L., O. B. Spiller, M. Okroj, S. Chanas, J. A. Aitken, S. W. Wong, B. Damania, A. M. Blom, and D. J. Blackbourn.** 2007. Molecular characterization of the rhesus rhadinovirus (RRV) ORF4 gene and the RRV complement control protein it encodes. J Virol **81:**4166-76.

57. **Miller, G., L. Heston, E. Grogan, L. Gradoville, M. Rigsby, R. Sun, D. Shedd, V. M. Kushnaryov, S. Grossberg, and Y. Chang.** 1997. Selective switch between latency and lytic replication of Kaposi's sarcoma herpesvirus and Epstein-Barr virus in dually infected body cavity lymphoma cells. J Virol **71:**314-24.

58. **Moorman, N. J., D. O. Willer, and S. H. Speck.** 2003. The gammaherpesvirus 68 latency-associated nuclear antigen homolog is critical for the establishment of splenic latency. J Virol **77:**10295-303.

59. **O'Connor, C. M., B. Damania, and D. H. Kedes.** 2003. De novo infection with rhesus monkey rhadinovirus leads to the accumulation of multiple intranuclear capsid species during lytic replication but favors the release of genome-containing virions. J Virol **77:**13439-47.

60. **O'Connor, C. M., and D. H. Kedes.** 2007. Rhesus monkey rhadinovirus: a model for the study of KSHV. Curr Top Microbiol Immunol **312:**43-69.

61. **Orzechowska, B. U., M. F. Powers, J. Sprague, H. Li, B. Yen, R. P. Searles, M. K. Axthelm, and S. W. Wong.** 2008. Rhesus macaque rhadinovirus-associated non-Hodgkin's lymphoma: animal model for KSHV associated malignancies. Blood.

62. **Pan, H. Y., Y. J. Zhang, X. P. Wang, J. H. Deng, F. C. Zhou, and S. J. Gao.** 2003. Identification of a novel cellular transcriptional repressor interacting with the latent nuclear antigen of Kaposi's sarcoma-associated herpesvirus. J Virol **77:**9758-68.

63. **Pearce, M., S. Matsumura, and A. C. Wilson.** 2005. Transcripts encoding K12, v-FLIP, v-cyclin, and the microRNA cluster of Kaposi's sarcoma-associated herpesvirus originate from a common promoter. J Virol **79:**14457-64.

64. **Pratt, C. L., R. D. Estep, and S. W. Wong.** 2005. Splicing of rhesus rhadinovirus R15 and ORF74 bicistronic transcripts during lytic infection and analysis of effects on production of vCD200 and vGPCR. J Virol **79:**3878-82.

65. **Radkov, S. A., P. Kellam, and C. Boshoff.** 2000. The latent nuclear antigen of Kaposi sarcoma-associated herpesvirus targets the retinoblastoma-E2F pathway and with the oncogene Hras transforms primary rat cells. Nat Med **6:**1121-7.

66. **Rainbow, L., G. M. Platt, G. R. Simpson, R. Sarid, S. J. Gao, H. Stoiber, C. S. Herrington, P. S. Moore, and T. F. Schulz.** 1997. The 222- to 234-kilodalton latent nuclear protein (LNA) of Kaposi's sarcoma-associated herpesvirus (human herpesvirus 8) is encoded by orf73 and is a component of the latency-associated nuclear antigen. J Virol **71:**5915-21.

67. **Renne, R., C. Barry, D. Dittmer, N. Compitello, P. O. Brown, and D. Ganem.** 2001. Modulation of cellular and viral gene expression by the latency-associated nuclear antigen of Kaposi's sarcoma-associated herpesvirus. J Virol **75:**458-68.

68. **Renne, R., D. Blackbourn, D. Whitby, J. Levy, and D. Ganem.** 1998. Limited transmission of Kaposi's sarcoma-associated herpesvirus in cultured cells. J Virol **72:**5182-8.

69. **Renne, R., D. Dittmer, D. Kedes, K. Schmidt, R. C. Desrosiers, P. A. Luciw, and D. Ganem.** 2004. Experimental transmission of Kaposi's sarcoma-associated

herpesvirus (KSHV/HHV-8) to SIV-positive and SIV-negative rhesus macaques. J Med Primatol **33:**1-9.

70. **Renne, R., M. Lagunoff, W. Zhong, and D. Ganem.** 1996. The size and conformation of Kaposi's sarcoma-associated herpesvirus (human herpesvirus 8) DNA in infected cells and virions. J Virol **70:**8151-4.

71. **Renne, R., W. Zhong, B. Herndier, M. McGrath, N. Abbey, D. Kedes, and D. Ganem.** 1996. Lytic growth of Kaposi's sarcoma-associated herpesvirus (human herpesvirus 8) in culture. Nat Med **2:**342-6.

72. **Rice, P., I. Longden, and A. Bleasby.** 2000. EMBOSS: the European Molecular Biology Open Software Suite. Trends Genet **16:**276-7.

73. **Sakurada, S., H. Katano, T. Sata, H. Ohkuni, T. Watanabe, and S. Mori.** 2001. Effective human herpesvirus 8 infection of human umbilical vein endothelial cells by cell-mediated transmission. J Virol **75:**7717-22.

74. **Sarid, R., J. S. Wiezorek, P. S. Moore, and Y. Chang.** 1999. Characterization and cell cycle regulation of the major Kaposi's sarcoma-associated herpesvirus (human herpesvirus 8) latent genes and their promoter. J Virol **73:**1438-46.

75. **Schafer, A., X. Cai, J. P. Bilello, R. C. Desrosiers, and B. R. Cullen.** 2007. Cloning and analysis of microRNAs encoded by the primate gamma-herpesvirus rhesus monkey rhadinovirus. Virology **364:**21-7.

76. **Schwam, D. R., R. L. Luciano, S. S. Mahajan, L. Wong, and A. C. Wilson.** 2000. Carboxy terminus of human herpesvirus 8 latency-associated nuclear antigen mediates dimerization, transcriptional repression, and targeting to nuclear bodies. J Virol **74:**8532-40.

77. **Searles, R. P., E. P. Bergquam, M. K. Axthelm, and S. W. Wong.** 1999. Sequence and genomic analysis of a Rhesus macaque rhadinovirus with similarity to Kaposi's sarcoma-associated herpesvirus/human herpesvirus 8. J Virol **73:**3040-53.

78. **Shamay, M., A. Krithivas, J. Zhang, and S. D. Hayward.** 2006. Recruitment of the de novo DNA methyltransferase Dnmt3a by Kaposi's sarcoma-associated herpesvirus LANA. Proc Natl Acad Sci U S A **103:**14554-9.

79. **Soulier, J., L. Grollet, E. Oksenhendler, P. Cacoub, D. Cazals-Hatem, P. Babinet, M. F. d'Agay, J. P. Clauvel, M. Raphael, L. Degos, and et al.** 1995. Kaposi's sarcoma-associated herpesvirus-like DNA sequences in multicentric Castleman's disease. Blood **86:**1276-80.

80. **Staudt, M. R., and D. P. Dittmer.** 2006. Promoter switching allows simultaneous transcription of LANA and K14/vGPCR of Kaposi's sarcoma-associated herpesvirus. Virology **350:**192-205.

81. **Stedman, W., Z. Deng, F. Lu, and P. M. Lieberman.** 2004. ORC, MCM, and histone hyperacetylation at the Kaposi's sarcoma-associated herpesvirus latent replication origin. J Virol **78:**12566-75.

82. **Storey, J. D., and R. Tibshirani.** 2003. Statistical significance for genomewide studies. Proc Natl Acad Sci U S A **100:**9440-5.

83. **Talbot, S. J., R. A. Weiss, P. Kellam, and C. Boshoff.** 1999. Transcriptional analysis of human herpesvirus-8 open reading frames 71, 72, 73, K14, and 74 in a primary effusion lymphoma cell line. Virology **257:**84-94.

84. **Verma, S. C., S. Borah, and E. S. Robertson.** 2004. Latency-associated nuclear antigen of Kaposi's sarcoma-associated herpesvirus up-regulates transcription of human telomerase reverse transcriptase promoter through interaction with transcription factor Sp1. J Virol **78:**10348-59.

85. **Verma, S. C., K. Lan, and E. Robertson.** 2007. Structure and function of latency-associated nuclear antigen. Curr Top Microbiol Immunol **312:**101-36.

86. **West, J., and B. Damania.** 2008. Upregulation of the TLR3 pathway by Kaposi's sarcoma-associated herpesvirus during primary infection. J Virol **82:**5440-9.

87. **Wong, L. Y., G. A. Matchett, and A. C. Wilson.** 2004. Transcriptional activation by the Kaposi's sarcoma-associated herpesvirus latency-associated nuclear antigen is facilitated by an N-terminal chromatin-binding motif. J Virol **78:**10074-85.

88. **Wong, L. Y., and A. C. Wilson.** 2005. Kaposi's sarcoma-associated herpesvirus latency-associated nuclear antigen induces a strong bend on binding to terminal repeat DNA. J Virol **79:**13829-36.

89. **Wong, S. W., E. P. Bergquam, R. M. Swanson, F. W. Lee, S. M. Shiigi, N. A. Avery, J. W. Fanton, and M. K. Axthelm.** 1999. Induction of B cell hyperplasia in simian immunodeficiency virus-infected rhesus macaques with the simian homologue of Kaposi's sarcoma-associated herpesvirus. J Exp Med **190:**827-40.

90. **Ye, F. C., F. C. Zhou, S. M. Yoo, J. P. Xie, P. J. Browning, and S. J. Gao.** 2004. Disruption of Kaposi's sarcoma-associated herpesvirus latent nuclear antigen leads to abortive episome persistence. J Virol **78:**11121-9.

91. **You, J., V. Srinivasan, G. V. Denis, W. J. Harrington, Jr., M. E. Ballestas, K. M. Kaye, and P. M. Howley.** 2006. Kaposi's sarcoma-associated herpesvirus latency-associated nuclear antigen interacts with bromodomain protein Brd4 on host mitotic chromosomes. J Virol **80:**8909-19.

CHAPTER 5

SUMMARY, CONCLUSIONS AND FUTURE DIRECTIONS

General Conclusions

KSHV is etiologically associated with three human neoplastic diseases, namely KS (8), PEL (6), and MCD (22, 40). KS is a vascular malignancy of endothelial origin, whereas PEL and MCD are lymphoproliferative disorders of B cell origin (8). KSHV encodes a plethora of transforming/tumorigenic proteins and cellular homologs that perturb normal cellular signaling pathways. The cellular functions affected by KSHV include cell growth and proliferation, cell death, innate and adaptive immunity. The ideal outcome for the virus is efficient viral replication and persistent infection of the host to benefit its own survivorship.

KSHV lifecycle exhibits lytic and latent phases of infection. During a lytic infection, the virus replicates its linear viral genomes and expresses more than 80 transcripts in a highly orchestrated temporal order, resulting in the production and release of infectious particles. In latency, the KSHV viral genome is circularized and exists as an extra-chromosomal episome. The latent virus only expresses a very small subset of latent transcripts (e.g. LANA) in the infected cells and produces no functional or infectious viral particles. Despite different roles in the viral lifecycle, both latent and lytic proteins of KSHV can be tumorigenic/oncogenic: the lytic viral proteins may mediate paracrine secretion of growth and angiogenic factors essential for tumor growth and development. The latent viral proteins may enhance the survival and proliferation of the infected cells.

The KSHV K1 and LANA proteins, which are the subjects of this dissertation, have been implicated in tumorigenesis and oncogenesis. The K1 ORF is located at the far left end of the KSHV genome (25), and is the positional equivalent of RRV R1 and HVS STP. It is therefore not surprising K1 and R1 can functionally substitute STP to

immortalize T lymphocytes (11, 15). Although K1 has been shown to perturb BCR cell signaling (15, 28, 42) and inhibit apoptosis in B cells (42) and have oncogenic properties (e.g. transformation of rodent fibroblasts (15) and induction of tumor formation in mice (15)), the mechanism of action contributing to these phenotypes is largely not known. Our lab and others have shown that while K1 gene expression could be detected in latently infected cells, it was induced to a higher level during lytic replication and thus K1 behaved like an early gene (7, 10, 24, 26, 39). We therefore sought to understand the role of K1 during various aspects of the lifecycle, i.e. latency, *de novo* lytic replication, and lytic reactivation, using RRV as a model system.

The LANA oncoprotein can suppress the activity of the tumor suppressors p53 (20) and Rb (36), and promote cell cycle progression by sequestering GSK-3β that leads to subsequent activation of CCND1 and Myc (3, 21). In addition, LANA is critical for the maintenance of the viral genomes in infected cells (13, 37, 44) and can inhibit Rta transactivation of viral promoters and thus the release of viral progeny (29). One would therefore speculate that depletion of LANA will result in a virus that is even more highly lytic but fails to establish and/or maintain latency. Because there is no cure or vaccine for KSHV as well as other rhadinovirus infections, we generated a LANA knockout virus in RRV and characterized its biological properties *in vitro*. A future goal is to explore its vaccine potential *in vivo* using a rhesus macaque model system.

The research work I performed under the supervision of Dr. Blossom Damania has generated new questions and hypotheses. Addressing the unresolved puzzles will stimulate further research and provide new insights into the oncogenic pathways usurped by KSHV as well as the basic virology of KSHV and other rhadinoviruses. My work also

provides further rationales for targeting K1 and its binding partners, especially Hsp90, to treat KSHV-associated lymphomas and for the use of a LANA knockout virus as a vaccine to prevent rhadinovirus infection and/or tumor development. The conclusions for the chapters will be reiterated below, with future directions and specific remarks wherever relevant and applicable.

The role of Hsp90 and Hsp40 in K1 expression and function

Despite the known signal transduction pathway and functions of K1, relatively little is known about how K1 protein expression and function are modulated. Using TAP, we identified Hsp90β and the ER-associated Hsp40/Erdj3 protein as the cellular partners of K1. This was corroborated by co-immunoprecipitations that confirmed these protein-protein interactions. We have further shown that K1's interaction with Hsp90β (but not Hsp40/Erdj3) is dependent on the presence of ATP and perhaps ATP hydrolysis by Hsp90β. To test specifically whether Hsp90 ATPase activity is essential for its interaction with K1, it will be worthwhile to test if Hsp90 inhibitors can also disrupt or abrogate the interaction between K1 and Hsp90.

Hsp90 has been show to regulate subcellular trafficking and function of viral proteins in KSHV and other herpesviruses (4, 18, 23). Our finding that K1 is a viral client protein of Hsp90 and the ER-associated Hsp40/Hsp70 system is novel and intriguing, because it implies that the protein expression of the K1 viral oncogene can be manipulated with existing Hsp90 inhibitors as well as siRNA/small hairpin RNAs targeting Hsp90 and/or Hsp40/Erdj3 chaperones. By performing confocal immunofluorescence assays, we showed that K1 interacts and colocalizes with Hsp90 and

Hsp40/Erdj3 in KSHV-positive PEL B cell lines. K1 and Hsp90 expression can also be detected in PEL tumors in our immunohistochemical study. Thus, our data validate Hsp90 as an important therapeutic target for treating KSHV-associated lymphomas.

Using the Hsp90 inhibitor geldanamycin (GA), we showed that Hsp90 ATPase activity and chaperoning function are required for optimal expression of K1. GA inhibits all the known Hsp90 homologs. Thus, it is possible that Hsp90 homologs other than Hsp90α and Hsp90β may also associate with K1 and modulate its expression and function. Future work addressing this possibility may elucidate if a general Hsp90 inhibitor or an isoform-specific Hsp90 is more preferable to target K1-driven pathways. The use of an isoform-specific Hsp90 inhibitor may cause fewer side effects than a general Hsp90 inhibitor *in vivo*. Similar to GA treatment, genetic knockdown of either Hsp90β or Hsp40/Erdj3 using siRNA also dramatically reduced K1 protein expression. Interestingly, we did not see much effect of K1 on the expression of levels of Hsp90 or Hsp40. It is plausible that instead of regulating the protein expression of Hsp90/ER-associated Hsp40, K1 modulates the chaperoning function of Hsp90 and/or ER-associated Hsp70 (that requires Erdj3 as a co-chaperone for optimal chaperoning activity). Future experiments testing K1's effect on the ATPase activity of Hsp90 and ER-associated Hsp70 will address this possibility.

While depletion of both endogenous Hsp90β and ER-associated Hsp40 negated the ability of K1 to prevent Fas-mediated apoptosis, depletion of only Hsp90β or Hsp40 by itself had no effect. One explanation is that knockdown of both Hsp90β and Hsp40 reduced K1 expression levels more robustly than single knockdowns of these proteins. A second possibility is that there are two different pools of K1 whose expression and/or

function are regulated by Hsp90β and Hsp40. K1 has been shown to be expressed on the plasma membrane as well as in the ER (30). Since Hsp90β is predominantly cytosolic and Hsp40/Erdj3 is ER-associated, one may speculate that these different pools of K1 are topologically distinct (Fig. 1). Hence, knockdown of the ER-restricted chaperone may reduce K1 levels in the ER, but not affect cytosolic or cell surface levels of K1, and *vice versa*. A simple experiment to test this in the future is to repeat the Hsp40/Erdj3 and Hsp90 knockdown experiments and perform immunofluorescence assays for K1-Hsp90 and K1-Hsp40/Erdj3 colocalization and also fluorescently label the ER or endosome compartment with an ER-tracker (e.g. glibenclamide that binds to ER-specific sulphonylurea receptors of ATP-sensitive K+ channels) or endosome marker (e.g. EEA1 and CD71/transferring receptor). Alternatively, we can perform the individual knockdown experiments and then fractionate the 293-K1 cells to obtain the cytosolic, ER, and membrane fractions and repeat the co-immunoprecipitation assays for K1-Hsp90 and K1-Erdj3. If the K1-Hsp90 and K1-Erdj3 complexes are topologically exclusive, we may only see the former complex predominantly in the cytosolic/endosome compartment and the latter in the ER compartment, respectively, by IFA or co-IP. With the control siRNAs transfected, we will detect K1-Erdj3 complex localized predominantly in the ER, and the majority of K1-Hsp90 complex in other compartments (e.g. plasma membrane, endosome, or cytosol). With Hsp90 siRNA transfection, we will detect mostly K1-Erdj3 complex in the ER, whereas with Erdj3 siRNAtransfection, K1-Hsp90 complex in other subcellular compartments. It will be interesting to see whether knockdown of Hsp90 will result in the enrichment of the Hsp40 colocalizing and interacting with K1 and *vice versa*.

Such a result may explain why single knockdown of Hsp90 or Erdj3 did not induce caspase-3 activation or cell death in 293-K1 cells relative to 293-Vec cells.

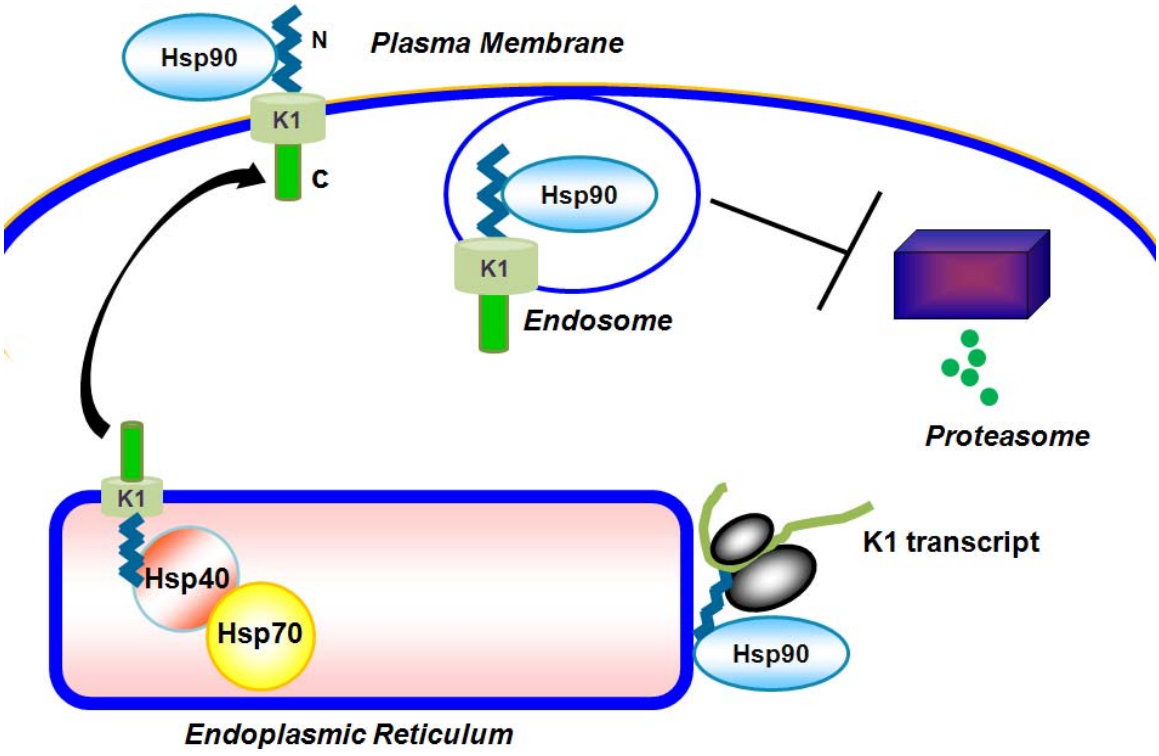

Figure 1. A working model for the interaction of K1 with Hsp90 and ER-associated Hsp40. K1-interacting complexes may be topologically distinct as shown. N: N-terminal domain of K1; C: C-terminal domain of K1.

Targeting Hsp90 and K1 as a therapeutic approach to PEL and other KSHV-associated malignancies

Our data showed that inhibition of Hsp90 activity by 17-AAG and 17-DMAG at low concentrations resulted in cell growth inhibition and cell-cycle arrest at G0/G1 phase. Furthermore, preliminary data (not shown) demonstrate that stable knockdown of K1 in BCBL-1 cells by shRNA also suppressed PEL cell proliferation. These data suggest the relevance of targeting Hsp90 and K1 as a potential therapeutic to PEL. To determine if

Hsp90 is also efficacious against KSHV-derived tumorigenic endothelial cells in the future, we will measure the IC_{50} and/or LC_{50} of Hsp90 inhibitors in long term-infected telomere-immortalized human umbilical vein endothelial (TIVE) cells that stably harbor KSHV. A key future direction is to test if Hsp90 inhibitor or stable knockdown of Hsp90 or K1 by shRNA can prevent the formation and/or progression of PEL-like or KS-like tumors in mouse models. Our lab as well as the Dittmer lab have established long term-infected TIVE cells (LTC)-severe combined immunodeficient (SCID) and PEL-SCID mouse xenograft models that have been shown to reflect KS and PEL tumorigenesis, respectively (5, 10, 35, 45).

We also speculate that there are several other KSHV proteins that utilize molecular chaperones to modulate their expression and function. Future experiments generating TAP-tagged molecular chaperones such as Hsp90 and Erdj3 and performing tandem affinity purification in reactivated KSHV-positive PEL or tumorigenic endothelial cell lines may identify additional KSHV proteins that interact with them. Similar experiments may also be performed in RRV-infected RhF lysates to identify RRV proteins that bind Hsps. All of the above experiments may provide even further insights and rationale for using inhibitors against molecular chaperones for KSHV-derived cancer therapy.

Investigation of the role of K1 in the viral lifecycle using RRV R1 as a model

The KSHV K1 protein has been shown to transform cells, inhibit apoptosis, and perturb cellular signaling pathways in B cells and endothelial cells (reviewed in (47)), yet its role in the KSHV lifecycle has not been well studied. K1 is expressed at low levels

during latency (7, 10, 17, 25, 38) and is upregulated during lytic infection (24, 26, 31, 39) where it demonstrates early kinetics. The role of K1 during latency versus lytic replication may depend on the level of K1 expression. Chandriani and Ganem recently reported using a very sensitive, limiting dilution-based assay that K1 RNA was present at low levels in latently infected cells in a context-dependent fashion (7).

Using overexpression systems, two laboratories previously studied the role of K1 on reactivation in B cells, albeit with conflicting data: Lee *et al*. observed in the KSHV-positive BCBL-1 cells that K1 overexpression resulted in the suppression of lytic reactivation by TPA treatment (31), whereas Lagunoff *et al*. showed in KSHV-negative BJAB B cells that K1 overexpression augmented lytic reactivation upon KSHV Rta overexpression (27). Notably, Lagunoff *et al*. also found that introduction of a K1 dominant negative mutant into BCBL-1 cells, followed by KSHV Rta-mediated induction of lytic replication, diminished lytic gene expression by up to 80% (27). These inhibitory effects could be overcome by TPA (27). Thus, these two publications reported contradictory results.

To this day, the role of K1 during lytic *de novo* infection/reactivation and latency still remains unclear. Similar to the situation of K1, while R1 appears to be the positional and functional homolog of K1, R1's role in RRV lifecycle has not been sufficiently addressed. By utilizing an overlapping set of cosmids developed by Bilello *et al.* (2), we generated a R1 functional knockout virus (RRVΔR1/GFPcc) of RRV and examined its replicative properties. Our findings should shed light onto the role of R1 and K1 in KSHV and RRV biology.

RRVΔR1/GFPcc and the revertant virus replicated on RhF with growth kinetics that were similar to those of the wild-type control viruses at single-step growth or multiple-step growth. However, disruption of R1 resulted in a mutant virus less capable of establishing and maintaining latency as well as reactivating in BJAB cells. This suggests that R1 fine-tunes the lytic activity of RRV during these phases of the viral lifecycle. Since our data imply that R1 modulates latent infection and lytic reactivation, one may speculate that R1 should have some effect during *de novo* lytic replication. One possibility for not observing this could be due to cell-type specificity. While K1 expression has been detected in KSHV-associated tumors, and K1 function and signaling have been demonstrated in B and endothelial cells, R1 function has only been described in B cells. Thus, rhesus fibroblasts might not represent the natural cell type in which R1 signals or functions. The SH2 binding motifs in R1 might be specific for SH2-binding proteins in lymphocytes and/or endothelial cells only. Alternatively, since RhF is a highly lytic system that supports efficient RRV infection, our experimental setup might not be sensitive enough to detect minor suppressive effects of R1 on *de novo* replication under a high background of lytic replication. Hence, we are currently in the process of performing viral infections at very low MOIs (e.g. 0.01) which may potentially address this question.

We are also comparing the replicative kinetics or RRVΔR1/GFPcc, Revertant, RRV-GFPcc, and RRV-J in immortalized human umbilical vein endothelial cells (HUVEC) that support *de novo* lytic infection to a lesser extent than RhF. Our preliminary data (not shown) revealed that RRVΔR1/GFPcc in HUVEC resulted in slightly less infectious particles and viral genomes when compared to the other three

viruses at 0.1 MOI. Interestingly, no difference was seen in all four viruses at higher MOIs (1 and 5). This suggests that R1 might modestly enhance lytic infection of HUVEC at low MOIs. However, these experiments were only performed once and will need to be repeated.

In our B cell model, while RRVΔR1/GFPcc-infected BJAB cells released less virions than RRV-GFPcc-infected BJAB cells, the former were able to produce similar levels of viral particles upon more robust reactivation induced by TPA/NaB/TSA cocktail or KSHV Rta/Orf50 transactivation activity. Thus, R1 signaling might be complemented by some of the signaling events activated by TPA, NaB, and TSA, or by Rta-mediated transactivation of viral and/or cellular promoters. In agreement with our finding, Lagunoff *et al*. reported blockage of lytic replication by K1 ITAM mutants that could be overcome by TPA treatment, thus suggesting that TPA-mediated signaling pathways could substitute for the loss of K1 signaling (27). An interesting observation from this study is that KSHV Rta/Orf50 was able to reactivate RRV from latency, which implies that KSHV Rta can functionally complement or substitute RRV Rta. This finding echoes our previous observation that the Rta of RRV and murine gammaherpesvirus-68 (MHV-68) can functionally substitute for their KSHV homolog.

An alternative and valid interpretation of the data is that as a glycoprotein, R1 (or K1) may function to optimize efficient maturation and/or egress of the virus particles from B cells. This could also account for the observed enrichment of intracellular viral genomes in the RRVΔR1/GFPcc infected B cells, and reduction of extracellular viral genomes in the supernatant in the RRVΔR1/GFPcc infected B cells compared to RRV-GFPcc infected B cells. To rule out this possibility, electron microscopy to examine and

compare the number, subcellular distribution, and morphology of viral particles within RRVΔR1/GFPcc and RRV-GFPcc infected BJAB cells will be performed in the future.

To address the mechanism by which R1 affects the viral lifecycle, we may determine whether R1 may affect viral genes and assess whether those viral genes are Rta-responsive in the near future. We will subject isolated viral RNA from RRVΔR1/GFPcc or RRV-GFPcc infected BJAB cells to the RRV quantitative real-time PCR array developed by the Dittmer lab as previously described (14, 48), in order to assess the transcriptional profile of all RRV viral genes. We are in the progress of generating BJAB cell lines stably and latently infected with RRVΔR1/GFPcc or RRV-GFPcc for the RRV viral array.

In addition to its role in latency maintenance or lytic reactivation *in vitro*, R1 may function as an immunoregulatory protein *in vivo*. KSHV K1 has been shown to downregulate the BCR surface expression (30) that may otherwise lead to apoptosis. Thus K1 modulation of BCR signal transduction may provide a long-term survival advantage *in vivo*. Indeed, K1 expression has been shown to protect cells from Fas-mediated apoptosis (42, 46). Like K1, R1 activates B-cell signaling pathways (9). We have preliminary data supporting that R1also increases the phosphorylation of Akt (S473), FKHR and Bad involved in the PI3K/Akt pathway (data not shown) (1, 42, 46). Since the same PI3K/Akt pathway activated by K1 is pro-survival and controls Fas-mediated apoptosis (41, 43), R1 may exhibit a similar phenotype to K1 *in vitro*. Future experiments comparing the ability of RRVΔR1/GFPcc or control RRV-GFPcc to inhibit apoptosis upon Fas-induction will address whether R1 can also protect cells from apoptosis in the context of the whole virus during lytic replication and latency.

It will be interesting to assess whether rhesus macaques co-infected with SIV and RRVΔR1/GFPcc (or RRV-GFPcc) would develop B cell hyperplasia and persistent lymphadenopathy (16, 33, 49). Because R1 is the positional homolog of STP that has been shown to be critical for transformation *in vivo* (15) and R1 deregulates signal transduction in B-cells (9), RRVΔR1/GFPcc may be defective in inducing B cell hyperplasia in rhesus macaques.

In conclusion, we have generated a recombinant RRV designated RRVΔR1/GFPcc, in which the R1 ORF has been disrupted by a GFP expression cassette. This R1 deletion virus displayed suppressed lytic activity in our B cell model for latency and reactivation, but had no significant effect on replication during *de novo* infection on rhesus fibroblasts at MOIs of 1 and 5. By determining the functional role of R1 in the RRV lifecycle, we may shed light on the role of K1 in KSHV lifecycle. This knowledge may guide future therapeutic strategy against rhadinovirus infection as well as KSHV infection and KSHV-associated malignancies.

The role of RRV LANA in the context of the whole-virus infection

The various functions of KSHV LANA (K-LANA) have been extensively studied (reviewed in (13, 44, 47)). By comparison, relatively little is known about R-LANA. Given our previous finding that R-LANA can inhibit RRV Rta-mediated transactivation of a subset of lytic viral genes (12), we hypothesized that a R-LANA knockout virus would be more lytic and display dysregulated transcription compared to the wild-type RRV. In order to gain insight into the role of LANA in RRV infection and replication, we

generated RRVΔLANA/GFP and a revertant virus (RRV_{REV}). We found that RRVΔLANA/GFP displayed increased lytic activity in RhF. Disruption of R-LANA also resulted in a global upregulation of RRV mRNA transcripts as assayed by a QPCR RRV array. Because Rta is necessary and sufficient for initiating and orchestrating the lytic viral transcriptional cascade, we speculate that the lytic behavior of RRVΔLANA/GFP in our permissive RhF tissue culture system was largely due to unhampered Rta transactivation activity when R-LANA was no longer expressed. Altogether, our data suggest that R-LANA suppresses lytic replication during *de novo* infection in RhF. For future studies, it will be important to test if R-LANA has similar effects on HUVEC that also supports lytic replication. An established role of LANA in viral persistence in endothelial cells may prove important for KS development.

RRVΔLANA/GFP exhibited elevated lytic activity in both viral production as well as global gene transcription that can be explained by unrestrained Rta transactivation activity. Several possible mechanisms could explain how R-LANA might inhibit Rta transactivation of Rta-responsive genes in the wild-type virus. The most obvious explanation is chromatin remodeling, as R-LANA has been implicated in recruiting histone deacetylases (HDACs) (12) , the result of which may lead to histone modification of Rta-responsive viral promoters. Additionally, Lu *et al*. have reported that Rta transcription is specifically repressed by KSHV LANA during viral latency (32). In addition to recruiting HDACs for transcription repression (12), R-LANA might sequester histone acetyltransferases (HATs) from Rta or Rta-dependent viral promoters. Our finding that R-LANA decreased the gene expression of the HAT, NCOA3, suggests that R-LANA might also repress HAT-mediated transcription. Other possibilities by which R-

LANA could inhibit Rta function include affecting Rta protein levels and modification of Rta post-translationally in order to downregulate Rta transactivation function. Our preliminary data have excluded these two possibilities (unpublished data). Interestingly, a significant number of RRV genes that were upregulated in the RRVΔLANA/GFP infected cells compared to the RRV-GFP infected cells have not been previously identified as being Rta-responsive in either the KSHV or RRV viral systems. It is plausible that R-LANA acts as a direct transcriptional repressor of a sub-set of viral genes, independent of its inhibition of Rta transactivation.

Furthermore, several cellular genes reported to be repressed by KSHV LANA in either B cells or endothelial cells were found to be derepressed in cells infected with RRVΔLANA/GFP compared to RRV-GFP. A future experiment will be to identify all cellular transcripts whose expression is altered by the presence of R-LANA during *de novo* lytic infection in the context of the whole virus. Specifically, we will subject mRNA isolated from RRVΔLANA/GFP vs. RRV-GFP infected RhF to Agilent Rhesus Macaque Gene Expression Microarray to profile cellular gene expression.

Finally, RRVΔLANA/GFP also failed to efficiently establish and maintain latency in BJAB cells. This was similar to what was observed with the KSHV LANA deletion mutant BAC36-ΔLNA in 293 cells (50).

RRVΔLANA/GFP as a vaccine candidate against rhadinovirus infection

A future goal of our study is to investigate RRVΔLANA/GFP infection in rhesus macaques to determine its behavior *in vivo*. Given the biological properties of the

RRVΔLANA/GFP recombinant virus, we hypothesize that such a virus would make a good candidate vaccine, which will protect against challenge with wild-type RRV-GFP virus. This is because the highly lytic nature of this virus resulted in the dysregulated expression of multiple lytic viral genes, which should expose the virus to the host innate and adaptive arms of the immune system to a greater extent than the wild-type RRV-GFP virus. Hence, we hypothesize that the host should be able to mount a robust immune response against the RRVΔLANA/GFP virus, which may help protect the host from subsequent challenge with wild-type RRV. Furthermore, the inability of this virus to establish latency in dividing cells means that unlike the wild-type RRV-GFP and other herpesviruses, this virus should be lost from proliferating cells since R-LANA is not expressed. It is possible that although R-LANA is required for the establishment of latency in dividing cells, it is not required for the establishment of latency in non-dividing cells, in which case low amounts of the RRVΔLANA/GFP virus may still be detected in non-dividing cells (e.g. macrophages and dendritic cells that can support KSHV infection). We will determine if this is the case when we isolate macrophages and dendritic cells from blood for viral DNA analysis. If RRVΔLANA/GFP can persist in these non-dividing presenting immune cells, booster vaccinations may not be needed as there will be persistently high immune responses to confer long-term protection.

A critical criterion for vaccines is safety. Importantly, RRVΔLANA/GFP virus could not achieve long-term latency in infected B cells that serve as the natural reservoir for rhadinoviruses. This should minimize the time and likelihood for the recombinant virus to transform infected B cells into lymphomatous cells. The presumably rampant clearance of this highly lytic virus should also discourage full-blown viral dissemination

as well as prolonged systemic symptoms in the host. Because both KSHV and RRV encode a number of cellular homologs, a legitimate concern is that RRVΔLANA/GFP genome may recombine with or integrate into the host cell genome. Another concern is that while herpesviruses have relatively stable DNA genomes, RRVΔLANA/GFP may still slowly mutate to lose its high lytic activity and revert back to the wild-type phenotype. With these potential problems in mind, we are currently evaluating the RRVΔLANA/GFP as a vaccine candidate in rhesus macaques in collaboration with Dr. Ronald Desrosiers at Harvard Medical School. We will determine the biological characteristics of the RRVΔLANA/GFP recombinant virus in terms of its persistence, viral load levels in the oral cavity and blood, anti-viral antibodies, and complete blood counts (CBC) present in the RRVΔLANA/GFP infected rhesus macaques (Table 1). We will also perform subsequent experiments to use it as a vaccine to protect against subsequent challenge with the wild-type RRV (Table 2).

In conclusion, we have created a RRVΔLANA/GFP that is more lytic than RRV-GFP, wild-type RRV H26-95, or a revertant RRV_{REV} virus. This recombinant virus displays higher viral loads in rhesus fibroblasts as well as increased expression of a multitude of RRV viral genes during lytic replication in rhesus fibroblasts. Additionally, cellular genes that are normally repressed by LANA are derepressed in RRVΔLANA/GFP infected cells compared to RRV-GFP infected cells. Furthermore, the RRVΔLANA/GFP recombinant virus also fails to successfully establish latent infection in B lymphocytes. These unique properties prompt us to investigate the vaccine potential of RRVΔLANA/GFP in the future by utilization of a rhesus macaque model system.

Table 1: Biological characterization of the RRVΔLANA/GFP recombinant virus

Mm # (TBD)	Strain	Route
1) XX-XX	RRV-GFP	IV
2) XX-XX	RRV-GFP	IV
3) XX-XX	RRV-GFP	IV
4) XX-XX	RRVΔLANA/GFP	IV
5) XX-XX	RRVΔLANA/GFP	IV
6) XX-XX	RRVΔLANA/GFP	IV

All 6 animals will be from the superclean SPF group and are RRV negative. (TBD=to be determined).

Week	Date	Plasma	PBMC load	Cell. Immune responses	Flow Cyt.	LN Biopsy	RRV gene profiling	CBC
-1		X	X	X	X		X	X
0		X	X	X	X		X	X
1		X	X	X	X		X	X
2		X	X	X	X	X	X	X
3		X	X	X	X		X	X
4		X	X	X	X	X	X	X
8		X	X	X	X		X	X
10		X	X	X	X		X	X
12		X	X	X	X	X	X	X
Twice per month thereafter		X	X	X	X		X	X

Pre - Temperature discs will be implanted into each animal. Temperature will be recorded daily for the first month

LN biopsies - Histopathological examination. Single cell suspension will be used for quantitative culture, and for flow cytometry, and for viral DNA levels

Table 2: Vaccination with RRVΔLANA/GFP virus and challenge with WT RRV

Mm # (TBD)	Strain		Route
1) XX-XX	None (PBS)		IV
2) XX-XX	None (PBS)		IV
3) XX-XX	RRVΔLANA/GFP	($1x10^6$)	IV
4) XX-XX	RRVΔLANA/GFP	($1x10^6$)	IV
5) XX-XX	RRVΔLANA/GFP	($1x10^7$)	IV
6) XX-XX	RRVΔLANA/GFP	($1x10^7$)	IV

All 6 animals will be from the superclean SPF group and are RRV negative. (TBD=to be determined).

Week	Date	Plasma	PBMC load	Cell. Immune responses	Flow Cyt.	LN Biopsy	RRV gene profiling	CBC
-1		X	X	X	X		X	X
0 (Challenge)		X	X	X	X		X	X
1		X	X	X	X		X	X
2		X	X	X	X	X	X	X
3		X	X	X	X		X	X
4		X	X	X	X	X	X	X
8		X	X	X	X		X	X
10		X	X	X	X		X	X
12		X	X	X	X	X	X	X
Twice per month thereafter		X	X	X	X		X	X

Pre - Temperature discs will be implanted into each animal. Temperature will be recorded daily for the first month

LN biopsies - Histopathological examination. Single cell suspension will be used for quantitative culture, and for flow cytometry, and for viral DNA levels

REFERENCES

1. **Bilello, J. P., S. M. Lang, F. Wang, J. C. Aster, and R. C. Desrosiers.** 2006. Infection and persistence of rhesus monkey rhadinovirus in immortalized B-cell lines. J Virol **80:**3644-9.

2. **Bilello, J. P., J. S. Morgan, B. Damania, S. M. Lang, and R. C. Desrosiers.** 2006. A genetic system for rhesus monkey rhadinovirus: use of recombinant virus to quantitate antibody-mediated neutralization. J Virol **80:**1549-62.

3. **Boshoff, C.** 2003. Kaposi virus scores cancer coup. Nat Med **9:**261-2.

4. **Burch, A. D., and S. K. Weller.** 2005. Herpes simplex virus type 1 DNA polymerase requires the mammalian chaperone hsp90 for proper localization to the nucleus. J Virol **79:**10740-9.

5. **Burnside, K. L., J. T. Ryan, H. Bielefeldt-Ohmann, A. Gregory Bruce, M. E. Thouless, C. C. Tsai, and T. M. Rose.** 2006. RFHVMn ORF73 is structurally related to the KSHV ORF73 latency-associated nuclear antigen (LANA) and is expressed in retroperitoneal fibromatosis (RF) tumor cells. Virology **354:**103-15.

6. **Cesarman, E., Y. Chang, P. S. Moore, J. W. Said, and D. M. Knowles.** 1995. Kaposi's sarcoma-associated herpesvirus-like DNA sequences in AIDS-related body-cavity-based lymphomas. N Engl J Med **332:**1186-91.

7. **Chandriani, S., and D. Ganem.** 2010. Array-based transcript profiling and limiting-dilution RT-PCR analysis identify additional latent genes in KSHV. J Virol.

8. **Chang, Y., E. Cesarman, M. S. Pessin, F. Lee, J. Culpepper, D. M. Knowles, and P. S. Moore.** 1994. Identification of herpesvirus-like DNA sequences in AIDS-associated Kaposi's sarcoma. Science **266:**1865-9.

9. **Damania, B., M. DeMaria, J. U. Jung, and R. C. Desrosiers.** 2000. Activation of lymphocyte signaling by the R1 protein of rhesus monkey rhadinovirus. J Virol **74:**2721-30.

10. **Damania, B., J. H. Jeong, B. S. Bowser, S. M. DeWire, M. R. Staudt, and D. P. Dittmer.** 2004. Comparison of the Rta/Orf50 transactivator proteins of gamma-2-herpesviruses. J Virol **78:**5491-9.

11. **Damania, B., M. Li, J. K. Choi, L. Alexander, J. U. Jung, and R. C. Desrosiers.** 1999. Identification of the R1 oncogene and its protein product from the rhadinovirus of rhesus monkeys. J Virol **73:**5123-31.

12. **DeWire, S. M., and B. Damania.** 2005. The latency-associated nuclear antigen of rhesus monkey rhadinovirus inhibits viral replication through repression of Orf50/Rta transcriptional activation. J Virol **79:**3127-38.

13. **Dittmer, D.** 2008. KSHV viral latent lifecycle. *In* B. Damania and J. Pipas (ed.), DNA Tumor Viruses. Springer.

14. **Dittmer, D. P., C. M. Gonzalez, W. Vahrson, S. M. DeWire, R. Hines-Boykin, and B. Damania.** 2005. Whole-genome transcription profiling of rhesus monkey rhadinovirus. J Virol **79:**8637-50.

15. **Duboise, M., J. Guo, S. Czajak, H. Lee, R. Veazey, R. C. Desrosiers, and J. U. Jung.** 1998. A role for herpesvirus saimiri orf14 in transformation and persistent infection. J Virol **72:**6770-6.

16. **Estep, R. D., M. F. Powers, B. K. Yen, H. Li, and S. W. Wong.** 2007. Construction of an infectious rhesus rhadinovirus bacterial artificial chromosome for the analysis of Kaposi's sarcoma-associated herpesvirus-related disease development. J Virol **81:**2957-69.

17. **Fakhari, F. D., and D. P. Dittmer.** 2002. Charting latency transcripts in Kaposi's sarcoma-associated herpesvirus by whole-genome real-time quantitative PCR. J Virol **76:**6213-23.

18. **Field, N., W. Low, M. Daniels, S. Howell, L. Daviet, C. Boshoff, and M. Collins.** 2003. KSHV vFLIP binds to IKK-gamma to activate IKK. J Cell Sci **116:**3721-8.

19. **Fowler, P., S. Marques, J. P. Simas, and S. Efstathiou.** 2003. ORF73 of murine herpesvirus-68 is critical for the establishment and maintenance of latency. J Gen Virol **84:**3405-16.

20. **Friborg, J., Jr., W. Kong, M. O. Hottiger, and G. J. Nabel.** 1999. p53 inhibition by the LANA protein of KSHV protects against cell death. Nature **402:**889-94.

21. **Fujimuro, M., and S. D. Hayward.** 2003. The latency-associated nuclear antigen of Kaposi's sarcoma-associated herpesvirus manipulates the activity of glycogen synthase kinase-3beta. J Virol **77:**8019-30.

22. **Gessain, A., A. Sudaka, J. Briere, N. Fouchard, M. A. Nicola, B. Rio, M. Arborio, X. Troussard, J. Audouin, J. Diebold, and G. de The.** 1996. Kaposi sarcoma-associated herpes-like virus (human herpesvirus type 8) DNA sequences in multicentric Castleman's disease: is there any relevant association in non-human immunodeficiency virus-infected patients? Blood **87:**414-6.

23. **Iscovich, J., A. Fischbein, J. Fisher-Fischbein, L. S. Freedman, S. M. Eng, P. Boffetta, A. Vudovich, C. Glasman, R. Goldschmidt, M. Livingston, B.**

Heger-Maslansky, P. Brennan, and P. S. Moore. 2000. Seroprevalence of Kaposi's sarcoma-associated herpesvirus in healthy adults in Israel. Anticancer Res **20:**2119-22.

24. **Jenner, R. G., M. M. Alba, C. Boshoff, and P. Kellam.** 2001. Kaposi's sarcoma-associated herpesvirus latent and lytic gene expression as revealed by DNA arrays. J Virol **75:**891-902.

25. **Kedes, D. H., M. Lagunoff, R. Renne, and D. Ganem.** 1997. Identification of the gene encoding the major latency-associated nuclear antigen of the Kaposi's sarcoma-associated herpesvirus. J Clin Invest **100:**2606-10.

26. **Krishnan, H. H., P. P. Naranatt, M. S. Smith, L. Zeng, C. Bloomer, and B. Chandran.** 2004. Concurrent expression of latent and a limited number of lytic genes with immune modulation and antiapoptotic function by Kaposi's sarcoma-associated herpesvirus early during infection of primary endothelial and fibroblast cells and subsequent decline of lytic gene expression. J Virol **78:**3601-20.

27. **Lagunoff, M., D. M. Lukac, and D. Ganem.** 2001. Immunoreceptor tyrosine-based activation motif-dependent signaling by Kaposi's sarcoma-associated herpesvirus K1 protein: effects on lytic viral replication. J Virol **75:**5891-8.

28. **Lagunoff, M., R. Majeti, A. Weiss, and D. Ganem.** 1999. Deregulated signal transduction by the K1 gene product of Kaposi's sarcoma-associated herpesvirus. Proc Natl Acad Sci U S A **96:**5704-9.

29. **Lan, K., D. A. Kuppers, S. C. Verma, and E. S. Robertson.** 2004. Kaposi's sarcoma-associated herpesvirus-encoded latency-associated nuclear antigen inhibits lytic replication by targeting Rta: a potential mechanism for virus-mediated control of latency. J Virol **78:**6585-94.

30. **Lee, B. S., X. Alvarez, S. Ishido, A. A. Lackner, and J. U. Jung.** 2000. Inhibition of intracellular transport of B cell antigen receptor complexes by Kaposi's sarcoma-associated herpesvirus K1. J Exp Med **192:**11-21.

31. **Lee, B. S., M. Paulose-Murphy, Y. H. Chung, M. Connlole, S. Zeichner, and J. U. Jung.** 2002. Suppression of tetradecanoyl phorbol acetate-induced lytic reactivation of Kaposi's sarcoma-associated herpesvirus by K1 signal transduction. J Virol **76:**12185-99.

32. **Lu, F., L. Day, S. J. Gao, and P. M. Lieberman.** 2006. Acetylation of the latency-associated nuclear antigen regulates repression of Kaposi's sarcoma-associated herpesvirus lytic transcription. J Virol **80:**5273-82.

33. **Mansfield, K. G., S. V. Westmoreland, C. D. DeBakker, S. Czajak, A. A. Lackner, and R. C. Desrosiers.** 1999. Experimental infection of rhesus and pig-tailed macaques with macaque rhadinoviruses. J Virol **73:**10320-8.

34. **Moorman, N. J., D. O. Willer, and S. H. Speck.** 2003. The gammaherpesvirus 68 latency-associated nuclear antigen homolog is critical for the establishment of splenic latency. J Virol **77:**10295-303.

35. **Ossevoort, M., A. Zaldumbide, A. J. te Velthuis, M. Melchers, M. E. Ressing, E. J. Wiertz, and R. C. Hoeben.** 2007. The nested open reading frame in the Epstein-Barr virus nuclear antigen-1 mRNA encodes a protein capable of inhibiting antigen presentation in cis. Mol Immunol **44:**3588-96.

36. **Radkov, S. A., P. Kellam, and C. Boshoff.** 2000. The latent nuclear antigen of Kaposi sarcoma-associated herpesvirus targets the retinoblastoma-E2F pathway and with the oncogene Hras transforms primary rat cells. Nat Med **6:**1121-7.

37. **Rainbow, L., G. M. Platt, G. R. Simpson, R. Sarid, S. J. Gao, H. Stoiber, C. S. Herrington, P. S. Moore, and T. F. Schulz.** 1997. The 222- to 234-kilodalton latent nuclear protein (LNA) of Kaposi's sarcoma-associated herpesvirus (human herpesvirus 8) is encoded by orf73 and is a component of the latency-associated nuclear antigen. J Virol **71:**5915-21.

38. **Samaniego, F., S. Pati, J. E. Karp, O. Prakash, and D. Bose.** 2001. Human herpesvirus 8 K1-associated nuclear factor-kappa B-dependent promoter activity: role in Kaposi's sarcoma inflammation? J Natl Cancer Inst Monogr**:**15-23.

39. **Sarid, R., J. S. Wiezorek, P. S. Moore, and Y. Chang.** 1999. Characterization and cell cycle regulation of the major Kaposi's sarcoma-associated herpesvirus (human herpesvirus 8) latent genes and their promoter. J Virol **73:**1438-46.

40. **Soulier, J., L. Grollet, E. Oksenhendler, P. Cacoub, D. Cazals-Hatem, P. Babinet, M. F. d'Agay, J. P. Clauvel, M. Raphael, L. Degos, and et al.** 1995. Kaposi's sarcoma-associated herpesvirus-like DNA sequences in multicentric Castleman's disease. Blood **86:**1276-80.

41. **Suhara, T., H. S. Kim, L. A. Kirshenbaum, and K. Walsh.** 2002. Suppression of Akt signaling induces Fas ligand expression: involvement of caspase and Jun kinase activation in Akt-mediated Fas ligand regulation. Mol Cell Biol **22:**680-91.

42. **Tomlinson, C. C., and B. Damania.** 2004. The K1 protein of Kaposi's sarcoma-associated herpesvirus activates the Akt signaling pathway. J Virol **78:**1918-27.

43. **Uriarte, S. M., S. Joshi-Barve, Z. Song, R. Sahoo, L. Gobejishvili, V. R. Jala, B. Haribabu, C. McClain, and S. Barve.** 2005. Akt inhibition upregulates FasL, downregulates c-FLIPs and induces caspase-8-dependent cell death in Jurkat T lymphocytes. Cell Death Differ **12:**233-42.

44. **Verma, S. C., K. Lan, and E. Robertson.** 2007. Structure and function of latency-associated nuclear antigen. Curr Top Microbiol Immunol **312:**101-36.

45. **Wang, L., D. P. Dittmer, C. C. Tomlinson, F. D. Fakhari, and B. Damania.** 2006. Immortalization of primary endothelial cells by the K1 protein of Kaposi's sarcoma-associated herpesvirus. Cancer Res **66:**3658-66.

46. **Wang, S., H. Maeng, D. P. Young, O. Prakash, L. E. Fayad, A. Younes, and F. Samaniego.** 2007. K1 protein of human herpesvirus 8 suppresses lymphoma cell Fas-mediated apoptosis. Blood **109:**2174-82.

47. **Wen, K. W., and B. Damania.** 2010. Kaposi sarcoma-associated herpesvirus (KSHV): molecular biology and oncogenesis. Cancer Lett **289:**140-50.

48. **Wen, K. W., D. P. Dittmer, and B. Damania.** 2009. Disruption of LANA in rhesus rhadinovirus generates a highly lytic recombinant virus. J Virol **83:**9786-802.

49. **Wong, S. W., E. P. Bergquam, R. M. Swanson, F. W. Lee, S. M. Shiigi, N. A. Avery, J. W. Fanton, and M. K. Axthelm.** 1999. Induction of B cell hyperplasia in simian immunodeficiency virus- infected rhesus macaques with the simian homologue of Kaposi's sarcoma- associated herpesvirus. J Exp Med **190:**827-40.

50. **Ye, F. C., F. C. Zhou, S. M. Yoo, J. P. Xie, P. J. Browning, and S. J. Gao.** 2004. Disruption of Kaposi's sarcoma-associated herpesvirus latent nuclear antigen leads to abortive episome persistence. J Virol **78:**11121-9.